Alpha-Synuclein in Parkinson's Disease: Molecular Pathogenesis and Development of Genome Engineering-Based Silencing Approaches

Sabrina M. Heman-Ackah

Balliol College

University of Oxford

A thesis submitted for the degree of

Doctor of Philosophy

Michaelmas 2015

Title of Thesis: Alpha-Synuclein in Parkinson's Disease: Molecular Pathogenesis and Development of Genome Engineering-Based Silencing Approaches

Name of Candidate: Sabrina M. Heman-Ackah

College of Candidate: Balliol College, University of Oxford

Degree for which Thesis is Submitted*:* Doctor of Philosophy

Term and Year of Submission: Michaelmas 2015

Abstract

The ability to reprogram adult somatic cells into induced pluripotent stem cells (iPSCs) and subsequent development of protocols for their differentiation into disease-relevant cell types have enabled in-depth molecular analyses of multiple disease states as hitherto impossible. Parkinson's disease (PD) is one such example, in which the dopaminergic neurons that manifest pathology are embedded in an inaccessible region of the midbrain, the substantia nigra pars compacta, making it unfeasible to obtain samples of the affected region from living patients. Overabundance of alpha-synuclein, encoded by the SNCA gene, has long been implicated in the pathogenesis of PD. However, the precise mechanism by which overexpression of alpha-synuclein leads to the demise of dopaminergic neurons remains elusive. Neurons differentiated from PD patient-specific iPSCs carrying multiplications of the SNCA gene may provide a means to recapitulate molecular phenotypes of the disease *in vitro*. The application of CRISPR/Cas9 to mammalian systems is likewise revolutionizing the utilization of genome editing in the study of molecular contributors to the pathogenesis of numerous diseases, including PD. In this body of work, I have utilized the double-nicking CRISPR/Cas9 system to mediate site-specific mutagenesis of SNCA in PD patient-specific iPSCs harboring a triplication of the SNCA gene locus, resulting in isogenic cells which can be used to phenocopy normal alpha-synuclein expression from two alleles. I have further demonstrated the utility of nuclease null or "dead" Cas9, for transcriptional silencing of alpha-synuclein expression. Finally, I have used these systems to interrogate phenotypic outcomes of SNCA triplication, demonstrating that alpha-synuclein induces endoplasmic reticulum stress and aberrant activation of a highly conserved arm of the unfolded protein response. The tools generated in these studies can be applied in future efforts to dissect the contributions of alpha-synuclein overexpression to PD pathogenesis and as a platform for the discovery of disease-modifying therapeutic approaches for PD.

Acknowledgements

Professor Matthew J.A. Wood for offering mentorship, support, advice, and allowing just enough space and freedom to encourage my development into an independent scientist.

Dr. Andrew R. Bassett for guidance and generosity which contributed immensely to the completion of the work presented here.

Collaborators at the University of Oxford, including Rowan Flynn, Dr. Sally A. Cowley, Professor Tudor A. Fulga, and Dr. Caleb Webber.

The NIH Center for Regenerative Medicine and other collaborators at the NIH, including Dr. Richard J. Youle.

Friends and Wood Lab members, past and present, including Yi (Fiona) Lee, Caroline (Caz) Woffindale, Karin Meijboom, Tirsa van Westering, Carlo Rinaldi, Raquel Manzano, Thomas Merritt, Yoshitsugu (Yoshi) Aoki, Misa Aoki, Andrew Breglio, Melissa Bowerman, Anna Coenen-Stass, Ghulam Dar, Olivier de Jong, Andrew Douglas, Samir (Samme) El Andaloussi, Katie Fletcher, Caroline Godfrey, Martina Hallegger, Suzan Hammond, Gareth Hazell, Justin Hean, Kenji Hyodo, Anja Krueger, Jinghuan Li, Imre Mager, Graham McClorey, Mary McMenamin, Helen Ody, Aisling O'Loughlin, Inna Uliyakina, Pieter Vader, Miguel Varela, Eduard Willms, Joanna Zapisek and Katharina Zauner, for the countless ways in which they have enriched my experiences in the lab and in Oxford.

My siblings, Selena, Sam, Yolanda and Lillian, for being my role models and my support system. My dad, for modeling diligence in the pursuit of higher education. My mom, for her humble wisdom, her unwavering love and her inspiring faith.

Table of Contents

List of Abbreviations

AD	Alzheimer's disease
ALS	amyotrophic lateral sclerosis
BER	base excision repair
Cas9	CRISPR-associated protein 9
CMA	chaperone-mediated autophagy
CRISPR	clustered regularly interspaced short palindromic repeat
crRNA	CRISPR RNA
DA	dopaminergic, in reference to neurons
DAT	dopamine transporter
DBS	deep brain stimulation
DLB	dementia with Lewy bodies
DM	diabetes mellitus
DSB	double strand break
EB	embryoid body
ER	endoplasmic reticulum
ERAD	endoplasmic reticulum associated protein degradation
ET	essential tremor
GBA	β-glucocerebrosidase
GPi	globus pallidus internus
gRNA	guide RNA
GWAS	genome-wide association studies
HD	Huntington's disease

HDR	homology directed repair
hESC	human embryonic stem cell
indel	insertion/deletion
iPSC	induced pluripotent stem cell
IVF	*in vitro* fertilization
LB	Lewy body
mDA	midbrain dopaminergic, in reference to neurons
MEF	mouse embryonic fibroblast
mESC	mouse embryonic stem cell
miRNA	microRNA
MOMP	mitochondrial outer membrane pore
MPP+	1-methyl-4-phenylpyridinium
MPTP	1-methyl-4-phenyl-1,2,3,6-tetrahydropyridine
mRNA	messenger RNA
MSA	multiple systems atrophy
MSC	mesenchymal stem cell
NHEJ	non-homologous end joining
NPC	neuronal precursor cell
NSC	neural stem cell
NUC	nuclease lobe, in reference to Cas9
PAM	protospacer adjacent motif
PCB	polychlorinated biphenyl
PD	Parkinson’s disease
PDD	PD with dementia

PI	PAM-interacting domain, in reference to Cas9
REC	recognition lobe, in reference to Cas9
RIDD	regulated IRE1a-mediated decay
RNAi	RNA interference
ROS	reactive oxygen species
sgRNA	single guide RNA
shRNA	short hairpin RNA
siRNA	short interfering RNA
SMA	spinal muscular atrophy
SN	substantia nigra
SNc	substantia nigra pars compacta
SNO	*S*-nitrosylation
SNP	single-nucleotide polymorphism
SRP	signal recognition particle
STN	subthalamic nucleus
TALENs	transcription activator-like effector nucleases
TBI	traumatic brain injury
TCE	trichloroethylene
tracrRNA	trans-activating crRNA
UPR	unfolded protein response
UK	United Kingdom
UPS	ubiquitin proteasome system
US	United States of America
ZFNs	zinc finger nucleases

Chapter 1: Introduction

1.1 Parkinson's Disease

1.1.1 Epidemiology of Parkinson's Disease

Parkinson's disease (PD) is a progressive neurodegenerative disease manifesting primarily as a debilitating movement disorder, commonly accompanied by mild cognitive impairment which frequently advances to dementia[1]. It is the second most common neurodegenerative disease, following Alzheimer's disease (AD)[2]. An estimated 1 million people in the US[3] and 127,000 people in the UK currently suffer from PD, equaling about 1 in 500 people[4]. The disease affects an estimated 7 – 10 million people worldwide[3]. Men are 1.5 times more likely than women to suffer from PD[3], and the incidence increases with age, the majority of patients being diagnosed after the age of 50[3].

1.1.2 Environmental Risk Factors

The most important risk factor for the development of PD is age, although both environmental and genetic factors are thought to contribute to the etiopathogenesis of the disease. The first evidence of an environmental contribution to PD pathogenesis derived from the observation of Parkinsonism in individuals who were inadvertently exposed to 1-methyl-4-phenyl-1,2,3,6-tetrahydropyridine (MPTP), a byproduct of illicit opioid synthesis which is oxidized to the mitochondrial complex I inhibitor, 1-methyl-4-phenylpyridinium (MPP+), and taken up by the dopamine

transporter (DAT) into dopaminergic (DA) neurons[5, 6]. Since this discovery, several other agents have been identified as either PD causative or contributory environmental factors. Examples include the pesticide rotenone, which acts similarly to MPP+ by inhibiting mitochondrial complex I, and the herbicide paraquat which causes oxidative stress through the generation of superoxide radicals, excessive oxidation of nicotinamide adenine dinucleotide phosphate (NADPH), and consumption of the important antioxidant, glutathione[7, 8]. In addition, exposure to certain metals such as manganese[9] and lead[10], solvents such as trichloroethylene (TCE)[11] and organic pollutants such as polychlorinated biphenyls (PCBs)[11] have been associated with a greater risk of developing PD. In recent years, traumatic brain injury (TBI) has also been identified as a potential risk factor for the development of secondary Parkinsonism[12].

1.1.3 Genetic Risk Factors

In addition to these environmental risk factors, a group of 18 chromosomal loci (denoted PARK and known as PD-related genes) have been identified as putative genetic contributors to PD pathogenesis[13]. Although the majority (90%) of PD is sporadic in etiology, six of these genes have been unequivocally linked to heritable monogenic PD[13]. These genes and their proposed role in PD pathogenesis are described in Table 1.1. The first of these genes to be identified, SNCA (PARK1/PARK4), encoding alpha-synuclein, is the primary focus of this work and is discussed further in Section 1.2. Several polymorphic variants identified by linkage analysis,

as well as single-nucleotide polymorphisms (SNPs) identified by genome-wide association studies (GWAS), have been described as genetic risk factors for the development of PD, although not all of these have been substantiated in follow-up studies[13]. Recently, other disease-associated genes have been identified and well-validated as risk factors for PD such as the Gaucher's disease-associated gene, β-glucocerebrosidase (GBA)[14-17]. Although monogenic PD comprises less than 10% of all PD cases, much can be learned about the disease from careful investigation of these genes and particular attention to the unifying pathways on which they converge.

1.1.4 Clinical Features

The clinical features of PD were first described by James Parkinson in his 1817 article, "An Essay on the Shaking Palsy"[18]. As the title suggests, the four clinical hallmarks of PD are the primary motor symptoms including tremor, rigidity, bradykinesia/akinesia and postural instability. The primary motor symptoms of PD result from the loss of dopamine signaling in the striatum, a consequence of the selective death of DA neurons in the midbrain substantia nigra pars compacta (SNc)[19-21]. The precise reason for the selective vulnerability of midbrain DA neurons is yet to be uncovered. However, the link between the lack of dopaminergic stimulation in PD and the manifestation of these four hallmark features is elucidated by examining the role of dopamine in regulating motor circuits between the basal ganglia and the motor cortex[22]. There are two such regulatory circuits in which dopamine acts to stimulate movement: the direct pathway and the

indirect pathway[22]. Simply stated, dopamine acts through the D_1 receptor to stimulate the direct pathway and through the D_2 receptor to inhibit the indirect pathway. Since the direct pathway is excitatory and the indirect pathway is inhibitory, the net action of dopamine is to promote movement via its concerted actions to stimulate the direct (excitatory) pathway and inhibit the indirect (inhibitory) pathway. When approximately 60% of DA neurons residing in the midbrain SNc are lost, the resultant 80-85% depletion of dopamine content in the striatum manifests as the hallmark motor symptoms of PD[23, 24].

1.1.5 Current Treatments

An understanding of this critical role of dopamine in regulating movement led to the most commonly utilized therapeutic approach for PD—dopamine replacement[25-28]. However, pharmacologic replacement of dopamine is not without side effects. Most notably, long term treatment with dopamine has been shown to cause cognitive deficits[29] and behavioral disturbances[30] in PD patients. Furthermore, after a variable period of time, many patients begin to experience switching from an “on-medication” to “off-medication” state in a rapid and unpredictable manner, despite compliance with their dopamine regimen [31].

The necessity for a treatment option for patients who experience this on-off phenomenon inspired the development of deep brain stimulation (DBS)[32]. Despite its name, DBS acts to provide an inhibitory electrical

impulse to neurons neighboring the implanted electrodes, which are typically placed at the subthalamic nucleus (STN)[33-35] or globus pallidus internus (GPi)[36] for treatment of PD. DBS revolutionized the treatment of PD and provides symptomatic relief for many patients who undergo this procedure. However, no surgery is without risk, and not all patients who incur the risks associated with the surgery benefit from this approach. Additionally, the technology is still in its infancy—since DBS has been clinically available for less than a decade, the long term effects of electrode implantation and stimulation remain an active area of investigation. In a study published in 2015, investigators examined pathoanatomical changes associated with electrode implantation in PD and essential tremor (ET) patients, finding that tissue in long-term contact with electrodes exhibited astrogliosis, T-cell infiltration and multinucleated giant cells[37]. The investigators also found amyloid precursor protein-positive axonal swellings in the brain tissue surrounding the electrically active parts of the electrode. Furthermore, it is unclear whether DBS will retain the same clinical effectiveness that is often seen immediately after electrode programming with long-term treatment. Although clearly of great clinical value, neither dopamine replacement nor DBS aim to slow or reverse the underlying neurodegeneration that causes PD or to preserve remaining midbrain DA neurons.

Importantly, PD patients also experience a wide range of non-motor symptoms that are not treated by either dopamine replacement or DBS. Progressive cognitive impairment leading to dementia is one of the most

common and important non-motor symptoms of PD. An extremely high reported cumulative prevalence of 80% of PD patients suffer from comorbid dementia[1]. Although little is known about the mechanisms underlying dementia in association with PD, pathological changes due to the abnormal accumulation of alpha-synuclein protein aggregates (i.e. alpha-synucleinopathy) have been shown to be sufficient to lead to a global dementia with cortical and subcortical elements, resulting in particularly severe executive and visuospatial impairments[38]. There are currently no mechanism-based therapies available for these features of Parkinsonism, the development of which has been hindered, in part, by a lack of access to the affected brain regions in living patients. Induced pluripotent stem cells (iPSCs) provide an unprecedented ability to characterize the role of molecular mediators, such as alpha-synuclein, in the development of motor and cognitive symptoms of PD due to the demise of DA and cortical neurons, respectively – the use of iPSCs in disease modeling and therapeutic development is discussed below in Section 1.3.

1.2 Alpha-Synuclein in PD Pathogenesis

Alpha-synuclein was first identified when it was purified from the electric organ of the Pacific electric ray, *Torpedo californica*, in a screen for synaptic proteins and was so named because of its apparent localization to the synapse and nucleus[39]. Alpha-synuclein is encoded by the six exon SNCA gene located on the long arm of chromosome 4, position 4q21.3-

22[40]. Alpha-synuclein is perhaps one of the most strongly implicated mediators of PD pathogenesis of both genetic and sporadic etiology, and is the major constituent of Lewy bodies (LBs), the pathological hallmark of PD[41]. The direct contributions of alpha-synuclein at the level of the gene, transcript and protein as well as convergence with other genes and environmental contributors implicated in the etiopathogenesis of PD will be discussed in this section.

1.2.1 Point Mutations

SNCA was the first gene for which mutations were identified to cause monogenic autosomal dominant PD[13]. In 1990, Golbe et al. first described a large family with autosomal dominant Parkinsonism, diagnosed in more than 60 family members over five generations, with symptoms ranging from typical PD to diffuse LB disease and often with concomitant dementia[42]. In 1996, Polymeropoulos et al. discovered that the causative mutation in this family was a G-to-A transition at nucleotide 209 of the SNCA gene, which resulted in an alanine-to-threonine substitution at position 53 of the alpha-synuclein protein (A53T)[43, 44]. Since the discovery of the A53T mutation in this Italian kindred, the same mutation has been identified in three Greek families. It has been further demonstrated that rodents and non-human primates virally transduced to overexpress A53T alpha-synuclein develop neurodegeneration characterized by the formation of alpha-synuclein-positive inclusions[45-47]. It is worth noting, however, that a threonine residue naturally appears at position 53 in rodent

alpha-synuclein. Thus any phenotypes observed in transgenic rodent models carrying this variant are likely the result of overexpression[44, 48]. Since this raises the possibility that A53T is actually a rare normal variant in humans, it was not until alpha-synuclein was identified as the major component of LBs in sporadic PD and other forms of dementia with LBs[41], and the identification of the A30P mutation in a German family[48], that alpha-synuclein was confirmed as a causative mediator of PD. Five other pathogenic substitutions have subsequently been identified: E46K in a Spanish family[49], A18T in a male of Polish origin and A29S in a female of Polish origin[50], H50Q in a Caucasian English female[51], and G51D in a French family[52].

1.2.2 Multiplications

A set of linkage analysis studies revealed that, in addition to the point mutations which cause Parkinsonian syndromes, enhanced expression of wild-type alpha-synuclein via multiplications of the SNCA gene also causes familial Parkinsonism[53, 54]. In 2003, Singleton et al. discovered that a genomic triplication of the SNCA locus was causative of PD in a large family, known as the Iowa kindred[53]. Singleton et al. described a 1.61 – 2.04 Mb triplicated region, containing 16 additional annotated or putative triplicated genes. Some of these genes may participate in fundamental cellular processes that could further affect neuronal physiology and contribute to PD pathogenesis, including CEB1, HERC3, FAM13A1, TIG2, MMRN and KIAA1680. CEB1 is an interferon-induced E3 ubiquitin ligase

that mediates ISGylation of target proteins[55]. HERC3 is an E3 ubiquitin ligase which localizes to vesicular structures containing beta-COP, ARF, and Rab5 and has been proposed to function in vesicle trafficking[56]. FAM13A1 is a RhoGAP (Rho GTPase-activating protein) which has recently been identified as a candidate AD-associated gene in a transcriptome analysis of post-mortem brain regions from affected individuals[57]. Interestingly, some of the triplicated genes may provide insight into how the triplicated region came to exist – TIGD2, for example, is part of the Tigger subfamily of DNA transposons in humans, elements that move by excision and reintegration in the genome[58]. MMRN is a large soluble endothelial protein, which may function in extracellular matrix formation and cell adhesion[59]. KIAA1680 belongs to the KIAA family of genes, some of which have been described as mediators of neuron migration[60].

Additional families with PD caused by triplications[54, 61] as well as duplications[62] of SNCA were subsequently identified. Multiplications of SNCA can present with a wide range of clinical symptoms, including cognitive impairment and dementia[1]. Intriguingly, genomic duplication of SNCA more closely phenocopies sporadic PD than SNCA triplication, the latter of which is more severe and more often associated with prominent dementia. Much as for the A53T mutation, it has been demonstrated that overexpression of wild-type alpha-synuclein by viral transduction in rodents and non-human primates is sufficient to cause alpha-synuclein cytotoxicity and neurodegeneration[45-47]. Three important implications follow

from the observation that multiplications of SNCA cause Parkinsonism: 1) the pathologic properties of alpha-synuclein are not dependent on mutations that alter the alpha-synuclein protein product (i.e. point mutations), 2) overexpression of wild-type alpha-synuclein is sufficient to cause disease in a dose-dependent manner and 3) alpha-synuclein overexpression may be a common theme in PD whereby smaller increases in alpha-synuclein, either due to increased expression or decreased clearance, may contribute to sporadic disease[63, 64].

1.2.3 Polymorphisms and Gene Variants

Focused assessment of genes involved in monogenic forms of PD as risk factor loci has led to an increased understanding of the role common variability in these genes plays in the disease process. This is particularly notable for SNCA, for which several polymorphisms and risk variants associated with PD have been identified. A recent meta-analysis of GWAS data replicated the finding that a SNP locus, rs356182, within the SNCA gene is associated with PD susceptibility[65]. In addition to SNPs within the coding regions of the SNCA gene, several risk loci have been identified within regulatory regions of the SNCA gene and are thought to influence susceptibility to PD by altering rates of SNCA transcription. For example, Rep1 is a mixed polypurine-pyrimidine repeat within the promoter region of SNCA, approximately 10 kb upstream of the start of transcription. Rep1 has been characterized as a negative modulator of SNCA transcriptional activity and risk variants of this polymorphism have been linked to

increased alpha-synuclein levels[63, 66-69]. In addition, variants in the 3' UTR[70] of SNCA have been identified as determinants of disease risk. These polymorphisms which, similar to SNCA gene multiplications, result in increased levels of alpha-synuclein suggest that increased alpha-synuclein levels are central to the etiology of PD[63].

1.2.4 Transcript Isoforms

Among the first evidence that altered alpha-synuclein transcript levels contribute to PD pathogenesis was the observation of elevated alpha-synuclein mRNA in DA neurons microdissected from PD patients compared to age-matched controls[71, 72]. Alpha-synuclein is expressed from at least three different promoters, and alternative splicing generates four transcript isoforms. Six exons encode the full-length SNCA-140 mRNA, while three alternatively spliced variants skipping exons 3, 5 or both generate the three isoforms SNCA-126, -112 and -98, respectively[73]. To date, only the SNCA-140 and SNCA-112 transcript isoforms have translated protein correlates annotated in the National Center for Biotechnology Information (NCBI) Reference Sequence (RefSeq) database[74].

McLean et al.[73] characterized the differential expression of all SNCA transcript isoforms in PD post-mortem brain regions, and in a transgenic mouse model of alpha-synuclein overexpression. The authors found increased levels of SNCA-140 in the substantia nigra (SN) of PD patients

compared to other brain regions in PD patients and the SN of control patients. SNCA-126 was similarly elevated in the SN of PD cases compared to controls. There were no observable differences in SNCA-112 and SNCA-98 expression levels between PD cases and controls. Finally, the authors found region-specific alterations in alpha-synuclein transcript splicing in 2- vs. 15-month old alpha-synuclein overexpressing (ASO) mice. The differential expression of alpha-synuclein transcript isoforms in PD patients and animal models highlights that understanding the physiological and pathological determinants of alpha-synuclein mRNA splicing may aid in revealing the function of alpha-synuclein as well as the development of targeted therapeutic strategies.

1.2.5 Alpha-Synuclein Protein Structure, Function and Tissue Distribution

Alpha-synuclein is one of three members of the synuclein family of proteins, which is further comprised of beta-synuclein, encoded by SNCB on chromosome 5q35[75], and gamma-synuclein, encoded by SNCG on chromosome 10q23[76]. Structurally, alpha-synuclein is 140 amino acids long and consists of three domains: an N-terminal KTKEGV repeat region[39, 77, 78], a central hydrophobic non-amyloid component (NAC) region[78, 79], and an acidic C-terminal region (Figure 1.1)[80]. At low concentrations, alpha-synuclein exists in its native random coil, unfolded conformation[78, 81]. However, the N-terminal domain (residues 1 – 60) of alpha-synuclein can undergo a conformational shift from random coil to alpha-helical structure,

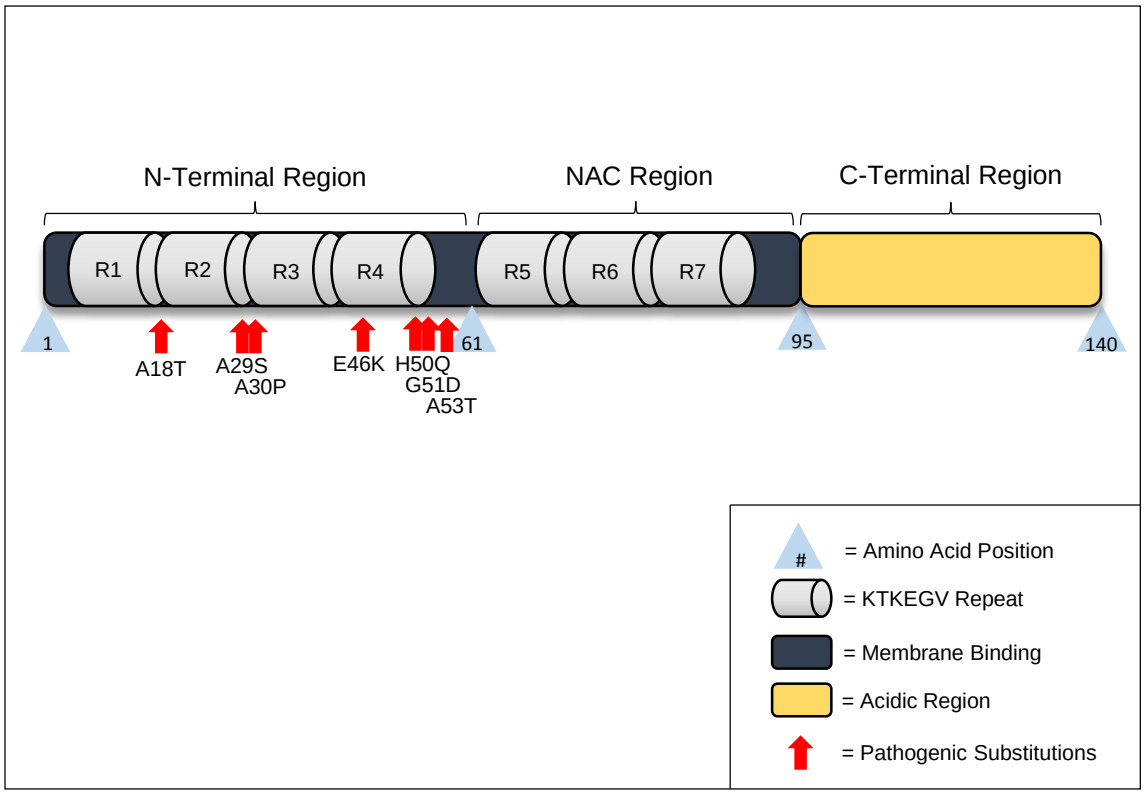

Figure 1.1 Domain Architecture of Alpha-Synuclein Protein.

Figure 1.1 Domain Architecture of Alpha-Synuclein Protein

Schematic representation of alpha-synuclein domain architecture. Alpha-synuclein has two functional domains: residues 1 – 94 represent the membrane binding region (dark blue) and residues 95 – 140 represent the acidic region (yellow). Within these two domains, there are three regions: the N-terminal region (residues 1 – 64), the NAC region (residues 65 – 94) and the C-terminal region (residues 95 – 140). The membrane binding region contains 7 KTKEGV repeats (grey cylinders), four of which occur in the N-terminal region, 3 of which occur in the NAC region. All seven currently known PD pathogenic substitutions occur within the N-terminal region (red arrows).

enabling alpha-synuclein to interact with small vesicles containing acidic phospholipids[82]. While the A53T mutation has no observable effect on this lipid binding property of alpha-synuclein, the A30P mutation disrupts, and the E46K mutation enhances the ability of alpha-synuclein to bind lipids[83, 84]. It remains to be determined if and how the more recently identified pathogenic substitutions, A18T, A29S, H50Q and G51D, affect the lipid binding properties of alpha-synuclein.

The central NAC domain (residues 61 – 94) of alpha-synuclein is a hydrophobic region that forms the beta-pleated sheet structure responsible for alpha-synuclein fibrillization, and residues 71 – 82 specifically are necessary for the aggregation of alpha-synuclein into fibrillar structures[85]. Beta-synuclein, which is highly homologous to alpha-synuclein except that it lacks a large portion of the central NAC domain[86], is not found in filamentous inclusions in PD[87] and does not form fibrils *in vitro*[87, 88]. Likewise, gamma-synuclein, which has less homology to alpha-synuclein than beta-synuclein, is not found in filamentous inclusions in PD[87]. In contrast, gamma-synuclein is capable of forming fibrils *in vitro*, albeit at a much slower rate than alpha-synuclein[88]. The C-terminal domain (residues 95 – 140) consists of a hydrophilic, glutamate-rich amino acid series[77] which is thought to inhibit alpha-synuclein fibril formation[89-91].

Increased protein concentrations are hypothesized to promote these conformational transformations leading to a partially folded intermediate

which, through a nucleation-dependent mechanism, generates alpha-synuclein oligomers and fibrils that can form more organized structures such as LBs[92-96]. In addition to their aggregation-prone state, these oligomeric and fibrillar structures are thought to have cytotoxic properties such as the ability to permeabilize membranes[97]. Complexity of alpha-synuclein aggregation and ability to form cytotoxic species could be a major factor in the progressive nature of PD[98], and underscores the importance of developing therapeutic strategies that reduce alpha-synuclein production as early as possible.

Although the precise normal function of alpha-synuclein remains unknown, several studies have implicated alpha-synuclein in the regulating various aspects of dopamine neurotransmission[99], dopamine transporter trafficking[100-102] and dopamine biosynthesis[103], as well as inhibition of phospholipases[104, 105]. Alpha-synuclein is expressed throughout the central nervous system, the highest levels being found in the olfactory bulb, cerebral cortex, striatum, and to a lesser extent, the thalamus[106]. Alpha-synuclein has also been identified in other cell types, including neurons of the cardiac plexus[107], red blood cells[108, 109], platelets[110] and T-lymphocytes[111]. Further study of alpha-synuclein function may inform insights regarding its tissue-specific and pathogenic roles. Regardless of its precise function, it is clear that overexpression and polymerization of alpha-synuclein are critical mediators of PD pathogenesis.

1.2.6 Toxins

Two co-contributors of relevance to PD have been shown to elevate native alpha-synuclein levels: toxins and aging[64]. Mice[112] and non-human primates[113, 114] stimulated with MPTP demonstrate enhanced alpha-synuclein expression as a neuronal response. Alpha-synuclein is upregulated during development, and it is thought that this serves to promote neuronal plasticity. In addition, evidence has shown that alpha-synuclein is involved in maintaining synaptic plasticity in the adult brain[115, 116]. Thus, the upregulation of alpha-synuclein in response to toxins may represent an attempt to promote plastic recovery and improve neurotransmission[64]. Severe or persistent insult may subsequently result in damage and death to neurons. Upregulation of alpha-synuclein in response to toxins is accompanied by alterations in the protein such as phosphorylation, oxidation and nitration, which may promote aggregation and result in a toxic gain-of-function. Of note, paraquat also induces a conformational protein change that accelerates the formation of alpha-synuclein fibrils[117]. These findings support the notion that environmental exposures contribute to PD by enhancing alpha-synuclein expression and promoting toxic modifications of the protein.

1.2.7 Aging

Aging is one of the strongest risk factors for PD. Several age-related changes have been described in the nigrostriatal system of healthy patients including dopamine depletion, decreased neuronal tyrosine

hydroxylase (TH) expression[118-120], loss of TH+ fibers[120, 121], distorted cell bodies[122], dendritic swelling[122] and neuromelanin accumulation[123]. These morphological alterations are accompanied by functional changes, including an increased susceptibility to toxic damage, such as that observed in response to MPTP in older vs. younger non-human primates[119]. These age-dependent changes likely contribute to the susceptibility of DA neurons to the neurodegenerative process underlying PD. Importantly, a robust age-related elevation in alpha-synuclein levels has also been described in SNc DA neurons of humans and non-human primates[124, 125]. Several important features of age-related alpha-synuclein accumulation have been uncovered including the findings that the strength of alpha-synuclein expression is negatively correlated with TH expression[125], the effect is selective to alpha-synuclein since other members of the synuclein family are unaltered by aging[124, 125], and the effect may be species-specific, since rodent alpha-synuclein levels are either stable or decline during aging[126, 127]. Many mechanisms might explain the enhanced alpha-synuclein expression observed in the aging brain. If alpha-synuclein is overexpressed in response to neuronal stress, the increased alpha-synuclein levels observed in SNc DA neurons may represent an adaptive response to the life-long burden of oxidative stress from dopamine metabolism. Alternatively, alpha-synuclein may accumulate secondary to age-related impairments in the ubiquitin-proteasome system (UPS) and autophagy protein clearance pathways, which are known to be less efficient in the aging brain[128, 129]. Age-related changes in alpha-synuclein expression may thus form the precipitating

event upon which other insults ultimately culminate in neurodegeneration in PD.

1.2.8 Therapeutic Strategies for Modulation of Alpha-Synuclein

Because of the central role of alpha-synuclein in both genetic and sporadic forms of PD, strategies to modulate its pathogenic actions may represent an important advance towards a disease-modifying therapy. There are three main approaches to the development of alpha-synuclein targeting therapeutics: 1) inhibiting its expression, 2) enhancing its clearance, and 3) inhibiting the formation of aggregated forms (Figure 1.2). RNA interference (RNAi) currently represents the best-described strategy for therapeutically inhibiting gene expression[130]. Short hairpin (shRNA) or short inhibitory (siRNAs) RNAs can be designed to target alpha-synuclein mRNA, resulting in its selective degradation[131-134]. As alpha-synuclein protein is cleared either by the UPS or autophagy, chemical enhancers of these pathways may represent a strategy to augment alpha-synuclein clearance[135]. Finally, a number of agents have been used to inhibit alpha-synuclein aggregation, including natural compounds, such as flavonoids, and small molecules[136, 137]. Very recent evidence has shown that antibodies against misfolded alpha-synuclein can also be used to inhibit its spread to neighboring cells[138]. The primary limitation to each of the above approaches is that they aim to modulate alpha-synuclein expression at stages beyond its production, thus the influence of post-transcriptional and post-translational modifications and half-life of alpha-synuclein mRNA and

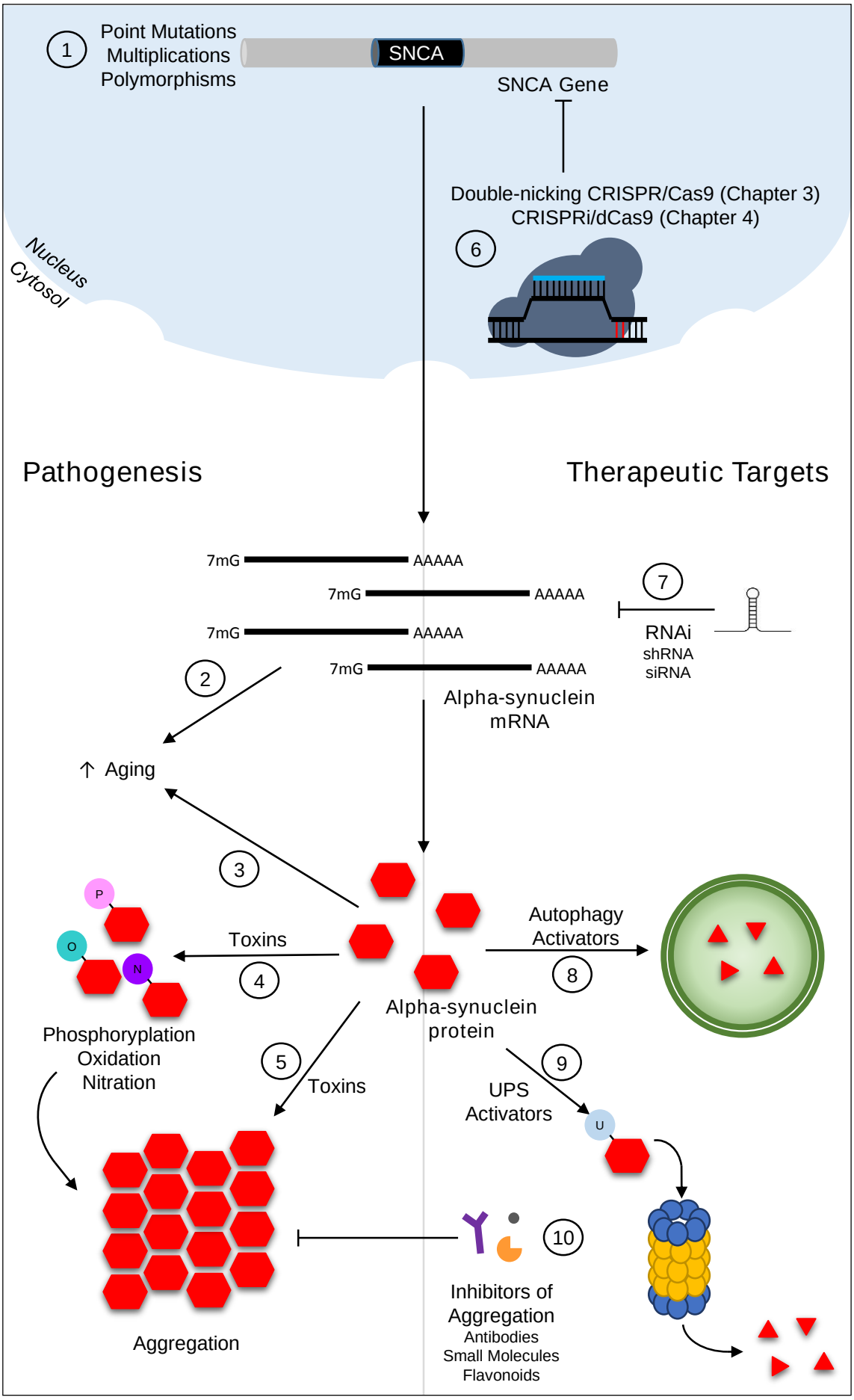

Figure 1.2 Alpha-Synuclein as a Target for Therapeutic Intervention in PD Pathogenesis

Figure 1.2 Alpha-Synuclein as a Target for Therapeutic Intervention in PD Pathogenesis

The left panel of the figure demonstrates reported mechanisms of alpha-synuclein induced neurotoxicity, including point mutations, multiplications and polymorphisms at the level of the SNCA gene (1), increased alpha-synuclein mRNA (2) and protein (3) levels due to aging, toxin-induced phosphorylation, oxidation and nitration of alpha-synuclein (4) which promote protein aggregation, and alpha-synuclein aggregation directly induced by toxin exposure (5). The right panel of the figure represents methods for therapeutic modulation of alpha-synuclein, including RNAi-mediated silencing of alpha-synuclein mRNA (7), chemical activation of autophagy (8) and ubiquitin-proteasome system (UPS) (9) protein clearance pathways and the use of antibodies, small molecules and flavonoids to inhibit alpha-synuclein aggregation (10). Notably, CRISPR/Cas9-based methods for modulation of alpha-synuclein expression presented in this work act at the level of the SNCA gene (6), an earlier time-point in the production of alpha-synuclein than any other currently available alpha-synuclein-targeting therapeutic strategies.

protein must be controlled in order to effect a clinical outcome. Two alternative strategies for altering alpha-synuclein gene expression are presented in this work, both of which act prior to the formation of functional alpha-synuclein transcript or protein by directly targeting the SNCA gene (Chapters 3 and 4).

For many neurodegenerative diseases, the therapeutic benefits observed in humans are diminished or in some cases, opposite, to what is observed in pre-clinical animal models, resulting in the failure of many promising neurodegenerative disease therapies in early stage clinical trials. The use of human, patient-specific pre-clinical models of neurodegenerative diseases could greatly enhance the screening of novel therapeutic strategies for these conditions.

1.3 iPSC Models of PD

Since their discovery by Kazutoshi Takahashi and Shinya Yamanaka in 2006[139], iPSCs have been well recognized for their potential applications in regenerative medicine and disease modeling. Pivotal studies in stem cell research leading to the discovery of iPSCs are briefly reviewed here, followed by a discussion of the application of iPSCs to the study of PD cellular and molecular pathogenesis and the development of cell replacement therapy.

1.3.1 Human Embryonic Stem Cells

The derivation of mouse embryonic stem cells (mESCs) was first described in 198[140, 141]. Approximately 17 years later, the conditions necessary for maintaining human embryonic stem cells (hESCs) in culture were described by James Thomson[142]. hESC lines are developed by subcultivation of the inner cell mass of pre-implantation blastocysts, produced by *in vitro* fertilization (IVF). Although several attempts were made to culture hESCs as early as the 1980s, the medium for cultivating IVF embryos was suboptimal. In addition, species-specific differences between mice and humans prevented direct application of techniques for mESC culture to hESCs. It wasn't until the 1990s, when experience with culture of non-human primate embryonic stem cells[143, 144] led to improvements in the culture conditions for human IVF-derived embryos and allowed the development of a method for long-term hESC culture. Although the potential for hESCs in biomedical research was tremendous, the derivation of these cells from human IVF-derived embryos raised a number of ethical and legal concerns that culminated in the implementation of policies to halt the production of new hESC lines in the US in 2001. This is among many reasons for the rapid implementation of iPSCs upon their discovery in 2006.

1.3.2 Human iPSCs

iPSCs are adult somatic cells which have been reprogrammed to a pluripotent state using defined genetic or chemical factors. Much as

mESCs were sustainable in the laboratory before hESCs, the first iPSCs were reprogrammed from mouse embryonic fibroblasts (MEFs)[139]. In a screen of 24 candidate genes, selected based on their known links to embryonic stem cell pluripotency, Takahashi and Yamanaka found four factors that were sufficient to reprogram somatic cells: Oct4, Sox2, Klf4 and c-Myc[139]. Much more rapidly than for embryonic stem cells, this system was adapted to human cells[145, 146]. The development of human iPSCs was a long sought after discovery, which opened novel avenues for biomedical research and regenerative medicine. Human iPSCs can be derived from patients with specific diseases, allowing investigators to define molecular phenotypes and probe the mechanisms underlying pathogenesis for diseases in which the relevant cell type is inaccessible in patients. The first studies to demonstrate the value of iPSCs in disease modeling verified that disease-specific phenotypes can be observed in disease-relevant differentiated cells from patients with familial dysautonomia[147] and spinal muscular atrophy (SMA)[148]. In addition, human iPSCs offer the unique opportunity for the development of gene therapy coupled with autologous cell replacement for the treatment of degenerative conditions[149]. Indeed the first iPSC-based clinical trial began in September 2014, an attempt to transplant autologous iPSC-derived retinal pigment epithelium for treatment of macular degeneration. Advancements in culture techniques have led to the development of feeder-free and xeno-free culture systems for iPSCs[150], eliminating concerns about contaminating human iPSCs with mouse-derived feeder cells, macromolecules and viruses, and enhancing the potential of these cells in biomedical research and therapeutic

development. The utility of iPSCs in the study of disease and development of cell replacement therapy is contingent upon the ability to derive relevant cell types from them – methods to derive neural cell populations for PD research are discussed below.

1.3.3 Neural Differentiation of iPSCs

Many of the principles that had been developed from prior work on directed differentiation of hESCs were applied and optimized to develop protocols for the derivation of neural cell populations from human iPSCs. In general, the *in vitro* differentiation of neural cell types from stem cells follows the same pattern as *in vivo* derivation of neural cell types during development[151, 152], progressing through 1) neural induction and multipotent progenitor formation, 2) neural cell type specification (known as patterning in development) and 3) maturation (Figure 1.3). Similar to hESCs[153, 154], iPSCs were initially differentiated into neural cell types using mouse-derived stromal cells as a growth substrate[147] or via a pluripotent embryoid body (EB) stage[155]. Neural induction of EBs is prompted by the application of the growth factors, noggin and FGF2, which stimulate the generation of multipotent neural stem cells (NSCs) by inhibiting BMP signaling and promoting self-renewal, respectively[156]. The resultant spheroids are known as neurospheres. Seeding neurospheres on a growth matrix, such as Geltrex, promotes the expansion of NSCs in a characteristic neural rosette formation[157] which mimics the formation of the neural tube during development[152]. Neural rosettes can be manually isolated, and an

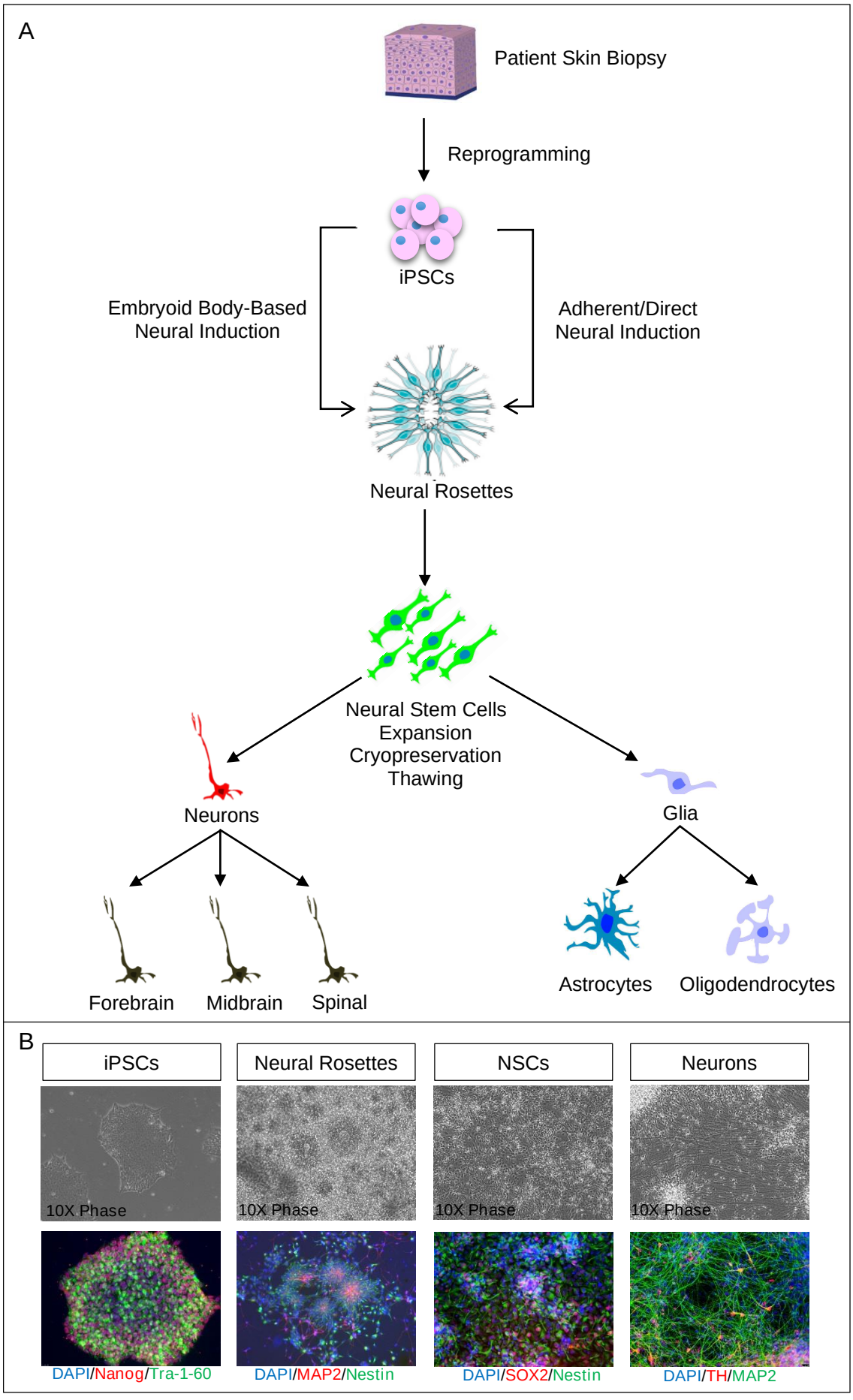

Figure 1.3 Differentiation of Neural Derivatives from iPSCs

Figure 1.3 Differentiation of Neural Derivatives from iPSCs

A) Schematic representation of iPSC differentiation into neural derivatives, demonstrating the key stages of reprogramming, neural induction, propagation of a neural stem cell population and terminal differentiation into neuronal and glial subtypes.

B) Representative images of iPSCs, neural rosettes, neural stem cells (NSCs), and terminally differentiated neurons from experiments performed throughout thesis studies. Phase images taken under 10x magnification are shown in the top panels. Immunostaining for stage-specific markers is shown in the bottom panels, including for Nanog and Tra-1-60 for iPSCs, MAP2 and Nestin for neural rosettes, SOX2 and Nestin for neural stem cells, and TH and MAP2 for neurons.

expandable NSC population devoid of contaminating alternate lineage cell types can be acquired by sequential suspension culture, seeding and manual isolation[157], or sorting with NSC-specific markers[158]. These populations of NSCs are self-renewing and will proliferate in culture for approximately 50 passages. Alternatively, iPSC-derived neural rosettes can be directly differentiated into neurons, astrocytes or oligodendrocytes, without deriving an expandable intermediate NSC population. A major advance in the induction of neural cell types from iPSCs was the development of an adherent culture method for deriving neural rosettes. This procedure is known as dual SMAD inhibition and involves the use of Noggin and SB431542, a small molecule inhibitor of SMAD signaling, to promote neural induction of iPSCs[159]. Importantly, this method involves a feeder-free culture system and bypasses the EB stage, thereby obviating two sources of variability in protocols for differentiating iPSC-derived NSCs[159]. Similar to EB-derived NSCs, rosettes derived from adherent culture dual SMAD inhibition can be manually isolated for expansion or directly differentiated into neuronal cell types.

A great deal of effort has been devoted to deriving specific neuronal subpopulations from iPSCs and iPSC-derived NSCs. Although protocols for such directed differentiations have significantly improved, it remains challenging to derive a homogenous population of one neuronal subtype from iPSCs or iPSC-derived NSCs. The primary cell type of interest to those investigating PD has long been the A9 midbrain DA (mDA) neuron, the most vulnerable neuronal subpopulation in PD, which is well described

to degenerate and is often absent or sparse in post-mortem samples from PD patients. Many efforts to derive A9 mDA neurons from iPSCs have been reported, generally converging on a sequential exposure of NSCs to the midbrain-specifying growth factors, FGF8 and SHH, the neuronal maturation growth factors, BDNF and GDNF and the antioxidant, ascorbic acid to aid the survival of dopamine-producing neurons which are prone to oxidative stress from dopamine metabolism[159, 160]. Again, these protocols progressed from the differentiation of hESCs on PA6 mDA-promoting mouse stromal cells, which drove the differentiation of DA neurons through variable release of growth factors[161], to xeno-free and feeder-free chemically defined protocols[157, 159]. As cortical neuron degeneration is the closest pathological correlate to cognitive decline, a more recent effort to evaluate the source of cognitive deficits experienced by 80% of PD patients has led to an effort to derive cortical neurons from patient-specific iPSCs[162, 163]. Still other neural cell types such as astrocytes[164], and oligodendrocytes [165] can be derived from iPSCs and may be useful in examining PD-relevant phenotypes, such as intercellular propagation of alpha-synuclein, and in elucidating the mechanism by which alpha-synuclein exerts distinct cell-specific pathological outcomes in PD compared to other synucleinopathies.

1.3.4 Applications of iPSC-Derived Neurons in Cell Replacement Therapy and Investigations of PD Cellular and Molecular Pathogenesis

Since the discovery that nigrostriatal dopamine depletion secondary to SNc DA neuron degeneration is the primary pathogenic event in PD, investigators have sought a means of therapeutically replacing dopamine. As discussed above (Section 1.1.5), pharmacologic replacement of dopamine can provide symptomatic relief, but is not without consequence. Grafting of dopamine-producing cells has long been acknowledged as a potentially long-lasting, focal treatment for PD[166]. Several sources for cell replacement therapy have been evaluated prior to the discovery of iPSCs, including fetal tissue grafts[167, 168], hESCs[169, 170], NSCs[171, 172] and mesenchymal stem cells (MSCs)[173, 174]. More recently, efforts to evaluate the efficacy of autologous iPSC-derived DA neuron grafts have advanced from studies in rodents[175] to those in non-human primates[176-178]. The primary advantages of such iPSC-derived graft sources are that 1) the proliferative capacity of iPSCs make them a renewable graft source and 2) iPSC-derived grafts would allow autologous transplantation, circumventing complications associated with immune rejection. However, iPSC-derived DA neuron grafts are not without their own set of limitations, chief among them the tumorigenic potential of residual transplanted iPSCs. It is possible that methods to generate iPSCs without the use of tumorigenic pluripotency factors like c-Myc[179], to excise other potentially tumorigenic pluripotency genes after reprogramming[180], to improve protocols for differentiating

iPSCs into DA neurons[170], and to optimize protocols for direct conversion of fibroblasts into DA neurons[181] may obviate these problems in the future.

iPSCs have now also been used in a number of studies that have yielded important insights into the mechanisms of monogenic PD-related genes in the pathogenesis of PD – the findings from these studies are summarized in Table 1.1. Although iPSCs have been shown to be important for elucidating PD-relevant phenotypes that could not have been gleaned from previous models, there are a number of limitations to using iPSCs for disease modeling. Foremost among these is that when comparing iPSC derivatives of healthy controls to those of PD patients, there exists an inherent difference in the genetic background. Such studies can be further complicated by variability between iPSC lines derived from the same individual. Perhaps one of the most important developments in the use of iPSCs as a disease model for PD was the development of isogenic control iPSCs. A set of elegant papers demonstrated the utility of this approach[163, 182], using site-specific nucleases to introduce the alpha-synuclein A53T PD-associated mutation to healthy control cells, and conversely to allow the insertion of a transgene to correct the same mutation in iPSCs derived from a PD patient who carried this mutation. This process is known as genome engineering. Genome engineering in human iPSCs is notoriously time consuming, laborious and costly. However, recent advances in genome engineering have revolutionized such efforts in mammalian systems, opening novel opportunities to control for genetic variability in

studies of complex diseases and to transcriptionally modulate the expression of disease-relevant genes.

1.4 Genome Engineering

Genome engineering refers to the process of making targeted modifications to the genome, its contexts (i.e. epigenetic marks), or its outputs (i.e. transcripts)[183]. Among the first breakthroughs in genome engineering was the discovery of the ability to make highly precise alterations to the genome via the incorporation of exogenous templates during homologous recombination[184]. However a major limitation of this approach is the infrequency with which the intended recombination events occur. The introduction of double strand breaks (DSBs) at the intended site of integration greatly enhances the frequency with which successful integration occurs via a process known as homology directed repair (HDR)[185-190]. Furthermore, in the absence of an HDR template, DSBs are repaired by the endogenous, non-homologous end joining (NHEJ) pathway, which is somewhat error-prone and therefore can generate insertion and deletion (indel) mutations at the cut site[191]. Thus, the ability to design nucleases to generate DSBs at a desired genomic site greatly enhances the efficiency and precision of HDR- and NHEJ-mediated genome editing.

1.4.1 Programmable Nucleases

Four major classes of programmable nucleases have been engineered to introduce site-specific DSBs: 1) meganucleases[192], 2) zinc finger nucleases (ZFNs)[193, 194], 3) transcription activator-like effector nucleases (TALENs)[195-198] and 4) the RNA-guided DNA endonuclease, CRISPR (clustered regularly interspaced short palindromic repeat)/Cas9 (CRISPR-associated protein 9), from the type II bacterial adaptive immune system[199, 200]. Meganucleases, ZFNs and TALENs all require labor intensive construction and extensive screening for functionality. For meganucleases, this is because there is no clear DNA target of specific protein residues. ZFNs, although more modular in their design, may exhibit context-dependent specificity making it difficult to predict their target sites in DNA, and resulting in a necessity to screen for paired combinations that bind and cleave efficiently at a desired target sequence[201]. TALENs are more predictable: one 34 amino acid module binds to one base, and each arm in a pair of TALENs is essentially independent of the other (i.e. not as affected by context-dependent effects), unlike ZFNs. TALENs are, however, difficult to assemble since there is a requirement for 18-20 highly repetitive sequences in a particular order (although some very elegant cloning strategies have been developed). Importantly, meganucleases, ZFNs and TALENs all function through protein-DNA recognition, whereas Cas9 uses guide RNAs (gRNAs) to recognize target DNA via Watson-Crick base pairing. This greatly enhances the utility of the CRISPR/Cas9 system for multiplex genome modifications via the delivery of a single

effector protein (Cas9) and libraries of gRNAs, as opposed to the introduction of multiple target-specific proteins.

1.4.2 CRISPR/Cas9

In bacteria, CRISPR loci consist of a set of CRISPR-associated (Cas) genes and a series of repeat sequences, interspaced by variable sequences corresponding to foreign genetic elements (CRISPR arrays)[183]. This system serves as an adaptive immune system, wherein CRISPR arrays are transcribed and endonucleolytically processed into small CRISPR RNAs (crRNAs)[202]. These hybridize to noncoding trans-activating crRNA (tracrRNA) to guide Cas9 to target sequences[203] and cause cleavage of the DNA[204, 205] adjacent to a protospacer adjacent motif (PAM)[206]. This led to the recognition that three components are essential for reconstituting the type II CRISPR nuclease system as a tool for genome engineering: Cas9, mature crRNA and tracrRNA. It was later discovered that crRNA and tracrRNA can be fused to generate a single guide RNA (sgRNA) that encodes Cas9 target sequence specificity[204].

There are three types of CRISPR systems: types I, II and III[207, 208]. Cas9 is exclusively associated with the type II CRISPR system, which is further subcategorized into type IIA, IIB and IIC based on structural diversity of the associated Cas9 genes[209, 210]. Specifically, type IIC CRISPR systems contain a minimal set of Cas genes, including Cas9, Cas1 and Cas2, whereas type IIA and IIB also contain Csn2 and Cas4 genes,

respectively[210]. Structurally, Cas9 proteins are characterized by a domain architecture including an alpha-helical recognition (REC) lobe, a nuclease (NUC) lobe comprised of the HNH and RuvC nuclease domains and a PAM-interacting (PI) C-terminal domain[211]. Cas9 proteins exhibit structural diversity regardless of their subtype classification, conferred largely by length differences in the REC domain[183]. Importantly, the variable conservation of this domain has presented a promising approach for minimizing Cas9 size via the generation of Cas9 mutants with recombined, truncated or eliminated REC2 domains (mutants lacking REC2 retain approximately 50% cleavage activity)[211]. This enhances the applications of the CRISPR system to models requiring delivery by highly tropic viruses with low packaging limits, such as AAV. Although *Streptococcus pyogenes* Cas9 (SpCas9) has been the most widely applied in genome editing efforts to date, smaller Cas variants from different species, such as *Staphylococcus aureus* Cas9 (SaCas9)[212] and *Acidaminococcus* and *Lachnospiraceae* Cpf1[213], may similarly aid packaging into small viruses.

The PAM serves as the DNA target search mechanism for Cas9[183]. The commonly utilized *Streptococcus pyogenes* Cas9 (SpCas9), can recognize target DNA sequences flanked primarily by 5'-NGG[199, 214], and to some extent 5'-NAG[214, 215]. The PAM initiates the transition of Cas9 from binding to cleavage conformations, and the formation of the RNA-DNA heteroduplex, even prior to the recognition of guide-sequence complementarity[216]. The recognized PAM is specific to each Cas9 species and ortholog[183]. This has two primary implications: 1) delivery of different Cas9 proteins with different PAM requirements can serve as a strategy to

differentially regulate gene activity at different target sites and 2) the targeting range of a particular Cas9 can be modified by rational design[217] and/or orthogonal replacement of the PI domain[183].

1.4.3 CRISPR/Cas9 as a Tool for Mammalian Genome Editing

In 2013, the CRISPR/Cas9 system was used for the first time to conduct genome editing in mammalian cells, revolutionizing genome editing for biomedical applications[199, 200]. The comparative ease of design, relative cost-effectiveness, and robustness of targeted DSB induction conferred by the CRISPR/Cas9 system has made it an attractive and rapidly adapted tool for genome editing in eukaryotic systems. The minimal requirement of a PAM immediately downstream of selected target sites is both advantageous and problematic in CRISPR/Cas9 gene editing applications. Although this feature significantly simplifies the design of gene targeting tools, off-target modifications are a great concern particularly for clinical applications such as gene therapy, in which permanent modifications are made to the genome. The specificity of target recognition has been enhanced by the generation of Cas9 nickases with point mutations in either the RuvC (D10A) or HNH (H840A) nuclease domains[204, 205, 218]. In contrast to wild-type Cas9 which directs DSBs through the use of both nuclease domains, individual Cas9 nickases generate single-strand breaks (SSBs), which are rapidly repaired by the high-fidelity base excision repair (BER) pathway[219]. The use of two appropriately spaced sgRNAs on opposing DNA strands with SpCas9 HNH^{+}/$RuvC^{-}$

(D10A) or SpCas9 HNH$^-$/RuvC$^+$(H840A) doubles the number of nucleotides required to be recognized for DSBs to occur and necessitates specific orientation and spacing of the two sites[220, 221]. This system can thus improve specificity by up to 1,500 times compared to wild-type Cas9 without compromising cleavage activity[220]. **In Chapter 3, I will describe the use of the double-nicking CRISPR/Cas9 system to mediate mutagenesis of two copies of SNCA in PD patient-derived iPSCs harboring a triplication of the SNCA gene locus, with the objective of generating an isogenic iPSC line with normalized alpha-synuclein expression for future detailed characterization.**

1.4.4 CRISPR/Cas9 as a Tool for Transcriptional Modulation in Mammalian Systems

Abolishing the endonuclease activity of both HNH and RuvC domains (SpCas9 HNH$^-$/RuvC$^-$, H840A and D10A) generates a nuclease null or dead Cas9 (dCas9), which can be used as an RNA-guided DNA binding protein[222]. In addition, dCas9 can be fused to transcriptional activators to induce gene expression. Recently, dCas9 has also been coupled to epigenetic modifiers to study the effects of epigenome modifications at specific chromosomal loci. Furthermore, this approach has been used to repress transcription either by DNA binding alone, or by coupling to transcriptional repressor domains, a method known as CRISPR interference (CRISPRi). These dCas9 applications are reviewed in depth in Chapter 6. **In Chapter 4, I explore the utility of CRISPRi for robust**

silencing of alpha-synuclein, among other genes which cause proteinopathy-related neurodegeneration, and define mechanistic determinants of dCas9-sgRNA/target DNA interactions for efficient gene repression by CRISPRi.

1.5 Endoplasmic Reticulum Stress and the Unfolded Protein Response in PD Pathogenesis

Endoplasmic reticulum (ER) stress-induced activation of the unfolded protein response (UPR) has gained increasing attention as a pathogenic mediator of proteinopathy-related neurodegenerative diseases, including PD. In this work, the influence of overabundant alpha-synuclein on ER stress and UPR activation will be explored. The physiological and pathological roles of the ER and the UPR in normal and disease states are first reviewed here.

1.5.1 Physiological Functions of the ER

The ER is composed of a membranous sheet, comprising more than half of the total membranes in eukaryotic cells and enclosing a single internal space, known as the ER cisternal space or ER lumen. The ER can be subdivided into two compartments: the rough ER (so named because it is studded with ribosomes) and the smooth ER. The ER plays central roles in lipid biogenesis, protein synthesis, and maintenance of cellular proteostasis, as discussed below (the primary reference for this section is

Alberts B, Johnson A, Lewis J, et al. Molecular Biology of the Cell. 4th edition. 2002.).

1.5.1.1 The ER in Lipid Biogenesis

The ER membrane synthesizes nearly all of the major classes of lipids required for the biogenesis of new cell membranes, including phospholipids and cholesterol. Whereas cholesterol is synthesized in the ER lumen, phospholipid synthesis occurs exclusively on the cytosolic side of the ER membrane. A phospholipid translocator, known as scramblase, mediates the flipping of newly synthesized phospholipids from the ER cytosolic domain to the ER luminal domain to promote equilibration of the membrane. In addition to producing phospholipids and cholesterol, the ER also generates ceramide, the precursor for glycosphingolipids and sphingomyelin, essential building blocks of the myelin sheath that insulates neuronal axons. The ER forms a continuous network with the Golgi apparatus, endosomes, lysosomes and plasma membrane, with which it communicates via the exchange of vesicles, transporting lipids and proteins. The maintenance of membrane integrity of these organelles is dependent on the transport of newly synthesized phospholipids from the ER. In contrast, mitochondria and peroxisomes are spatially distinct from this communication system and thus require the use of water-soluble carriers, known as phospholipid transfer proteins, to obtain phospholipids made at the ER. Since these proteins act to distribute phospholipids randomly, a net transport of lipids from lipid-rich (ER) to lipid-poor

(mitochondria and peroxisomes) membranes is thought to be sufficient for maintenance of mitochondrial and peroxisomal membranes.

1.5.1.2 The ER in Protein Synthesis

Both luminal and transmembrane proteins containing an ER signal sequence are directed, with ribosome bound, to the surface of the ER membrane. The ER signal sequence is recognized by a signal recognition particle (SRP), a six subunit protein complexed with one small RNA, which cycles between the cytosol and the ER and binds to the SRP receptor in the ER membrane. Binding to the SRP receptor brings the SRP-ribosome complex to a protein translocator, at which time the SRP and SRP receptor are released and the growing polypeptide chain is transferred across the ER membrane. This translocator is known as the Sec61 complex, and consists of three protein domains, each composed of three transmembrane protein subunits that assemble to form a pore structure in the ER membrane. The ER signal sequence is recognized again by a binding site in the translocator which may help to ensure that only ER-destined proteins enter the lumen. Protein translocation typically occurs as a co-translational process, however some proteins are imported into the ER lumen post-translationally with the help of accessory proteins. In eukaryotes the accessory proteins that associate with the Sec61 complex and mediate this process are Sec62, Sec63, Sec71, and Sec72. Proteins that are translocated post-translationally also require binding by chaperone proteins in the cytosol to prevent premature folding.

Transmembrane proteins contain multiple ER signal sequences that occur throughout the polypeptide chain and lack an adjacent signal peptidase recognition site. In contrast, soluble proteins have only one N-terminal ER signal sequence which is cleaved on the luminal side of the ER membrane by a signal peptidase following synthesis.

Many of the soluble proteins synthesized in the ER are *en route* to other destinations. However, many are ER resident proteins, directed to remain within the ER lumen by a four-amino-acid-long C-terminal ER retention signal. In certain cell types (i.e. secretory cells) and under cellular stress conditions, ER proteins may exist at high concentrations within the ER lumen. As high protein concentrations may result in molecular crowding, a prerequisite for protein misfolding and aggregation, the function of many ER resident proteins is to assist in the proper folding and assembly of proteins that are synthesized or translocated there. For example, protein disulfide isomerase (PDI) is an ER resident enzyme that catalyzes the formation of disulfide bonds from free sulfhydryl groups, thereby aiding protein folding. The ER resident binding protein, 78 kDa glucose regulated protein (GRP78)/binding immunoglobulin protein (BiP), recognizes incorrectly folded proteins and subunits that have not yet assembled by binding to exposed amino acid sequences that would normally be found at the interior of correctly folded or assembled proteins. BiP is an ATPase that acts as a molecular timer by regulating binding and release of unassembled protein subunits, preventing them from aggregating and retaining them in the ER to allow time for assembly and folding to occur[223].

When the presence of misfolded proteins in the ER exceeds its protein-folding capacity, BiP serves a critical role in mediating activation of the unfolded protein response (UPR) (Figure 1.4).

1.5.2 The UPR

The UPR is an evolutionarily conserved pathway that aims to restore ER homeostasis and directs the cell to undergo apoptosis when ER stress is unresolvable. Activation of the UPR is controlled by three master regulators: inositol-requiring enzyme 1a (IRE1a), eukaryotic translation initiation factor 2 alpha kinase 3 (EIF2AK3, more commonly known as PERK) and activating transcription factor 6 (ATF6). Each of these master regulators is an ER transmembrane protein with a luminal domain that is capable of directly or indirectly sensing misfolded proteins. In direct sensing, misfolded proteins act as ligands to trigger activation of the UPR master regulators[224, 225]. BiP is thought to inhibit activation of the UPR master regulators under physiologic conditions[226]. In indirect sensing, BiP-mediated inhibition of the UPR master regulators is alleviated as BiP dissociates from the UPR master regulators to bind accumulated misfolded proteins, for which it has a higher affinity[226]. The outputs of all of the master regulators first attempt to restore protein-folding capacity to the ER by promoting ER biogenesis and upregulating the transcription of protein-folding chaperones and ER-associated protein degradation (ERAD) enzymes. Despite this commonality, each arm of the UPR is activated uniquely and has a distinct set of targets.

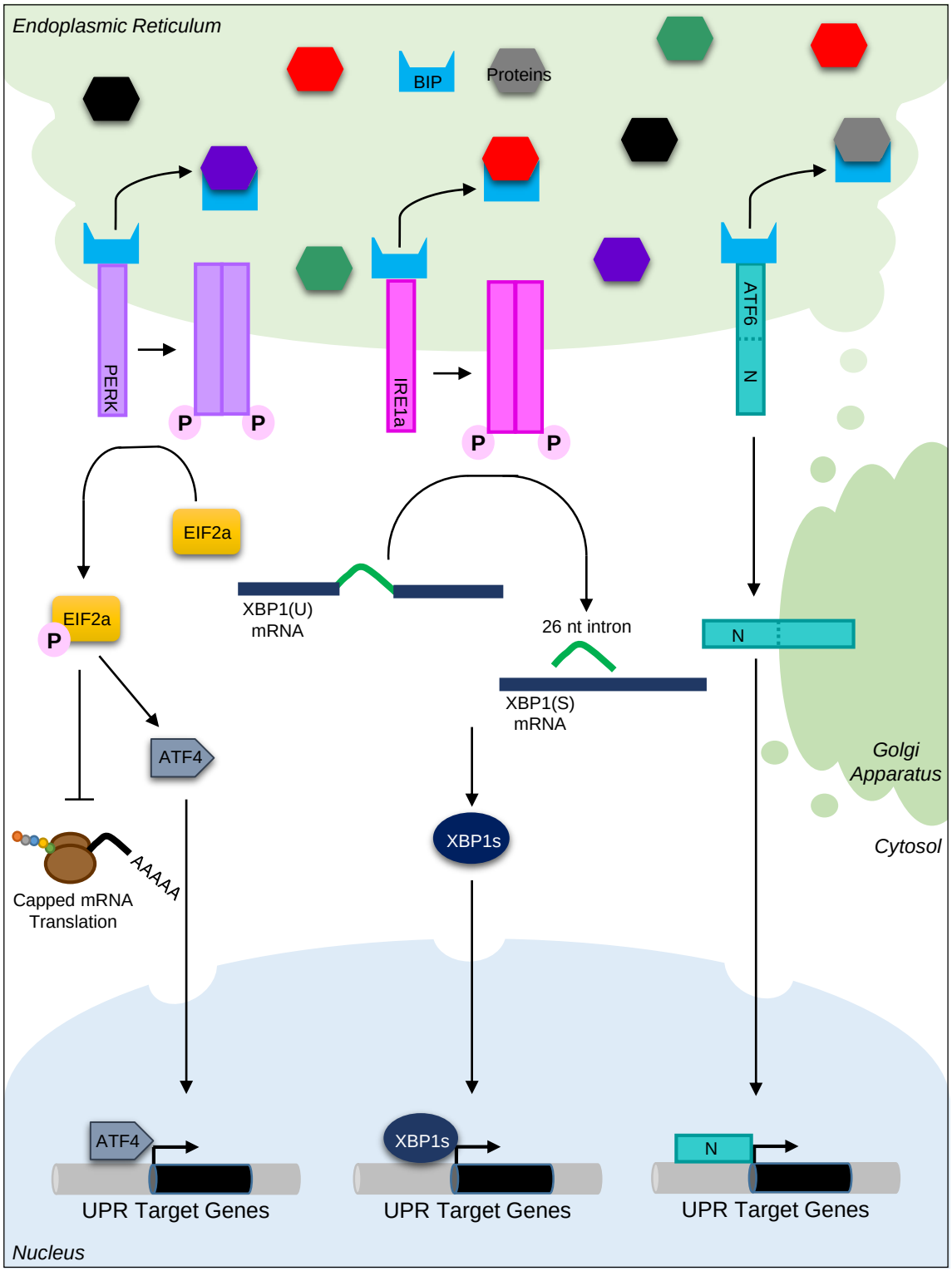

Figure 1.4 The Unfolded Protein Response

Figure 1.4 The Unfolded Protein Response

Conditions that promote an overload of misfolded proteins at the ER stimulate the UPR pathway. BiP dissociates from the UPR master regulators to bind unfolded proteins, for which it has a higher affinity. This alleviates the repression of the UPR master regulators, PERK, IRE1a and ATF6. Upon activation, PERK mediates the phosphorylation of EIF2a, resulting in a general attenuation of protein translation and selective translation of ATF4 protein, which translocates the nucleus to activate UPR target genes. Activated IRE1a mediates the excision of a 26 nt intron from XBP1 mRNA, forming XBP1(S) mRNA which can be translated into the functional XBP1s transcription factor that acts in concert with ATF4 to restore ER homeostasis. ATF6 activation requires transit to the Golgi apparatus where it is cleaved by site1 and site 2 proteases, releasing its cytosolic domain for translocation to the nucleus where it aids the effort to restore ER proteostasis.

IRE1a is the most conserved of the three UPR master regulators and is the only ER stress sensor in yeast[227]. IRE1a has two activities: 1) a serine-threonine kinase domain and 2) an endoribonuclease (RNase) domain[228, 229]. Under conditions of ER stress, IRE1a's serine-threonine kinase activity trans-autophosphorylates and activates the RNase domain[230], which specifically cleaves a 26 nucleotide intron from x-box binding protein 1 (XBP1). Splicing of XBP1's exons allows its translation into the functional XBP1s transcription factor[231, 232]. XBP1s then translocates to the nucleus where it activates the transcription of ER chaperones and ERAD enzymes in an attempt to restore ER homeostasis[233]. IRE1a also signals to the cytosol by binding adapter proteins, triggering activation of alarm pathways through ASK1/JNK and NF-kB, leading to autophagy, apoptosis and inflammatory responses[234]. IRE1a can also degrade mRNA encoding proteins that are predicted to be difficult to fold[235]. PERK is a serine kinase which phosphorylates eukaryotic translation initiation factor 2 alpha (EIF2a) when activated[236, 237]. Phosphorylation of EIF2a inhibits its activity, leading to a general attenuation of protein translation, and allowing the cell time to deal with the burden of misfolded proteins before producing more[238]. Specifically, PERK phosphorylates the serine 51 residue of EIF2a, which depletes the EIF2a-GTP-Met-tRNA complex that is required for initiation of cap-dependent mRNA translation[239]. Phosphorylation of EIF2a allows the selective translation of ATF4, whose targets act in concert with XBP1s targets to rescue ER stress. In the presence of ER stress, ATF6 transits to the Golgi apparatus, where it is cleaved by Site-1 and Site-2 proteases to release its transcription factor domain, ATF6(N)[240]. ATF6(N)

translocates to the nucleus and acts in concert with XBP1s and ATF4 to produce ER chaperones and ERAD enzymes in an attempt to rescue ER stress.

If ER stress is chronic or irreparable, the UPR can transform into an alternate signaling platform that destroys the cell: the terminal UPR[239]. Although the molecular details of the terminal UPR remain under active investigation, it is apparent that each arm of the UPR can ultimately lead to the activation of pro-apoptotic outputs in the presence of irremediable ER stress. The IRE1a target, XBP1s, can activate transcription of the terminal UPR effector, CHOP, which transcribes pro-apoptotic BIM and inhibits anti-apoptotic BCL-2[241]. In addition, IRE1a can form high-order oligomers with affinity for targets other than XBP1, leading to the degradation of mRNAs that produce ER chaperones and ERAD enzymes, thereby worsening the burden of ER stress[242, 243]. In addition, regulated IRE1a-mediated decay (RIDD) destroys non-coding RNAs such as miR-17 which normally inhibits the expression of the pro-death genes, caspase-2 and TXNIP[244, 245]. This de-repression of caspase-2 and TXNIP commits the cell to death by apoptosis and inflammasome activation, respectively[244]. In addition, sustained EIF2a-mediated inhibition of translation is incompatible with cell survival, and long-term activation of PERK can lead to direct activation of CHOP to encourage cell death[239]. ATF6 is thought to have pro-apoptotic activity under conditions of chronic ER stress, but the molecular details of ATF6-mediated cell death remain to be elucidated.

The pro-apoptotic activity of the terminal UPR is thought to converge on the activation of four BH3-only proteins: BIM, BID, NOXA and PUMA[246-248]. The BH3-only proteins are a family of pro-apoptotic proteins containing a short alpha-helix domain necessary for their killing activity[249]. When activated, they disable anti-apoptotic proteins and trigger mitochondrial permeabilization by recruitment of BAX and BAK, components of the mitochondrial outer membrane pore (MOMP)[250]. The formation of the MOMP allows the release of cytochrome c into the cytosol, and the ensuing apoptotic cascade that ends in cell death[250]. ER stress-induced cytotoxicity and cell death have been implicated in numerous and varied disease conditions – some examples follow.

1.5.3 Non-Neurological Diseases Affected by ER Stress and UPR Activation

1.5.3.1 Diabetes Mellitus

Pancreatic beta cells contain a highly developed ER to accommodate the high demand for insulin processing and secretion. Under healthy conditions, beta cells serve a critical role in maintaining normoglycemia by enhancing insulin secretion in post-prandial and fasted states, until the levels of blood glucose normalize, at which time the stimulus for insulin release is attenuated. The ER of beta cells is responsible for processing the insulin precursor, preproinsulin to proinsulin by the formation of three intramolecular disulfide bonds that promoting its folding[251]. Proinsulin is then further processed in the Golgi apparatus by the removal of C-peptide,

forming functional insulin that can be packaged into secretory granules for stimulus-induced release[251]. Diabetes mellitus (DM) results when there is an insufficient mass of beta cells to produce the required amount of insulin in fasted and post-prandial states to maintain normoglycemia.

There are several examples of mouse models and human genetic diseases for which evidence suggests that ER stress may be a crucial factor promoting DM onset and progression. The Akita diabetic mouse expresses a proinsulin variant, Ins2 (C96Y), which lacks one of the cysteines necessary to form one of the intramolecular disulfide bonds of properly folded insulin. The Ins2 variant causes a dominant gain-of-function diabetic syndrome by acting as a proteotoxin trapped at the ER, exhausting homeostatic UPR outputs and promoting terminal UPR activation[252-255]. Rare cases of human infantile diabetes have been reported due to Akita-like mutations in human insulin[256]. In addition, PERK knockout in mice causes a diabetic syndrome which results from massive and rapid beta cell apoptosis and culminates in frank pancreatic insufficiency. The ER of beta cells in PERK knockout mice is distended with electron-dense protein deposits and pancreatic islets exhibit a high rate of apoptosis with a marked decline in beta cell proliferation[239]. Again, a rare human diabetic syndrome, Wolcott-Rallison syndrome, is caused by PERK null mutations and patients display many of the same features as recapitulated by PERK knockout mice[257]. Another genetic example of ER-stress induced diabetes is Wolfram syndrome, a human genetic disorder caused by mutations in WFS1, which is phenocopied by WFS1 knockout in mice. WFS1 is an ER

transmembrane protein which is thought to normally contribute to protein assembly, ERAD and processing of ATF6 and when mutated causes early-onset diabetes, optic and auditory defects and neurodegeneration[258-260].

Although the aforementioned genetic causes of DM are rare, they offer insight into the unifying biological processes that may underlie common diabetic syndromes in humans. Several studies have confirmed that beta cells function at higher basal levels of UPR activation than other secretory cell types. Thus as ER stress levels rise, beta cells are more prone to cross a threshold promoting transition from the homeostatic to the terminal UPR. The upstream stressors that initiate DM type 1, 2 and gestational diabetes are unique, but are perhaps unified by the scheme of UPR-mediated beta cell death culminating in endocrine pancreatic failure.

1.5.3.2 Cancer

Several studies have demonstrated sustained activation of all three arms of the UPR in many primary tumor types. However, whether UPR activation ultimately promotes tumor death or survival is an area of intense investigation. Among the types of tumors found to have UPR activation are malignant gliomas[261] and carcinomas of the breast[262], stomach[263], esophagus[264] and liver[265]. Myeloma[266] as an example, illustrates the complexity of UPR activation in cancers. The IRE1a/XBP1s axis of the UPR is thought to be critical for plasma cell development – indeed, in mice,

IRE1a and XBP1 are both required for differentiation of B lymphocytes into plasma cells[267, 268]. About half of all myelomas show unusually high levels of XBP1s and mice expressing a transgene of XBP1s develop a plasma cell malignancy that phenocopies myeloma[266]. The first-line treatment for myeloma, bortezomib, is a proteasome inhibitor that is thought to exert its anti-myeloma action by preventing the removal of misfolded proteins by ERAD, leading to ER stress-induced apoptosis[269, 270]. This evidence would suggest a pro-oncogenic role for IRE1a/XBP1s in myeloma development. However, several lines of evidence contradict these findings, including the finding that XBP1s downregulation correlates with resistance to bortezomib[271-273]. In addition, only two of 38 myeloma patients screed by whole-genome and whole-exome sequencing were found to have XBP1 mutations and these were loss-of-function[274]. This highlights that the contribution of the UPR to disease states, and certainly cancers, may be more complicated and nuanced that might have been predicted.

1.5.3.3 Heart Disease, Stroke and Ischemia-Reperfusion Injury

Reductions in blood flow rapidly induce protein misfolding and ER stress. In addition, when blood flow is restored, reperfusion leads to oxidative stress with resultant alterations in the redox status of the ER that affect protein folding[239, 275, 276]. UPR activation has been well-documented in atherosclerotic plaques, and ER stress-induced apoptosis of macrophages and endothelial cells worsens the progression of atherosclerosis[277]. Cardiac myocytes within and adjacent to the site of a

myocardial infarction activate the UPR, and genetic ablation of ASK1 (a member of the IRE1a/ASK1/JNK alarm signaling cascade) in mice preserves cardiac function, indicating that UPR activation may be pathogenic in the infarcted heart[278]. Similarly, in the brain regions surrounding a stroke, evidence suggests that neuronal loss is secondary to ER stress-induced apoptosis, and mice deficient in the terminal UPR effector CHOP incur less neuronal loss than wild-type controls[279].

1.5.4 ER Stress and UPR Activation in Proteinopathy-Related Neurodegeneration

Accumulation of misfolded proteins in the brain is a common feature of many neurodegenerative diseases including PD, ALS, AD, and Huntington's disease (HD). In superoxide dismutase 1 (SOD1) ALS mouse models, chronic ER stress was found to be the earliest pathological event, occurring in vulnerable neurons during the pre-symptomatic stage of the disease[280]. It was thus thought that targeting the UPR may provide a neuroprotective therapy for ALS. Targeting the PERK signaling branch of the UPR, however, produced an unexpected outcome which was partially protective and partially pathogenic. Activation of EIF2a phosphorylation was protective, likely due to the resultant attenuation of protein translation[280, 281]. Similar EIF2a-induced neuroprotection has been observed in TDP43 ALS zebrafish and *Caenorhabditis elegans* (*C. elegans*) models[282]. In contrast, ATF4 activation was detrimental, resulting in activation of terminal UPR components CHOP and BIM[283]. Interestingly,

ablation of terminal UPR apoptotic effectors PUMA, BIM and ASK1 protects against ALS in experimental models[284-286]. In addition, targeting XBP1 has been shown to protect against ALS in experimental models by enhancing protein clearance through autophagy[287] – importantly, this was one of the first reports of an interconnection between the UPR and autophagy in the context of neurodegeneration. Similar results have been observed for models of HD, wherein XBP1 knockout conferred neuroprotection which was mediated by enhanced autophagy[288]. Conflicting results have been obtained regarding the role of the UPR in AD pathology. For example, overexpression of XBP1 in a Drosophila melanogaster model of AD protected against amyloid-beta toxicity[289]. In contrast, XBP1 ablation in a C. elegans model of AD protected against amyloid-beta toxicity[290]. These findings indicate the need for patient-specific models to evaluate the contributions of ER stress to AD pathology. Another report suggested that ER stress may act in a vicious pathogenic cycle with amyloid-beta, wherein ER stress affects the generation of amyloid-beta and amyloid-beta in turn initiates apoptosis via UPR activation of JNK3[291]. The elucidation of such reciprocal relationships between the proteins that mediate proteinopathy-related neurodegeneration and the UPR, as well as mechanisms to activate homeostatic and silence terminal UPR activation will aid in the development of neuroprotective disease-modifying therapies for these diseases in the future.

1.5.5 ER Stress and UPR Activation in PD

Among the earliest evidence for a role of ER stress in PD pathogenesis was the finding of ER stress responsive genes, including homocysteine-inducible ER stress protein (HERP), BiP and PDI, at elevated levels in the SNc of PD patients, and in complexes with LBs[292-294]. The UPR is the major cell stress signature engaged by PD-inducing neurotoxins, including MPTP, 6-OHDA and rotenone, with a clear activation of the PERK and IRE1a signaling pathways being observed in PD models challenged with these toxins[295, 296]. In addition, targeting UPR components has been shown to impact the survival of DA neurons in response to neurotoxin exposure[234].

Each of the six genes which cause monogenic heritable PD (alpha-synuclein, leucine-rich repeat kinase (LRRK2), Parkin, PINK1, DJ-1 and ATP13A2) have been associated with ER stress. PD-causative mutations in the gene encoding LRRK2 were first identified in 2004[297, 298], and have since been described as the single most common cause of inherited PD[299]. Much as for alpha-synuclein, the precise normal function of LRRK2 is unknown. LRRK2 is so named because of the identification of a leucine-rich repeat domain and a kinase domain, however, the validation of *in vivo* physiological substrates of LRRK2 kinase activity remains an active area of investigation[299]. Indeed, the first rigorously-validated physiological substrates of LRRK2 kinase activity, a subset of Rab GTPases, were characterized just this year[300]. The presence of leucine-rich and ankyrin-like repeats, as well as a WD40 domain suggests that LRRK2 may serve

as a scaffold for protein-protein interactions[299]. In addition, WD40 domains in other proteins serve as lipid-interacting motifs[301], suggesting that LRRK2 may interact with intracellular membranes[299]. Consistent with this notion, post-mortem analysis of healthy control compared to PD patient brains revealed that LRRK2 is present both within Lewy bodies and at the ER, the presence in both locations being 50% higher in the brains of PD patients with the pathogenic LRRK2 G2019S mutation, suggesting that this mutation may partly mediate neurodegeneration through ER stress caused by ER retention of mutant LRRK2 protein[302]. In C. elegans, wild-type LRRK2 was found to be neuroprotective in response to human alpha-synuclein overexpression and treatment with the dopaminergic neurotoxin, 6-hydroxydopamine (6-OHDA)[303]. Furthermore, it was found that this neuroprotection was mediated through the upregulation of BiP[303]. In addition, C. elegans lacking the LRRK2 homolog were found to be hypersusceptible to experimental ER stress, a phenotype which was rescued in PINK1 knockout worms[304]. This suggests that LRRK2 and PINK1 may act antagonistically in a common stress pathway involving the ER that contributes to pathogenesis in PD. Parkin is an E3 ubiquitin ligase that is thought to function in the UPS, an important component of the ERAD pathway[234]. The overexpression of a Parkin substrate, Parkin-associated endothelin receptor-like receptor (Pael-R), induces ER stress and SNc degeneration in mice, a phenotype which is enhanced by Parkin deficiency[305, 306]. Parkin has also been demonstrated to be a downstream UPR target, activated by ATF4 in response to ER stress[307]. Downregulation of DJ-1 has been shown to enhance cellular susceptibility to ER stress[308],

and mutations in ATP13A2 are known to trigger its retention at the ER, causing chronic ER stress and cell death[309].

1.5.6 Alpha-Synuclein-Induced ER-Stress and UPR Activation

Recent literature which has strongly implicated an interplay between the UPR pathway, and the critical PD-related pathogenic protein, alpha-synuclein is reviewed here. Because proteinopathy, secondary to disrupted proteostasis, is a prominent feature of PD, efforts to elucidate the role of the UPR in PD have erupted over the past several years. In particular, since alpha-synucleinopathy is a common feature of genetic and sporadic forms of PD, it is of great interest to evaluate the interplay between ER handling of overabundant or mutated alpha-synuclein via the UPR and the pathogenic actions of alpha-synuclein which interfere with this process. In elucidating the role of ER stress and UPR activation as mediators of alpha-synuclein-induced neurotoxicity in PD, there is great potential to unveil novel targets for therapeutic intervention.

1.5.6.1 Evidence of ER Stress-Induced UPR Activation in Post-Mortem PD Brains

Hoozemans et al. 2007[310] was the first study to demonstrate UPR activation in DA neurons from post-mortem SNc of PD patients relative to age-matched controls. In this study, the authors found that phosphorylated PERK (pPERK) and its target, phosphorylated EIF2a (pEIF2a), were

detectable in neuromelanin-containing DA neurons of PD cases. Phosphorylation of EIF2a by pPERK causes a general attenuation of mRNA translation, while selective transcripts, such as AFT4 mRNA, are specifically translated to promote restoration of ER homeostasis, or in cases of ongoing or severe ER stress, to promote ER stress-induced cell death[310]. Neuromelanin-containing pigmented DA neurons of the SNc have been demonstrated to be selectively vulnerable to neurodegeneration in PD[311]. Notably, neither pPERK nor pEIF2a were detectable in age-matched controls, supporting a role for PERK-mediated UPR activation in the etiopathogenesis of PD. Strikingly, DA neurons containing higher levels of alpha-synuclein were found to express higher levels of pPERK, suggesting a functional relationship between alpha-synuclein accumulation and ER stress. More recently, Baek et al. 2015[312] examined levels of GRP78/BiP as a marker of ER stress and UPR activation in PDD and DLB compared to AD postmortem brain tissue, with the aim of examining levels of UPR activation in the context of co-existing synucleinopathy and amyloidopathy, compared to amyloidopathy alone. The authors found elevated levels of GRP78/BiP in PDD and DLB cases compared to AD and control cases, particularly in the cingulate gyrus and parietal cortex. Consistent with the findings reported by Hoozemans et al. 2007, it was further demonstrated that synuclein pathology was positively correlated with GRP78/BiP levels in the cingulate gyrus. This finding highlights that levels of UPR activation due to synucleinopathy may vary based on the level of alpha-synuclein expression in different brain regions. Furthermore, co-occurrence of other proteinopathies may enhance ER stress and UPR

activation, potentially resulting in an earlier switch from cytoprotective to cytotoxic outcomes and possibly contributing to the etiopathogenesis of neurodegeneration in these different disease contexts.

1.5.6.2 PERK-Mediated UPR Activation is Strongly Implicated in Experimental Models of PD with Alpha-Synucleinopathy

In 2011, Bellucci et al.[313] defined the functional relationship that Hoozemans et al. 2007 proposed between alpha-synuclein accumulation and ER stress. In this study, it was demonstrated that accumulation of alpha-synuclein in the ER results in its association with GRP78/BiP and consequent derepression of the UPR master regulators. Consistent with previous reports of alpha-synuclein-induced PERK activation, Bellucci et al. found induction of ATF4 translation, a downstream event specific to the PERK-activated arm of the UPR pathway. These events were described in both cell culture and animal models of PD, including SYN120-transfected HEK293 cells, glucose-deprived differentiated SH-SY5Y cells, and SYN120 mouse substantia nigra. In a subsequent study using a rat model of PD induced by human alpha-synuclein locally overexpressed in the SNc, Gorbatyuk et al. 2012[314] found that alpha-synuclein induces both the PERK and ATF6 arms of the UPR, as well as the terminal UPR effector, CHOP. Consistent with the report from Bellucci et al., Gorbatyuk et al. described alpha-synuclein in complexes with GRP78/BiP. Furthermore, it was demonstrated that AAV delivery of GRP78/BiP cDNA diminished alpha-synuclein-induced neurotoxicity by attenuating ER

stress and apoptosis, leading to survival of TH+ nigral neurons. Importantly, this provides proof-of-principle that genetically altering the expression of molecular modulators of ER stress may provide therapeutic benefit for PD.

1.5.6.3 A53T Mutant Alpha-Synuclein Induces ER Stress

Mutations in SNCA are an overall rare cause of PD, however the alanine-to-threonine substitution at position 53 (A53T) is the most frequent mutation type identified[315]. The identification of cellular pathways involved in the molecular and cellular pathogenesis of PD in such monogenic forms of the disease may enable the application of such knowledge to elucidate the source of pathology in more enigmatic sporadic cases. For example, Smith et al. 2005[316] reported that ER stress is integral to A53T mutant alpha-synuclein induced pathology. Levels of several ER stress markers were elevated in their Tet-Off inducible A53T alpha-synuclein expressing PC12 cell culture model, including GRP78/BiP, pEIF2a and CHOP, as well as the ER resident inducer of apoptosis, caspase-12. The authors described a sequential activation of PD-related cytopathological changes in response to induced expression of A53T alpha-synuclein, including 1) inhibition of proteasome activity and increased intracellular reactive oxygen species (ROS), 2) activation of mitochondrial cell death pathways and 3) ER stress-induced cell death. A53T-induced neurotoxicity was partially rescued by RNAi-mediated inhibition of caspase-12 and application of the ER stress inhibitor, salubrinal, an EIF2a inhibitor.

Following on from these observations, Colla et al. 2012[317] provided the first evidence for ER-stress in a vertebrate model of A53T alpha-synuclein-induced neurotoxicity, the A53T transgenic mouse. In contrast to Smith et al., Colla et al. noted that UPR activation was not accompanied by an increase in EIF2a phosphorylation, but was evidenced by defective ER-associated protein degradation (ERAD), increased neuronal expression of ER chaperones and cleavage of caspase-12. Interestingly, it was also found that overabundance of wild-type alpha-synuclein in neuroblastoma models was sufficient to induce ER stress as represented by elevated GRP78/BiP levels.

1.5.6.4 Overabundance of Wild-Type Alpha-Synuclein Induces ER Stress

The finding that overabundance of wild-type alpha-synuclein is an inducer of ER stress is consistent with other reports on alpha-synucleinopathy-induced UPR activation by accumulation of the unmutated protein, and is of much significance since this scenario is more representative of sporadic PD cases where alpha-synucleinopathy is not accompanied by mutations in the SNCA gene. Jiang et al. 2010[318] developed an alpha-synuclein Tet-Off BE2-M17D (3D5) inducible cell line to examine the effects of stable alpha-synuclein overexpression and treatment with histone deacetylase (HDAC) inhibitors on alpha-synuclein aggregation and cytotoxicity. After 10 days of retinoic acid differentiation, Tet was either removed to induce alpha-synuclein overexpression (α-Syn+) or maintained at 2 μg/mL to repress expression (α-Syn-). The authors then treated the cells with HDAC

inhibitors. Consistent with previous reports[319-321], HDAC inhibitors were found to induce an ER stress response. Furthermore, the authors found that the stress response was more enhanced in α-Syn+ cells than in α-Syn- cells. The authors noted that the different responses of the α-Syn+ and α-Syn- cells to HDAC inhibitors, may be in part, if not entirely, due to basal differences in the expression of ER stress markers, suggested by the following observations: 1) alpha-synuclein overexpression alone elicited an ER stress response, signified by higher GRP78/BiP and pEIF2a levels, regardless of whether it led to the formation of filamentous alpha-synuclein inclusions, 2) salubrinal treatment protected cultures from HDAC-induced cytotoxicity, 3) treatment with tunicamycin (TM), an ER stress-inducer, resulted in alpha-synuclein oligomer accumulation, and 4) this too was reversed by treatment with salubrinal. The primary conclusions therefore were that wild-type alpha-synuclein can elicit an ER stress response, sensitizing cells to further insults and that ER stress can promote aggregation of wild-type alpha-synuclein.

1.5.6.5 The Role of ER Stress in Alpha-Synuclein Aggregation

As aggregation is a prominent feature of alpha-synucleinopathy, several investigations have sought to determine whether ER stress contributes to the formation of, or cellular response to, toxic aggregation-prone alpha-synuclein species. Following an earlier study in which they demonstrated that oligomeric species of amyloid-beta activated the IRE1a-dependent ER stress response[289], Castillo-Carranza et al. 2012[322] investigated

whether oligomeric forms of other aggregation-prone proteins, including alpha-synuclein, would similarly lead to activation of the IRE1a axis of the UPR. By treating SH-SY5Y neuroblastoma cells with homogenous preparations, they found that alpha-synuclein oligomers, but not monomers or fibers, potently induced XBP1 splicing, the downstream event following activation of the UPR master regulator, IRE1a. This suggests that toxic oligomeric forms of alpha-synuclein are capable of eliciting a precise ER stress response. Supporting a role for ER stress in the formation of toxic alpha-synuclein oligomers, Colla et al. 2012[323] showed that alpha-synuclein which accumulates within the ER forms toxic oligomeric species within mouse and human brains with alpha-synucleinopathies, contributing to disease progression. Treatment with salubrinal was found to reduce the accumulation of alpha-synuclein oligomers at the ER. This suggests that ER stress contributes to the formation of oligomeric forms of alpha-synuclein.

Tissue transglutaminase (tTG) is an enzyme which catalyzes molecular protein cross-linking, and tTG-induced cross-links have been described in alpha-synuclein oligomers and aggregates[324-328]. Wilhelmus et al. 2011[329] established a granular pattern of expression of tTG in PD brains, consistent with melanized neurons[329]. In addition to tTG, these granules expressed markers of ER stress, including protein disulfide isomerase (PDI), ERp57, calreticulin and pPERK. Moreover, alpha-synuclein aggregates were observed in tTG granule-containing neurons, providing further evidence for an interaction between tTG-mediated alpha-synuclein

aggregation and ER-stress activation. Further to the evidence supporting a role for ER stress in alpha-synuclein polymerization, post-translational modifications of alpha-synuclein have been similarly demonstrated to promote its aggregation and activation of ER stress. In 2008, Sugeno et al. demonstrated that Ser129 phosphorylation of alpha-synuclein promoted its aggregation. Interestingly, the authors demonstrated that Ser129 phosphorylation of alpha-synuclein is required for alpha-synuclein-induced ER stress and activation of the PERK arm of the UPR with concomitant elevation of pEIF2a[330]. Taken together, these findings highlight the interplay between alpha-synuclein aggregation and ER stress as pathogenic events in PD.

1.5.6.6 ER Stress in Toxin-Induced Models of PD

ER stress has also been implicated as a pathogenic mediator of toxin-induced aggregation of alpha-synuclein. Arsenite-infusion in the rat substantia nigra induced alpha-synuclein aggregation and expression of ER stress markers, culminating in neuronal apoptosis[331]. PDI is a multifunctional ER resident protein with oxidoreductase, disulfide bond isomerase and chaperone properties, which is induced by the UPR. S-nitrosylation (SNO) of PDI has been associated with PD and AD. Xu et al. 2014a[332] demonstrated that exposure of organotypic brain slices to manganese (Mn), a known activator of ER stress and implicated environmental cause of PD, induced nitrosative stress and formation of SNO-PDI. Furthermore, it was demonstrated that formation of SNO-PDI is

a key event in Mn-induced alpha-synuclein oligomerization. In the same year, Kabiraj et al.[333] demonstrated that SNO-PDI induces aggregation of alpha-synuclein and provokes the deposition of alpha-synuclein with its binding partner, synphilin-1, in Lewy-body like deposits. A small molecule, ellagic acid, which scavenges NO and NO_2 radicals was found to alleviate nitrosative-stress-induced aggregation of alpha-synuclein and alpha-synuclein/synphilin-1 composites. In a separate study, Xu et al. 2014b[131] demonstrated that exposure of organotypic brain slices to Mn induces ER stress associated with alpha-synuclein overexpression. Mn was found to induce the expression of GRP78/BiP, GRP94, CHOP, and caspase-12. Alpha-synuclein overexpression was specifically associated with an activation of the PERK arm of the UPR as evidenced by increased expression of pPERK, pEIF2a and induction of ATF4 expression. RNAi-mediated silencing of alpha-synuclein reversed these outcomes. Interestingly, although Mn was found to induce IRE1 expression and XBP1 splicing, this was not rescued by RNAi-mediated silencing of alpha-synuclein. Therefore, the authors suggest that Mn-induced alpha-synuclein overexpression is associated with a selective activation of the PERK arm of the UPR.

1.5.6.7 Catecholamine Toxicity as a UPR Trigger: The Selective Vulnerability of DA Neurons in PD

Catecholamine-induced neurotoxicity, following from the production of oxidized metabolites, has long been implicated in the pathogenesis of

neurodegenerative diseases[334]. Dopamine itself is considered to be particularly neurotoxic, and this feature has been described as a potential explanation for the selective vulnerability of DA neurons in PD[335]. Gomez-Santos et al. 2005[336] found that dopamine caused elevations of CHOP, CEBPb and alpha-synuclein levels in SH-SY5Y neuroblastoma cells. Overexpression of CEBPb alone also caused an elevation of alpha-synuclein levels. Since alpha-synuclein contains CEBPb regulatory zones within the promoter region, the authors propose that CEBPb homodimers or heterodimers of CEBPb/CHOP, could serve as mediators of alpha-synuclein elevation in response to dopamine-induced stress. Interestingly, overexpression of CHOP alone did not affect alpha-synuclein expression. However, inhibition of JNK and p38 MAPK tempered the elevation of CHOP levels in response to dopamine. The authors thus conclude that CHOP is activated in response to ER stress signaling mediated by MAPKs in response to high dopamine levels. Similarly, Ito et al. 2010[337] evaluated the interaction between alpha-synuclein and catecholamine synthesis in a PC12 alpha-synuclein Tet-inducible cell culture system[337]. The authors observed nuclear induction of CHOP when alpha-synuclein was expressed. Also, consistent with other reports on alpha-synuclein-induced PERK-mediated UPR activation, the authors described elevated levels of pEIF2a. Paradoxically, the authors found that the IRE1a and ATF6 arms of the UPR were inhibited. They conclude that the co-occurrence of alpha-synuclein expression and catecholamine synthesis enhances ER stress which may contribute to PD pathology. Importantly, this highlights that distinct neuronal subpopulations may exhibit different ER stress

responses, based partially on endogenous neurotransmitter production, which can potentially be individually and specifically targeted for therapeutic benefit.

1.5.6.8 ER Stress Unifies Cellular Pathways Implicated in PD Pathology

Previous literature has provided compelling evidence for the role of alpha-synuclein in provoking ER stress, leading to UPR activation. Importantly, several lines of investigation have begun to demonstrate the interrelation of alpha-synuclein-induced ER stress and UPR activation with other cellular pathways which have been implicated in PD pathogenesis, further supporting a central role for these events in the molecular pathogenesis of PD. These studies are discussed below.

1.5.6.8.1 The Ubiquitin Proteasome System

Homocysteine-induced endoplasmic reticulum protein (HERP) is an ER resident membrane protein that is strongly induced by ER stress, but rapidly degraded by the ubiquitin proteasome system (UPS)[338]. Miura et al. 2010[339] describe a scenario in which HERP knockdown unexpectedly facilitates the clearance of alpha-synuclein, increases the levels of ubiquitinated proteins in the cytosol, and improves cell viability during proteasomal stress. The authors concluded that HERP may have a pathogenic action to delay the degradation of cytosolic proteins at the ubiquitination step.

1.5.6.8.2 Calcium Homeostasis

The ER has a well-established vital function in eukaryotic cells to sequester calcium from the cytosol, as cytosolic calcium release regulates a number of rapid intracellular signaling responses[340]. Defects in intracellular calcium homeostasis have been strongly implicated in PD pathogenesis (reviewed in Chan et al. 2009)[341]. In 2012, Belal et al.[342] found a PD-relevant link between ER stress and calcium homeostasis, specifically that A53T alpha-synuclein induces ER stress with accompanying disturbances in ER Ca^{2+} homeostasis that sensitize cells to ER stress-induced death. Furthermore, they found that HERP protects against A53T-induced cell death by restoring ER Ca^{2+} homeostasis. This protective role of HERP is in contrast to the findings from Miura et al. 2010 that HERP delays degradation of ubiquitinated cytosolic proteins and that HERP knockdown improves cell viability during proteasome inhibition. Taken together, these results suggest that modulation of HERP can differentially impact proteostasis as mediated by the ER and the cytosol, and thereby differentially impact cell fate as determined by the stress pathways involved.

1.5.6.8.3 Mitochondrial Dysfunction

Mitochondrial dysfunction is perhaps one of the most commonly implicated pathogenic events in PD, among other neurodegenerative diseases. Several studies have now linked mitochondrial dysfunction and ER stress to alpha-synucleinopathy in PD. Recently, Wang et al. 2014 have identified

another such link[343], showing that low levels of phosphatidylethanolamine, triggered by depletion of mitochondrial phosphatidylserine decarboxylase (PSD), causes ER stress which in turn results in high levels of alpha-synuclein and the occurrence of alpha-synuclein cytoplasmic foci. RNAi depletion of PSD exacerbates this phenotype in *Caenorhabditis elegans* (*C. elegans*), whereas supplemental ethanolamine rescues neurodegeneration.

DNJ-27, the *C. elegans* ortholog of human ERdj5, is an ER-resident thioredoxin protein required as a disulfide reductase for the degradation of misfolded proteins. In 2014, Muñoz-Lobato et al.[344] found that DNJ-27 is specifically induced by IRE1a/XBP1. *C. elegans* models of PD, AD and HD expressing human alpha-synuclein, amyloid-beta and polyQ proteins, respectively, show protein aggregation and concordant motility phenotypes which are enhanced by RNAi-mediated silencing of DNJ-27/ERdj5. Conversely, these effects are ameliorated by overexpression of DNJ-27/ERdj5. Importantly, silencing of DNJ-27/ERdj5 results in mitochondrial fragmentation and disrupted cytoplasmic proteostasis, which are rescued by DNJ-27/ERdj5 overexpression. The authors present an interesting hypothesis that inhibition of DNJ-27/ERdj5 (and presumably other UPR components that assist in the elimination of misfolded proteins from the ER) compromises ERAD, resulting in an increased load of misfolded proteins translocated to the cytosol for degradation. In healthy cells, other protein clearing mechanisms such as the UPS and autophagy (or in dividing cells, mitosis) would clear these proteins. However, in

neurodegenerative disease states, like PD, where these clearance mechanisms are also compromised, the long-standing overabundance of misfolded proteins in the cytosol results in sustained proteotoxicity.

1.5.6.8.4 RNA Processing

Similarly, Ray et al. used a *C. elegans* model to identify a link between ER-mediated proteostasis and RNA processing in neurodegeneration[345]. *C. elegans* RTCB-1 is a modifier of alpha-synuclein protein misfolding, as demonstrated by the fact that RNAi depletion of RTCB-1 enhanced alpha-synuclein induced neurodegeneration. HSPC117, the human ortholog of RTCB-1, is a tRNA splicing ligase with alternative functions in RNA repair and unconventional splicing. The authors found that in *C. elegans*, the neuroprotection conferred by RTCB-1 requires similar RNA-ligase activity and is mediated through XBP1 of the UPR. This highlights a more general role for RNA processing pathways in conferring neuroprotection through interacting with mediators of proteostasis.

1.5.6.8.5 Intracellular Vesicle Transport

Besides the recognition of alpha-synuclein-induced activation of the PERK arm of the UPR, perhaps the most compelling implicated role of alpha-synuclein as a mediator of ER stress is in impairing vesicular transit from the ER to the Golgi apparatus. Cooper et al. 2006[346] demonstrated that one of the earliest defects to appear following expression of alpha-synuclein in

yeast is a block in ER-to-Golgi vesicular trafficking. A genome-wide screen demonstrated that the largest class of modifiers of alpha-synuclein-induced toxicity acted at this step, Ypt1p. The mammalian homolog of Ypt1p, Rab1, further rescued alpha-synuclein induced toxicity in three independent animal models of PD: *Drosophila*, *C. elegans* and primary rat midbrain cultures. They hypothesized that alpha-synuclein-induced blockage of ER-Golgi transport would result in an accumulation of proteins at the ER which would elicit an ER stress response through sequestration of GRP78/BiP. This is in agreement with the previously described activation of the PERK arm of the UPR, although the suggested mechanism of UPR activation is distinct: that the general accumulation of secreted proteins at the ER activates the UPR, rather than the accumulation of alpha-synuclein itself. Alpha-synuclein-induced blockade of ER-Golgi vesicular trafficking in PD models has been further confirmed in subsequent reports[347, 348]. In a recent publication, Credle et al. 2015[349] found that alpha-synuclein-induced inhibition of ER-Golgi trafficking may actually inhibit activation of the UPR by interfering with processing of the UPR master regulator, ATF6, which would typically traffic from the ER to the Golgi to be activated by cleavage with Golgi serine proteases. Alpha-synuclein-mediated inhibition of ATF6 processing occurs both directly through physical interactions between ATF6 and alpha-synuclein and indirectly through alpha-synuclein-induced inhibition of ATF6 processing into COPII vesicles. The blockage of ATF6 processing ultimately resulted in ERAD dysfunction. This represents a novel mechanism by which alpha-

synuclein-induced inhibition of ER-Golgi trafficking may directly impair the restoration of ER homeostasis by the UPR.

The Lindquist group further expanded on their findings of synucleinopathy-induced impairment of ER-Golgi trafficking in yeast, *C. elegans*, *Drosophila* and rat midbrain cultures[346, 347] by evaluating this process in cortical neurons derived from an A53T SNCA mutant iPSC line and corrected isogenic control in Chung et al. 2013[163]. Specifically, it was found that PDI and GRP78/BiP levels were elevated in A53T mutant cortical neurons compared to isogenic controls. Importantly, levels of the terminal UPR effector, CHOP, were not altered. The expression of ERAD substrates, glucocerebrosidase (GCase), neuroserpin and nicastrin, was further examined. While neuroserpin was unaffected, GCase and nicastrin accumulated at the ER in A53T mutant iPSC-derived neurons, as evidenced by declining post-ER forms. None of these phenotypes were observable at the iPSC stage. It was further demonstrated that ERAD dysfunction was rescued with synoviolin-1 (Syvn1) and *N*-arylbenzimidazole (NAB2), two highly conserved ubiquitin ligases which function in the ERAD and vesicle trafficking pathways, respectively.

Interestingly, despite a great deal of work evaluating activation of the UPR in mutant, exogenous or inducible alpha-synuclein overexpression models, little is known about the role of the UPR in the case of SNCA triplication, a known cause of monogenic, autosomal dominant PD with

prominent alpha-synucleinopathy. It is important to distinguish the effects of mutant, exogenous or inducible alpha-synuclein overexpression observed in neuroblastoma or animal models from features of endogenously overexpressed wild-type alpha-synuclein, as in the case of SNCA triplication, as certain features of endogenously overexpressed alpha-synuclein that may be intricately involved in the resultant pathology may not be recapitulated by previous model systems. The development of iPSCs has provided an unprecedented means of evaluating the molecular outcomes of such endogenously overexpressed alpha-synuclein and the availability of iPSCs derived from a patient with PD caused by SNCA triplication has allowed me to evaluate the role of the UPR in this disease context[350]. To date, I could identify only five manuscripts reporting phenotypes associated with SNCA triplication using these cells as a model[163, 350-353], and only one addressing SNCA triplication-induced ER stress[163]. The Chung et al. 2013 study provides the first evidence for ER stress in the case of SNCA triplication. Alongside the characterizations of ER stress in A53T mutant iPSC-derived cortical neurons, this paper demonstrates that cortical neurons derived from SNCA triplication iPSCs similarly express elevated levels of ER-stress markers, PDI and BiP, and accumulate ERAD substrates, GCase and nicastrin, closely phenocopying the A53T mutant. **In Chapter 5, I build on these initial observations, conducting a detailed analysis of alpha-synuclein-induced ER stress-mediated activation of the UPR in neuronal derivatives of iPSCs from a patient with PD caused by SNCA triplication.**

1.6 Summary

In this chapter I have reviewed key details of current knowledge regarding the pathogenic role of alpha-synuclein in PD. In addition, I have introduced the double-nicking CRISPR/Cas9 (Chapter 3) and CRISPRi/dCas9 (Chapter 4) systems which I have applied for modulation of alpha-synuclein expression in subsequent chapters. Finally, I have discussed the role of the UPR in PD pathogenesis and the convergence of alpha-synucleinopathy with ER stress-induced UPR activation in PD pathogenesis, which will be further explored in Chapter 5.

PD-Related Gene	Proposed Role in PD Pathogenesis	PD-Mutant iPSC Lines Generated	Phenotypes Observed in PD-Mutant iPSC Derivatives
Alpha-synuclein (SNCA/PARK1/ PARK4)	Point mutations and multiplications lead to overabundance, oligomerization, fibrillization and aggregation, resulting in the formation of LBs, the pathological hallmark of PD. Evidence has demonstrated alpha-synuclein-induced cellular dysfunction through actions at the nucleus, ER, mitochondria, lysosomes and proteasome.	Triplication (Devine et al. 2011)[1]	Doubled alpha-synuclein expression
		Triplication (Byers et al. 2011)[2]	Accumulation of alpha-synuclein Increased susceptibility to oxidative stress
		Triplication (Flierl et al. 2014)[3]	NPCs showed changes in growth, viability, cellular energy metabolism, and starvation- or toxin-induced stress resistance
		Triplication (Reyes et al. 2015)[4]	Alpha-synuclein secreted from SNCA triplication DA neurons is taken up by neighboring neurons
		Triplication (Heman-Ackah, see Chapter 5)	Activation of IRE1a arm of the UPR in NSC and neuron derivatives; compensated in NSCs, leading to terminal UPR activation and ER stress-induced cell death in neurons
		A53T (Chung et al. 2013)[5]	Increased nitrosative stress Accumulation of ERAD substrates ER stress
		A53T (Ryan et al. 2013)[6]	Increased nitrosative stress Increased oxidative stress Inhibition of MEF2C-PGC1α transcriptional network Mitochondrial dysfunction Apoptotic cell death
LRRK2 (PARK8)	The normal actions of LRRK2 are unknown and whether mutations lead to loss-of-function or gain-of-function in PD pathogenesis remains to be answered. Proposed physiological functions of LRRK2 such as neurite outgrowth, cytoskeletal maintenance, vesicle trafficking and autophagic protein degradation are currently thought to be lost when the gene is mutated, contributing to PD pathology.	Idiopathic PD G2019S (Sánchez-Danés et al. 2012)[7]	Reduced neurite number and arborization Reduced autophagic flux Accumulation of early autophagosomes
		G2019S (Orenstein et al. 2013)[8]	Blockage of CMA translocation complex formation Increased expression of LAMP-2A Accumulation of alpha-synuclein
		G2019S (Reinhardt et al. 2013)[9]	Decreased neurite length Increased ERK activation
		G2019S R1441C (Nguyen et al. 2011)[10]	Increased expression of oxidative stress response genes Accumulation of alpha-synuclein Enhanced sensitivity to caspase-3 activation Increased susceptibility to death due to cellular stressors
		G2019S R1441C (Cooper et al. 2012)[11]	Increased vulnerability to chemical stressors Diminished defense against oxidative stress

Parkin (PARK2)	Parkin is an E3 ubiquitin ligase that functions in the UPS and mitochondrial quality control by translocating to damaged mitochondria and mediating their selective removal via mitophagy. Parkin has also been shown to ubiquitinate mitochondrial outer membrane proteins, altering the balance between fission and fusion and facilitating mitochondrial motility to isolate damaged mitochondria from the mitochondrial network for mitophagy. Mutations in Parkin are thought to lead to a loss-of-function, resulting in defective mitophagy and accumulation of damaged mitochondria.	Compound heterozygous exon 3/5 deletion Homozygous exon 3 deletion (Jiang et al. 2012)[12]	Loss of Parkin function Increased transcription of monoamine oxidases Increased oxidative stress Decreased dopamine uptake Increased spontaneous dopamine release
		Compound heterozygous exon 3/5 deletion Homozygous exon 3 deletion (Ren et al. 2015)[13]	Decreased complexity of neuronal processes Decreased microtubule stability
		Homozygous exon 2-4 deletion Homozygous exon 6-7 deletion (Imaizumi et al. 2012)[14]	Increased oxidative stress Enhanced Nrf2 pathway activity Abnormal mitochondrial morphology Impaired mitochondrial homeostasis Alpha-synuclein accumulation
		V324A (Miller et al. 2013)[15]	Increased apoptosis Decreased dendrite length Decreased AKT activation
		R42P; exon 3 deletion Exon 3-4 deletion; 255A deletion R275W R42P (Shaltouki et al. 2015)[16]	Decreased DA neurogenesis Reduced mitochondrial volume fraction in TH+ neurons
PINK1 (PARK6)	PINK1 is thought to act upstream of Parkin in the mitophagy pathway, accumulating on damaged mitochondria and eliciting the translocation of Parkin. Similar to Parkin, mutations in PINK1 are thought to result in a loss-of-function leading to the accumulation of damaged mitochondria.	Nonsense Q456X Missense V170G (Seibler et al. 2011)[17]	Impaired Parkin recruitment Increased mitochondrial copy number Upregulated PGC1α
		Homozygous Q456X Compound heterozygous D525N/W577R (Cooper et al. 2012)[11]	Increased vulnerability to chemical stressors Diminished defense against oxidative stress
		Q456X (Miller et al. 2013)[15]	Increased apoptosis Decreased dendrite length Decreased AKT activation

DJ-1 (PARK7)	The precise function of DJ-1 remains to be discovered, however it has demonstrated roles in oxidative stress response, cellular transformation and RNA binding. Recent evidence suggests that DJ-1 may function in a common mitochondrial quality control pathway with PINK1 and Parkin.	None to date	N/A
ATP13A2 (PARK9)	The ATP13A2 gene encodes a lysosomal ATPase, which is aberrantly localized to the ER when bearing all mutations associated with PD. Loss of ATP13A2 activity is thought to contribute to PD pathology by reducing the capacity of lysosomes to degrade proteins (including alpha-synuclein) and clear autophagosomes. Mutations in ATP13A2 cause a rare variant of PD known as Krufor-Rakeb syndrome.	None to date	N/A

Table 1.1 Genes Which Cause Monogenic PD and Mutant Phenotypes Observed in Patient-Specific iPSC-Derived Models

LBs = Lewy Bodies; NPCs = neural progenitor cells; ER = endoplasmic reticulum; ERAD = ER-associated protein degradation; CMA = chaperone-mediated autophagy; UPS = ubiquitin proteasome system

Footnotes

1. Devine MJ, Ryten M, Vodicka P, Thomson AJ, Burdon T, Houlden H, et al. Parkinson's disease induced pluripotent stem cells with triplication of the alpha-synuclein locus. Nature communications. 2011;2:440.
2. Byers B, Cord B, Nguyen HN, Schule B, Fenno L, Lee PC, et al. SNCA triplication Parkinson's patient's iPSC-derived DA neurons accumulate alpha-synuclein and are susceptible to oxidative stress. PloS one. 2011;6(11):e26159.

3. Flierl A, Oliveira LM, Falomir-Lockhart LJ, Mak SK, Hesley J, Soldner F, et al. Higher vulnerability and stress sensitivity of neuronal precursor cells carrying an alpha-synuclein gene triplication. PloS one. 2014;9(11):e112413.
4. Reyes JF, Olsson TT, Lamberts JT, Devine MJ, Kunath T, Brundin P. A cell culture model for monitoring alpha-synuclein cell-to-cell transfer. Neurobiology of disease. 2015;77:266-75.
5. Chung CY, Khurana V, Auluck PK, Tardiff DF, Mazzulli JR, Soldner F, et al. Identification and rescue of alpha-synuclein toxicity in Parkinson patient-derived neurons. Science (New York, NY). 2013;342(6161):983-7.
6. Ryan SD, Dolatabadi N, Chan SF, Zhang X, Akhtar MW, Parker J, et al. Isogenic human iPSC Parkinson's model shows nitrosative stress-induced dysfunction in MEF2-PGC1alpha transcription. Cell. 2013;155(6):1351-64.
7. Sanchez-Danes A, Richaud-Patin Y, Carballo-Carbajal I, Jimenez-Delgado S, Caig C, Mora S, et al. Disease-specific phenotypes in dopamine neurons from human iPS-based models of genetic and sporadic Parkinson's disease. EMBO molecular medicine. 2012;4(5):380-95.
8. Orenstein SJ, Kuo S-H, Tasset I, Arias E, Koga H, Fernandez-Carasa I, et al. Interplay of LRRK2 with chaperone-mediated autophagy. Nat Neurosci. 2013;16(4):394-406.
9. Reinhardt P, Schmid B, Burbulla LF, Schondorf DC, Wagner L, Glatza M, et al. Genetic correction of a LRRK2 mutation in human iPSCs links parkinsonian neurodegeneration to ERK-dependent changes in gene expression. Cell stem cell. 2013;12(3):354-67.
10. Nguyen HN, Byers B, Cord B, Shcheglovitov A, Byrne J, Gujar P, et al. LRRK2 mutant iPSC-derived DA neurons demonstrate increased susceptibility to oxidative stress. Cell stem cell. 2011;8(3):267-80.
11. Cooper O, Seo H, Andrabi S, Guardia-Laguarta C, Graziotto J, Sundberg M, et al. Pharmacological rescue of mitochondrial deficits in iPSC-derived neural cells from patients with familial Parkinson's disease. Science translational medicine. 2012;4(141):141ra90.
12. Jiang H, Ren Y, Yuen EY, Zhong P, Ghaedi M, Hu Z, et al. Parkin controls dopamine utilization in human midbrain dopaminergic neurons derived from induced pluripotent stem cells. Nature communications. 2012;3:668.
13. Ren Y, Jiang H, Hu Z, Fan K, Wang J, Janoschka S, et al. Parkin mutations reduce the complexity of neuronal processes in iPSC-derived human neurons. Stem cells (Dayton, Ohio). 2015;33(1):68-78.
14. Imaizumi Y, Okada Y, Akamatsu W, Koike M, Kuzumaki N, Hayakawa H, et al. Mitochondrial dysfunction associated with increased oxidative stress and alpha-synuclein accumulation in PARK2 iPSC-derived neurons and postmortem brain tissue. Molecular brain. 2012;5:35.
15. Miller JD, Ganat YM, Kishinevsky S, Bowman RL, Liu B, Tu EY, et al. Human iPSC-based modeling of late-onset disease via progerin-induced aging. Cell stem cell. 2013;13(6):691-705.
16. Shaltouki A, Sivapatham R, Pei Y, Gerencser AA, Momcilovic O, Rao MS, et al. Mitochondrial alterations by PARKIN in dopaminergic neurons using PARK2 patient-specific and PARK2 knockout isogenic iPSC lines. Stem cell reports. 2015;4(5):847-59.
17. Seibler P, Graziotto J, Jeong H, Simunovic F, Klein C, Krainc D. Mitochondrial Parkin recruitment is impaired in neurons derived from mutant PINK1 induced pluripotent stem cells. The Journal of neuroscience : the official journal of the Society for Neuroscience. 2011;31(16):5970-6.

Chapter 2: Materials and Methods

2.1 HEK293T, SH-SY5Y and BE(2)-M17 Cell Culture

Human Embryonic Kidney (HEK)293T cells were thawed from frozen stocks by agitation in a 37°C waterbath. For recovery, 1 mL fresh HEK293T Culture Medium was added dropwise to the cryovial containing 1 mL of recovered cells, and the entire 2 mL contents was added dropwise to a 15 mL conical tube containing 8 mL fresh HEK293T Culture Medium, consisting of DMEM (Life Technologies) supplemented with 10% HyClone FBS (GE Healthcare). Cells were pelleted by centrifugation at 1500 rpm for 5 min at 25°C. During centrifugation, 14 mL of fresh HEK293T Culture Medium was added to a T75 flask and equilibrated at 37°C and 5% CO_2. Medium was aspirated from pelleted cells. The cell pellet was resuspended with 1 mL fresh HEK293T Culture Medium and seeded into pre-equilibrated T75 flasks. Cells were stored in a 37°C, 5% CO_2 incubator. Medium was changed 24 hours after thawing and every third day thereafter. When cells reached 80% confluence (approximately once per week), they were passaged with TrypLE (Life Technologies) and quenched with 1 volume of fresh HEK293T Culture Medium. A subcultivation ratio of 1:100 was used for maintenance, otherwise cells were seeded at the densities described in the following sections for the relevant experimental setup.

SH-SY5Y neuroblastoma cells were cultured as above with the notable exception that SH-SY5Y cells grow in two phases: adherent and non-adherent. Thus, media changes required the collection of spent medium, centrifugation at 1500 rpm for 5 min at 25°C to pellet non-adherent cells, resuspension in fresh SH-SY5Y Culture Medium (DMEM, supplemented with 10% HyClone FBS) and re-seeding onto adherent cells. Cells were passaged when reaching 80% confluence, as described above, with a subcultivation ratio of 1:4 for maintenance. Non-adherent cells were discarded during passaging. Cells were seeded at the densities described in the following sections for the relevant experimental setup.

BE(2)-M17 neuroblastoma cells were cultured, as described above, in BE(2)-M17 Culture Medium, consisting of OptiMEM (Life Technologies) supplemented with 10% HyClone FBS. Cells were passaged when reaching 80% confluence, as described above, with a subcultivation ratio of 1:7 used for maintenance and at the densities described in the following sections for the relevant experimental setup.

2.2 iPSC Culture

2.2.1 iPSC Source

NIH Center for Regenerative Medicine (NCRM)-5 iPSCs, derived from CD34+ cord blood of a healthy control male subject with normal alpha-synuclein (NAS) expression levels, were obtained from the NIH Center for

Regenerative Medicine (NIH CRM) and are distributed through RUDCR Infinite Biologics at Rutgers University. ND34391G iPSCs, derived from fibroblasts of 55-year-old female patient with PD caused by alpha-synuclein triplication (AST), were obtained from the Coriell Institute and are distributed through the NINDS Repository Fibroblasts and iPSCs Collection. NCRM-5 and ND34391G iPSCs were quality controlled by comparison to the following established iPSC lines: NCRM-1 iPSCs, derived from CD34+ cord blood of a healthy control male subject, obtained from the NIH CRM and distributed through RUDCR Infinite Biologics at Rutgers University; Normal Human Dermal Fibroblasts (NHDF)-1 iPSCs, derived from fibroblasts of a healthy control 44-year-old female subject and obtained from the James Martin Stem Cell Facility; ND38477C iPSCs, derived from fibroblasts of a 50-year-old male patient with PD caused by a compound heterozygous 255A and exon 3-4 deletion in the PARK2 gene, obtained from the Coriell Institute and distributed through the NINDS Repository Fibroblasts and iPSCs Collection.

2.2.2 Thawing and Recovery

NCRM-1, also known as NIH-Lonza (NL)-1, and NCRM-5, also known as NL-5, healthy control iPSCs were obtained as frozen cryostocks from the NIH Center for Regenerative Medicine. NHDF1 healthy control iPSCs were obtained as a frozen cryostock from the James Martin Stem Cell Facility. One hour before thawing cells, 2 mg of BD Matrigel Matrix Growth Factor Reduced (BD Biosciences) was diluted in 12 mL DMEM/F-12

(11320-074, Life Technologies), and 6-well tissue culture dishes were coated with 1 mL per well. Matrigel-coated plates were incubated at 37°C, 5% CO_2 during medium preparation and cell thawing. Complete Essential 8 (E8) Medium (Life Technologies) was prepared by adding 1 mL 50X E8 Supplement to 49 mL E8 Basal Medium. For each cell line, 9 mL Complete E8 Medium was aliquoted to individually labelled 15 mL conical tubes and allowed to warm to room temperature. ROCK inhibitor, Y27632 (Tocris Bioscience), was added to a final concentration of 10 µM. Frozen cryostocks were thawed by agitation in a 37°C water bath. For recovery, 1 mL of Complete E8 Medium containing ROCK inhibitor was added dropwise to 1 mL of thawed cells. The entire 2 mL volume was added back to the 15 mL conical tubes, containing 8 mL Complete E8 Medium with ROCK inhibitor. Cells were pelleted by centrifugation at 1500 rpm for 5 min. Medium was aspirated and cells were resuspended in 2 mL Complete E8 Medium supplemented with ROCK inhibitor and seeded onto Matrigel-coated plates. Plates were quickly and gently rocked side-to-side and front-to-back to evenly distribute cells while placing in a 37°C, 5% CO_2 incubator. After 24 hours, 100% Complete E8 Medium without ROCK inhibitor was replaced.

ND34391G (SNCA triplication) and ND38477C (PARK2 compound heterozygous exon 3-4 deletion and 255A deletion) iPSCs were obtained from the Coriell Institute. ND34391G iPSCs were received as live feeder-based cultures; ND38477C iPSCs were received as a frozen cryostock. CF-1 mouse embryonic fibroblast (MEF) feeders (GlobalStem) were

prepared 1 – 4 days before seeding iPSCs. To prepare feeders, 6-well tissue culture dishes were coated with 1 mL per well 0.1% gelatin in water (StemCell Technologies) and incubated at 37°C, 5% CO_2 for 20 min during MEF Medium preparation and CF-1 MEF thawing. MEF Medium, consisting of DMEM (Life Technologies) supplemented with 10% HyClone FBS (GE Healthcare) and 1X MEM Non-Essential Amino Acids (Life Technologies), was aliquoted at 9 mL per 15 mL conical tube and allowed to warm to room temperature. CF-1 MEFs were thawed and seeded as described above. 1 x 10^6 feeders were used to coat 1 x 6-well plate. Frozen cryostocks of ND38477C iPSCs were thawed as above and seeded onto MEFs in Human iPSC Culture Medium, consisting of DMEM/F12 (10565-018, Life Technologies), 20% KnockOut Serum Replacement (Life Technologies), 1X GlutaMAX (Life Technologies), 1X MEM Non-Essential Amino Acids, 0.1 mM beta mercaptoethanol (Sigma) and 10 ng/mL bFGF (R&D Systems), supplemented with 10 µM ROCK inhibitor. After 24 hours, 100% Human iPSC Culture Medium without ROCK inhibitor was replaced. Passaging of ND34391G and ND38477C iPSCs during feeder-based culture was accomplished via the StemPro EZPassage tool (Life Technologies), with 10 µM ROCK inhibitor supplemented for the first 24 hours after passaging. For feeder-free adaptation, cells were passaged with Collagenase IV (Stem Cell Technologies) onto Matrigel-coated plates in Complete E8 Medium, supplemented with 10 µM ROCK inhibitor for the first 24 hours after passaging.

2.2.3 Maintenance and Passaging

Following feeder-free adaptation of all iPSC lines, cells were maintained by 100% daily replacement of Complete E8 Culture Medium. When cells reached 70% confluence, they were passaged with Dulbecco's phosphate buffered saline/ethylenediaminetetraacetic acid (DPBS/EDTA) solution, containing 0.5 mM EDTA (Life Technologies) in calcium- and magnesium-free DPBS (Life Technologies). Cells were rinsed twice with 1 mL per well DPBS/EDTA solution to remove excess media before applying 1 mL DPBS/EDTA solution for dissociation. Cells were observed with the EVOS FL Imaging System (Life Technologies) for rounding colony edges and central dissociation, which typically occurred within 1.5 – 5 min. DPBS/EDTA solution was aspirated and cells were gently dislodged from the plate by pipetting with Complete E8 Culture Medium, without ROCK inhibitor. Cells were collected to labelled 15 mL conical tubes and pelleted by centrifugation at 1500 rpm for 5 min (NCRM-1, NCRM-5 and NHDF1) or at 200 x g for 2 min (ND34391G, ND38477C). Medium was aspirated and cells were seeded at a subcultivation ratio between 1:6 and 1:24 in Complete E8 Culture Medium, supplemented with 10 µM ROCK inhibitor for the first 24 hours after passaging.

2.2.4 Cryopreservation

When cells reached 70 – 80 % confluence they were cryopreserved by DBPS/EDTA passaging, as described above, pelleting and resuspsending in 1 mL CryoStor CS10 (StemCell Technologies) per 6-well of cells.

Cryovials were then placed on dry ice until freezing medium solidified, and subsequently transferred to a CoolCell Freezing Container (Biocision) for short term (less than 1 month) storage at -80, or to liquid nitrogen for long term storage.

2.3 Generation, Maintenance and Neuronal Differentiation of iPSC-Derived NSCs

NCRM-5 NSCs were derived from NCRM-5 iPSCs by the NIH Center for Regenerative Medicine, using PSC Neural Induction Medium (Life Technologies) per the manufacturer's instructions. NCRM-5 NSCs were maintained in StemPro NSC SFM (Life Technologies), containing Knockout DMEM, 1X StemPro Neural Supplement, 1X GlutaMAX, 20 ng/mL EGF and 20 ng/mL bFGF. C1158 NSCs were derived from ND34391G (SNCA triplication) iPSCs via the Applied StemCell NSC Generation Service, using the Chambers protocol[354]. C1158 NSCs were maintained on Geltrex in Applied StemCell NSC Expansion Medium, containing 1:1 Neurobasal (Life Technologies) and DMEM/F-12 (11320-033, Life Technologies), 1X B27 supplement (Life Technologies), 1X N2 supplement (Life Technologies), 1X GlutaMAX, and 20 ng/mL bFGF (Peprotech). All NSCs were grown on Geltrex LDEV-Free Reduced Growth Factor Basement Membrane Matrix (Life Technologies)-coated plates, prepared by applying a dilution of 60 µL of Geltrex in 12 mL of DMEM/F12 (11320-074, Life Technologies) at tissue culture dish-dependent coating volumes (i.e. 1 mL per well of 6-well tissue culture

dish), and equilibrating at 37°C, 5% CO_2 for one hour prior to cell seeding. Notably, variability introduced by the derivation of NSCs has been minimized to the extent possible by using protocols based on chemically defined medium for neural induction in adherent culture format. All NSCs were passaged with StemPro Accutase Cell Dissociation Reagent (Life Technologies) and quenched with 5 volumes of medium per 1 volume of Accutase applied. NSCs could be maintained for more than 50 passages, while retaining NSC marker expression and neuronal differentiation capacity.

Two days prior to seeding NSCs for cortical neuron differentiation, 0.01% poly-L-ornithine solution (Sigma-Aldrich) was diluted 1:5 in culture grade water (Life Technologies) and applied to coat tissue culture vessels in the following volumes: 0.5 mL per 12-well, 1 mL per 6-well, 6 mL per T75 flask). After 24 hours, poly-L-ornithine solution was aspirated, tissue culture vessels were rinsed twice in culture grade water and laminin (Life Technologies) was applied at a final concentration of 10 µg/mL in the same coating volume as was used for poly-L-ornithine. On the day of seeding (day 0 of differentiation), laminin was aspirated from tissue culture vessels and approximately 1 x 10^5 NSCs per cm^2 (5 x 10^5 NSCs to 12-wells, 1 x 10^6 NSCs to 6-wells or 7.5 x 10^6 NSCs to T75 flasks) were seeded onto poly-L-ornithine/laminin-coated tissue culture vessels in the respective NSC culture medium. On day 1, 100% medium was replaced with Neuronal Differentiation Medium consisting of Neurobasal, 1X B27 supplement, 1X GlutaMAX, 20 ng/mL BDNF (R&D Systems) and 20 ng/mL

GDNF (R&D Systems). 50% medium was replaced every other day, accounting for volume lost by evaporation and avoiding exposure of differentiating neurons to air. On day 7, cortical neuron progenitors were dissociated with Accutase and re-seeded onto poly-L-ornithine/laminin-coated tissue culture vessels to retain the initial cell density. Cells were re-seeded in Neuronal Differentiation Medium containing 0.5 mM dbcAMP (Sigma) to promote maturation. Post-mitotic neurons were not passaged beyond day 7. Cells were processed for analysis between days 10 and 15.

Differentiation of TH+ enriched neurons (20 – 50% of the final population) was accomplished by following the Swistowski protocol[157]. For dopaminergic differentiation, NSCs were seeded as above in the respective NSC culture medium. On day 1, 100% medium was replaced to DA1 Medium consisting of Neurobasal, 1X B27 supplement, 1X GlutaMAX, 1X MEM Non-Essential Amino Acids, 200 ng/mL SHH (R&D Systems) and 100 ng/mL FGF8b (R&D Systems). 100% DA1 Medium was replaced every other day for 14 days. On day 14, cells were dissociated with Accutase and re-seeded onto poly-L-ornithine/laminin-coated tissue culture vessels to retain the initial cell density. On day 15, 100% medium was replaced with DA2 Medium consisting of Neurobasal, 1X B27 supplement, 1X GlutaMAX, 1X MEM Non-Essential Amino Acids, 20 ng/mL BDNF, 20 ng/mL GDNF and 200 mM ascorbic acid. 50% DA2 Medium was replaced every other day for an additional 14 days. Cells were fixed or processed for analysis on day 28.

2.4 CRISPR/Cas9 Construction and Testing

For Cas9-mediated mutagenesis, specifically NHEJ-induced indel formation, the double-nicking (D10A mutant) CRISPR/Cas9 system was used to minimize off-target effects, as cooperative nicking at off-target sites occurs at a significantly reduced rate compared to wild-type Cas9. Single guide RNAs (sgRNAs) were manually designed based on principles described in Ran et al. 2013[220]. Specifically, SNCA exon 4-targeting sgRNAs were 20 nt long and were spaced with 0 nt offset between them (according to the -4 to 20 bp offset suggested) on opposing DNA strands. In the first iteration of genome editing, the pX335 plasmid (Addgene plasmid #42335)[199] was used to co-express sgRNAs and Cas9 nickases. In the second iteration of genome editing, pX461 (Addgene plasmid #48140)[355] and pX462 (Addgene plasmid #48141)[355] were used to co-express sgRNA-Cas9 nickases with EGFP or puromycin acetyltransferase, respectively, allowing simultaneous visual- and drug-selection. The cleavage efficiency of sgRNA-Cas9 nickases was tested extensively in HEK293T cells, SH-SY5Y cells and BE(2)-M17 cells by SURVEYOR assay, sequencing of indel mutations, qPCR for alpha-synuclein transcript levels and ELISA for alpha-synuclein protein levels before proceeding to gene targeting in iPSCs. For SURVEYOR assay, plasmids expressing each sgRNA were transfected in equimolar ratios, as described below (Section 2.6). Cells were collected for gDNA extraction with the DNEasy Blood and Tissue Kit (Qiagen) 48 hours after transfection. The targeted region was amplified with Pfu polymerase and SURVEYOR PCR Primers (Table 3.1), followed by heteroduplex formation and

SURVEYOR nuclease digestion. Cleavage products were visualized on a 2% agarose gel with 1X GelRed. Quantification of band intensity using ImageJ, as described in Ran et al. 2013[220], was used as an initial approximation of sgRNA cleavage efficiency. For sequencing, PCR products were cloned into ZeroBlunt pCR vector (LifeTechnologies) and transformed into TOP10 *E. coli* (Life Technologies). At least 20 bacterial clones were analyzed either by MiniPrep (Qiagen) or colony PCR followed by ExoSAP-IT treatment (Affymetrix) and sequencing with the PCR forward primer. A definitive cleavage efficiency was calculated as the number of indel mutations detected by sequencing divided by the total number of clones analyzed. Analyses of alpha-synuclein transcript and protein levels were performed as described below (Sections 2.7 and 2.9).

Nuclease null or dead Cas9 (dCas9) (D10A and H840A mutant), which lacks endonuclease activity was used for CRISPRi experiments. CRISPRi constructs were generated from the pAC154-dual-dCas9VP160-sgExpression vector (Addgene #48240) by replacement of the VP160 domain with a 2A ribosome skipping site and puromycin acetyl transferase gene, with or without substitution of the sgRNA backbone, as described below. For inhibition of transcript elongation, sgRNAs were designed to align at SNCA exon 1, exon 2, exon 4, the exon 1/2 slice donor and exon 1/2 splice acceptor, and were expressed from a dCas9 vector with an unmodified sgRNA backbone. Constructs for template and non-template strand TSS targeting of SNCA, APP and MAPT were designed to align directly over the TSS, or immediately upstream or downstream of the TSS

without overlapping. TSS-targeting sgRNAs were co-expressed in a dCas9 vector containing a modified F+E sgRNA backbone. F+E refers to two modifications of the sgRNA backbone: the F modification is an A – U basepair flip which abolishes a putative RNA Polymerase III terminator (4 consecutive U's) in the sgRNA stem-loop, the E modification is an extended dCas9-binding hairpin structure[356]. For cloning, sgRNA oligos were annealed and subsequently ligated into Cas9 nickase, dCas9 or dCas9 F+E vectors digested with *Bbs* I (ThermoFisher Scientific), and transformed into Stbl3 *E.Coli* (Life Technologies).

2.5 High Resolution Melt (HRM) Analysis of Targeted iPSC Clones

For HRM analysis, HRM master mix was generated, consisting of 10 µL MeltDoctor HRM Master Mix (Life Technologies), 1.2 µL (5 µM) forward primer, 1.2 µL (5 µM) reverse primer and 6.6 µL nuclease-free water for a volume of 19 µL per reaction. gDNA was extracted from iPSC clones using the DNEasy Blood and Tissue Kit (Qiagen). Samples were diluted to 20 ng/µL and 1 µL of template was added to each well for a final reaction volume of 20 µL. gDNA extracted from ND34391G (SNCA triplication) iPSCs was run as the reference sample. Samples were run in duplicate and the experiment was repeated, with the same four clones identified as variants. Cycling was performed on a 7500 Fast System (Life Technologies) with the following program: 95°C for 10 min, 40 cycles of 95°C for 15 sec and 60°C for 1 min, followed by the high resolution melt curve program, 95°C for 10 sec (100%), 60°C for 1 min (100%), 95°C for

15 sec (1%), 60°C for 15 sec (100%). High Resolution Melt Analysis Software (Applied Biosystems) was used for data analysis to call variants.

2.6 Lipofectamine 2000 and Neon Transfection

HEK293T and BE(2)-M17 cells were transfected in triplicate 24-well format with Lipofectamine 2000 (Life Technologies). One day prior to transfection, cells were seeded at a density of 1.3 x 10^5 cells per well. After 24 hours, 1500 ng of DNA was diluted in 75 µL OptiMEM. In a separate tube, 7.5 µL Lipofectamine 2000 was diluted in 75 µL OptiMEM. DNA was added dropwise to Lipofectamine and the mixture was incubated at room temperature for 5 min. 50 µL DNA-lipid complexes were added to triplicate wells, with 500 ng final DNA applied per well. After 24 hours, 1 volume of medium was added. Cells were collected for analysis 48 (SURVEYOR assay) or 72 (qPCR, ELISA) hours post-transfection.

SH-SY5Y cells and iPSCs were transfected using the Neon Transfection System (Life Technologies) with the Neon Transfection System 10 µL Kit (Life Technologies), per the manufacturer's instructions. Briefly, cells were subcultured as described above until reaching 70 – 80 % confluency. Two hours prior to transfection, 100% Complete E8 Medium containing 10 µM ROCK inhibitor was replaced on iPSCs. SH-SY5Y cells were dissociated with TrypLE and iPSCs were dissociated with Accutase. TrypLE dissociation was quenched with 1 volume, and Accutase dissociation with 5 volumes, of culture medium. Cells were counted and distributed at a

density of 2.5×10^5 (SH-SY5Y) or 1×10^6 (iPSCs) cells per 15 mL conical tube. Cells were pelleted by centrifugation at 1500 rpm for 5 min (SH-SY5Y) or 200 x g for 2 min (iPSCs) at room temperature, washed in 3 mL 1X phosphate buffered saline (PBS) and re-pelleted. Plasmids were distributed to separate tubes for each transfection reaction at 2 µg per tube. For Cas9 nickase experiments, equivalent amounts of each SNCA Cas9 Nickase sgRNA (Table 3.1) were used (i.e. 1 µg SNCA Cas9 Nickase sgRNA1, 1 µg SNCA Cas9 Nickase sgRNA 2). A CAG-driven tdTomato expression plasmid was used as a transfection control and Endotoxin Free Buffer TE (Qiagen) was included as a non-transfected control. Washed cells were resuspended in 10 µL Resuspension Buffer R and transferred to tubes containing DNA. DNA and cell mixture was then electroporated via aspiration into the 10 µL Neon tip. A different Neon tube was used for each cell type, plasmid and control condition. A different Neon tip was applied every two transfections, or when changing cell type, plasmid or control condition. Settings for SH-SY5Y transfection were as follows: 1,100 V, 50 ms, 1 pulse. Settings for iPSC transfection were as follows: 1,400 V, 20 ms, 1 pulse. Cells were dispensed directly into culture vessels containing pre-equilibrated (37°C, 5% CO_2) medium. iPSCs were seeded onto CF-1 (GlobalStem) normal or DR4 (Global Stem) multi-drug resistant MEFs in Complete E8 Medium containing 10 µM ROCK inhibitor for the first 24 hours. On the day after transfection, cell debris was gently removed by washing once with DPBS, and 100% complete culture medium was replaced.

2.7 RNA Extraction, Reverse Transcription and qPCR

Total RNA, including miRNA, was extracted using the miRNeasy Mini Kit (Qiagen) as follows. Culture medium was aspirated and cells were washed once with 1X PBS (Life Technologies). 700 µL Qiazol lysis reagent was added directly to cultured cells and incubated at room temperature for 5 min. Lysates were collected by pipetting into labelled 1.5 mL microcentrifuge tubes. 140 µL chloroform was added to each sample. The mixture was vigorously shaken for 15 sec and allowed to settle at room temperature for 3 min. Samples were centrifuged at 12,000 x g for 15 min at 4°C. The aqueous phase (350 µL) was collected into new labelled 1.5 mL microcentrifuge tubes. 1.5 volume (525 µL) of 100% ethanol was added to each sample and mixed thoroughly by pipetting. 525 µL of sample was applied to labelled RNeasy Mini Spin Columns and centrifuged at 8,000 x g for 30 sec at room temperature. Flow-through was discarded and the remaining sample was applied to the column and centrifuged at 8,000 x g for 30 sec at room temperature. Flow-through was discarded. Columns were washed successively as follows: 700 µL Buffer RLT followed by centrifugation at 8,000 x g for 30 sec, 500 µL Buffer RPE followed by centrifugation at 8,000 x g for 30 sec, 500 µL Buffer RPE followed by centrifugation at 8,000 x g for 2 min. Columns were transferred to fresh 2 mL collection tubes and dried by centrifugation at maximum speed (17,200 x g) for 1 min. Columns were transferred to fresh labelled 1.5 mL microcentrifuge tubes and RNA was eluted in 30 µL RNase-free water by centrifugation at 8,000 x g for 1 min. RNA concentration was

determined by spectrophotometric analysis using a NanoDrop 2000 (ThermoFisher Scientific).

Reverse transcription was performed with SuperScriptIII First-Strand Synthesis SuperMix for qRT-PCR (Life Technologies). 1 µg RNA was diluted in 8 µL DEPC-treated water. 10 µL 2X RT Reaction Mix and 2 µL RT Enzyme Mix were added to each sample to a final volume of 20 µL per RT reaction. RT was performed on a thermal cycler with the following program: 25°C for 10 min, 50°C for 30 min, 85°C for 5 min, 4°C hold. Samples were treated with 1 µL (2 U) E.coli RNase H at 37°C for 20 min. Synthesized cDNA was diluted 1:200 for qPCR or stored at -20°C until use. Note that when necessary to use less than 1 µg of RNA for cDNA synthesis (i.e. due to low RNA concentration), cDNA dilution for qPCR was scaled accordingly (i.e. if 500 ng RNA was used to make cDNA, a 1:100 dilution was used for qPCR).

For qPCR primer design, gene sequences were derived from RefSeqGene (human assembly GRCh38.p2) and primers were designed to generate a 75 – 150 bp product spanning an exon-exon junction using Primer3[357, 358]. Primer specificity was confirmed with PrimerBlast. For ChIP assays, specificity was further established by confirming the presence of a single qPCR product by agarose gel electrophoresis. Lyophilized primers were received from IDT and reconstituted to generate 100 µM stocks with nuclease-free water. Primers were diluted 1:10 to 10 µM for qPCR. Target-

specific master mixes were generated by mixing 10 µL KiCqStart SYBR Green Master Mix (Sigma-Aldrich), 0.6 µL (300 nM) forward primer, 0.6 µL (300 nM) reverse primer and 3.8 µL nuclease-free water for a final volume of 15 µL per reaction. 5 µL diluted cDNA template was added per reaction for a final reaction volume of 20 µL. Cycling was performed on a StepOnePlus Real-Time PCR System (Life Technologies) under standard cycling conditions with the following program: 95°C for 3 min, 40 cycles of 95°C for 15 sec and 60°C for 60 sec, followed by the instrument's melt curve program. Relative quantitation of qPCR data was performed on technical triplicates of biological triplicates, using a relevant control sample and beta-actin as the reference gene. Statistical analysis of significance was performed in SPSS (IBM) by one-way ANOVA with post-hoc Bonferonni where samples met the homogeneity of variances assumption, or Games Howell where samples did not meet the homogeneity of variances assumption, as determined by Levene's test of homogeneity of variance.

2.8 hPSC ScoreCard Analysis

For TaqMan hPSC ScoreCard (Life Technologies) analysis, 20 µL of cDNA from 1 µg of RNA, prepared as described above, was diluted in 610 µL of nuclease-free water. 630 µL of 2X TaqMan Fast Advanced Master Mix was added, and 10 µL of the reaction mixture was loaded per well into the plate, using a fresh tip for each well. Cycling was performed on a StepOnePlus Real-Time PCR System (Life Technologies) under fast cycling conditions

with the following program: 50°C for 2 min, 95°C for 20 sec and 40 cycles of 95°C for 1 sec and 60°C for 20 sec. The experiment was run twice for each sample and data were analyzed using hPSC ScoreCard Analysis Software (Life Technologies).

2.9 Protein Extraction and Quantification of Alpha-Synuclein Protein by ELISA

Protein was extracted for ELISA using Cell Extraction Buffer (Life Technologies) supplemented with 1 mM PMSF. Cells were seeded at a density of 1.3 x 10^5 cells per 24-well for assay. Cells were washed twice with cold 1X PBS (Life Technologies) before lysis in 200 µL Cell Extraction Buffer. Lysates were collected by pipetting into 1.5 mL microcentrifuge tubes and incubated on ice for 30 min with vortexting at 10 min intervals. Cellular debris was pelleted by centrifugation at 13,000 rpm for 10 min at 4°C. Clear lysate was aliquoted to microcentrifuge tubes for assay or stored at -80°C.

ELISA was performed using the Human Alpha-Synuclein ELISA Kit (KHB0061, Life Technologies), per the manufacturer's instructions. Samples and Alpha-Synuclein Standards were prepared in Sample Diluent Buffer and added to Alpha-Synuclein Antibody-coated assay wells in duplicate. Alpha-Synuclein Detection Antibody was added to assay wells and plates were incubated at room temperature for three hours. Assay wells were washed four times with 1X Wash Buffer and Anti-Rabbit

IgG HRP was added to each well. Plates were incubated for 30 min at room temperature. Assay wells were washed 4 times with 1X Wash Buffer and Stabilized Chromogen was added. Wells were incubated for 30 min at room temperature, after which an equal volume of Stop Solution was added and absorbance was read at 450 nm. A standard curve was created in GraphPad Prism 6 (GraphPad Software) and the program was used to calculate the unknown concentrations of alpha-synuclein in cell extracts. Statistical analysis of significance was performed on technical duplicates of biological triplicates in SPSS by one-way ANOVA with post-hoc Bonferonni where samples met the homogeneity of variances assumption, or Games Howell where samples did not meet the homogeneity of variances assumption, as determined by Levene's test of homogeneity of variance.

2.10 Immunostaining

For immunostaining, cells were fixed with 4% paraformaldehyde (PFA) diluted in 1X PBS. Fixative was removed and cells rinsed three times with 1X PBS for 5 min each wash. Cells were then blocked with a solution of 0.3% Triton X-100, 5% goat serum in 1X PBS for one hour at room temperature. Blocking reagent was aspirated and primary antibodies (as specified in the Materials and Methods section of relevant chapters) were applied in antibody dilution buffer (0.3% Triton X-100, 1% BSA in 1X PBS) for overnight incubation at 4°C. Primary antibodies were aspirated, and cells were rinsed three times with 1X PBS for 5 min each wash. Secondary

antibodies (as specified in the Materials and Methods section of relevant chapters) were applied for two hours at room temperature. Secondary antibodies were then removed and samples rinsed three times with 1X PBS for 5 min each. The cells were then mounted with VECTASHIELD Mounting Medium with DAPI (Vector Labs) and glass coverslips. Images were acquired using an EVOS FL Imaging System.

2.10.1 Pluripotency Immunostaining

The following antibodies were used for pluripotency immunostaining: Nanog (PeproTech, 500-P236), Tra-1-60 (Millipore, MAB4360), Oct4 (Cell Signaling, 2750), goat anti-rabbit IgG Alexa Fluor 488 (Life Technologies, A-11034) and goat anti-mouse IgM Alexa Fluor 555 (Life Technologies, A-21426).

2.10.2 Immunostaining of Neurons

The following antibodies were used for immunostaining of neurons: MAP2 (Cell Signaling, 4542), TUJ1 (Cell Signaling, 4466), goat anti-rabbit Alexa Fluor 488 (Life Technologies, A-11034) and goat anti-mouse Alexa Fluor 555 (Life Technologies, A-21424).

2.11 Chromatin Immunoprecipitation (ChIP) Assays

2.11.1 HA, H3 and H3K4me3 ChIP

HEK293T cells were seeded at a density of 1 x 10^6 cells per well to 6-well tissue culture dishes for triplicate transfections. Empty dCas9 F+E vector or dCas9 F+E vectors co-expressing TSS2-1, TSS2-2 or TSS2-3 sgRNAs were transfected with Lipofectamine 2000 (note: all dCas9 vectors express an HA tag). 7500 ng of DNA and 37.5 µL Lipofectamine 2000 were diluted separately in 375 µL OptiMEM. Diluted DNA was added to diluted Lipofectamine and incubated for 5 min at room temperature. 250 µL per well of DNA-lipid complexes were added dropwise to HEK293T cells, resulting in 2500 ng final DNA transfected per well. A plasmid expressing CAG-driven tdTomato was used as a transfection control. Cells were incubated at 37°C, 5% CO_2 for 48 hours. On day 1 of ChIP, cells were washed once with 1 mL 1X PBS, and then dissociated with 1 mL per well TrypLE. Dissociation was quenched by addition of 2 mL HEK293T Culture Medium and cells were triturated to disperse clumps into single cells with a P1000 pipette. Cells were collected into 15 mL conical tubes and counted on a hemocytometer. 2.2 x 10^6 cells were aliquoted to new labelled 15 mL conical tubes. Cells were pelleted by centrifugation at 1300 rpm for 5 min at room temperature. Medium was aspirated and cells were washed with 500 µL 1X PBS, pelleted by centrifugation at 1300 rpm for 5 min, resuspended in 500 µL 1X PBS and transferred to 1.7 mL microcentrifuge tubes. Crosslinking was performed by the addition of 13.5 µL 37% formaldehyde, gentle vortexing and incubation at room temperature for 10 min. Fixation was quenched by the addition of 57 µL

1.25 M glycine, gentle vortexing and incubation at room temperature for 5 min. Fixed cells were pelleted by centrifugation at 500 x g for 10 min at 4°C. Cells were washed twice with 500 µL 1X PBS, and then resuspended in 149.5 µL complete Buffer B (Diagenode) containing 1X Protease Inhibitor (Diagenode). Samples were vortexed and then incubated on ice for 5 min. Samples were sonicated in a 4°C waterbath using a Bioruptor on high setting with a program of 30 cycles, 30 sec on, 30 sec off.

Subsequently, 957 µL complete Buffer A (Diagenode) containing Protease Inhibitor (Diagenode) was added to dilute SDS. 100 µL of chromatin was analyzed for shearing efficiency by phenol:chloroform extraction and ethanol precipitation and products visualized on a 1.5% agarose gel. Insoluble material was removed by centrifugation at 16,000 x g for 15 min at room temperature, and soluble chromatin pre-cleared for one hour with 40 µL protein A agarose (Millipore) for HA ChIP or 10 µL protein G magnetic beads (Diagenode) for H3 and H3K4me3 ChIP. For all experiments, a sample of 40 µL was taken as 10% input. For HA ChIP, 400 µL of chromatin was used for mock ChIP with protein A beads alone and 400 µL for HA-dCas9 ChIP with a rat monoclonal anti-HA antibody (3F10 affinity matrix 11815016001, Roche). For H3 and H3K4me3 ChIP, 400 µL of chromatin was used for mock ChIP with protein G magnetic beads alone. 400 µL of chromatin was used for H3 ChIP with a rabbit anti-H3 antibody (ab1791, AbCam) and 400 µL of chromatin was used for H3K4me3 ChIP with a rabbit anti-H3K4me3 ChIP antibody (C15410003-50, Diagenode). Samples were incubated overnight at 4°C with rotation.

On day 2 of ChIP, samples were washed once in low salt wash buffer (0.1% SDS, 1% Triton X-100, 2 mM EDTA pH 8.0, 150 mM NaCl, 20 mM Tris-HCl pH 8.0), once in high salt wash buffer (0.1% SDS, 1% Triton X-100, 2 mM EDTA pH 8.0, 500 mM NaCl, 20 mM Tris-HCl pH 8.0), once in lithium chloride wash buffer (0.25 M LiCl, 1% NP-40, 1% sodium deoxycholate, 1 mM EDTA pH 8.0, 10 mM Tris-HCl pH 8.0) and twice in TE buffer (10 mM Tris-HCl pH 8.0, 1 mM EDTA). Chromatin was eluted from the beads with 100 µL elution buffer (1% SDS, 0.1 M $NaHCO_3$) for 5 min at 65°C and subsequently for 30 min at 25°C with agitation (800 rpm). Crosslinking was reversed overnight with 200 mM NaCl at 65°C alongside the input samples. On day 3 of ChIP, DNA was treated with 100 µg/ml RNase A (Ambion) for 90 min at 42°C and 200 µg/ml proteinase K (Roche) for one hour at 45°C before purification using ChIP DNA Clean and Concentrator Columns (Zymo). DNA was analyzed by qPCR and results are represented as % input. Statistical analysis of significance was performed on technical triplicates of biological triplicates in SPSS by one-way ANOVA with post-hoc Bonferonni where samples met the homogeneity of variances assumption, or Games Howell where samples did not meet the homogeneity of variances assumption, as determined by Levene's test of homogeneity of variance.

2.11.2 Phospho-Sensitive ChIP of RNA Polymerase II

Phospho-sensitive ChIP assays were performed as described by Stock et al.[359], including recent modifications published by the authors

(www.epigenesys.eu, Prot 48). HEK293T cells were seeded at a density of 6.8 x 10^6 cells per T75 flask for triplicate transfections. Empty dCas9 F+E vector or dCas9 F+E vectors co-expressing TSS2-1, TSS2-2 or TSS2-3 sgRNAs were transfected with Lipofectamine 2000. 13.06 µg of DNA and 65.28 µL Lipofectamine 200 were diluted separately in 652.8 µL OptiMEM. Diluted DNA was added to diluted Lipofectamine and incubated for 30 min at room temperature. The entire volume (1.306 mL) was added dropwise to HEK293T cells, resulting in 13.06 µg final DNA per flask. Cells were incubated at 37°C, 5% CO_2 for 48 hours. On day 1 of ChIP, fresh HEK293T Culture Medium containing 1% formaldehyde was prepared. Spent medium was aspirated and 15 mL of medium containing 1% formaldehyde was added to each flask. Cells were incubated at 37°C for 10 min. Glycine was added to a final concentration of 125 mM (1.5 mL of 1.25 M glycine) and incubated at room temperature for 5 min to quench the fixation. Cells were washed three times with ice cold 1X PBS. Sufficient swelling buffer (25 mM HEPES pH 7.9, 1.5 mM $MgCl_2$, 10 mM KCl, 0.1% NP-40, 5 mM NaF, 2mM Na_3VO_4, 1 mM PMSF and 1X Roche Complete Mini Protease Inhibitor Cocktail) was added to cover cells (3 mL) and samples were incubated on ice for 10 min. Cells were collected by scraping and nuclei were isolated by 50 strokes of Dounce homogenization with tight pestle. Nuclei were pelleted by centrifugation at 3000 x g at 4°C for 5 min, resuspended in sonication buffer (50 mM HEPES pH 7.9, 140 mM NaCl, 1 mM EDTA, 1% Triton X-100, 0.1% sodium deoxycholate, 0.1% SDS, 5 mM NaF, 2mM Na_3VO_4, 1 mM PMSF and 1X Roche Complete Mini Protease Inhibitor Cocktail), and counted on a

haemocytometer. 1 x 10^7 nuclei were sonicated in a 4°C waterbath using a Bioruptor on high setting with a program of 60 cycles, 30 sec on, 30 sec off.

Insoluble material was removed by centrifuging twice at 16,000 x g at 4°C for 15 min, keeping the supernatant. 100 µL of chromatin was analyzed for shearing efficiency by phenol:chloroform extraction and ethanol precipitation and products visualized on a 1.5% agarose gel. 20 µL of chromatin was stored at -20°C overnight as input, and 200 µL was added to each tube of unconjugated protein G magnetic beads, or protein G magnetic beads with rabbit anti-mouse bridging antibody (Jackson ImmunoResearch Laboratories, 315-005-044) and either mouse anti-nonphosphorylated PolII antibody (clone 8WG16, Covance MMS-126R) or mouse anti-Ser^5-phosphorylated PolII antibody (clone CTD4H8, Covance MMS128P). ChIP was performed on a rotating wheel overnight at 4°C. On day 2 of ChIP, chromatin was washed once with sonication buffer (without NaF, Na_3VO_4, PMSF or Roche Complete Mini Protease Inhibitor Cocktail), once with wash buffer A (50 mM HEPES pH 7.9, 500 mM NaCl, 1 mM EDTA, 1% Triton X-100, 0.1% sodium deoxycholate, and 0.1% SDS) once with wash buffer B (20 mM Tris-HCl pH 8.0, 1 mM EDTA, 250 mM LiCl, 0.5% NP-40, 0.5% sodium deoxycholate), and twice with TE buffer (10 mM Tris-HCl pH 8.0, 1 mM EDTA). Chromatin was eluted from beads by sequential incubation at 65°C for 5 min and rotation at room temperature for 15 min in elution buffer (50 mM Tris-HCl pH 7.5, 1 mM EDTA, 1% SDS). Crosslinking was reversed overnight, alongside input samples, with 160

mM NaCl with simultaneous RNase A treatment at a final concentration of 20 µg/mL at 65°C. On day 3 of ChIP, EDTA concentration was increased to 5 mM, 200 µg/mL proteinase K was added, and samples were incubated at 45°C for two hours. Chromatin was purified using Zymo ChIP DNA Clean and Concentrator Columns and samples were analyzed as % input by qPCR. Statistical analysis of significance was performed on technical triplicates of biological triplicates in SPSS by one-way ANOVA with post-hoc Bonferonni where samples met the homogeneity of variances assumption, or Games Howell where samples did not meet the homogeneity of variances assumption, as determined by Levene's test of homogeneity of variance.

Chapter 3: Generation of Isogenic Alpha-Synuclein Triplication iPSCs via Double-Nicking CRISPR/Cas9

3.1 Introduction

The recent generation of iPSCs from a PD patient harboring a triplication of the SNCA gene locus[350] has facilitated efforts to evaluate the role of alpha-synuclein overexpression in PD pathogenesis. Whereas one allele maintains a single copy of SNCA, a triplication on the other allele results in doubling of the total SNCA gene dosage. These cells have been utilized in a small number of pioneering studies, which used age-matched healthy controls for phenotypic comparisons to identify alpha-synuclein-related pathogenic changes, or to examine cell-to-cell transfer of alpha-synuclein[163, 350-353]. The utility of these cells would be greatly enhanced by the generation of an isogenic iPSC line, which would allow the careful characterization of phenotypic alterations resulting solely from alpha-synuclein overexpression, independent of background individual variations[163, 182], or differences due to the overexpression of other genes within the triplicated region[53]. In this chapter, I applied the double-nicking CRISPR/Cas9 system to generate an isogenic iPSC line by double knockout of SNCA in these iPSCs (Figure 3.1). It is worth noting that a broad definition of the term “isogenic” is applied throughout this text to refer to pairs (or sets) of unmodified and genetically engineered iPSCs derived from the same starting cells and therefore possessing the same, or very similar, genetic background.

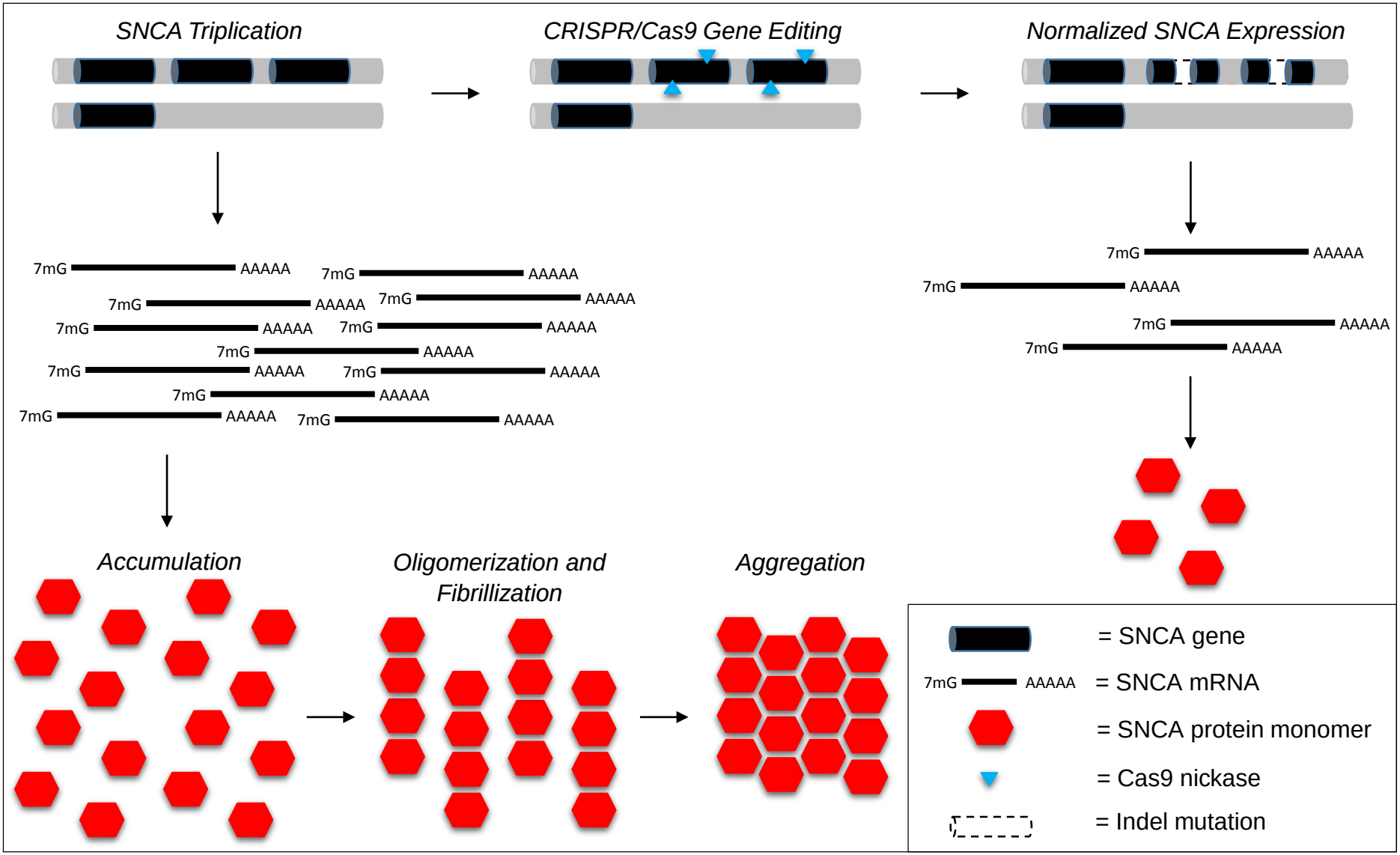

Figure 3.1 Schematic Representation of Gene Editing in SNCA Triplication iPSCs

Figure 3.1 Schematic Representation of Gene Editing in SNCA Triplication iPSCs

Triplication of the SNCA gene locus results in three copies of SNCA on one allele, and a single copy on the other allele. This leads to overexpression of alpha-synuclein at both transcript and protein levels. The overabundance of alpha-synuclein monomers initiates the cascade of proteinopathy-induced neurodegeneration, progressing through accumulation, oligomerization, fibrillization, and aggregation into intracellular inclusions and LBs. Using the double-nicking CRISPR/Cas9 system, I have conducted site-specific mutagenesis of two copies of SNCA in iPSCs derived from a patient with such a triplication. This results in a reduction of alpha-synuclein transcript levels and normalized expression.

3.2 Materials and Methods

The following materials and methods applied in this chapter are the same as those described in Chapter 2: HEK293T, SH-SY5Y and BE(2)-M17 cell culture; iPSC culture; CRISPR/Cas9 construction and testing; HRM analysis of targeted iPSC clones; Lipofectamine 2000 and Neon transfection; RNA extraction, reverse transcription and qPCR; hPSC ScoreCard analysis; protein extraction and quantification of alpha-synuclein protein by ELISA; immunostaining. Oligonucleotide sequences used in this chapter can be found in Table 3.1.

3.3 Results

3.3.1 Double Nickase-Mediated Indel Formation at SNCA Exon 4 Reduces Alpha-Synuclein Expression in Cellular Models

I first designed Cas9 nickase sgRNAs (Table 3.1) to target SNCA exon 4, which is expressed in all four alpha-synuclein transcript isoforms (Figure 3.2, A). Induction of DNA double-strand breaks by Cas9 nickases produced indel mutations through imperfect non-homologous end joining (NHEJ), which were detectable by SURVEYOR assay in HEK293T, BE(2)-M17 and SH-SY5Y cells (Figure 3.2, B). Indels were examined by sequencing, and the mutagenesis efficiency in each cell type was calculated (Figure 3.2, C). To confirm that the mutations generated were sufficient to alter alpha-synuclein expression, I analyzed total alpha-synuclein mRNA (Figure 3.2, D) and protein levels (Figure 3.2, E) by qRT-

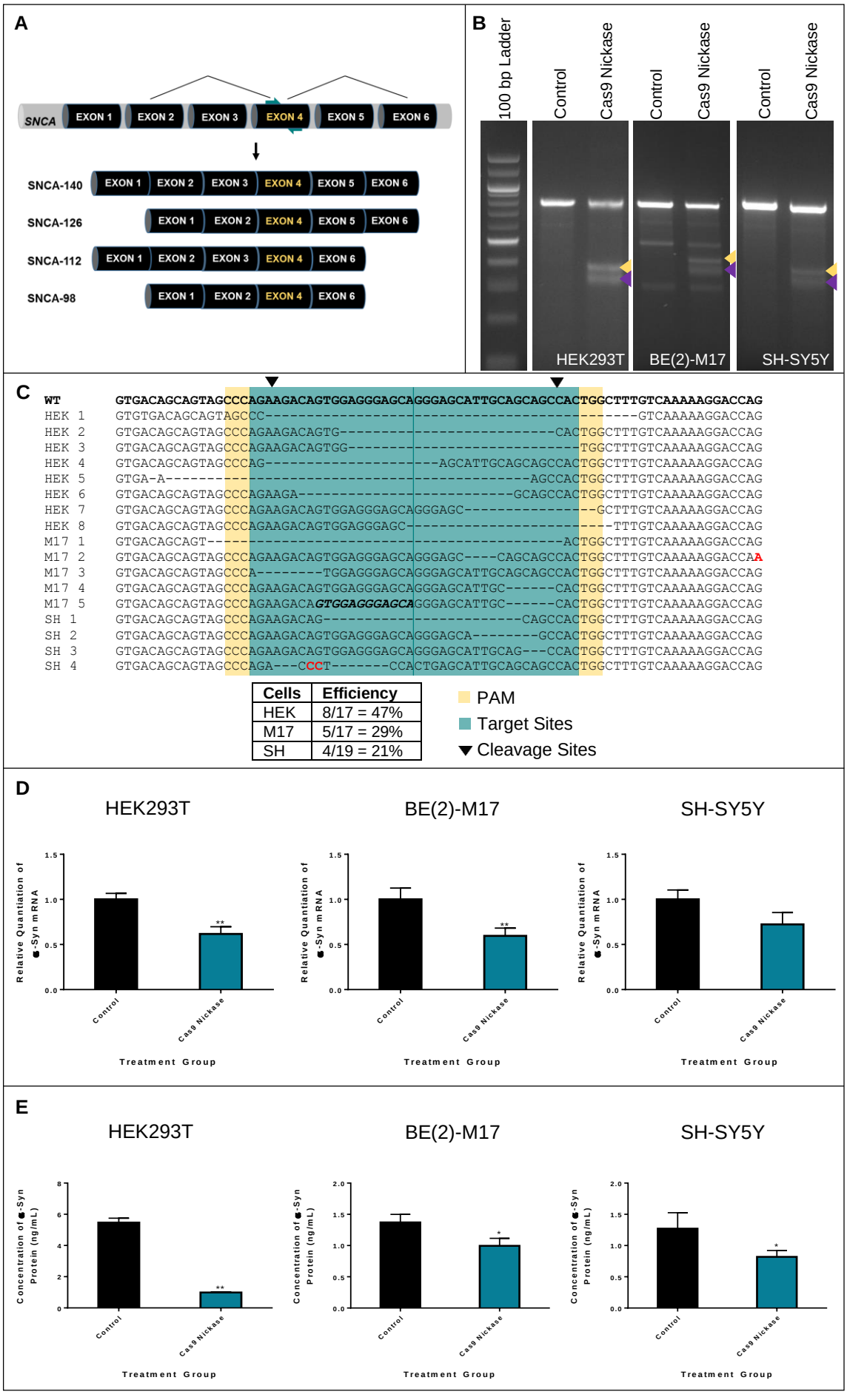

Figure 3.2 Site-Specific Mutagenesis of SNCA Exon 4 by Cas9 Nickases

Figure 3.2 Site-Specific Mutagenesis of SNCA Exon 4 by Cas9 Nickases

A) Schematic representation of sgRNAs (represented as teal arrows) aligning Cas9 nickases to SNCA exon 4, which exists in each of the four alpha-synuclein transcript isoforms generated by alternative splicing of exons 3 and 5.

B) SURVEYOR assay of Cas9 nickase-mediated cleavage at SNCA exon 4 in HEK293T, BE(2)-M17 and SH-SY5Y cells. Gold arrows = 408 bp cleavage products, purple arrows = 357 bp cleavage products.

C) Indels formed in HEK293T (HEK), BE(2)-M17 (M17) and SH-SY5Y (SH) cells by Cas9 nickase-mediated cleavage. Chart shows mutagenesis efficiency in each cell type. PAMs and sgRNA target sequences are highlighted in gold and teal, respectively. A 12 nt duplicated region is indicated in bold and italic text. Base pair mutations are indicated in bold red text.

D) qRT-PCR for total alpha-synuclein (α-Syn) mRNA, normalized to beta-actin, in HEK293T, BE(2)-M17 and SH-SY5Y cells. Data are represented as mean ± SEM of n = 3 non-transfected control wells and n = 3 SNCA Exon 4 Cas9 nickase-transfected wells. Statistical significance was determined by one-way ANOVA.

E) ELISA for alpha-synuclein (α-Syn) protein in HEK293T, BE(2)-M17 and SH-SY5Y cells. Data are represented as mean ± SEM of n = 3 non-transfected control wells and n = 3 SNCA Exon 4 Cas9 nickase-transfected wells. Statistical significance was determined by one-way ANOVA.

*$p \leq 0.05$ compared to control, **$p \leq 0.01$ compared to control

PCR and ELISA, respectively and detected a reduction in alpha-synuclein levels in pooled, targeted populations of each cell type.

3.3.2 Generation of Isogenic SNCA Triplication iPSCs

I then applied these Cas9 nickases to generate isogenic iPSCs derived from a PD patient with SNCA triplication. ND34391G (SNCA triplication) iPSCs were first quality controlled by morphological analysis, pluripotency immunostaining, karyotyping, and hPSC ScoreCard analysis (Figure 3.3, A – C). I further confirmed the genomic presence of four copies of SNCA using Type-IT CNV SYBR Green (Qiagen) qPCR assays (Figure 3.3, D). Vectors co-expressing sgRNAs and Cas9 nickase were then Neon transfected into iPSCs, which had been carefully dissociated into single cells by Accutase treatment. Transfected cells were plated onto feeders and allowed to recover for 4 days, after which individual colonies were manually picked with a glass-stretched pipette and seeded onto Matrigel-coated 96-well plates. Cells were then expanded from 96- to 6-well plate format. A cryostock was preserved and gDNA was extracted to perform mutation analysis. Of 24 clones, four (16.67%) were identified as variants by HRM analysis (Figure 3.4, A). SURVEYOR assay (Figure 3.4, B) and sequencing (Figure 3.4, C) confirmed one (4%) clone as a double knockout, containing an out-of-frame 31 bp deletion, an out-of-frame 40 bp insertion, and an in-frame 3 bp deletion. The double knockout clone, Clone 1-13, was quality controlled by pluripotency immunostaining, karyotyping and hPSC ScoreCard analysis (Figure 3.4, D and E). Finally,

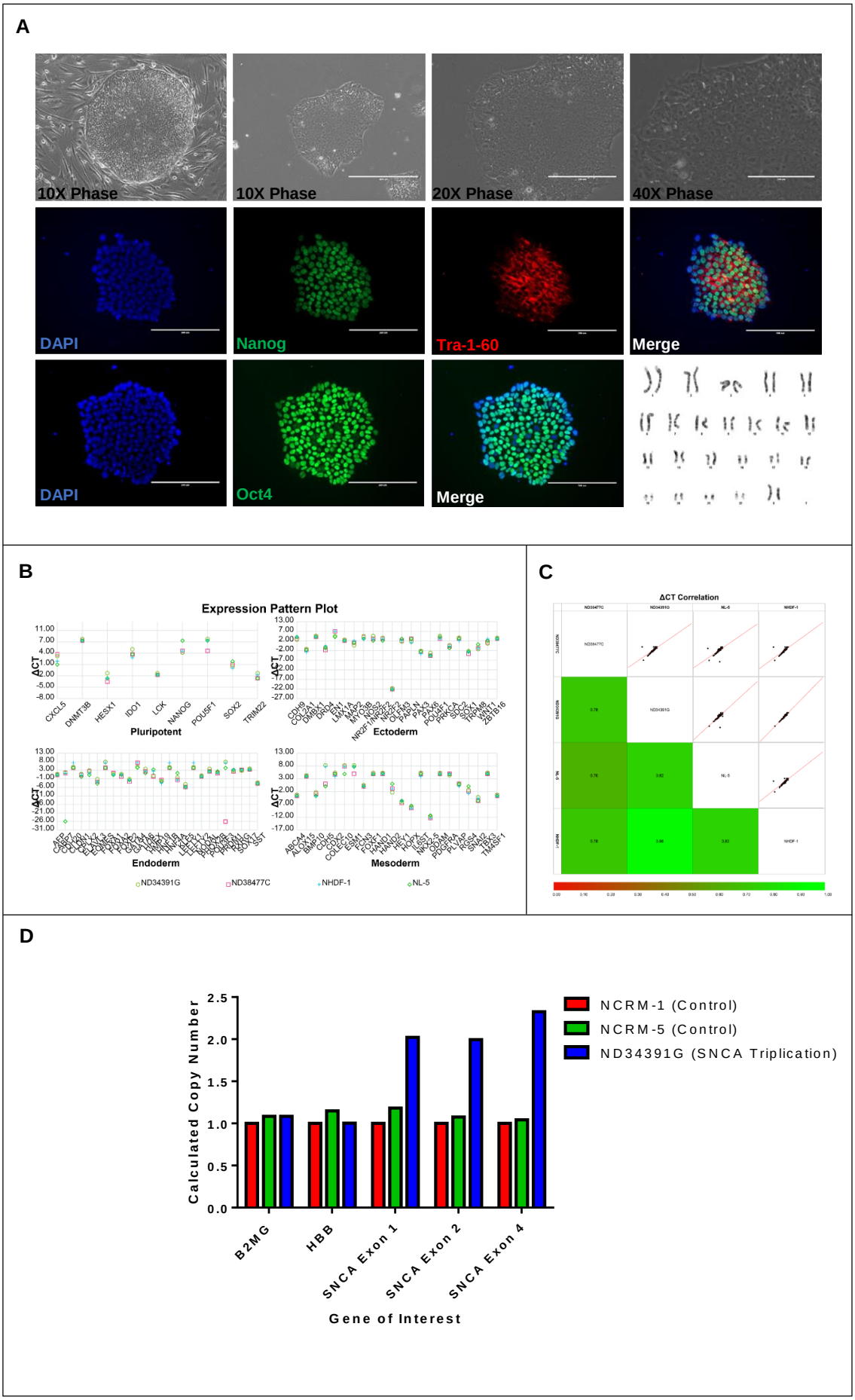

Figure 3.3 Quality Control of SNCA Triplication iPSCs Prior to Genome Editing

Figure 3.3 Quality Control of SNCA Triplication iPSCs Prior to Genome Editing

A) Morphology and pluripotency immunostaining of ND34391G (SNCA triplication) iPSCs. Top panel (left to right): feeder-based culture 10X, feeder-free culture 10X, 20X, and 40X. Middle panel (left to right): DAPI, Nanog, Tra-1-60, overlay. Bottom panel (left to right): DAPI, Oct4, overlay, normal 46,XX g-banded karyotype.

B) hPSC ScoreCard gene expression profiling of pluripotency, endodermal, mesodermal and ectodermal fate-specifying genes in ND34391G (SNCA triplication) iPSCs compared to other established iPSC lines, ND38477C (Parkin mutant), NHDF-1 (healthy control), and NCRM-5 (healthy control).

C) Scatterplots and corresponding correlation coefficients of hPSC ScoreCard Ct values for ND34391G (SNCA triplication) iPSCs, compared to ND34391G (Parkin mutant), NHDF-1 (healthy control) and NCRM-5 (healthy control) iPSCs.

D) Validation of SNCA triplication resulting in doubled SNCA copy number by Type-it CNV SYBR Green qPCR.

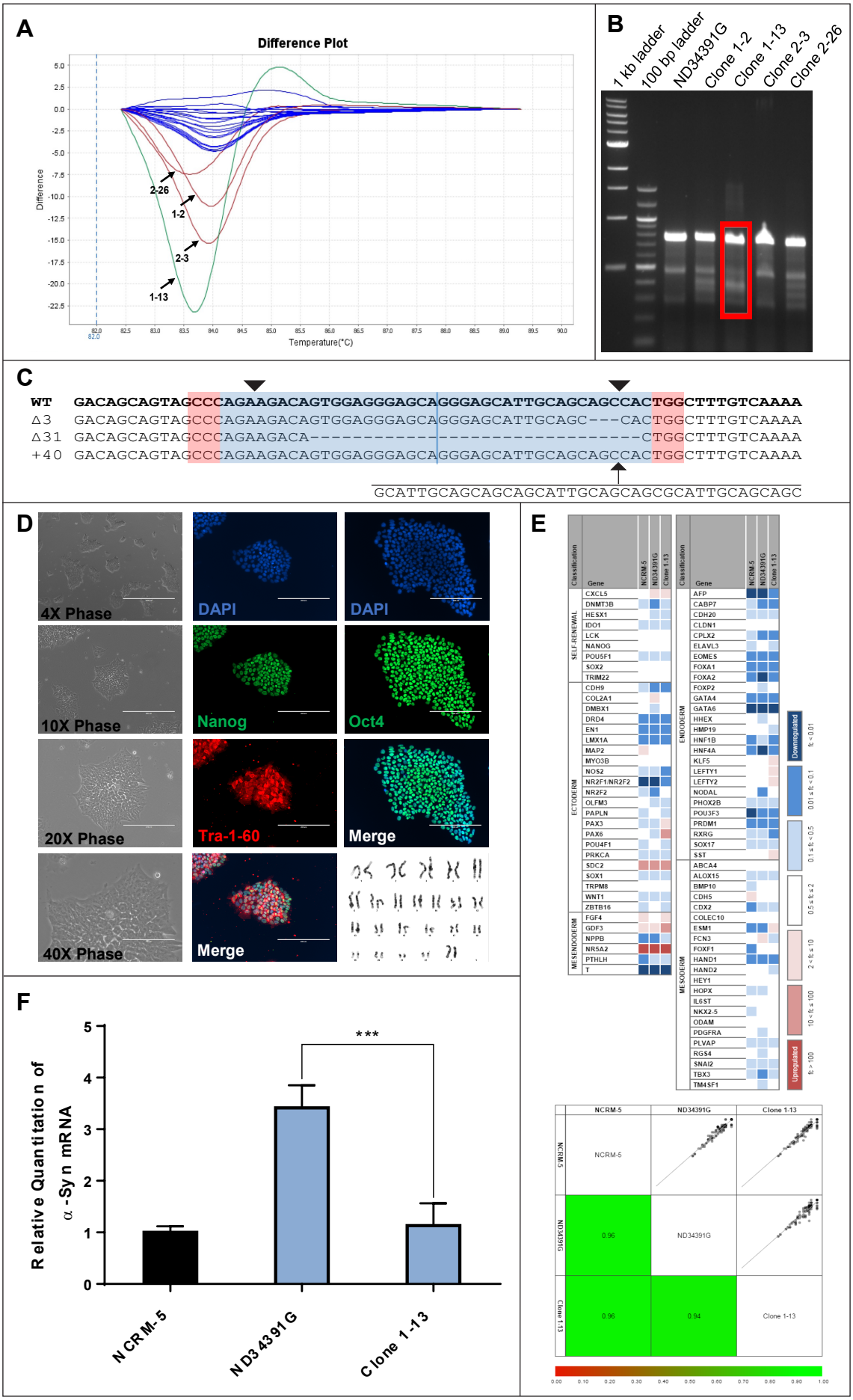

Figure 3.4 Double Knockout of SNCA in iPSCs Derived from a PD Patient with SNCA Triplication via Double-Nicking CRISPR/Cas9

Figure 3.4 Double Knockout of SNCA in iPSCs Derived from a PD Patient with SNCA Triplication via Double-Nicking CRISPR/Cas9

A) HRM analysis of all 24 iPSC clones and the ND34391G (SNCA triplication) reference sample.

B) SURVEYOR assay of four putative knockout iPSC clones identified by HRM screening. Cleavage products from SURVEYOR assay of Clone 1-13 are highlighted by red boxing.

C) Wild-type, 3 bp deletion, 31 bp deletion, and 40 bp insertion identified by sequencing of Clone 1-13. PAMs are highlighted in red, sgRNAs are highlighted in blue and downward pointing black arrows represent cleavage sites.

D) Left panel: morphology of Clone 1-13 iPSCs at magnifications of 4x, 10x, 20x and 40x, top to bottom. Central panel: immunostaining for DAPI, Nanog, Tra-1-60 and the merged image, top to bottom. Right panel: immunostaining for DAPI, Oct4 and the merged image, top to bottom. The bottom right panel demonstrates the normal 46,XX g-banded karyotype of Clone 1-13 iPSCs.

E) Top: hPSC ScoreCard analysis demonstrates that the expression of pluripotency genes and genes required for differentiation along endodermal, mesodermal and ectodermal lineages falls within the same range as the reference sample and is similar between the NCRM-5 (control), ND34391G (SNCA triplication) and Clone 1-13 (double knockout) iPSC lines. Bottom: Scatterplots and corresponding correlation coefficients of the hPSC ScoreCard Ct values for each sample further demonstrate that the edited Clone 1-13 (double knockout) iPSCs remain similar in their expression of pluripotency and differentiation related genes to the NCRM-5 (control) and ND34391G (SNCA triplication) iPSCs.

F) qRT-PCR for total alpha-synuclein (α-Syn) mRNA, normalized to beta-actin, shows a normalization of alpha-synuclein levels in Clone 1-13 (double knockout) iPSCs. Data are represented as mean ± SEM of n = 3 wells of NCRM-5 healthy control iPSCs, n = 3 wells of ND34391G SNCA triplication iPSCs, and n = 3 wells of Clone 1-13 isogenic iPSCs. Statistical significance was determined by one-way ANOVA. ***p ≤ 0.001

I examined the expression of alpha-synuclein in NCRM-5 (healthy control), ND34391G (SNCA triplication) and Clone 1-13 (double knockout) iPSCs, finding that alpha-synuclein levels in the double knockout iPSC line were reduced to levels comparable to the healthy control iPSC line (Figure 3.4, F), with silencing of transcript expression from the out-of-frame mutant alleles caused by nonsense-mediated decay. This double knockout clone will act as an isogenic iPSC line in downstream evaluations, as it mimics the expression of alpha-synuclein from two SNCA gene copies.

Notably, the other variants identified by HRM were confirmed to be single knockout clones by sequencing and may be useful in modeling SNCA duplication, another known cause of PD. Furthermore, triple and quadruple knockout clones were generated in a second iteration of gene editing with Clone 1-13 (Figure 3.5), resulting in a full set of SNCA triplication isogenic iPSC lines with varying SNCA gene dosage.

3.4 Discussion

Following its development in 2013, the double-nicking CRISPR/Cas9 system has been rapidly acknowledged as a highly specific tool for site-directed mutagenesis in a wide variety of genome editing applications[220]. I applied the double-nicking CRISPR/Cas9 system for editing of the important PD-related gene, SNCA. The Cas9 nickase sgRNAs designed in this study efficiently mediate site-specific double-strand breaks in exon 4 of the SNCA gene, as demonstrated by SURVEYOR assay in HEK293T

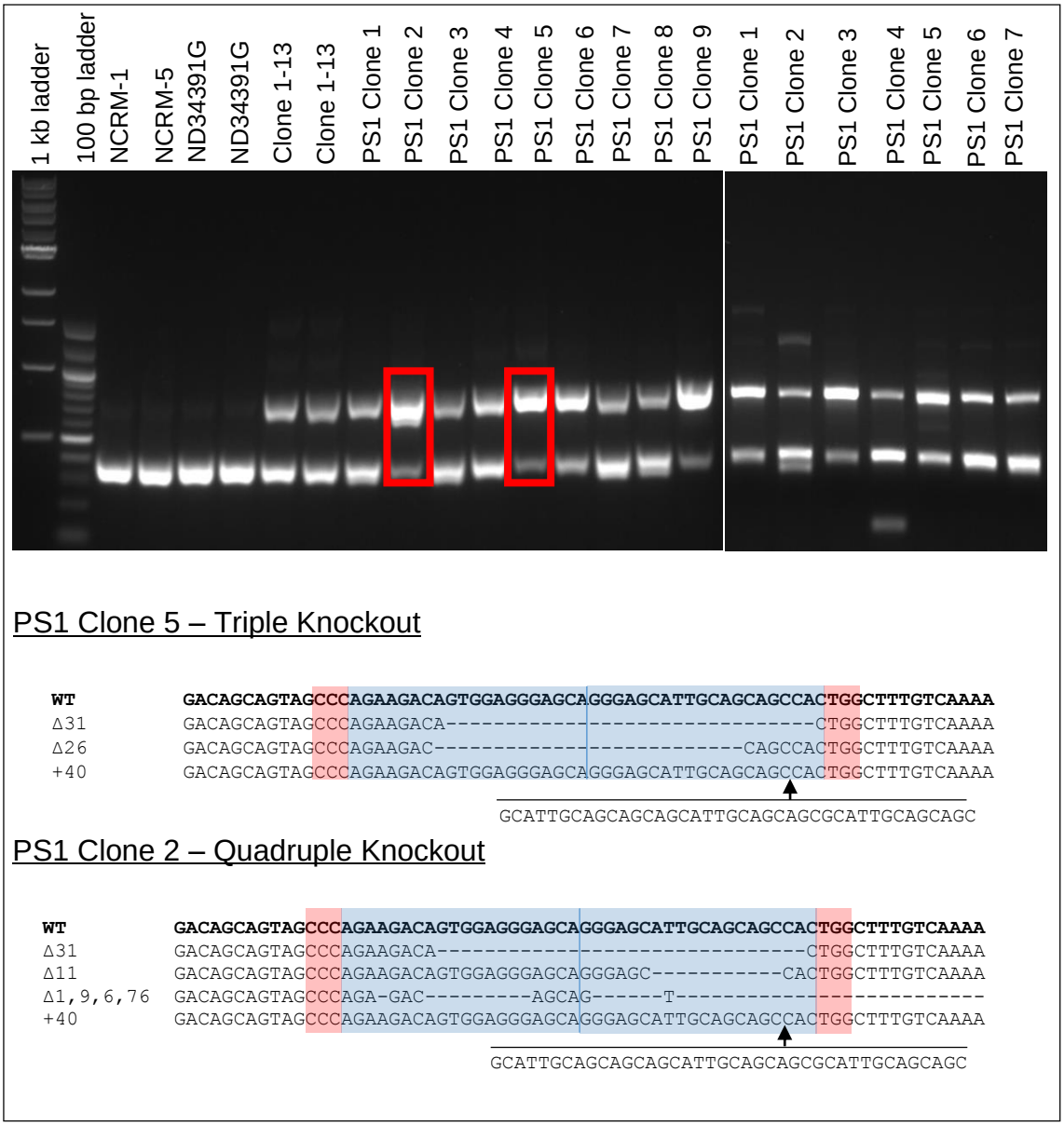

Figure 3.5 Triple and Quadruple Knockout Clones Generated in a Second Iteration of Gene Editing

Figure 3.5 Triple and Quadruple Knockout Clones Generated in a Second Iteration of Gene Editing

Clone 1-13 was used in a second iteration of gene editing with pX461 EGFP-expressing (Addgene plasmid # 48140) and pX462 puromycin acetyltransferase-expressing (Addgene plasmid # 48141) double-nickase CRISPR/Cas9 plasmids. Additionally, the right sgRNA was re-designed to overlap the 3 bp in-frame deletion generated in the first iteration of gene editing. This 3 bp deletion also resulted in a unique ApeKI restriction enzyme site which allowed iPSC clone screening by PCR amplification (with SURVEYOR PCR primers, Table 3.1) of the targeted region and subsequent restriction digest with ApeKI. Several clones demonstrated the anticipated restriction digest pattern of successfully targeted clones – a lighter band of smaller size indicating less digested product due to the loss of the unique restriction enzyme site. PS1 Clone 5 and PS1 Clone 2 (red boxes), were among those validated as triple and quadruple knockout clones by sequencing.

cells, and the commonly utilized *in vitro* PD models, BE(2)-M17 and SH-SY5Y neuroblastoma cells. In this study, these SNCA-targeting Cas9 nickase sgRNAs were applied towards the generation of an isogenic SNCA triplication iPSC line. They may further support other efforts to interrogate the contributions of alpha-synuclein expression levels to pathology in PD and other synucleinopathies due to the presence of SNCA gene multiplications[53, 62, 360], point mutations[44, 48, 49] or mutations that result in decreased clearance of alpha-synuclein protein, such as GBA mutations[361, 362].

Triplication of the SNCA gene locus was first described as the cause of an autosomal dominant, fully penetrant, early onset and rapidly progressive PD with concomitant dementia affecting a large family known as the Iowa kindred by Singleton et al. in 2003[53]. In 2011, Devine et al. generated iPSCs from a PD patient with SNCA triplication (AST) and a first-degree unaffected relative with normal alpha-synuclein expression (NAS)[350]. In this study, Devine et al. conducted a detailed comparison of DA neurons derived from AST and NAS iPSCs. The Singleton et al. paper reported that the size of the triplicated region was approximately 1.61 – 2.04 Mb. Devine et al. were able to further refine the triplicated region to determine an exact size of 1.505 Mb. Unexpectedly, AST iPSCs were found to produce a higher percentage (37%) of DA neurons, defined as tyrosine hydroxylase (TH, a DA neuron marker) and β III tubulin (TUJ1, a pan-neuronal marker) double-positive cells, compared to NAS iPSCs (28%), although this difference was not significant. Alpha-synuclein was expressed in all TUJ1-

positive cells, indicating that it is ubiquitously expressed across neuronal cell types. However, the authors observed heterogeneity of alpha-synuclein expression in neuronal cultures, which may reflect different levels of alpha-synuclein expression in different neuronal subtypes and in the relative proportions of these neuronal subtypes in the final differentiated cell population. These differences in alpha-synuclein expression may also reflect inter-experimental variations in neuronal maturation. Interestingly, the genes in the triplicated region, including SNCA, were expressed at higher levels in AST iPSCs and neurons, but not in AST fibroblasts. Consistent with this result, alpha-synuclein was not detectable in either NAS or AST fibroblasts. AST neurons expressed double the amount of alpha-synuclein mRNA and protein as NAS neurons. Expression of the paralogous genes, beta-synuclein (SNCB) and gamma-synuclein (SNCG) was either not altered (SNCB) or significantly lower (SNCG) in AST neurons compared to NAS neurons. Finally, the authors reported a greater than two-fold increase in secreted alpha-synuclein protein from AST neurons compared to NAS neurons.

Subsequent studies using AST iPSCs have built on these initial findings in an effort to define cellular and molecular phenotypes caused by alpha-synuclein overexpression and their contributions to PD pathogenesis. Consistent with the report by Devine et al., Byers et al. found that DA neurons differentiated from AST iPSCs expressed more alpha-synuclein than NAS neurons, derived from an unaffected sister[353]. Specifically, AST neurons expressed 1.44 times the amount of alpha-synuclein mRNA as

NAS iPSC-derived neurons and 7.17 times the amount of alpha-synuclein mRNA as hESC-derived neurons. In addition, AST neurons expressed twice the amount of alpha-synuclein protein as NAS iPSC- and hESC-derived neurons. The finding of heterogeneous neuronal alpha-synuclein expression described by Devine et al. was further supported in the Byers et al. report, which found that TH-positive neurons derived from AST iPSCs expressed variable amounts of alpha-synuclein. The authors noted that some AST neurons demonstrated an abnormally high expression of alpha-synuclein, but these neurons did not co-express TH, the rate-limiting enzyme in dopamine production. This finding is particularly interesting as it recapitulates an age-related phenomenon that may contribute to the pathogenic context in which PD develops in susceptible individuals: alpha-synuclein-induced dopamine depletion in the nigrostriatal system, which has been previously described in humans and monkeys[125]. Byers et al. additionally examined the baseline levels of 14 oxidative stress response genes in AST iPSC-, NAS iPSC- and hESC-derived DA neurons, and found that five of these genes (DNAJA1, HMOX2, UCHL1, HSPB1, and MAO-A) were differentially expressed. In addition, when the antioxidant, ascorbic acid, was withdrawn from the culture medium and the neurons were challenged with hydrogen peroxide, the authors observed a relative elevation in the levels of cleaved caspase-3 in AST neurons compared to NAS iPSC and hESC controls. These findings suggest that overabundance of alpha-synuclein sensitizes neurons to oxidative stress-induced cell death.

Flierl et al. subsequently published a report comparing neuronal precursor cells (NPCs) derived from AST iPSCs to NAS iPSC-derived NPCs from an unaffected sibling and an unrelated healthy control[351]. Consistent with the report by Byers et al, Flierl et al. reported increased oxidative stress in AST NPCs, as signified by increased production of reactive oxygen species and superoxide. The authors identified a range of other phenotypes in AST NPCs which may contribute to PD pathogenesis, including decreased proliferation, mitochondrial dysfunction, increased protein aggregation and caspase activation. The ability to observe these phenotypes in NPCs is significant for at least two reasons: 1) it suggests that PD-relevant pathogenic events may occur as early as neurogenesis, highlighting that there may be a neurodevelopmental component to PD pathogenesis[363] and 2) NPCs provide a relatively cost-effective means of screening for disease-modifying compounds which may have therapeutic efficacy at earlier stages of the disease[364]. To date, only two other reports have utilized the AST iPSC model. Chung et al. evaluated cortical neurons derived from the AST iPSC line alongside their characterizations of SNCA A53T and mutation-corrected isogenic iPSC-derived cortical neurons, finding that the pathogenic outcomes observed in the A53T mutant neurons were phenocopied in AST neurons and providing the first evidence that ER stress may contribute to pathology in the case of SNCA triplication[163]. Finally, Reyes et al. found that AST DA neurons secreted alpha-synuclein which was taken up by neighboring neurons[352].

Although each of the aforementioned studies have provided compelling insights into the pathogenic actions of overabundant alpha-synuclein due to SNCA triplication, an important limitation in all of these reports is the lack of an isogenic AST iPSC line. Isogenic iPSCs have provided a valuable means of controlling background genetic variability in studies using patient-specific iPSCs to model complex diseases. The sources of such background genetic variability when using iPSC models are multifarious and may include genetic alterations introduced during the reprogramming process[365, 366], residual transgene expression from reprogramming[180], and differences in experimental conditions during reprogramming and cell differentiation[367]. Furthermore, in contrast to early onset diseases for which robust phenotypes are rapidly manifested in the relatively immature disease-relevant cells differentiated from iPSCs, the more subtle phenotypic differences which occur due to complex late onset diseases may be overshadowed by individual genetic differences when comparing patient-specific iPSC derivatives to those of healthy controls[182].

In the case of SNCA triplication, there is a particular necessity for an isogenic iPSC line to validate that the reported phenotypes are specifically caused by overexpression of alpha-synuclein. Whereas uncharacterized background variation may obscure results when comparing patient-specific and healthy controls iPSC derivatives, the triplicated region is a well characterized source of variability as it is known to contain 16 other annotated or putative triplicated genes (for a full list, please see Singleton et al. 2003, Table S1). Due to the proposed roles of the other genes in the

triplicated region in such cellular processes as the UPS, vesicle trafficking, cytoskeletal dynamics, and neuronal migration (discussed in Section 1.2.2), it is impossible to reject the notion that the phenotypes described in previous reports might be partially attributable to the overexpression of these genes. Similarly, without the use of an isogenic iPSC line, it is impossible to exclude the possibility that the phenotypes observed may be explained in part by background individual genetic variability between PD patients and healthy controls.

In this chapter, I have developed an isogenic iPSC line to overcome this limitation. I used double-nicking CRISPR/Cas9[368] to mediate mutagenesis of two copies of SNCA, producing an iPSC line of the same genetic background as the AST iPSCs that expresses a normal level of alpha-synuclein. This iPSC line is not without its own set of limitations. First, a 3 bp deletion on one of the expressed alleles results in a deletion of an alanine at position 90 (A90). This deletion is not predicted to significantly affect downstream investigations of the contribution of alpha-synuclein overexpression to PD pathology since neither mutations nor deletions at position A90 have been identified as a cause of PD. In addition, A90 sits near the end of the last helical region of the alpha-synuclein protein before it becomes disordered, making it unlikely to dramatically affect protein structure. However, it is worth noting that this deletion may have unpredictable consequences – of particular concern is how this deletion may affect the lipid-binding properties and aggregation propensity of alpha-synuclein. As A90 is positioned within the membrane-binding region

(residues 1 – 95) of alpha-synuclein[369], it is possible that this deletion could enhance or inhibit the binding of alpha-synuclein to intracellular membranes. This could be experimentally evaluated by examining whether alpha-synuclein co-localizes to a greater or lesser extent with intracellular membrane-specific markers (i.e. for the plasma membrane, Golgi apparatus, ER and lysosomes) in neurons derived from these iPSCs. In addition, A90 is specifically localized to the NAC region (residues 61 – 94)[85] of the alpha-synuclein protein. Although residues 71 – 82 are responsible for formation of the beta-pleated sheet structure that promotes alpha-synuclein fibrillization[85], the proximity of the deletion at position A90 may influence alpha-synuclein aggregation. Interestingly, deletion of residues 85 – 94 has been found to inhibit fibril formation[370]. In addition, A90 is one of three sites (A18C, A90C and A140C) that have been targeted via site-directed mutagenesis to introduce cysteine resides that can be used for spin-labelling to examine long-range interactions between alpha-synuclein protein domains[371]. A90C spin-labelling has demonstrated that this residue interacts with all of the C-terminal residues of the alpha-synuclein protein[371]. Based on these findings, it is possible that a deletion of this residue might affect the native aggregation propensity of alpha-synuclein, although whether such a deletion would inhibit or enhance alpha-synuclein aggregation would need to be determined experimentally, for example by real-time quaking-induced conversion (RT-QuIC)[372].

Another limitation to these iPSCs is that it is not possible to validate which alleles have been targeted. In a perfect isogenic control, the two amplified

SNCA alleles would be selectively knocked out, leaving the two normally expressed alleles intact. Again, it is not predicted that this would affect downstream characterizations using these iPSCs as a control since the amplified region is large enough that the entire SNCA gene has been copied intact. However, the possibility remains that expression from one of the amplified alleles would differentially contribute to PD pathogenesis than expression from one of the normally expressed alleles. Allele-specific gene editing (in the absence of point mutations) has not yet been achieved, thus such an iPSC line is unattainable with current tools. Nevertheless, the isogenic iPSC line I have generated provides an opportunity to evaluate the contributions of alpha-synuclein overabundance due to SNCA triplication to PD pathogenesis without background individual variability or differences due to the contributions of the other genes in the triplicated region. Importantly, this approach can be complemented by the implementation of dCas9-mediated transcriptional activation of SNCA in healthy control iPSC-derived neurons, as done in Chapter 5.

I next aim to evaluate phenotypic differences between cortical neurons derived from this pair of SNCA triplication and isogenic iPSCs. Using co-culture, supernatant transfer, application of extracellular vesicles (i.e. exosomes) and direct innoculation experiments, they can be further applied in evaluations of how neuron-neuron and neuron-glial interactions promote alpha-synuclein propagation[373, 374]. Although my primary interest is in evaluating the role of alpha-synuclein in CNS derivatives, these iPSCs

can also be utilized to evaluate early alpha-synuclein-related pathogenic changes along multiple alternative developmental lineages implicated in PD pathogenesis[375]. Furthermore, these cells and their derivatives can be utilized for high throughput drug screening, aiding the development of novel therapeutic targets for PD, and other synucleinopathies. This pair of SNCA triplication and isogenic control iPSCs can be broadly applied for functional evaluations of differentiated derivatives to decipher phenotypic alterations which result solely from the overabundance of alpha-synuclein, independent of individual background variation.

Table 3.1 Table of Oligonucleotide Sequences

Primer	Forward	Reverse
SNCA Cas9 Nickase sgRNA 1	CACCGTGCTCCCTCCACTGTCTTCT	AAACAGAAGACAGTGGAGGGAGCAC
SNCA Cas9 Nickase sgRNA 2	CACCGGGAGCATTGCAGCAGCCAC	AAACGTGGCTGCTGCAATGCTCCC
HRM Analysis Primers	GAGCAAGTGACAAATGTTGGAGG	CACAAAACGTACACAGCCATACC
SURVEYOR PCR Primers	TGGCTTTACATTCCTGATCG	GGCACAAAGGGATTTGTTAC
ACTB qRT-PCR Primers	CACAGAGCCTCGCCTTTG	GCGGCGATATCATCATCCAT
SNCA qRT-PCR Primers	CCTTCTGCCTTTCCACCCT	TCCCTCCTTGGCCTTTGAAA

Chapter 4: Precision Modulation of Neurodegenerative Disease-Related Gene Expression via CRISPRi/dCas9

4.1 Introduction

Alpha-synuclein (encoded by SNCA), amyloid precursor protein (encoded by APP), and microtubule associated protein tau (encoded by MAPT) are well-known mediators of neurodegeneration through protein misfolding or accumulation, aggregation and deposition. The consequences of these molecular events are devastating neurodegenerative diseases, collectively known as proteinopathies, including PD, AD and the tauopathies. Here, I describe the application of CRISPRi/dCas9 for transcriptional silencing of these critical neurodegenerative disease-related genes. CRISPRi/dCas9 can be used as a novel tool for interrogation of genetic contributions to neurodegenerative diseases and such an approach could eventually be applied therapeutically to silence neurodegenerative disease-related genes. In addition to demonstrating that CRISPRi/dCas9 can be used for robust, reversible repression of SNCA, APP and MAPT gene expression, I have evaluated mechanistic determinants for efficient silencing by CRISPRi/dCas9. In this chapter, I present evidence that supports recent reports that dCas9 sgRNA position relative to transcription start sites (TSSs) is a key determinant of CRISPRi efficacy. Furthermore, I define the importance of sgRNA-mediated dCas9 binding affinity for effective gene silencing by CRISPRi. Finally, I evaluate the effects of sgRNA-mediated dCas9 binding on the abundance of active chromatin marks and RNA polymerase II occupancy at the SNCA

promoter. The findings presented in this chapter can be utilized towards the rational design of dCas9-specific sgRNAs for robust transcriptional silencing via CRISPRi.

4.2 Materials and Methods

The following materials and methods applied in this chapter are the same as those described in Chapter 2: HEK293T, SH-SY5Y and BE(2)-M17 cell culture; CRISPR/Cas9 construction and testing; Lipofectamine 2000 and Neon transfection; RNA extraction, reverse transcription and qPCR; protein extraction and quantification of alpha-synuclein protein by ELISA; ChIP assays. Sequences of sgRNA oligonucleotides can be found in Table 4.2 and qPCR primers can be found in Table 4.3.

4.3 Results

4.3.1. CRISPRi Targeting of Annotated SNCA TSSs Allows Robust Repression of Alpha-Synuclein Transcript and Protein Levels

I first examined if dCas9 could be used to induce transcriptional silencing of SNCA. As CRISPRi was previously shown to inhibit transcription elongation in *E.coli* and mammalian cells[222], I tested the possibility of inducing SNCA gene repression by targeting transcribed regions within exons expressed in all alpha-synuclein transcript isoforms (Figure 4.1, A and B). As it was previously thought that the dCas9-sgRNA complex could potentially interact with mRNA and alter its translation or stability[222], I also

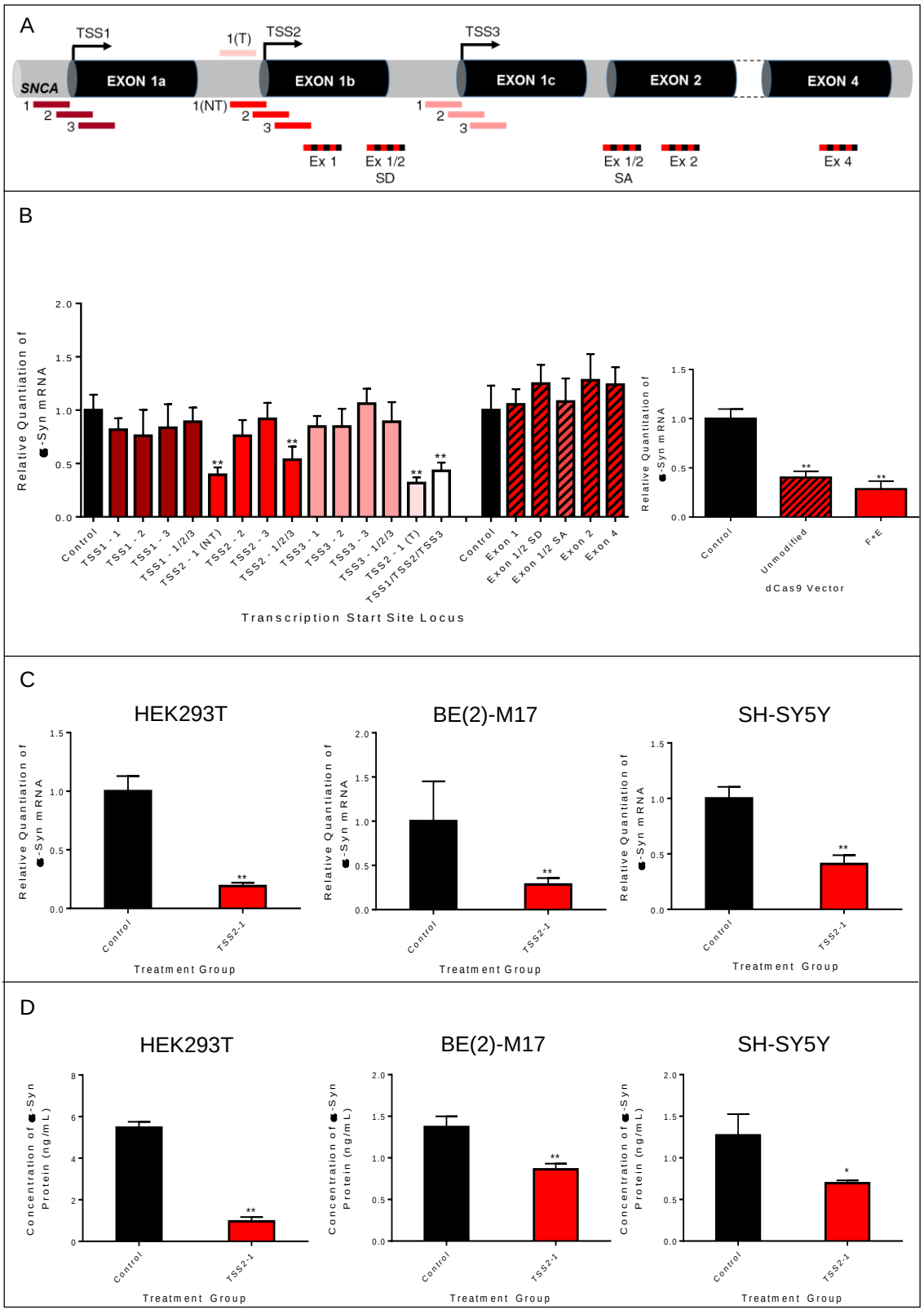

Figure 4.1 Screening of dCas9 sgRNAs Targeting SNCA Exons and Transcription Start Sites

Figure 4.1 Screening of dCas9 sgRNAs Targeting SNCA Exons and Transcription Start Sites

A) Schematic representation of SNCA exon- and TSS-targeting dCas9 sgRNA positions.

B) qRT-PCR screening of total alpha-synuclein (α-Syn) mRNA, normalized to beta-actin, in HEK293T cells transfected with SNCA exon- and TSS-targeting dCas9 sgRNAs (left). qRT-PCR for total alpha-synuclein (α-Syn) mRNA in HEK293T cells transfected with the most active SNCA TSS-targeting sgRNA, TSS2-1, identified by screening co-expressed in dCas9 vectors with unmodified or F+E modified sgRNA backbones. Data are represented as mean ± SEM of n = 3 non-transfected control wells and n = 3 wells of cells transfected with each individual and combination of dCas9 sgRNAs. Statistical significance was determined by one-way ANOVA.

C) qRT-PCR for total alpha-synuclein (α-Syn) mRNA, normalized to beta-actin, in HEK293T, BE(2)-M17 and SH-SY5Y cells transfected with the most active SNCA TSS-targeting dCas9 sgRNA, TSS2-1, identified by screening. Data are represented as mean ± SEM of n = 3 non-transfected control wells and n = 3 dCas9/TSS2-1 sgRNA-transfected wells. Statistical significance was determined by one-way ANOVA.

D) ELISA for alpha-synuclein (α-Syn) protein in HEK293T, BE(2)-M17 and SH-SY5Y cells transfected with the most active SNCA TSS-targeting dCas9 sgRNA, TSS2-1, identified by screening. Data are represented as mean ± SEM of n = 3 non-transfected control wells and n = 3 dCas9/TSS2-1 sgRNA-transfected wells. Statistical significance was determined by one-way ANOVA.

*$p \leq 0.05$ compared to control, **$p \leq 0.01$ compared to control

T = template strand, NT = non-template strand, SD = splice donor, SA = splice acceptor

attempted targeting of constitutive splice sites to examine whether this may interfere with binding of spliceosome components, and therefore reduce spliced transcript levels (Figure 4.1, A and B). However, no observable reduction in alpha-synuclein expression occurred using either method.

I next tested whether CRISPRi could induce efficient silencing of SNCA via inhibition of transcription initiation. Using the Eukaryotic Promoter Database (EPDnew human version 003)[376], I found three annotated TSSs for SNCA and designed sgRNAs to align directly over each TSS, immediately upstream or immediately downstream without overlapping (Figure 4.1, A). I screened these sgRNAs in HEK293T cells and found the TSS2-1 sgRNA to have strong repressive activity when transfected alone, or within any combination of SNCA TSS-targeting sgRNAs (Figure 4.1, B). The SNCA TSS2-1 sgRNA was also found to reduce alpha-synuclein transcript (Figure 4.1, C) and protein (Figure 4.1, D) levels in HEK293T, BE(2)-M17 and SH-SY5Y cells by qRT-PCR and ELISA, respectively.

As dCas9 has been described to have superior repressive activity when targeting the non-template strand of a gene[377], I tested whether an sgRNA aligning to the template strand at the same SNCA TSS2-1 locus would induce silencing. Indeed, the sgRNA aligning to the same position on the template strand was capable of inducing comparable silencing of alpha-synuclein transcript levels (Figure 4.1, A and B). This suggests that the

mechanism of this repression did not involve steric hindrance of RNA polymerase II elongation, as postulated previously[377].

All SNCA TSS-targeting sgRNAs were co-expressed from a dCas9 vector containing a modified sgRNA backbone with A – U flip (F) and stem extension (E), so called dCas9 F+E[378]. Since exon-targeting sgRNAs were co-expressed from a dCas9 vector containing an unmodified sgRNA backbone, I tested whether SNCA gene expression would be similarly repressed when the same SNCA TSS2-1 sgRNA was expressed from the dCas9 vector with the unmodified sgRNA backbone. I found that the SNCA TSS2-1 sgRNA remained capable of inducing robust silencing even when expressed from the unmodified sgRNA backbone (Figure 4.1, B), further supporting the notion that repressive activity of dCas9 is primarily dependent on proximity to the TSS.

Although total alpha-synuclein levels were reduced in HEK293T, BE(2)-M17 and SH-SY5Y cells, not all SNCA isoforms were equally affected by either Cas9 nickase- (from Chapter 3) or dCas9-mediated silencing in each cell type. Whereas all isoforms were repressed by both methods in HEK293T cells (Figure 4.2, A), and dCas9 induced silencing of all isoforms in BE(2)-M17 cells (Figure 4.2, B), Cas9 nickase resulted in a relative elevation of SNCA-112 and SNCA-98 isoforms in BE(2)-M17 cells (Figure 4.2, B). In SH-SY5Y cells, all isoforms were silenced by both techniques, except SNCA-112 which demonstrated a relative increase in expression in response to both approaches (Figure 4.2, C). These cell type-specific

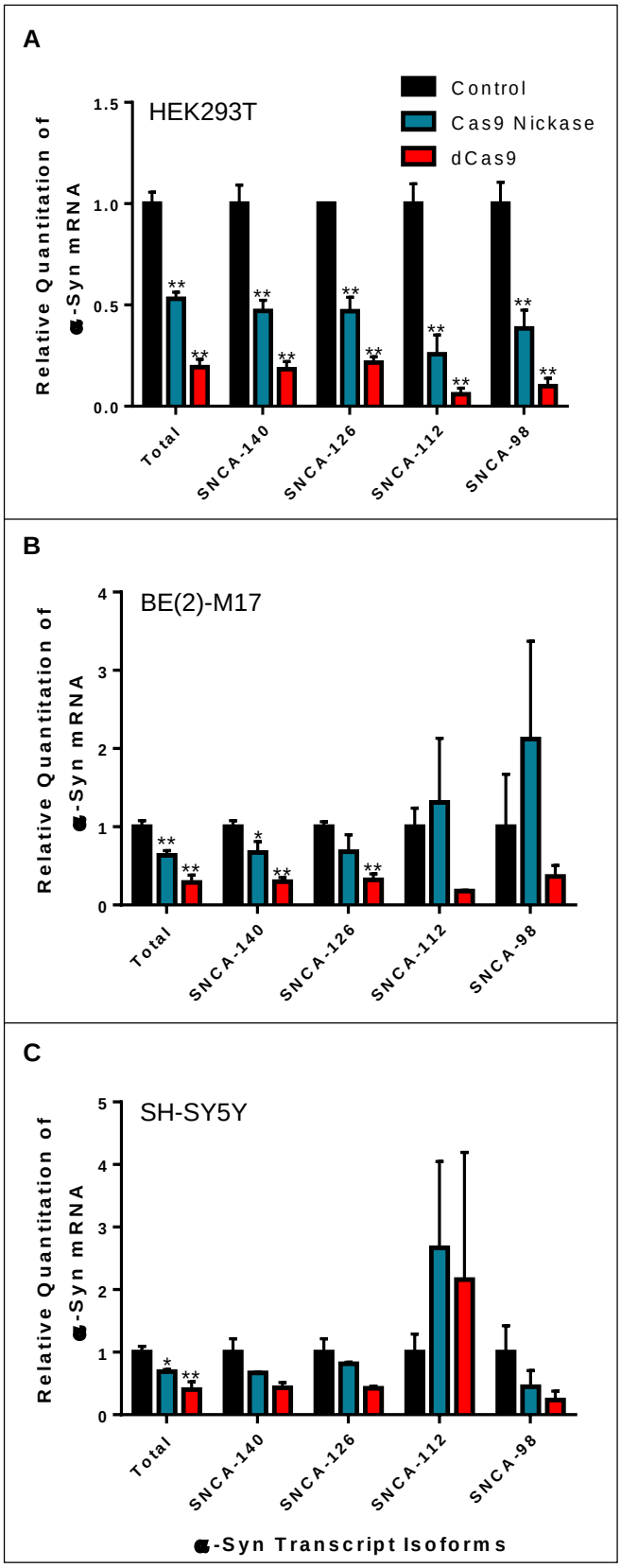

Figure 4.2 Alpha-Synuclein Transcript Isoform Expression Following CRISPR/Cas9-Mediated Transcriptional Silencing

Figure 4.2 Alpha-Synuclein Transcript Isoform Expression Following CRISPR/Cas9-Mediated Transcriptional Silencing

qRT-PCR analysis of total alpha-synuclein (α-Syn) mRNA, normalized to beta-actin, and SNCA-140, SNCA-126, SNCA-112 and SNCA-98 transcript isoform expression in n = 3 Cas9 nickase (teal bars) and n = 3 dCas9 transfected (red bars) wells of (A) HEK293T, (B) BE(2)-M17, and (C) SH-SY5Y cells compared to n = 3 non-transfected control (black bars) wells of each cell type. All data are represented as mean ± SEM. Statistical significance was determined by one-way ANOVA.

*p ≤ 0.05 compared to control, **p ≤ 0.01 compared to control

effects are likely explained by differences in the relative usage of different promoters and differences in transcript isoform expression. Despite this complexity, reductions in total alpha-synuclein transcript and protein levels were acheivable in all cell types using either silencing approach.

4.3.2 sgRNA-Mediated Binding Affinity of dCas9 is a Critical Determinant of Transcriptional Repression by CRISPRi

I next sought to define mechanistic determinants of CRISPRi, first by evaluating whether sgRNA-mediated dCas9 binding affinity could explain the differences in repressive activity of different sgRNAs targeting the same TSS. As dCas9 is expressed with an HA tag, I used an anti-HA antibody to perform ChIP of dCas9 from HEK293T cells transfected with an empty dCas9 vector, lacking sgRNA expression, or a dCas9 vector co-expressing SNCA TSS2-1, TSS2-2 or TSS2-3 sgRNAs (Figure 4.3, A). TSS2-1, the most active sgRNA, and TSS2-2, a weakly active sgRNA showed enrichment at the SNCA genomic locus encompassing all three sgRNAs. In contrast, TSS2-3, an inactive sgRNA, was not enriched. This suggests that differences in binding affinity between different sgRNAs as well as their position relative to the TSS are both critical for efficient CRISPRi.

To further evaluate the mechanism of gene silencing by dCas9 in the absence of a repressive domain, I conducted a set of ChIP assays to examine the effect of dCas9 binding on the presence of the active

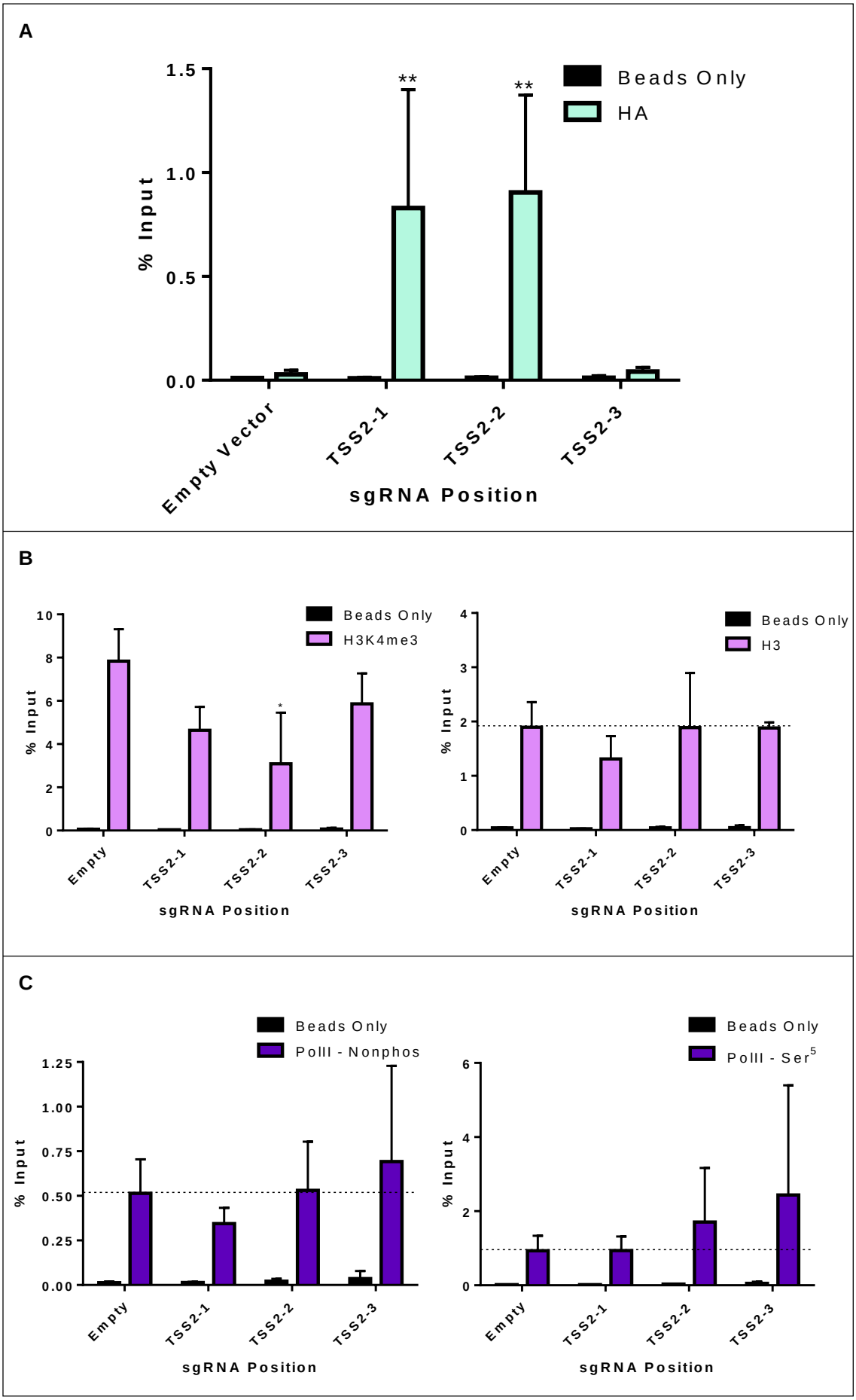

Figure 4.3 Evaluation of Mechanistic Determinants for Efficient CRISPRi

Figure 4.3 Evaluation of Mechanistic Determinants for Efficient CRISPRi

A) HA ChIP of HEK293T cells transfected with empty dCas9 F+E vector or TSS2-1, TSS2-2, or TSS2-3 sgRNA co-expressing dCas9 F+E vectors.

B) H3K4me3 ChIP (left) and H3 ChIP (right) of HEK293T cells transfected with empty dCas9 F+E vector or TSS2-1, TSS2-2, or TSS2-3 sgRNA co-expressing dCas9 F+E vectors.

C) Phospho-sensitive ChIP of nonphosphorylated (left) and Ser^5 phosphorylated (right) RNA polymerase II in HEK293T cells transfected with empty dCas9 F+E vector or TSS2-1, TSS2-2, or TSS2-3 sgRNA co-expressing dCas9 F+E vectors. All data are represented as mean ± SEM of n = 3 individual ChIP experiments, each performed with n = 1 flask of HEK293T cells transfected with each of empty dCas9 F+E vector or TSS2-1, TSS2-2, or TSS2-3 sgRNA co-expressing dCas9 F+E vectors. Statistical significance was determined by one-way ANOVA.

*p ≤ 0.05 compared to control, **p ≤ 0.01 compared to control

chromatin marker, H3K4me3, and the occupancy of RNA polymerase II transcription pre-initiation (non-phosphorylated) and initiation (Ser^5 phosphorylated) phospho-isoforms. TSS2-1 and TSS2-2 sgRNAs induced a trend of reduced H3K4me3 chromatin marks compared to empty vector control and TSS2-3 sgRNA, although this effect was significant only for the moderately active, TSS2-2 sgRNA (Figure 4.3, B). I further confirmed that these effects were not confounded by H3 eviction (Figure 4.3, B). Ser^5 phosphorylated (initiation) RNA polymerase II occupancy at the SNCA promoter was not affected by any of the sgRNAs, however there as a slight decline in nonphosphorylated (pre-initiation) RNA polymerase II occupancy in response to the most active, TSS2-1 sgRNA, which was not observable for any other sgRNAs (Figure 4.3, C). This suggests that inhibition of RNA polymerase II binding at the stage of transcription pre-initiation may contribute to dCas9 silencing activity in the absence of a repressive domain.

4.3.3 Multiplex CRISPRi Silencing of Genes Mediating Proteinopathy-Induced Neurodegeneration

Finally, I examined whether the TSS-targeting approach could be applied to silence other genes known to induce proteinopathy-induced neurodegeneration. I designed sgRNAs to align to the one annotated TSS of MAPT (Figure 4.4, A) and five annotated TSSs of APP (Figure 4.4, B). MAPT was reduced by approximately 80%, whereas the most active TSS-targeting sgRNA produced approximately 40% repression of APP. I noted an inverse relationship between the level of repressive activity achievable

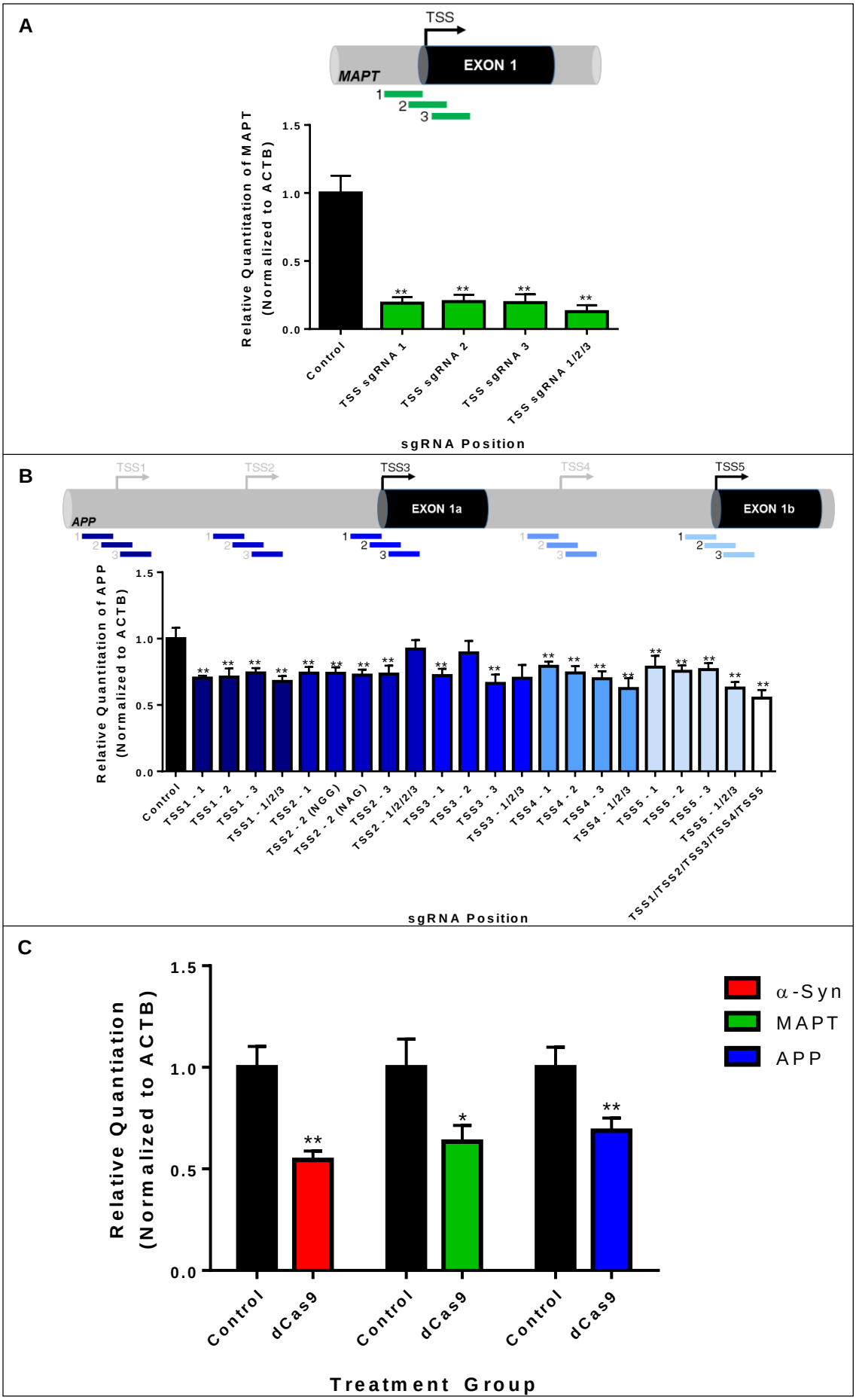

Figure 4.4 Multiplex Transcriptional Silencing of Genes Mediating Proteinopathy-Induced Neurodegeneration by CRISPRi

Figure 4.4 Multiplex Transcriptional Silencing of Genes Mediating Proteinopathy-Induced Neurodegeneration by CRISPRi

A) qRT-PCR for microtubule associated protein tau (MAPT) mRNA in HEK293T cells transfected with dCas9 sgRNAs targeting MAPT TSS.

B) qRT-PCR screening for amyloid precursor protein (APP) mRNA in HEK293T cells transfected with dCas9 sgRNAs targeting five annotated APP TSSs. TSSs represented in black are identified in EPDnew as well as in RefSeqGene, whereas those represented in grey are putative annotated TSSs in EPDnew. Note that the sequence overlapping TSS2 possessed two potential sgRNA binding sites, one with the canonical 5'-NGG PAM, labelled TSS2-2 (NGG), and one with the 5'-NAG PAM, labelled TSS2-2 (NAG). Each sgRNA was tested individually, and the combination of all TSS2-targeting sgRNAs is represented by TSS2-1 – 1/2/2/3, wherein each TSS2-2 sgRNA is represented.

C) qRT-PCR for alpha-synuclein (α-Syn), microtubule associated protein tau (MAPT) and amyloid precursor protein (APP) mRNA in HEK293T cells simultaneously transfected with the most active TSS-targeting dCas9 sgRNAs for each gene.

All data are represented as mean ± SEM of n = 3 non-transfected control wells and n = 3 wells of cells transfected with each individual and combination of dCas9 sgRNAs. Statistical significance was determined by one-way ANOVA.

*$p \leq 0.05$ compared to control, **$p \leq 0.01$ compared to control

and the number of TSSs that exist for a gene, where MAPT having one TSS was reduced by 80%, SNCA having three TSSs was reduced by 60% and APP having five TSSs was reduced by 40%. I finally examined the possibility of targeting all three genes simultaneously and was able to knock down expression of all of the genes at the same time, demonstrating the feasibility of using dCas9/CRISPRi to perform complex manipulations of gene expression profiles (Figure 4.4, C).

4.3.4 Evaluation of Putative Off-Target Silencing by CRISPRi

Putative off-targets of the SNCA TSS2-1 sgRNA were identified by a BLAT search (Table 4.1). Three putative off-target candidates were chosen for evaluation based on the likelihood that altering their expression would produce a phenotypic outcome (i.e. presence within the coding region or promoter of a gene) as well as the directionality of sgRNA complementarity (i.e. the sgRNA would align to the non-template strand). With these criteria, THRB, AK093107 and MIPEPP3 were chosen for analysis by qRT-PCR in SNCA TSS2-1 sgRNA-transfected HEK293T cells (Figure 4.5). Among these three putative off-target genes, THRB was the only one validated to undergo off-target silencing by the SNCA TSS2-1 sgRNA. AK093107 appeared to be activated nearly 2-fold and MIPEPP3 expression was unchanged.

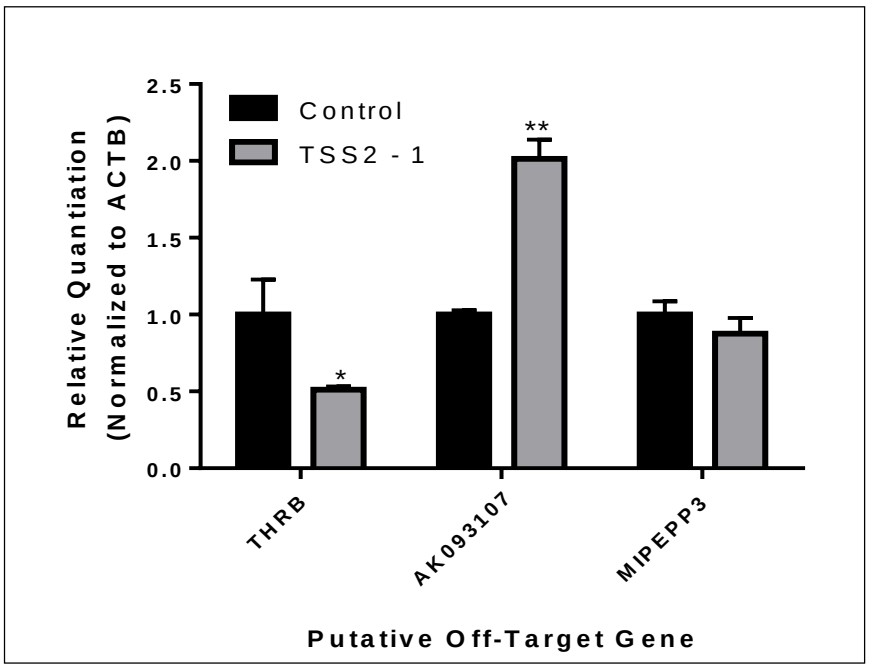

Figure 4.5 qRT-PCR for Putative Off-Target Genes in SNCA TSS2-1 sgRNA Transfected HEK293T Cells

Figure 4.5 qRT-PCR for Putative Off-Target Genes in SNCA TSS2-1 sgRNA Transfected HEK293T Cells

Of three putative off-target genes examined, one (THRB) showed decreased expression, one (AK093107) showed increased expression and one (MIPEPP3) showed no alteration. Data are represented as mean ± SEM of n = 3 non-transfected control wells and n = 3 dCas9/TSS2-1 sgRNA-transfected wells. Statistical significance was determined by one-way ANOVA.

*p ≤ 0.05 compared to control, **p ≤ 0.01 compared to control

4.4 Discussion

In addition to its role as a primary mediator of PD, alpha-synuclein pathology has been described as a common feature of other synucleinopathies, including PD with dementia (PDD), dementia with LBs (DLB) and multiple systems atrophy (MSA)[379, 380]. Comorbidity is often observed between the synucleinopathies and other neurodegenerative diseases which share the common molecular events of protein misfolding or accumulation, aggregation and deposition, collectively known as proteinopathies[381]. For example, overabundance of amyloid precursor protein, encoded by the APP gene, which aggregates to form β-amyloid is a well-established mechanism of AD pathology[382, 383]. Accumulation of hyperphosphorylated microtubule associated protein tau, encoded by the MAPT gene, is the central event of the tauopathies, of which AD[384] and frontotemporal dementia with Parkinsonism linked to tau mutations on chromosome 17 (FTDP-17)[385] are notable examples. The co-occurrence of synucleinopathy with β-amyloid and tau pathology in cases that have been attributed purely to one disease classification has spurred the concept of a continuum between these diseases[381]. Thus, the development of novel tools for interrogating genetic contributions to the common processes of proteinopathies could result in therapies that benefit patients across a broad spectrum of neurodegenerative disorders[381, 386].

Catalytically dead Cas9 (dCas9) has been applied in an, as of yet, relatively small set of papers for diverse applications and in varied model

systems, the findings of which are synthesized with the results presented in this chapter below.

Qi et al. published the first study reporting that dCas9, lacking endonuclease activity, could be applied as an RNA-guided DNA binding protein for regulation of gene expression[222]. Shortly thereafter, Gilbert et al. reported that dCas9-mediated gene repression (CRISPRi) and activation (CRISPRa), could be enhanced by fusion of dCas9 to transcriptional repressor and activator domains, respectively[377]. The same group subsequently published a protocol to facilitate the design, construction and testing of sgRNAs for use in this system in Larson et al. 2013[387].

Among the first studies to demonstrate that CRISPRi could be applied to interrogate the functions of genes involved in complex human diseases were those of Gilbert et al. 2014[388] and Lawhorn et al. 2014. Gilbert et al. demonstrated that CRISPRi can be used on a genome-wide scale to interrogate gene function in the presence or absence of repressor domains. Lawhorn et al., applied CRISPRi to silence expression of the important tumor suppressor gene TP53 (p53)[389]. The authors evaluated the efficacy of dCas9-mediated transcriptional silencing in the presence and absence of a KRAB transcriptional repressor domain. This report demonstrated that dCas9 alone can mediate efficient CRISPRi, achieving up to 86% transcriptional silencing, in the absence of a repressor domain. This is consistent with the results presented in this chapter which suggest

that, even in the absence of repressive domains, CRISPRi represents a robust system for transcriptional silencing of eukaryotic genes in a position-dependent manner, specifically, when proximal to the TSS of a gene. Interestingly, I observed that the number of TSSs for a gene was inversely correlated to the level of repressive activity that could be achieved by CRISPRi. This may be explained by the presence of focused versus dispersed promoters or genomic features such as CpG islands versus TATA promoters[390]. This finding is particularly important to the broad application of this technique for gene silencing, given that many genes have multiple TSSs[391]. Similar position dependence for efficient CRISPRi, specifically TSS proximity, has recently been observed at other human genes, suggesting that this may be a general phenomenon[392].

Other studies have validated the finding that dCas9 alone can efficiently and reproducibly mediate efficient CRISPRi by preventing the binding of endogenous transcription factors to *cis*-elements[393 394]. In addition, it has been demonstrated that dCas9-repressor domain fusion proteins also exert their gene regulatory actions via *cis*-elements. Kearns et al. fused dCas9 to a histone demethylase, LSD1, as a tool for examining the roles of defined and novel enhancers in the maintenance of pluripotency in mESCs[395]. This study provided some mechanistic insight into the activity of both the dCas9-LSD1 and dCas9-KRAB fusion proteins in gene silencing. The KRAB effector induced a loss of the active histone marker, H3K27ac, and an induction of the repressive histone markers, H3K27me3 and H3K9me3 at the TBX3 promoter. In contrast, the LSD1 effector did

not induce changes in histone markers at the promoter, but resulted in a strong loss in H3K4me2 and H3K27ac at an enhancer region. The authors therefore caution that the KRAB effector may have the unintended side effect of heterochromatin spreading and functions through promoter silencing, rather than decommissioning the enhancer, as in LSD1-mediated gene silencing.

Coupling of dCas9 to transcriptional activator domains allows the conversion of dCas9 into a programmable synthetic transcription factor. VP64 was the first transcriptional activator domain fused to dCas9 and was found to robustly induce transcriptional activation[396, 397]. Kearns et al. reported the first study to evaluate the possibility of using dCas9-VP64 to control the differentiation state of hESCs[398]. Specifically, dCas9-VP64 was used to activate expression of SOX17, a mediator of endoderm development. In addition, dCas9-KRAB was used to silence the important pluripotency gene, OCT4. This study established the feasibility of using dCas9 as an effector to promote the differentiation of pluripotent stem cells along a desired developmental lineage. In addition, this study attempted to dissect the mechanism of dCas9-mediated gene repression using four components: dCas9, dCas9-KRAB, an OCT4 sgRNA 158 bp upstream of the TSS (OCT4A-158), and an OCT4 sgRNA 12 bp upstream of the TSS (OCT4A-12). No morphological changes were observed in hESC cultures transfected with dCas9 and OCT4A-158. However, morphological changes were observed in hESC cultures transfected with dCas9 and OCT4A-12, with patches of downregulated Oct4 and Nanog and rare

SOX17-positive cells. Strikingly, both sgRNAs induced morphological changes when co-transfected with the dCas9-KRAB effector. Thus, the authors conclude that the activity of the sgRNA OCT4A-12 is partially dependent on inhibition of RNA polymerase II or other components of the basal transcription machinery, whereas the activity of the OCT4A-158 sgRNA is entirely dependent on KRAB domain activity.

Dead Cas9 can also be applied to promote the expression of pluripotency genes for reprogramming applications. Hu et al. used dCas9-VP64 to activate the expression of OCT4 in human HEK293T and mouse NIH3T3 cells[399]. The authors found that epigenetic modification of the OCT4 gene locus was central to its efficient activation, as co-transfection with the histone acetyltransferase, p300, enhanced CRISPRa and silencing of p300 with siRNA attenuated the efficiency of CRISPRa-mediated OCT4 transcriptional activation. Subsequent reports have built on this finding, developing a dCas9-p300 fusion which uses the p300 catalytic core to induce H3K27ac histone marks at target sites, and induces robust transcriptional activation with a single sgRNA[400]. This is useful for activing gene expression via dCas9 targeting at both promoters and enhancers, since the mechanism of gene activation in this case is the addition of the enhancer activating chromatin mark, H3K27ac by the p300 histone acetyltransferase. Gao et al. compared the relative efficacy of dCas9 and designer TALE transcription factors in inducing expression of OCT4 and Nanog reprogramming factors[394]. They showed that dCas9 is more efficient for gene repression via physical interference of transcription factor binding

at enhancers, but relatively weaker in active histone marker recruitment and recruitment of gene activating complexes compared to TALE transcription factors. They also constructed dCas9 expression constructs with VP64 fused to the N-terminus, C-terminus or both of dCas9, and found that the construct in which VP64 was expressed to both ends of dCas9 was most efficient in transcriptional activation. Other efforts to optimize the transcriptional activation domain for CRISPRa lead to the development of SunTag[388, 401] and MS2/PP7[402, 403] amplification systems, VP160 (10 tandem repeats of the VP16 transcriptional activator) by Cheng et al.[397] and the rational design of a tripartite transcriptional activation domain containing VP64, p65 and Rta domains (VPR) by Chavez et al.[404].

Engineered DNA-binding molecule-mediated chromatin immunoprecipitation, or enChIP, in which genomic regions are immunoprecipitated with antibodies to tags (i.e. HA) fused to dCas9, was developed to interrogate chromatin structure and associated proteins at specific genomic loci[405, 406]. Such an approach was used in this chapter to characterize the influence of differential sgRNA binding affinity of dCas9 on the efficiency of CRISPRi-mediated silencing of SNCA. Wu et al. and Kuscu et al. used enChIP-seq to conduct a genome-wide analysis of dCas9 binding in mouse ESCs[407] and human HEK293T cells[408], respectively. Both papers reported a large number of off-target binding sites for dCas9, although a low frequency of mutagenesis was observed when the same sgRNAs were introduced with a nuclease-competent Cas9. Wu et al. defined a 5-nucleotide seed region, in addition to the PAM,

which is required for dCas9 target binding and attributed the large number of off-target effects to this minimal requirement for dCas9 binding. This suggests that dCas9 may have more off-target activity than previously anticipated or reported. Note, however, that this could also be an artifact of crosslinking in ChIP, since this stabilizes even transient interactions. Recent unpublished work from Jennifer Doudna's group suggests that there is a requirement for perfect complementarity to achieve stable binding and cleavage by Cas9 proteins.

Overcoming off-target effects will necessarily involve improvements in the specificity of the dCas9 protein and the rational design of dCas9 sgRNAs. Oakes et al. presented a general method for screening or selection to promote directed evolution of dCas9, generating novel proteins with new functionalities that may overcome off-target binding[409]. In addition, new information about structure-function determinants of dCas9 interactions with DNA may contribute to efforts to overcome the off-target effects of dCas9 by defining novel features of the dCas9 protein which confer specificity to associated sgRNA sequences[410]. Xu et al. defined new sequence determinants in the design of sgRNAs for efficient CRISPRi/a[411]. Specifically, 19-nt spacers were found to have better efficiency than 17-, 18- and 20-nt spacers and purine-rich spacers were preferred. In contrast to CRISPR/Cas9 sgRNAs where a few nucleotides of the spacer adjacent to the PAM dominate sequence preference (likely due to sequence requirements for DNA cleavage), nucleotides throughout the spacer of CRISPRi/dCas9 sgRNAs were found to collectively contribute to sgRNA

efficiency. The authors developed an algorithm for CRISPRi/dCas9 sgRNA prediction, but noted that chromatin states and transcription factor binding may influence CRISPRi efficacy, in ways that cannot be predicted by the sequence context alone. In this chapter, I have demonstrated that sgRNA-mediated dCas9 binding affinity is a critical factor for the repressive activity of dCas9 in CRISPRi. This may be due to differences in the inherent binding affinity of individual sgRNAs, or chromatin structure around these regions. Consistent with this notion, and the hypothesis proposed by Xu et al., recent data suggests that Cas9 can bind more effectively to sequences within DNase hypersensitive sites that are associated with promoter regions[412].

Given that there is no loss of H3 signal (i.e. no H3 eviction due to dCas9 binding), the reduction of the H3K4me3 active chromatin marker in TSS2-1 and TSS2-2 sgRNA transfected cells may signify that the binding of the K4me3 histone methyltransferase complex may be affected by dCas9. This is typically the MLL complex at CpG island promoters through a CxxC domain binding non-methylated CpGs. How this is linked to transcription is still unclear, but the data presented here perhaps suggest that this could act in parallel with RNA polymerase II recruitment.

The finding that the pre-initiation (nonphosphorylated), but not initiation (Ser^5 phosphorylated), phospho-isoform of RNA polymerase II is affected by dCas9 binding suggests that dCas9 may inhibit the recruitment of the cyclin-dependent kinases (CDK7, CDK8 and CDK9) that mediate RNA

polymerase II C-terminal domain (CTD) phosphorylation during the transition from pre-initiation to initiation phases[413]. This suggests that efficient CRISPRi in mammalian cells may require blockage of transcription earlier than the previously postulated elongation phase. These findings regarding the mechanism of CRISPRi will be useful in the rational design of sgRNAs for CRISPRi, and may eventually be incorporated with other experimentally validated determinants of CRISPRi efficacy, such as those presented by Xu et al., to aid in defining new algorithms to predict activity of CRISPRi at particular genomic loci.

Methods to exert spatiotemporal and quantitative control of gene expression using dCas9 have also been developed. Wu et al., described the use of a blue light responding system to control sgRNA activity in cells which constitutively express dCas9 and demonstrated that this system can be used to quantitatively titrate the levels of target gene expression indirectly, as blue light intensity results in a decline in sgRNA expression and a resultant increase in target gene expression[414]. A similar report by Polstein and Gersbach has demonstrated that light-activated CRISPR-Cas9 effector (LACE) can be used to directly induce transcription of endogenous genes in the presence of blue light[415]. Balboa et al. demonstrated the feasibility of exerting temporal control of dCas9-mediated gene activation, achieved using a dCas9-VP192 (12 tandem repeats of the VP16 transcriptional activator) fused to the dihydrofolate reductase (DHFR) destabilizer domain (DD) wherein gene expression can be controlled by the introduction of trimethroprim[416]. This system can be

combined with other inducible systems such as TetON to exert tighter temporal control over gene expression. In addition, methods to execute transcriptional activation and transcriptional repression of different target genes within the same cell have recently been developed[402]. This technique uses dCas9 as a single effector, while using scaffold RNAs which encode both target specificity and regulatory action. This system will likely enable the use of dCas9 for recapitulating pleiotropic disease states in model systems and directing cell fates, both of which will require the activation of complex transcriptional networks.

Fusion of dCas9 to endonuclease domains re-instates the DNA cleavage capacity of the protein, while conferring added specificity. Specifically, dCas9 has been fused to the *Fok* I catalytic domain, which mediates cleavage of TALENs, to produce a novel nuclease-competent genome editing system[417]. The *Fok* I-dCas9 (fCas9) fusion is similar to the double-nickase CRISPR/Cas9 system in that it requires the appropriate alignment of two sgRNAs at an appropriate distance and on opposing DNA strands to conduct cleavage generating DNA double-strand breaks. The fCas9 system has been shown to have lower off-target mutagenesis rates than the double-nicking CRISPR/Cas9 system[417], and has been used to generate knockout mice[418, 419]. Compared to wild-type Cas9 and Cas9 nickase, fCas9 presented the best balance between mutation and birth rates[419]. In addition to the dimerization dependent cleavage conferred by the use of the *Fok* I domain, methods to further reduce the off-target activity of fCas9 have been employed, including sgRNA truncation[420].

Published protocols for designing fCas9 nucleases which take these advancements into consideration are already available[421].

Other bodies of work have demonstrated the wide utility of dCas9 in basic and translational research applications. dCas9 has been used for CRISPRa-mediated transcriptional activation in plants[422] and *Drosophila*[423] and for CRISPRi-mediated transcriptional silencing of genes in *Mycobacterium*[424] and *Actinomyces*[425] and miRNAs in murine[426], porcine[426], and bovine[427] cells. CRISPRi can be used to control gene expression in *E. coli*[222, 428], and since silencing cassettes are transferrable between *E. coli* cells, this approach could be applied to control bacterial populations[429] and for metabolic engineering[430]. In addition, dCas9 has been employed at the interface of computational biology and living systems to evaluate and manipulate outputs of synthetic circuits[431]. Others have already proposed that dCas9 could be used in future medical applications, for example to alter the expression of genes that promote stem cell graft survival in the ischemic heart[432] to mediate epigenetic modifications in tumor cells for treatment of cancer[433], and to treat graft-versus-host disease[434]. dCas9 has also been shown to have anti-bacterial and anti-viral applications[435-439]. Genome-wide sgRNA libraries for CRISPRi and CRISPRa have been described as a tool for screening and mapping complex transcriptional pathways[388], and such CRISPRi libraries have been demonstrated to perform similarly to optimized RNAi libraries in genome-wide screens[440]. Finally, dCas9 has been used for a variety of imaging applications. Anton et al. developed a dCas9-eGFP fusion protein to examine the location of

specific genome sequences in the nuclear architecture of mESCs[441]. Similar systems have been developed for live imaging of single[442] and multiple genomic loci, using multicolor fluorescence tagging of distinct dCas9 bacterial orthologs[443], as well as imaging fixed cells and primary tissue sections[444].

Much as the Golden Gate TALEN and TALE Effector Kits enhanced the accessibility of TALEN-mediated genome editing, similar CRISPRi/dCas9 effector toolkits have been developed[445, 446]. Despite the relative accessibility of dCas9-mediated transcriptional regulation, I could identify only one report which has used this system for any neuroscience-relevant applications: the Chavez et al. report indicated that co-transfection of dCas9-VPR with sgRNAs targeting neurogenin 2 (NGN2) and neuronal differentiation factor 1 (NEUROD1) was sufficient to induce the differentiation of neurons from iPSCs. Importantly, no reports to date have used this system for interrogating the contributions of disease-associated genes to the pathogenesis of any neurodegenerative diseases.

In this chapter, I have demonstrated that dCas9 can be utilized for multiplex transcriptional silencing of genes mediating proteinopathy-induced neurodegenerative diseases. In particular, I have shown that sgRNAs targeting SNCA reduce alpha-synuclein mRNA and protein levels across multiple cell lines. In addition, I have demonstrated that sgRNAs targeting other genes mediating proteinopathy-induced

neurodegenerative diseases, including MAPT and APP, can be silenced with this approach. Although results presented here support the position-dependence of dCas9 for CRISPRi, as well as present new findings regarding sgRNA binding affinity as a critical determinant of CRISPRi, and begin to explore the impact of dCas9 on chromatin structure and RNA polymerase recruitment, further work will be needed to ascertain the precise mechanism of action of CRISPRi towards the development of CRISPRi-mediated therapeutic approaches for neurodegenerative diseases.

In addition, further studies in human iPSC and animal models will need to be carried out to assess the viability of dCas9-mediated gene silencing for therapy in proteinopathy-induced neurodegenerative diseases. Assuming such investigations are successful, a remaining complication to the clinical translation of this technology is the lack of a robust approach for delivery of dCas9 protein and gene-specific sgRNAs to affected brain regions, primarily due to the requirement of crossing the blood-brain barrier (BBB). Advances in the delivery of biologic agents across the BBB may be adapted to overcome this limitation. For example, dCas9 could be re-engineered to cross the BBB by fusion to proteins that are known to facilitate BBB transfer. Fusion of dCas9 to BBB-penetrating neurotrophins, IgGs (where the IgG is a genetically engineered monoclonal antibody against human insulin receptor or transferrin receptor[447]), lysosomal enzymes, cell-penetrating peptides, or decoy receptors could enable the crossing of dCas9 protein across the BBB[448]. Such approaches would

require the use of 1) a separate delivery system for sgRNAs, 2) the engineering of a dCas9/BBB-penetrating fusion protein-sgRNA complex, or 3) a method to complex dCas9/BBB-penetrating fusion protein with sgRNA before delivery. Recent improvements in methods for loading of exosomes[449] and lipid nanoparticles[450] may enhance their utility as carriers of dCas9 and sgRNA for delivery across the BBB. Direct injection of dCas9 and sgRNA via neurosurgical techniques would bypass the BBB, however this approach would entail invasive procedures and rely on diffusion of dCas9 and sgRNA into cells neighboring the injection site[451]. Viral-mediated delivery is perhaps the best described approach for gene therapy in the brain. Indeed, all of the major classes of viral vectors have already been engineered and tested as vehicles for Cas9 and sgRNA delivery, including retrovirus, lentivirus, adenovirus and AAV[452]. Furthermore, the feasibility of generating retroviral, lentiviral, adenoviral and AAV vectors which co-express Cas9 and sgRNA has been demonstrated[453-456]. Further to demonstrating the feasibility of viral mediated delivery of dCas9, lentiviral vectors for delivery of dCas9 and sgRNAs have been developed and tested in CRISPRi and CRISPRa applications[388]. Importantly, AAV-mediated delivery of nuclease-competent Cas9 and sgRNAs has been demonstrated to induce robust gene editing in the mouse brain[457], and a similar approach could be applied with CRISPRi since the size of the dCas9 and sgRNA co-expression cassettes are similarly compatible with packaging into AAV vectors. This provides early support for the idea that CRISPR/Cas9-based strategies can be

utilized for studies of neurodegeneration, and perhaps eventually as tools in the treatment of brain diseases.

Taken together, these studies and the results presented in this chapter support further development of CRISPRi for biomedical research and therapeutic applications. CRISPRi represents a valuable approach to gene silencing, comparable to RNAi, the current state-of-the-art in gene repression, in ease of production and cost. Much as was learned from the rapid adaptation of RNAi in biomedical research, it is essential to evaluate and report off-target effects of dCas9 sgRNAs utilized for CRISPRi. Comparably, the action of both methods is guided by roughly 18 – 20 nt of target sequence complementarity, and thus it would be predicted that as many off-target effects might be observable in CRISPRi as were ultimately found for RNAi. However, whereas RNAi requires a region of only 6 – 8 nt of seed sequence[458] to exert activity at specific target sites, CRISPR/Cas9 sgRNAs require a minimum of 12 nt of seed sequence complementarity[459] (possibly more for CRISPRi/dCas9), making off-target effects less likely than for RNAi, and on-target effects more predictable. Indeed, it is remarkable that only one of three targets predicted to cause off-target activity with a single sgRNA exert a repressive effect – this is in contrast to the high frequency off-target activity observable with single Cas9 sgRNAs[460], or single siRNAs[461]. In addition, dCas9 can tolerate fewer mismatches within the sgRNA sequence than Cas9[214, 460, 462], and in contrast to RNAi, requires a protospacer adjacent motif (PAM) for repressive activity[377]. Furthermore, the present study and others[392] have demonstrated

that CRISPRi is only robust when targeting at or near the TSS of a gene. With a high sensibility to the potential for off-target effects of CRISPR/Cas9 and CRISPRi/dCas9, several leaders in the field have embarked upon efforts to enhance the specificity of both Cas9 and dCas9. Perhaps the most promising among these efforts for CRISPRi are the aforementioned coupling of dCas9 to transcriptional repressor domains[377, 395], which exert their functions either by interacting with native transcription factor machinery or by altering the chromatin structure within promoter and enhancer regions. In contrast to the present study, where dCas9 was used in the absence of such repressor domains, such fusion proteins may add a layer of specificity to exert more precise transcriptional control only at loci where such effector domains would naturally act. Another considerable advantage of dCas9 as a tool for gene expression alteration is the ability to activate gene expression at the same endogenous genomic loci from which gene expression can be silenced by coupling dCas9 to transcriptional activator domains[399, 400, 404]. In the short term, this presents one method to circumvent concerns that phenotypes observed by dCas9-mediated gene silencing might be exclusively attributed to off-target effects – if phenotypic outcomes follow a specific pattern with repression vs. activation, and off-target genes are not similarly altered, it builds confidence that the phenotypes observed are due to alterations in expression of the target gene of interest, rather than any off-target effects. Another approach that can be borrowed from RNAi is to use many sgRNAs with similar repressive (or activating) activity to evaluate phenotypes[458] – if the same phenotype is observed with different sgRNAs that possess

different off-target profiles, it again brings more confidence to phenotypic evaluations deriving from gene expression manipulations by CRISPRi/a.

With growing knowledge of the mechanisms by which CRISPRi can be induced efficiently and specifically, CRISPRi can be expanded to dissect the roles of genes with putative gain of function roles in other neurodegenerative diseases such as c9orf72 in ALS/frontotemporal dementia (FTD)[463] and LRRK2 in PD[464]. Further, CRISPRi can be employed in the development of therapy for diseases involving numerous systems in which gene overexpression induces pathology, such as HD[465], amyloidosis[466] and several cancers[467]. CRISPRi may thus soon emerge as a novel means of transcriptional repression for numerous investigations of genetic contributions to disease and therapeutic silencing of disease-associated genes.

Chromosome	Orientation	Start	End	Length	Associated Gene
4	***Plus***	***90758331***	***90758353***	***23***	***SNCA***
6	Minus	25279491	25279511	21	LRRC16A
6	Minus	4961574	4961594	21	
18	Minus	14960136	14960156	21	
15	Minus	53961171	53961191	21	WDR72
3	Plus	95781606	95781626	21	
3	Plus	24381807	24381827	21	THRB
3	Plus	11766698	11766718	21	
22	Plus	48098101	48098121	21	AK093107
2	Plus	13910169	13910189	21	
13	Plus	21918196	21918216	21	MIPEPP3
12	Plus	41110196	41110216	21	CNTN1
1	Plus	197949260	197949280	21	
3	Minus	74215356	74215375	20	
2	Minus	63130906	63130925	20	EHBP1
3	Plus	47591480	47591499	20	
2	Plus	126027228	126027247	20	
2	Plus	119330402	119330421	20	
2	Plus	48791736	48791755	20	STON1/STON1-GTF2A1L
1	Plus	214853230	214853249	20	
1	Plus	197334723	197334742	20	CRB1
1	Plus	165085242	165085261	20	
1	Plus	113980542	113980561	20	MAGI3

Table 4.1 BLAT-Identified Putative Off-Target Genes of SNCA TSS2-1 dCas9 sgRNA

Grey text indicates genes that were examined by qRT-PCR in SNCA TSS2-1 sgRNA transfected HEK293T cells (see also Figure 4.5).

Sequence Name	Forward	Reverse
SNCA Exon 1 dCas9	CACCGCGCACCTCACTTCCGCGTCG	AAACCGACGCGGAAGTGAGGTGCGC
SNCA Exon 1/2 SD dCas9	CCACGCCCGCTAACCTGTCGTCGAA	AAACTTCGACGACAGGTTAGCGGGC
SNCA Exon 1/2 SA dCas9	CCACGTGAATTCCTTTACACCACAC	AAACGTGTGGTGTAAAGGAATTCAC
SNCA Exon 2 dCas9	CACCGAGCAGCCACAACTCCCTCCT	AAACAGGAGGGAGTTGTGGCTGCTC
SNCA Exon 4 dCas9*	CACCGTGCTCCCTCCACTGTCTTCT	AAACAGAAGACAGTGGAGGGAGCAC
SNCA TSS1-1 dCas9 F+E	CACCGTCGGAAGATTAGTTAAGCAC	AAACGTGCTTAACTAATCTTCCGAC
SNCA TSS1-2 dCas9 F+E	CACCGAAGCCTTTGCTTTCTGTGCC	AAACGGCACAGAAAGCAAAGGCTTC
SNCA TSS1-3 dCas9 F+E	CACCGTTCCTGGATCACACCAGAA	AAACTTCTGGTGTGATCCAGGAAC
SNCA TSS2-1 dCas9 and dCas9 F+E	CACCGCTCCTCCTTCTCCTTCTCCT	AAACAGGAGAAGGAGAAGGAGGAGC
SNCA TSS2-1 Template dCas9 F+E	CACCGCGAGGAGAAGGAGAAGGAGG	AAACCCTCCTTCTCCTTCTCCTCGC
SNCA TSS2-2 dCas9 F+E	CACCGCCCCTCTCTTGGGCCCCTTC	AAACGAAGGGGCCCAAGAGAGGGGC
SNCA TSS2-3 dCas9 F+E	CACCGCACTTCCGCGTCGCGGCGCT	AAACAGCGCCGCGACGCGGAAGTGC
SNCA TSS3-1 dCas9 F+E	CACCGAACCCCGCGCCAGCCACCCG	AAACCGGGTGGCTGGCGCGGGGTTC
SNCA TSS3-2 dCas9 F+E	CACCGCTCAGCTATCTACCCTGAGC	AAACGCTCAGGGTAGATAGCTGAGC
SNCA TSS3-3 dCas9 F+E	CACCGAACAGCAGGCCCAAGTGTGA	AAACTCACACTTGGGCCTGCTGTTC
MAPT TSS-1 dCas9 F+E	CACCGCGAAGAGGGCGCGTTCCTG	AAACCAGGAACGCGCCCTCTTCGC
MAPT TSS-2 dCas9 F+E	CACCGTGGGTGGCGGTGACTGCGA	AAACTCGCAGTCACCGCCACCCAC
MAPT TSS-3 dCas9 F+E	CACCGAGCGGCGCTGCTGTTGGTGC	AAACGCACCAACAGCAGCGCCGCTC
APP TSS1-1 dCas9 F+E	CACCGTAACCCCCAACGTCAAAAGC	AAACGCTTTTGACGTTGGGGGTTAC

APP TSS1-2 dCas9 F+E	CACCGAGTGAAGCTTAAAGGAAAT	AAACATTTCCTTTAAGCTTCACTC
APP TSS1-3 dCas9 F+E	CACCGAGAGGTGGGGCAGGCGTTTC	AAACGAAACGCCTGCCCCACCTCTC
APP TSS2-1 dCas9 F+E	CACCGCTTGAATCATCCGACCCCGC	AAACGCGGGGTCGGATGATTCAAGC
APP TSS2-2 (NGG) dCas9 F+E	CACCGAGGTGAGTCCTAGGACGCTG	AAACCAGCGTCCTAGGACTCACCTC
APP TSS2-2 (NAG) dCas9 F+E	CACCGCTGAGGCTCTAGAAAAGTC	AAACGACTTTTCTAGAGCCTCAGC
APP TSS2-3 dCas9 F+E	CACCGAGAGGGACGGTGCAGGATCA	AAACTGATCCTGCACCGTCCCTCTC
APP TSS3-1 dCas9 F+E	CACCGCGGCGGCGGGGCTCAGAGCC	AAACGGCTCTGAGCCCCGCCGCCGC
APP TSS3-2 dCas9 F+E	CACCGACCGCTGCCGAGGAAACTGA	AAACTCAGTTTCCTCGGCAGCGGTC
APP TSS3-3 dCas9 F+E	CACCGCCACCGCCGCCGTCTCCCG	AAACCGGGAGACGGCGGCGGTGGC
APP TSS4-1 dCas9 F+E	CACCGCCAACTTCTAAGCTAACAA	AAACTTGTTAGCTTAGAAGTTGGC
APP TSS4-2 dCas9 F+E	CACCGAACTTCTACCACGCACAGCA	AAACTGCTGTGCGTGGTAGAAGTTC
APP TSS4-3 dCas9 F+E	CACCGCAGAGCTTCCATCCTCGGGA	AAACTCCCGAGGATGGAAGCTCTGC
APP TSS5-1 dCas9 F+E	CACCGCGTGTTCTCCAAAAAAGAG	AAACCTCTTTTTTGGAGAACACGC
APP TSS5-2 dCas9 F+E	CACCGCCCACCAGCCTATCCTTCTC	AAACGAGAAGGATAGGCTGGTGGGC
APP TSS5-3 dCas9 F+E	CACCGTTAGAGATTGGACTTTCAGC	AAACGCTGAAAGTCCAATCTCTAAC

Table 4.2 Table of sgRNA Oligonucleotides

*The same sgRNA was used to make the SNCA exon 4-targeting dCas9 vector as was used to generate the SNCA exon 4-targeting Cas9 nickase sgRNA 1 vector.

Table 4.3 Table of qPCR Primers

Primer Name	Forward	Reverse
ACTB qRT-PCR	**CACAGAGCCTCGCCTTTG**	**GCGGCGATATCATCATCCAT**
SNCA qRT-PCR (Total)	**CCTTCTGCCTTTCCACCCT**	**TCCCTCCTTGGCCTTTGAAA**
SNCA-140 qRT-PCR	**GTGGCAACAGTGGCTGAGAA**	**CCTTCTTCATTCTTGCCCAACTG**
SNCA-126 qRT-PCR	**CTCTATGTAGTGGCTGAGAAGACC**	**CCTTCTTCATTCTTGCCCAACTG**
SNCA-112 qRT-PCR	**GTGGCAACAGTGGCTGAGAA**	**TGATACCCTTCCTTGCCCAAC**
SNCA-98 qRT-PCR	**CTCTATGTAGTGGCTGAGAAGACC**	**TGATACCCTTCCTTGCCCAAC**
SNCA ChIP qPCR	**AGATAGGGACGAGGAGCACG**	**CCCGCACGCACCTCACTT**
MAPT qRT-PCR	**CCTCGCCTCTGTCGACTATC**	**CTCTTGGTCTTGGTGCATGG**
APP qRT-PCR	**GGTTTGGCACTGCTCCTG**	**CAGAACATGGCAATCTGGGG**
THRB qRT-PCR	**AGGGCACTGGTAATTTGGCT**	**ATGTGTGGAACTTGGCACC**
AK093107 qRT-PCR	**TTGGGCCCAGTTCTCCTTTT**	**CTTCCCCGGGTCCTGAATC**
MIPEPP3 qRT-PCR	**AGCCTTGAAGCCGGGATC**	**CGGTCCACAAGCAATTCTGT**

Chapter 5: The IRE1a Axis of the UPR is Selectively Activated in Neural Derivatives of PD Patient-Specific SNCA Triplication iPSCs

5.1 Introduction

In this chapter, I provide evidence that the overabundance of wild-type alpha-synuclein, ensuing from SNCA triplication, results in activation of the IRE1a arm of the UPR, culminating in CHOP-mediated apoptosis of PD patient-specific iPSC-derived neurons. In addition to providing novel insights into the role of pathogenic levels of alpha-synuclein in eliciting a specific cellular stress response in PD, this finding highlights the IRE1a arm of the UPR as a potential target for therapeutic development.

5.2 Materials and Methods

The materials and methods applied in this chapter are the same as those described in Chapter 2, including the following: iPSC culture; generation, maintenance and neuronal differentiation of iPSC-derived NSCs; CRISPR/Cas9 construction and testing; RNA extraction, reverse transcription and qPCR; immunostaining. Sequences of qPCR primers used this chapter are listed in Table 5.1.

5.3 Results

5.3.1 SNCA Triplication NSCs and Neurons Display Intracellular Inclusions and Decreased Final Cell Density Compared to Healthy Controls

NCRM-5 healthy control (henceforth normal alpha-synuclein = NAS) and ND34391G PD-patient derived (henceforth alpha-synuclein triplication = AST) iPSCs were differentiated into a homogenous intermediate neural stem cell (NSC) population by dual SMAD inhibition using an established protocol[159], as described in Chapter 2 (Figure 5.1, A and B). This approach is used to minimize the presence of endodermal, mesodermal and non-neural ectodermal derivatives in the final population, to reduce the time required for neuronal maturation and to limit the requirement for expensive growth factors in the differentiation protocol. NSCs were further differentiated into neurons, closely following the protocol for cortical neuron differentiation described in Chung et al. 2013[163], which is adapted from previous reports[159, 162, 468]. This protocol produces a near-homogenous (~85 – 90%) population of neurons which express the neuronal markers, MAP2 and TUJ1 (Figure 5.1, C). At all stages of differentiation, AST derivatives are morphologically comparable to their NAS counterparts, with two exceptions. First, a subset of AST NSCs and neurons, but not iPSCs, contain phase-bright intracellular inclusions (see red arrows to inserts in Figure 5.1, B). Alpha-synuclein immunostaining demonstrates that alpha-synuclein-dense foci appear at approximately the same perinuclear location as these phase-bright intracellular inclusions, indicating that these inclusions are likely at least partially composed of

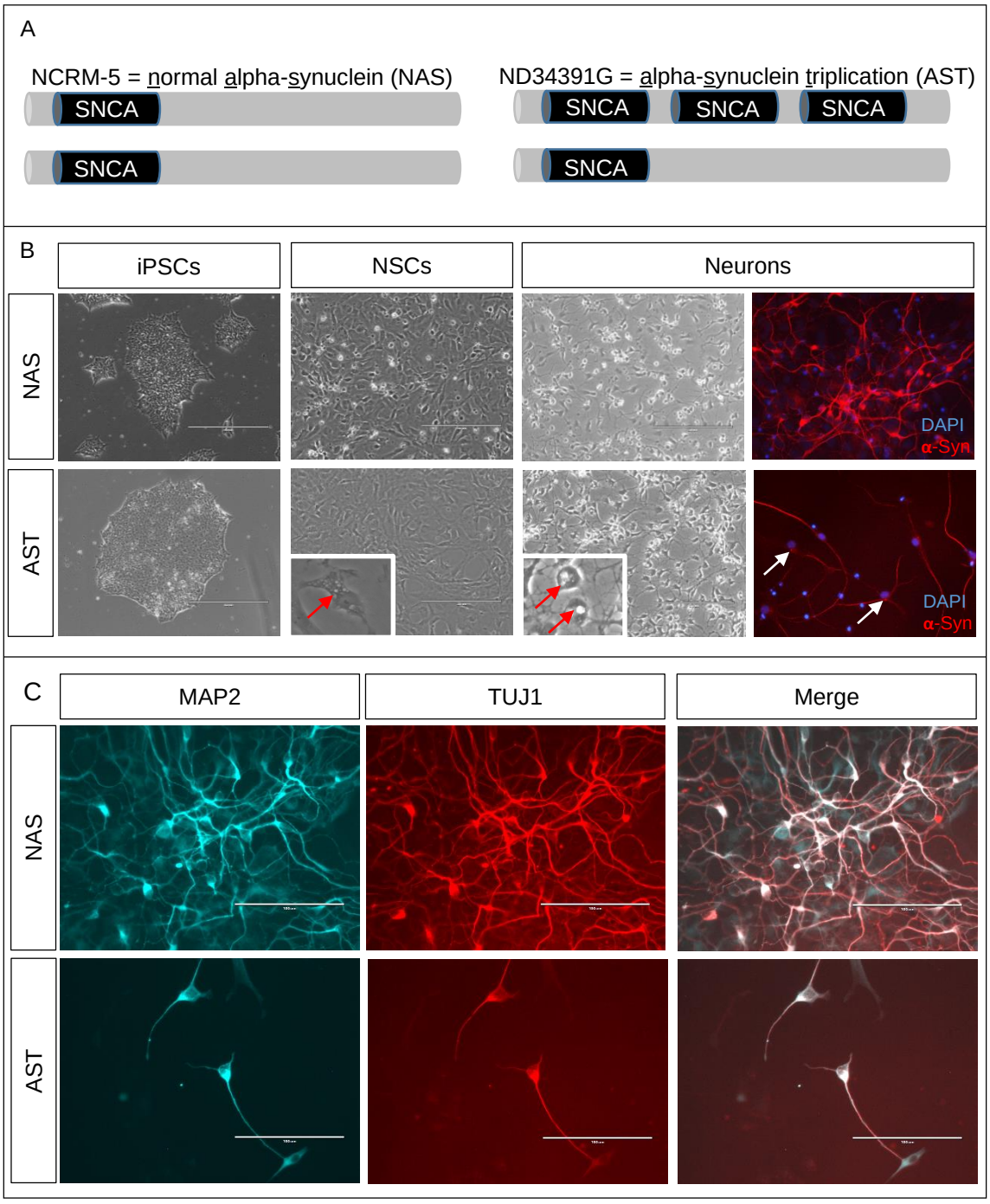

Figure 5.1 Morphological and Immunohistochemical Characterizations of iPSC-Derived Neurons.

Figure 5.1 Morphological and Immunohistochemical Characterizations of iPSC-Derived Neurons

A) Schematic representation of SNCA gene locus copy number in NCRM-5 healthy control (normal alpha-synuclein = NAS) iPSCs/derivatives and ND34391G PD patient-derived (alpha-synuclein triplication = AST) iPSCs/derivatives.

B) Morphology of NAS and AST iPSCs (10x magnification), NSCs (20x magnification) and neurons (20x magnification). Intracellular inclusions are highlighted in expanded view inserts by red arrows. Far right neuronal panels show alpha-synuclein immunostaining, which demonstrated alpha-synuclein-dense foci in the same approximate perinuclear location as these phase-bright intracellular inclusions (white arrows).

C) Immunofluorescence labeling of NAS and AST neurons with the pan-neuronal markers, MAP2 (40x magnification) and TUJ1 (40x magnification). Overlay is shown in the right panel (40x magnification).

alpha-synuclein (Figure 5.1, B). Second, despite seeding the same number of cells, there was a noticeable decline in cell density in the AST neuronal differentiations, particularly after dbcAMP-induced neuronal maturation between days 7 - 15 (Figure 5.1, C).

5.3.2 Neural Derivatives of SNCA Triplication iPSCs Express Elevated Levels of Alpha-Synuclein mRNA Compared to their iPSC Precursors

Interestingly, despite the presence of four genomic copies of alpha-synuclein in AST iPSCs, NSCs and neurons, the relative expression of alpha-synuclein mRNA as measured by qRT-PCR varied widely across these differentiation stages (Figure 5.2). AST iPSCs expressed three times the amount of alpha-synuclein mRNA as NAS iPSCs, roughly correlating to the number of genomic copies of alpha-synuclein. AST NSCs in contrast, expressed 36 times the amount of alpha-synuclein mRNA as NAS NSCs, whereas AST neurons expressed 17 times the amount of alpha-synuclein mRNA as NAS neurons.

5.3.3 The IRE1a Axis of the UPR is Strongly Activated in Neural Derivatives of iPSCs Bearing a Triplication of the SNCA Gene Locus

I next explored whether the overabundance of wild-type alpha-synuclein in AST triplication iPSCs, NSCs and neurons would lead to an activation of the UPR (Figure 5.3). In general, I found that the expression levels of UPR components are not distinguishable in AST iPSCs compared to NAS

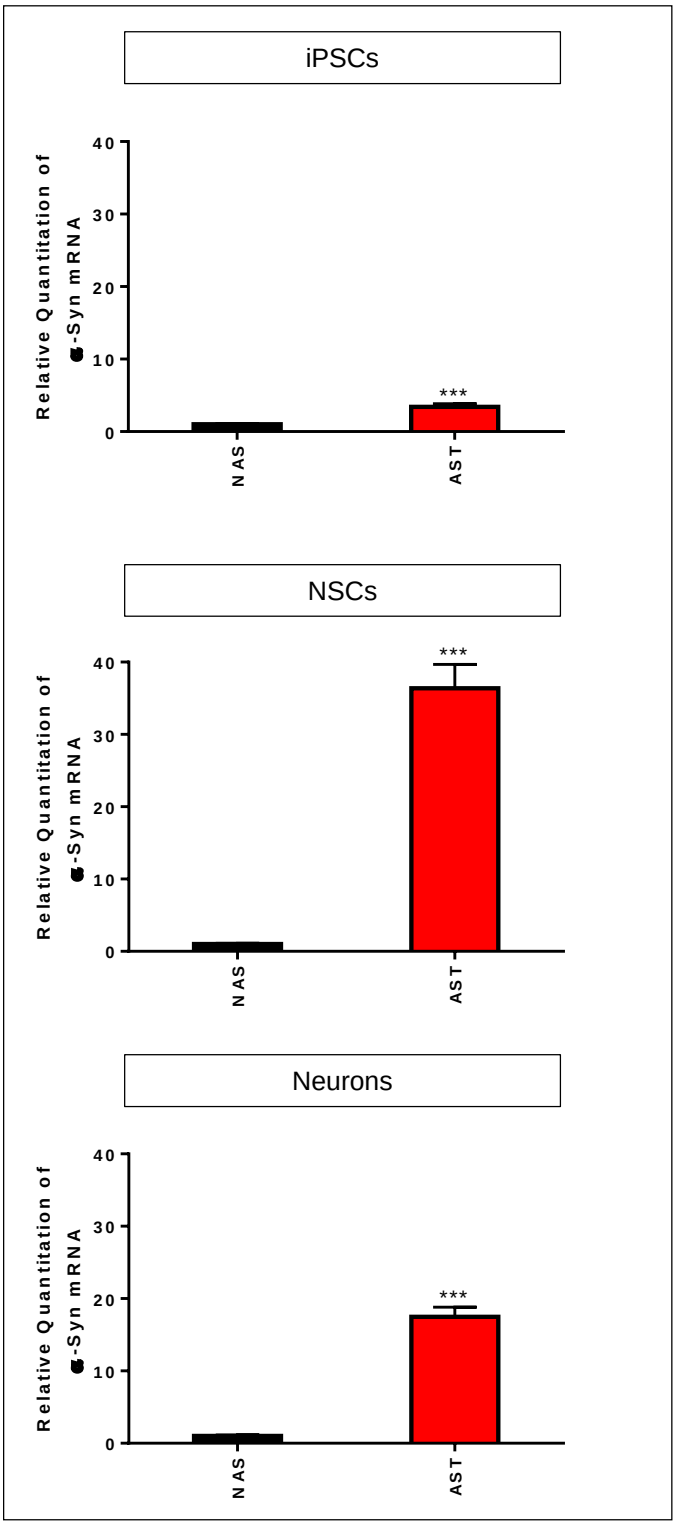

Figure 5.2 Alpha-Synuclein Expression Levels in iPSCs and Neural Derivatives

Figure 5.2 Alpha-Synuclein Expression Levels in iPSCs and Neural Derivatives

Examination of alpha-synuclein (α-Syn) mRNA levels in NAS and AST iPSCs, NSCs and neurons by qRT-PCR. AST iPSCs express 3X alpha-synuclein compared to NAS iPSCs. AST NSCs and neurons express 36X and 17X alpha-synuclein compared to NAS NSCs and neurons, respectively. Data are represented as mean ± SEM of n = 3 NAS wells and n = 3 AST wells at each differentiation stage: iPSCs, NSCs and neurons. Statistical significance was determined by one-way ANOVA.

*** = $p \leq 0.001$

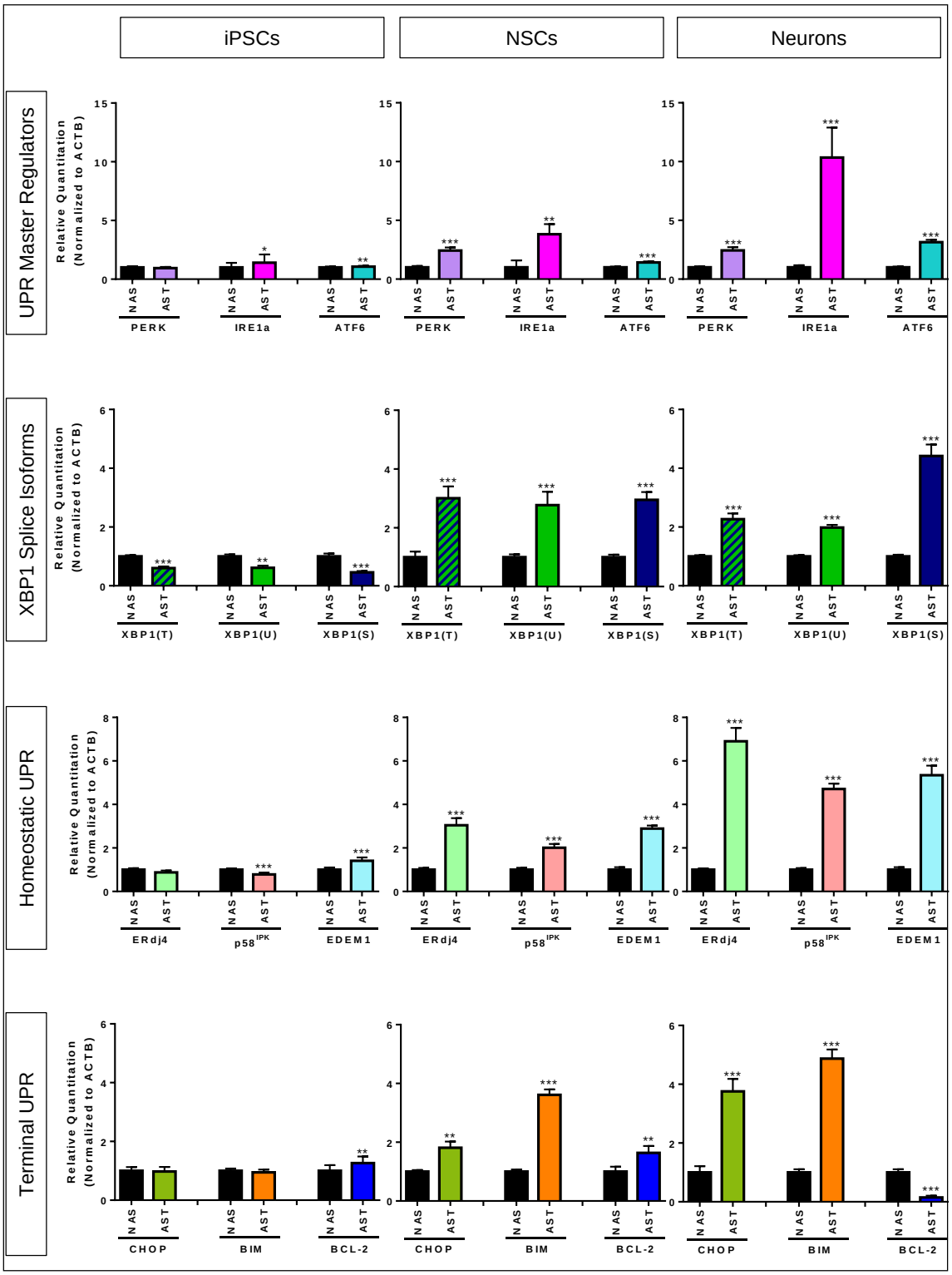

Figure 5.3 The IRE1a Axis of the UPR is Activated in iPSC-Derived NSCs and Neurons Bearing an SNCA Triplication

Figure 5.3 The IRE1a Axis of the UPR is Activated in iPSC-Derived NSCs and Neurons Bearing an SNCA Triplication

UPR gene expression profiling by qRT-PCR comparing NAS and AST iPSCs, NSCs and neurons. AST iPSCs generally lack UPR activation compared to NAS iPSCs. Activation of the IRE1a axis becomes evident in AST NSCs and amplified in AST neurons compared to NAS NSCs and NAS neurons, respectively. Notably, terminal UPR activation is attenuated in AST NSCs compared to AST neurons, as evidenced by the lesser induction of CHOP and BIM, and compensatory activation of BCL-2. Data are represented as mean ± SEM of n = 3 NAS wells and n = 3 AST wells at each differentiation stage: iPSCs, NSCs and neurons. Statistical significance was determined by one-way ANOVA.

* = $p \leq 0.05$, ** = $p \leq 0.01$ and *** = $p \leq 0.001$

iPSCs. This is in contrast to the clear activation of the UPR in AST NSCs and neurons compared to their NAS equivalents. I began by examining the expression of the UPR master regulators, PERK, ATF6 and IRE1a in AST NSCs and neurons by qRT-PCR. Surprisingly, all of the UPR master regulators were elevated in AST NSCs and neurons, compared to NAS controls. However, IRE1a demonstrated a clear and strong activation, approximately 4-fold in AST NSCs and 10-fold in AST neurons compared to NAS controls. As activated IRE1a is known to have endoribonuclease activity that induces the non-canonical splicing of a 26-nucleotide intron from XBP1 mRNA, I next examined the expression of total (T), unspliced (U) and spliced (S) XBP1. Interestingly, using primers specific for different spliced forms of XBP1, I showed that all splice isoforms were elevated in AST NSCs, however, a clear induction of XBP1 splicing was additionally observed in AST neurons. I next examined the expression of well-described XBP1s homeostatic and terminal UPR targets. Several components of the homeostatic UPR machinery were found to be elevated in AST NSCs and neurons, with the response magnified in AST neurons compared to NSCs. These include the ER chaperone, ERdj4, the PERK phosphorylation inhibitor and UPR fate-switching molecular timer, $p58^{IPK}$, and the ERAD mediator, EDEM1. Finally, the pro-apoptotic terminal UPR components CHOP and BIM were mildly elevated AST NSCs. The anti-apoptotic BCL-2 is concomitantly activated in AST NSCs, indicating a compensatory effort to evade apoptosis. In contrast, AST neurons appear to have committed to undergoing apoptosis due to the stronger activation of pro-apoptotic CHOP and BIM and repression of anti-apoptotic, BCL-2.

5.3.4 Transcriptional Activation of SNCA via dCas9-VPR in Healthy Control iPSC-Derived Neurons Induces the IRE1a Axis of the UPR

As NSCs from the AST isogenic iPSC line described in Chapter 3 are still in production, I could not yet evaluate whether IRE1a-mediated UPR activation is attenuated in neuronal derivatives from cells of the same genetic background as the AST iPSC-line wherein alpha-synuclein expression has been normalized. I therefore considered the possibility that the IRE1a activation observed may be a cell line-specific effect. I thus endeavored to determine whether activation of IRE1a was similarly induced by endogenous alpha-synuclein overexpression in NAS neurons. Nuclease-null Cas9 (dCas9) has been shown to induce endogenous gene expression when fused to a rationally-designed tripartite transcriptional activator, VP64-p65-Rta (VPR)[404]. When dCas9-VPR and the TSS2-2 sgRNA (please see Chapter 4) were co-transfected into NAS neurons, I observed an 8-fold upregulation of alpha-synuclein expression (Figure 5.4). After only 48 hours of alpha-synuclein induction, IRE1a levels are elevated nearly 2-fold. This suggests that endogenous activation of alpha-synuclein is sufficient to induce IRE1a-specific activation of the UPR, and that such activation may be an early contributing event in PD pathogenesis. The ability to perform such modulations of alpha-synuclein expression enable timecourse experiments to be performed to establish the order of cytopathogenic events upon alpha-synuclein overexpression.

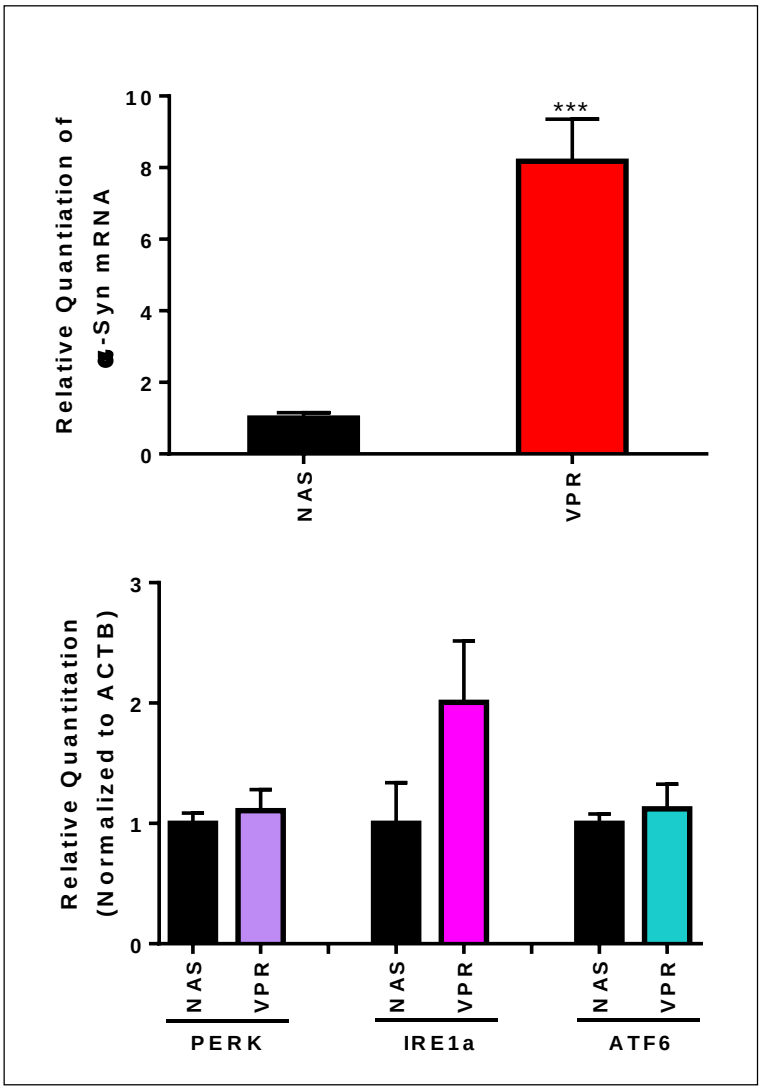

Figure 5.4 Transcriptional Activation of SNCA via dCas9-VPR in NAS Neurons Induces IRE1a Expression

Figure 5.4 Transcriptional Activation of SNCA via dCas9-VPR in NAS Neurons Induces IRE1a Expression

Co-transfection of dCas9-VPR with the TSS2-2 sgRNA in NAS neurons (VPR) induced alpha-synuclein (α-Syn) mRNA expression up to 8X that of non-transfected NAS neurons (NAS). After 48 hours, IRE1a expression is upregulated 2-fold in dCas9-VPR/TSS2-2 sgRNA transfected NAS neurons. Data are represented as mean ± SEM of n = 3 NAS wells and n = 3 VPR wells. Statistical significance was determined by one-way ANOVA.

*** = $p \leq 0.001$.

5.4 Discussion

Although Devine et al.[350] did not report any significant difference in neurogenic potential between NAS and AST iPSC lines, the results presented here suggest that AST iPSC-derived neurons undergo apoptosis during maturation, resulting in a reduced final population of neurons in AST cultures compared to NAS controls. This discrepancy may be partially explained by the fact that Devine et al. differentiated DA neurons in their studies, whereas the neurons I have characterized have been generated using a protocol for cortical neuron differentiation. Based on this observation, the differences in neurogenic potential detected in my studies are consistent with previous reports which have hypothesized that alpha-synuclein overexpression may differentially contribute to neuronal pathology in different brain regions and neuronal subtypes.

Further, in this chapter, I have identified a visible cellular phenotype of SNCA triplication in NSCs and neurons, specifically, phase-bright cytosolic intracellular inclusions that are generally larger in neurons than in NSCs and morphologically resemble the characteristic proteinacous inclusions that result from canonical protein aggregation[469]. It is possible that these are the same or similar structures to those observed by Flierl et al. in NPC-derivatives[351], or those described by Byers et al. in DA neuron-derivatives[353] of the same SNCA triplication iPSCs. Immunostaining confirms that these inclusions are at least partly composed of aggregated alpha-synuclein, possibly in complex with ubiquitin or bound by autophagosomal

membranes resulting from the cell's attempt to rid itself of alpha-synuclein induced proteotoxicity via the UPS or autophagy pathways. Consistent with the notion that these inclusions are partially composed of alpha-synuclein, iPSCs, which express the least alpha-synuclein of the differentiation stages examined, do not show these structures. In subsequent experiments, electron microscopy will help identify the ultrastructural characteristics of these inclusions and immunolabeling, for example with antibodies to detect autophagic proteins and ubiquitin, will be used to decipher other components of their composition.

Previous reports have demonstrated that alpha-synuclein is ubiquitously expressed in human tissues throughout development[470]. Rodent models have revealed that during CNS development, alpha-synuclein mRNA levels peak early and then decline and stabilize at relatively high expression levels in adults[126]. Consistent with these results, I found that alpha-synuclein overexpressed from the same four genomic copies demonstrates a similar peak of expression in NSCs, and decline in neurons. This adds to the inference that there may be some as of yet undiscovered regulators of alpha-synuclein expression in neurons and speaks to the importance of examining the pathological influences of alpha-synuclein expression from its endogenous context.

Many studies have investigated the role of the IRE1a axis of the UPR in PD. Conditions that increase susceptibility to PD, such as

hyperhomocysteinemia[471] have been shown to activate XBP1 splicing[472]. In addition, environmental toxicants which cause PD have been demonstrated to activate the IRE1a arm of the UPR. Holtz et al. found that 6-OHDA induces XBP1 splicing and CHOP activation in MN9D dopaminergic neuroblastoma cells and primary mesencephalic neurons[295]. In separate reports, Yang et al. and Niso-Santano et al. found that paraquat induces apoptosis in SH-SY5Y neuroblastoma cells via the IRE1a/ASK1/JNK cascade[473, 474]. Exogenous delivery of XBP1s was shown to protect against DA neuron death in response to MPP+ and proteasome inhibitors in a cell culture model, and in response to MPTP in a mouse model[475]. Other studies have demonstrated that the IRE1a arm of the UPR may have distinct age-related influence on DA neuron survival. For example, Valdés et al. showed that developmental ablation of XBP1 protected against SNc DA neurodegeneration in response to 6-OHDA, and that this neuroprotective effect was mediated by preconditioning with an adaptive ER stress response[476]. In contrast, the same paper demonstrated that silencing XBP1 in adult animals resulted in chronic ER stress and resultant SNc DA neuron degeneration[476]. In adult animals, 6-OHDA-mediated SNc degeneration could be rescued by exogenous delivery of XBP1s[476]. Janyou et al. demonstrated that pharmacological agents which rescue thapsigarin-mediated ER stress-induced cell death in SK-N-SH cells act partially via inhibiting phosphorylation of IRE1a[477]. Finally, XBP1s has been intricately linked to the neuroprotective actions of the PD-related genes, Parkin and DJ-1[478].

Although these studies have contributed to our understanding of the IRE1a pathway in PD pathogenesis, they provide conflicting insights regarding whether this pathway is neuroprotective or neurotoxic in PD, and thus as to whether (and in which way) modulating this pathway might have any therapeutic advantage. Importantly, no previous studies have examined ER stress-induced UPR activation in the case of SNCA triplication. Whereas alpha-synuclein-induced PERK activation has been widely described, to my awareness, this is the first report of activation of the IRE1a axis of the UPR in the context of alpha-synuclein overabundance due to SNCA triplication. It is important to note that many of the previous reports describing PERK-mediated UPR activation have derived from studies on DA neurons in the SNc of post-mortem human brains or animal models, or dopaminergic-like neuroblastoma cell culture models. Although the motor symptoms of PD caused by the selective loss of dopaminergic neurons in the SNc are a well described phenomenon in PD, the impact of non-motor symptoms of PD on quality of life, such as cognitive decline, are increasingly recognized. Cognitive decline is experienced by approximately 80% of PD patients, and often progresses to dementia[479]. As cortical neuron degeneration is the strongest pathological correlate to cognitive decline[1], it is of interest to evaluate the role of cellular stress pathways in mediating cortical neuron degeneration in PD. Thus, I have focused my efforts on examining the role ER stress and UPR activation in neurons generated via a protocol established to produce forebrain-type cortical neurons[159, 162, 163, 468]. I thus cannot exclude the possibility that the relatively weak activation of the PERK and ATF6 pathways that I observed

is related to the neuronal type I am investigating: this would in fact be consistent with aforementioned studies which have demonstrated that different brain regions and neuronal subclasses may differentially activate the UPR in response to alpha-synuclein-induced neurotoxicity[312, 337]. Similarly, these different mechanisms of UPR activation may relate to differences in the levels of alpha-synuclein expression in these different models[312].

Although this is the first study to demonstrate that SNCA triplication induces IRE1a-specific activation of the UPR, the findings presented here stand in agreement with previous literature which has implied that alpha-synucleinopathy may activate this arm of the UPR. In their 2011 study, Bellucci et al.[313] infer that the IRE1a and ATF6 arms of the UPR may be activated in a similar manner to the reported activation of PERK due to derepression via alpha-synuclein sequestering BiP in the ER lumen in cell culture and animal models of PD. This inference is supported by the finding of elevated GRP78/BiP, which is itself a downstream target of the IRE1a and ATF6 arms of the UPR. In a subsequent review, Hoozemans et al. 2012[480], describe unpublished data that supports the presence of elevated phosphorylated IRE1a in neuromelanin-containing neurons of the SNc in postmortem PD patient samples compared to controls. In addition, Castillo-Carranza et al.[322] showed that IRE1a is specifically induced by alpha-synuclein oligomers. This perhaps suggests that overexpression of alpha-synuclein to the extent that it oligomerizes at the ER is crucial for

the activation of the IRE1a arm of the UPR that I observe in SNCA triplication neurons.

It remains to be determined whether IRE1a activation is protective or pathogenic, and it is likely that the outcome is context specific. For example, I observed activation of the IRE1a arm in both NSCs and neurons, but apoptotic death only in neurons. One explanation for this is that post-mitotic cells, such as neurons, are incapable of titrating the levels of aggregation prone proteins by division[481, 482]. The IRE1a pathway could therefore be adaptive in NSCs where division is capable of limiting the duration of the alpha-synuclein-induced ER stress insult, becoming pathogenic in neurons due to the long-lasting burden of accumulated alpha-synuclein. This is consistent with the fact that I observed higher levels of alpha-synuclein in AST NSCs than in AST neurons, but apoptotic induction only in neurons. Intriguingly, the loss of cellular density in differentiated AST neurons may be attributed to this elevated activation of apoptosis.

Interestingly, IRE1a is a mediator of another cell-fate determining pathway, termed regulated IRE1-dependent decay (RIDD)[227]. It is thought that when ER-stress reaches threshold, RIDD is activated, wherein the ribonuclease activity of IRE1a cleaves a selection of RNAs other than XBP1, including miR-17 which has been shown to control apoptosis by regulating the expression of caspase-2 and TXNIP. Via this pathway, IRE1a also

contributes to the cell's decision to undergo cell death. Thus, another possible explanation for the differential terminal activation of apoptosis in neurons is that prolonged activation of IRE1a leads to RIDD-induced cell death. Whether RIDD is involved in the neuronal response to SNCA triplication is something I am currently investigating.

In this chapter, I have demonstrated that overabundance of alpha-synuclein due to SNCA triplication results in activation of the IRE1a arm of the UPR, signaling via XBP1s to activate the terminal UPR effector, CHOP, and induction of neuronal apoptosis. These results are summarized in Figure 5.5. Based on the findings presented in this chapter, the IRE1a arm of the UPR represents an attractive therapeutic target for alpha-synucleinopathy-induced ER stress and UPR activation in cases of SNCA triplication, and perhaps more broadly in PD. However, as highlighted by previous literature, further studies of the contributions of downstream effectors of IRE1a activation (i.e. IRE1a/XBP1s/CHOP vs. IRE1a/ASK1/JNK vs. RIDD) and the differential actions of this pathway in different brain regions, neuronal subtypes, and stages of disease will be required in order to develop a safe and efficacious IRE1a-modulating UPR-based therapy for PD.

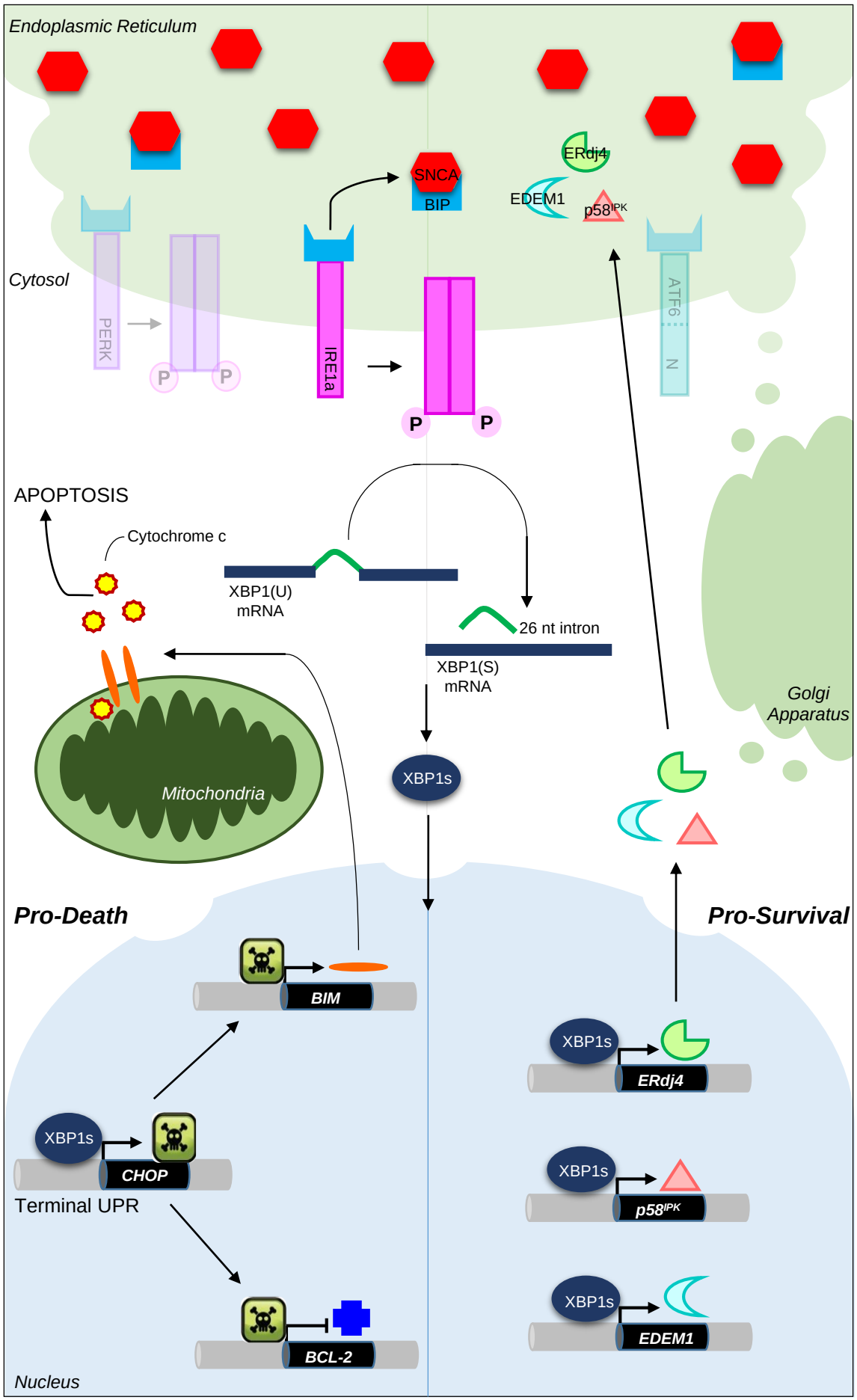

Figure 5.5 Schematic Representation of IRE1a Axis Activation as Observed in iPSC-Derived NSCs and Neurons Bearing an SNCA Triplication.

Figure 5.5 Schematic Representation of IRE1a Axis Activation as Observed in iPSC-Derived NSCs and Neurons Bearing an SNCA Triplication

I observed a cascade of events following from IRE1a activation, which are consistent with previous literature regarding the IRE1a axis of the UPR, but distinct in that SNCA triplication has not been previously linked to IRE1a-mediated activation of the UPR. Overabundance of alpha-synuclein led to increased IRE1a expression levels. Levels of XBP1 mRNA splicing were elevated resulting from the endoribonuclease activity of IRE1a in its activated form. The level of XBP1s homeostatic targets, ERdj4, p58IPK and EDEM1 were elevated. Interestingly, the terminal UPR was activated to differing degrees in the SNCA triplication NSCs and neurons. Specifically, the pro-apoptotic genes, CHOP and BIM, were elevated in both cases, but to a lesser extent in NSCs. Additionally, the anti-apoptotic gene, BCL-2, was activated in NSCs, consistent with compensation. However, BCL-2 was silenced in neurons, consistent with a commitment to undergo apoptosis.

Gene Name	Forward Primer	Reverse Primer
ACTB	CACAGAGCCTCGCCTTTG	GCGGCGATATCATCATCCAT
SNCA	CCTTCTGCCTTTCCACCCT	TCCCTCCTTGGCCTTTGAAA
PERK	ACGATGAGACAGAGTTGCGA	ATGACACCAAGGAACCGGAT
IRE1a	CCGTCCTCTGTCCGTACC	GGTTTCAGGAAGCGTCACTG
ATF6	GGACTCTTTCACAGGCTGGA	CGTCTCATTTGCTGCTTCCA
XBP1 (T)	AATGAAGTGAGGCCAGTGGC	ATACCGCCAGAATCCATGGG
XBP1 (U)	GCACTCAGACTACGTGCACC	ATACCGCCAGAATCCATGGG
XBP1 (S)	TGCTGAGTCCGCAGCAGGTG	ATACCGCCAGAATCCATGGG
ERdj4	GCAGTAGTCGGAGGGTGC	CGCTCTGATGCCGATTTTGG
$p58^{IPK}$	CTGGTGGATCTGCAGTACGA	TGTCCAGCTGCAAGTAATTTCT
EDEM1	TGACTCTTGTTGATGCATTGGA	AGACTTGGACGGTGGAATCT
CHOP	GCGACAGAGCCAAAATCAGA	TGCTTTCAGGTGTGGTGATG
BIM	AGTTCTGAGTGTGACCGAGA	TTGTGGCTCTGTCTGTAGGG
BCL-2	CTTGACAGAGGATCATGCTGT	TCGGATCTTTATTTCATGAGGCA

Table 5.1 Table of qPCR Primers

Chapter 6: Conclusions and Future Directions

6.1 General Conclusions and Deliverables

In this body of work, I have developed and utilized genome editing technologies to manipulate the expression of alpha-synuclein, a critical mediator of PD pathogenesis. I designed and implemented double-nicking CRISPR/Cas9 sgRNAs to induce DNA double-strand breaks in SNCA. This set of Cas9-nickase sgRNAs may assist a variety of other efforts to decipher the normal functions of alpha-synuclein and to study the influence of alpha-synuclein expression in PD pathogenesis. I contributed to the growing body of knowledge regarding determinants of CRISPRi efficacy through the design and rigorous testing of dCas9 sgRNAs to silence SNCA gene expression at the transcriptional level. Furthermore, I demonstrated that this approach can be applied to several genes involved in other proteinopathy-related neurodegenerative diseases.

At the start of this project, iPSCs had been generated from a healthy control patient and a PD patient with a triplication of the SNCA gene locus. In this body of work, I have delivered an isogenic SNCA triplication iPSC line that can be differentiated alongside healthy control and SNCA triplication iPSCs to enhance efforts to decipher those phenotypes which result specifically from alpha-synuclein overexpression without the interference of individual background differences or differences conferred by other genes within the triplicated locus. For immediate phenotypic

characterizations, I have exploited the use of services to generate high-quality NSCs from the healthy control and SNCA triplication iPSCs which are self-renewing, expandable for 50 or more passages and multipotent, capable of differentiating into neurons, astrocytes and oligodendrocytes. NSCs are under production from the isogenic iPSC line generated in this study and I aim to deposit all of these cell lines in a repository to extend their utility in efforts to investigate the role of alpha-synuclein overabundance in PD and other synucleinopathies.

Comparisons of healthy control and SNCA triplication neurons derived from these NSCs has revealed a new relationship between alpha-synuclein overexpression and activation of the UPR that has not been previously described. Although the literature strongly supports an interplay between alpha-synuclein and the UPR, there has been no evaluation of the status of UPR activation in the case of SNCA triplication in patient fibroblasts, patient-derived iPSCs, or iPSC derivatives to date. Having conducted this analysis for the first time, I discovered that neurons bearing an SNCA triplication exhibit a clear and strong activation of the IRE1a arm of the UPR leading to terminal UPR activation and apoptosis. Further evaluation of the pathogenic contributions of this pathway to alpha-synuclein-induced neuropathology in PD may eventuate in the development of UPR-directed, disease-modifying therapies for PD.

6.2 Future Directions

Does normalization of alpha-synuclein expression rescue IRE1a-mediated terminal UPR activation and neuronal apoptosis? In addition to providing the impetus for this question by identifying IRE1a pathway activation in neurons overexpressing alpha-synuclein due to SNCA triplication, this project has produced several tools that will enable it to be answered. The ability to induce alpha-synuclein expression via dCas9-VPR in healthy control neurons, nearly to the extent that it is overexpressed in AST neurons, allowed validation of the finding that alpha-synuclein overabundance induces activation of the IRE1a arm of the UPR and that this phenotype is not individual- or cell line- specific. The precision of such manipulations of SNCA gene expression will allow analysis of the temporal order of pathogenic changes following alpha-synuclein overexpression. When NSCs are available from the isogenic AST iPSCs generated in this study, I will characterize UPR activation in isogenic AST NSC and neuron derivatives. In parallel, I will evaluate whether silencing alpha-synuclein via CRISPRi in AST neurons affects the outcome of IRE1a activation. I hypothesize that 1) long-term dCas9-VPR-mediated activation of alpha-synuclein expression will result in IRE1a activation with resultant terminal UPR activation and apoptosis in healthy control neurons and 2) normalization of alpha-synuclein expression in AST neurons, either due to double-knockout (isogenic AST neurons) or dCas9-mediated silencing, will rescue terminal UPR activation and neuronal apoptosis. Ultimately, clinically available small molecule modifiers of UPR pathway activity, either alone or in combination with novel therapeutic methods for silencing alpha-

synuclein, could be employed to temper alpha-synuclein-induced terminal UPR activation and neuronal apoptosis in PD patients. In the future, CNS delivery of CRISPR/Cas9 may enhance the use of this system in gene therapy for PD via silencing of SNCA and terminal UPR components and activation of homeostatic UPR components to achieve neuronal proteostasis.

References

1. Svenningsson P, Westman E, Ballard C, Aarsland D. Cognitive impairment in patients with Parkinson's disease: diagnosis, biomarkers, and treatment. The Lancet Neurology. 2012;11(8):697-707.
2. Bertram L, Tanzi RE. The genetic epidemiology of neurodegenerative disease. Journal of Clinical Investigation. 2005;115(6):1449-57.
3. Parkinson's Disease Foundation. Statistics on Parkinson's 2015 [cited 2015 27 May].
4. Parkinson's UK. What is Parkinson's 2015 [cited 2015 27 May].
5. Langston JW, Ballard P, Tetrud JW, Irwin I. Chronic Parkinsonism in humans due to a product of meperidine-analog synthesis. Science. 1983;219(4587):979-80.
6. Nicklas WJ, Vyas I, Heikkila RE. Inhibition of NADH-linked oxidation in brain mitochondria by 1-methyl-4-phenyl-pyridine, a metabolite of the neurotoxin, 1-methyl-4-phenyl-1,2,5,6-tetrahydropyridine. Life sciences. 1985;36(26):2503-8.
7. Berry C, La Vecchia C, Nicotera P. Paraquat and Parkinson's disease. Cell death and differentiation. 2010;17(7):1115-25.
8. Franco R, Li S, Rodriguez-Rocha H, Burns M, Panayiotidis MI. Molecular mechanisms of pesticide-induced neurotoxicity: Relevance to Parkinson's disease. Chemico-biological interactions. 2010;188(2):289-300.
9. Couper J. Sur les effets du peroxide de manganese. Journal de chimie medicale, de pharmacie et de toxicologie. 1837;3:223-5.
10. Weisskopf MG, Weuve J, Nie H, Saint-Hilaire MH, Sudarsky L, Simon DK, et al. Association of cumulative lead exposure with Parkinson's disease. Environmental health perspectives. 2010;118(11):1609-13.
11. Goldman SM. Environmental toxins and Parkinson's disease. Annual review of pharmacology and toxicology. 2014;54:141-64.
12. Wong JC, Hazrati LN. Parkinson's disease, parkinsonism, and traumatic brain injury. Critical reviews in clinical laboratory sciences. 2013;50(4-5):103-6.
13. Klein C, Westenberger A. Genetics of Parkinson's disease. Cold Spring Harbor perspectives in medicine. 2012;2(1):a008888.

14. Goker-Alpan O, Schiffmann R, LaMarca ME, Nussbaum RL, McInerney-Leo A, Sidransky E. Parkinsonism among Gaucher disease carriers. Journal of medical genetics. 2004;41(12):937-40.
15. Lwin A, Orvisky E, Goker-Alpan O, LaMarca ME, Sidransky E. Glucocerebrosidase mutations in subjects with parkinsonism. Molecular genetics and metabolism. 2004;81(1):70-3.
16. Aharon-Peretz J, Rosenbaum H, Gershoni-Baruch R. Mutations in the glucocerebrosidase gene and Parkinson's disease in Ashkenazi Jews. The New England journal of medicine. 2004;351(19):1972-7.
17. Sidransky E. Heterozygosity for a Mendelian disorder as a risk factor for complex disease. Clinical genetics. 2006;70(4):275-82.
18. Parkinson J. An essay on the shaking palsy. 1817. The Journal of neuropsychiatry and clinical neurosciences. 2002;14(2):223-36.
19. Carlsson A, Lindqvist M, Magnusson T. 3,4-Dihydroxyphenylalanine and 5-hydroxytryptophan as reserpine antagonists. Nature. 1957;180(4596):1200.
20. Ehringer H, Hornykiewicz O. Distribution of noradrenaline and dopamine (3-hydroxytyramine) in the human brain and their behavior in diseases of the extrapyramidal system. Klinische Wochenschrift. 1960;38:1236-9.
21. Carlsson A, Lindqvist M, Magnusson T, Waldeck B. On the presence of 3-hydroxytyramine in brain. Science. 1958;127(3296):471.
22. Calabresi P, Picconi B, Tozzi A, Ghiglieri V, Di Filippo M. Direct and indirect pathways of basal ganglia: a critical reappraisal. Nat Neurosci. 2014;17(8):1022-30.
23. Jankovic J. Parkinson's disease: clinical features and diagnosis. Journal of neurology, neurosurgery, and psychiatry. 2008;79(4):368-76.
24. Wirdefeldt K, Adami HO, Cole P, Trichopoulos D, Mandel J. Epidemiology and etiology of Parkinson's disease: a review of the evidence. European journal of epidemiology. 2011;26 Suppl 1:S1-58.
25. Birkmayer W, Hornykiewicz O. [The L-3,4-dioxyphenylalanine (DOPA)-effect in Parkinson-akinesia]. Wiener klinische Wochenschrift. 1961;73:787-8.
26. Barbeau A. L-dopa therapy in Parkinson's disease: a critical review of nine years' experience. Canadian Medical Association journal. 1969;101(13):59-68.

27. Cotzias GC, Papavasiliou PS, Gellene R. Modification of Parkinsonism--chronic treatment with L-dopa. The New England journal of medicine. 1969;280(7):337-45.
28. Yahr MD, Duvoisin RC, Schear MJ, Barrett RE, Hoehn MM. Treatment of parkinsonism with levodopa. Archives of neurology. 1969;21(4):343-54.
29. Poletti M, Bonuccelli U. Acute and chronic cognitive effects of levodopa and dopamine agonists on patients with Parkinson's disease: a review. Therapeutic Advances in Psychopharmacology. 2013;3(2):101-13.
30. Park A, Stacy M. Dopamine-induced nonmotor symptoms of Parkinson's disease. Parkinson's disease. 2011;2011:485063.
31. Marsden CD, Parkes JD. "On-off" effects in patients with Parkinson's disease on chronic levodopa therapy. Lancet. 1976;1(7954):292-6.
32. Benabid AL, Chabardes S, Mitrofanis J, Pollak P. Deep brain stimulation of the subthalamic nucleus for the treatment of Parkinson's disease. The Lancet Neurology. 2009;8(1):67-81.
33. Benabid AL, Pollak P, Gross C, Hoffmann D, Benazzouz A, Gao DM, et al. Acute and long-term effects of subthalamic nucleus stimulation in Parkinson's disease. Stereotactic and functional neurosurgery. 1994;62(1-4):76-84.
34. Limousin P, Pollak P, Benazzouz A, Hoffmann D, Le Bas JF, Broussolle E, et al. Effect of parkinsonian signs and symptoms of bilateral subthalamic nucleus stimulation. Lancet. 1995;345(8942):91-5.
35. Limousin P, Krack P, Pollak P, Benazzouz A, Ardouin C, Hoffmann D, et al. Electrical stimulation of the subthalamic nucleus in advanced Parkinson's disease. The New England journal of medicine. 1998;339(16):1105-11.
36. Siegfried J, Lippitz B. Bilateral chronic electrostimulation of ventroposterolateral pallidum: a new therapeutic approach for alleviating all parkinsonian symptoms. Neurosurgery. 1994;35(6):1126-9; discussion 9-30.
37. Kronenbuerger M, Nolte KW, Coenen VA, Burgunder JM, Krauss JK, Weis J. Brain alterations with deep brain stimulation: New insight from a neuropathological case series. Movement disorders. 2015.
38. Possin KL. Visual spatial cognition in neurodegenerative disease. Neurocase. 2010;16(6):466-87.

39. Maroteaux L, Campanelli JT, Scheller RH. Synuclein: a neuron-specific protein localized to the nucleus and presynaptic nerve terminal. The Journal of neuroscience. 1988;8(8):2804-15.
40. Whittle AF, M. Genetics of Alpha-Synuclein. In: Dawson T, editor. Parkinson's Disease: Genetics and Pathogenesis. Informa Healthcare USA, Inc.; 2007. p. 75 - 82.
41. Spillantini MG, Schmidt ML, Lee VM, Trojanowski JQ, Jakes R, Goedert M. Alpha-synuclein in Lewy bodies. Nature. 1997;388(6645):839-40.
42. Golbe LI, Di Iorio G, Bonavita V, Miller DC, Duvoisin RC. A large kindred with autosomal dominant Parkinson's disease. Annals of neurology. 1990;27(3):276-82.
43. Polymeropoulos MH, Higgins JJ, Golbe LI, Johnson WG, Ide SE, Di Iorio G, et al. Mapping of a gene for Parkinson's disease to chromosome 4q21-q23. Science. 1996;274(5290):1197-9.
44. Polymeropoulos MH, Lavedan C, Leroy E, Ide SE, Dehejia A, Dutra A, et al. Mutation in the alpha-synuclein gene identified in families with Parkinson's disease. Science. 1997;276(5321):2045-7.
45. Lo Bianco C, Ridet JL, Schneider BL, Deglon N, Aebischer P. alpha -Synucleinopathy and selective dopaminergic neuron loss in a rat lentiviral-based model of Parkinson's disease. Proceedings of the National Academy of Sciences of the United States of America. 2002;99(16):10813-8.
46. Kirik D, Annett LE, Burger C, Muzyczka N, Mandel RJ, Bjorklund A. Nigrostriatal alpha-synucleinopathy induced by viral vector-mediated overexpression of human alpha-synuclein: a new primate model of Parkinson's disease. Proc Natl Acad Sci U S A. 2003;100(5):2884-9.
47. Eslamboli A, Romero-Ramos M, Burger C, Bjorklund T, Muzyczka N, Mandel RJ, et al. Long-term consequences of human alpha-synuclein overexpression in the primate ventral midbrain. Brain. 2007;130(Pt 3):799-815.
48. Kruger R, Kuhn W, Muller T, Woitalla D, Graeber M, Kosel S, et al. Ala30Pro mutation in the gene encoding alpha-synuclein in Parkinson's disease. Nature genetics. 1998;18(2):106-8.

49. Zarranz JJ, Alegre J, Gomez-Esteban JC, Lezcano E, Ros R, Ampuero I, et al. The new mutation, E46K, of alpha-synuclein causes Parkinson and Lewy body dementia. Annals of neurology. 2004;55(2):164-73.
50. Hoffman-Zacharska D, Koziorowski D, Ross OA, Milewski M, Poznanski J, Jurek M, et al. Novel A18T and pA29S substitutions in alpha-synuclein may be associated with sporadic Parkinson's disease. Parkinsonism & related disorders. 2013;19(11):1057-60.
51. Proukakis C, Dudzik CG, Brier T, MacKay DS, Cooper JM, Millhauser GL, et al. A novel alpha-synuclein missense mutation in Parkinson disease. Neurology. 2013;80(11):1062-4.
52. Lesage S, Anheim M, Letournel F, Bousset L, Honore A, Rozas N, et al. G51D alpha-synuclein mutation causes a novel parkinsonian-pyramidal syndrome. Annals of neurology. 2013;73(4):459-71.
53. Singleton AB, Farrer M, Johnson J, Singleton A, Hague S, Kachergus J, et al. alpha-Synuclein locus triplication causes Parkinson's disease. Science. 2003;302(5646):841.
54. Farrer M, Kachergus J, Forno L, Lincoln S, Wang DS, Hulihan M, et al. Comparison of kindreds with parkinsonism and alpha-synuclein genomic multiplications. Annals of neurology. 2004;55(2):174-9.
55. Wong JJ, Pung YF, Sze NS, Chin KC. HERC5 is an IFN-induced HECT-type E3 protein ligase that mediates type I IFN-induced ISGylation of protein targets. Proceedings of the National Academy of Sciences of the United States of America. 2006;103(28):10735-40.
56. Cruz C, Ventura F, Bartrons R, Rosa JL. HERC3 binding to and regulation by ubiquitin. FEBS letters. 2001;488(1-2):74-80.
57. Miller JA, Woltjer RL, Goodenbour JM, Horvath S, Geschwind DH. Genes and pathways underlying regional and cell type changes in Alzheimer's disease. Genome medicine. 2013;5(5):48.
58. Smit AF, Riggs AD. Tiggers and DNA transposon fossils in the human genome. Proceedings of the National Academy of Sciences of the United States of America. 1996;93(4):1443-8.
59. Hayward CP, Kelton JG. Multimerin. Current opinion in hematology. 1995;2(5):339-44.

60. Paracchini S, Thomas A, Castro S, Lai C, Paramasivam M, Wang Y, et al. The chromosome 6p22 haplotype associated with dyslexia reduces the expression of KIAA0319, a novel gene involved in neuronal migration. Human molecular genetics. 2006;15(10):1659-66.

61. Olgiati S, Thomas A, Quadri M, Breedveld GJ, Graafland J, Eussen H, et al. Early-onset parkinsonism caused by alpha-synuclein gene triplication: Clinical and genetic findings in a novel family. Parkinsonism & related disorders. 2015;21(8):981-6.

62. Chartier-Harlin MC, Kachergus J, Roumier C, Mouroux V, Douay X, Lincoln S, et al. Alpha-synuclein locus duplication as a cause of familial Parkinson's disease. Lancet. 2004;364(9440):1167-9.

63. Singleton AC, J. Genetics of Parkinson's Disease. In: Dawson T, editor. Parkinson's Disease: Genetics and Pathogenesis. Informa Healthcare USA, Inc.; 2007. p. 19 - 33.

64. McCormack AL, Di Monte DA. Enhanced alpha-synuclein expression in human neurodegenerative diseases: pathogenetic and therapeutic implications. Curr Protein Pept Sci. 2009;10(5):476-82.

65. Nalls MA, Pankratz N, Lill CM, Do CB, Hernandez DG, Saad M, et al. Large-scale meta-analysis of genome-wide association data identifies six new risk loci for Parkinson's disease. Nature genetics. 2014;46(9):989-93.

66. Chiba-Falek O, Nussbaum RL. Effect of allelic variation at the NACP-Rep1 repeat upstream of the alpha-synuclein gene (SNCA) on transcription in a cell culture luciferase reporter system. Human molecular genetics. 2001;10(26):3101-9.

67. Kruger R, Vieira-Saecker AM, Kuhn W, Berg D, Muller T, Kuhnl N, et al. Increased susceptibility to sporadic Parkinson's disease by a certain combined alpha-synuclein/apolipoprotein E genotype. Annals of neurology. 1999;45(5):611-7.

68. Tan EK, Matsuura T, Nagamitsu S, Khajavi M, Jankovic J, Ashizawa T. Polymorphism of NACP-Rep1 in Parkinson's disease: an etiologic link with essential tremor? Neurology. 2000;54(5):1195-8.

69. Linnertz C, Saucier L, Ge D, Cronin KD, Burke JR, Browndyke JN, et al. Genetic regulation of alpha-synuclein mRNA expression in various human brain tissues. PloS one. 2009;4(10):e7480.

70. Cardo LF, Coto E, de Mena L, Ribacoba R, Lorenzo-Betancor O, Pastor P, et al. A search for SNCA 3' UTR variants identified SNP rs356165 as a determinant of disease risk and onset age in Parkinson's disease. Journal of molecular neuroscience. 2012;47(3):425-30.

71. Cantuti-Castelvetri I, Keller-McGandy C, Bouzou B, Asteris G, Clark TW, Frosch MP, et al. Effects of gender on nigral gene expression and parkinson disease. Neurobiology of disease. 2007;26(3):606-14.

72. Grundemann J, Schlaudraff F, Haeckel O, Liss B. Elevated alpha-synuclein mRNA levels in individual UV-laser-microdissected dopaminergic substantia nigra neurons in idiopathic Parkinson's disease. Nucleic acids research. 2008;36(7):e38.

73. McLean JR, Hallett PJ, Cooper O, Stanley M, Isacson O. Transcript expression levels of full-length alpha-synuclein and its three alternatively spliced variants in Parkinson's disease brain regions and in a transgenic mouse model of alpha-synuclein overexpression. Molecular and cellular neurosciences. 2012;49(2):230-9.

74. Pruitt KD, Brown GR, Hiatt SM, Thibaud-Nissen F, Astashyn A, Ermolaeva O, et al. RefSeq: an update on mammalian reference sequences. Nucleic acids research. 2014;42:D756-63.

75. Spillantini MG, Divane A, Goedert M. Assignment of human alpha-synuclein (SNCA) and beta-synuclein (SNCB) genes to chromosomes 4q21 and 5q35. Genomics. 1995;27(2):379-81.

76. Lavedan C, Leroy E, Dehejia A, Buchholtz S, Dutra A, Nussbaum RL, et al. Identification, localization and characterization of the human gamma-synuclein gene. Human genetics. 1998;103(1):106-12.

77. George JM, Jin H, Woods WS, Clayton DF. Characterization of a novel protein regulated during the critical period for song learning in the zebra finch. Neuron. 1995;15(2):361-72.

78. Weinreb PH, Zhen W, Poon AW, Conway KA, Lansbury PT, Jr. NACP, a protein implicated in Alzheimer's disease and learning, is natively unfolded. Biochemistry. 1996;35(43):13709-15.
79. Ueda K, Fukushima H, Masliah E, Xia Y, Iwai A, Yoshimoto M, et al. Molecular cloning of cDNA encoding an unrecognized component of amyloid in Alzheimer disease. Proceedings of the National Academy of Sciences of the United States of America. 1993;90(23):11282-6.
80. Crowther RA, Jakes R, Spillantini MG, Goedert M. Synthetic filaments assembled from C-terminally truncated alpha-synuclein. FEBS letters. 1998;436(3):309-12.
81. Conway KA, Harper JD, Lansbury PT. Accelerated in vitro fibril formation by a mutant alpha-synuclein linked to early-onset Parkinson disease. Nature medicine. 1998;4(11):1318-20.
82. Davidson WS, Jonas A, Clayton DF, George JM. Stabilization of alpha-synuclein secondary structure upon binding to synthetic membranes. The Journal of biological chemistry. 1998;273(16):9443-9.
83. Jensen PH, Nielsen MS, Jakes R, Dotti CG, Goedert M. Binding of alpha-synuclein to brain vesicles is abolished by familial Parkinson's disease mutation. The Journal of biological chemistry. 1998;273(41):26292-4.
84. Choi W, Zibaee S, Jakes R, Serpell LC, Davletov B, Crowther RA, et al. Mutation E46K increases phospholipid binding and assembly into filaments of human alpha-synuclein. FEBS letters. 2004;576(3):363-8.
85. Giasson BI, Murray IV, Trojanowski JQ, Lee VM. A hydrophobic stretch of 12 amino acid residues in the middle of alpha-synuclein is essential for filament assembly. The Journal of biological chemistry. 2001;276(4):2380-6.
86. Jakes R, Spillantini MG, Goedert M. Identification of two distinct synucleins from human brain. FEBS letters. 1994;345(1):27-32.
87. Spillantini MG, Crowther RA, Jakes R, Hasegawa M, Goedert M. alpha-Synuclein in filamentous inclusions of Lewy bodies from Parkinson's disease and dementia with lewy bodies. Proceedings of the National Academy of Sciences of the United States of America. 1998;95(11):6469-73.
88. Biere AL, Wood SJ, Wypych J, Steavenson S, Jiang Y, Anafi D, et al. Parkinson's disease-associated alpha-synuclein is more fibrillogenic than beta-

and gamma-synuclein and cannot cross-seed its homologs. The Journal of biological chemistry. 2000;275(44):34574-9.

89. Hoyer W, Cherny D, Subramaniam V, Jovin TM. Impact of the acidic C-terminal region comprising amino acids 109-140 on alpha-synuclein aggregation in vitro. Biochemistry. 2004;43(51):16233-42.

90. Lowe R, Pountney DL, Jensen PH, Gai WP, Voelcker NH. Calcium(II) selectively induces alpha-synuclein annular oligomers via interaction with the C-terminal domain. Protein science. 2004;13(12):3245-52.

91. Murray IV, Giasson BI, Quinn SM, Koppaka V, Axelsen PH, Ischiropoulos H, et al. Role of alpha-synuclein carboxy-terminus on fibril formation in vitro. Biochemistry. 2003;42(28):8530-40.

92. Wood SJ, Wypych J, Steavenson S, Louis JC, Citron M, Biere AL. alpha-synuclein fibrillogenesis is nucleation-dependent. Implications for the pathogenesis of Parkinson's disease. The Journal of biological chemistry. 1999;274(28):19509-12.

93. Conway KA, Harper JD, Lansbury PT, Jr. Fibrils formed in vitro from alpha-synuclein and two mutant forms linked to Parkinson's disease are typical amyloid. Biochemistry. 2000;39(10):2552-63.

94. Uversky VN, Lee HJ, Li J, Fink AL, Lee SJ. Stabilization of partially folded conformation during alpha-synuclein oligomerization in both purified and cytosolic preparations. The Journal of biological chemistry. 2001;276(47):43495-8.

95. Uversky VN, Li J, Fink AL. Evidence for a partially folded intermediate in alpha-synuclein fibril formation. The Journal of biological chemistry. 2001;276(14):10737-44.

96. Shtilerman MD, Ding TT, Lansbury PT, Jr. Molecular crowding accelerates fibrillization of alpha-synuclein: could an increase in the cytoplasmic protein concentration induce Parkinson's disease? Biochemistry. 2002;41(12):3855-60.

97. Rochet JC, Outeiro TF, Conway KA, Ding TT, Volles MJ, Lashuel HA, et al. Interactions among alpha-synuclein, dopamine, and biomembranes: some clues for understanding neurodegeneration in Parkinson's disease. Journal of molecular neuroscience. 2004;23(1-2):23-34.

98. Gallegos S, Pacheco C, Peters C, Opazo CM, Aguayo LG. Features of alpha-synuclein that could explain the progression and irreversibility of Parkinson's disease. Frontiers in neuroscience. 2015;9:59.
99. Abeliovich A, Schmitz Y, Farinas I, Choi-Lundberg D, Ho WH, Castillo PE, et al. Mice lacking alpha-synuclein display functional deficits in the nigrostriatal dopamine system. Neuron. 2000;25(1):239-52.
100. Lee FJ, Liu F, Pristupa ZB, Niznik HB. Direct binding and functional coupling of alpha-synuclein to the dopamine transporters accelerate dopamine-induced apoptosis. FASEB journal. 2001;15(6):916-26.
101. Wersinger C, Prou D, Vernier P, Sidhu A. Modulation of dopamine transporter function by alpha-synuclein is altered by impairment of cell adhesion and by induction of oxidative stress. FASEB journal. 2003;17(14):2151-3.
102. Wersinger C, Prou D, Vernier P, Niznik HB, Sidhu A. Mutations in the lipid-binding domain of alpha-synuclein confer overlapping, yet distinct, functional properties in the regulation of dopamine transporter activity. Molecular and cellular neurosciences. 2003;24(1):91-105.
103. Perez RG, Waymire JC, Lin E, Liu JJ, Guo F, Zigmond MJ. A role for alpha-synuclein in the regulation of dopamine biosynthesis. The Journal of neuroscience. 2002;22(8):3090-9.
104. Jenco JM, Rawlingson A, Daniels B, Morris AJ. Regulation of phospholipase D2: selective inhibition of mammalian phospholipase D isoenzymes by alpha- and beta-synucleins. Biochemistry. 1998;37(14):4901-9.
105. Narayanan V, Guo Y, Scarlata S. Fluorescence studies suggest a role for alpha-synuclein in the phosphatidylinositol lipid signaling pathway. Biochemistry. 2005;44(2):462-70.
106. Iwai A, Masliah E, Yoshimoto M, Ge N, Flanagan L, de Silva HA, et al. The precursor protein of non-A beta component of Alzheimer's disease amyloid is a presynaptic protein of the central nervous system. Neuron. 1995;14(2):467-75.
107. Iwanaga K, Wakabayashi K, Yoshimoto M, Tomita I, Satoh H, Takashima H, et al. Lewy body-type degeneration in cardiac plexus in Parkinson's and incidental Lewy body diseases. Neurology. 1999;52(6):1269-71.

108. Miller DW, Hague SM, Clarimon J, Baptista M, Gwinn-Hardy K, Cookson MR, et al. Alpha-synuclein in blood and brain from familial Parkinson disease with SNCA locus triplication. Neurology. 2004;62(10):1835-8.
109. Barbour R, Kling K, Anderson JP, Banducci K, Cole T, Diep L, et al. Red blood cells are the major source of alpha-synuclein in blood. Neuro-degenerative diseases. 2008;5(2):55-9.
110. Hashimoto M, Yoshimoto M, Sisk A, Hsu LJ, Sundsmo M, Kittel A, et al. NACP, a synaptic protein involved in Alzheimer's disease, is differentially regulated during megakaryocyte differentiation. Biochemical and biophysical research communications. 1997;237(3):611-6.
111. Shameli A, Xiao W, Zheng Y, Shyu S, Sumodi J, Meyerson HJ, et al. A critical role for alpha-synuclein in development and function of T lymphocytes. Immunobiology. 2016;221(2):333-40.
112. Vila M, Vukosavic S, Jackson-Lewis V, Neystat M, Jakowec M, Przedborski S. Alpha-synuclein up-regulation in substantia nigra dopaminergic neurons following administration of the parkinsonian toxin MPTP. Journal of neurochemistry. 2000;74(2):721-9.
113. Kowall NW, Hantraye P, Brouillet E, Beal MF, McKee AC, Ferrante RJ. MPTP induces alpha-synuclein aggregation in the substantia nigra of baboons. Neuroreport. 2000;11(1):211-3.
114. Purisai MG, McCormack AL, Langston WJ, Johnston LC, Di Monte DA. Alpha-synuclein expression in the substantia nigra of MPTP-lesioned non-human primates. Neurobiology of disease. 2005;20(3):898-906.
115. Clayton DF, George JM. The synucleins: a family of proteins involved in synaptic function, plasticity, neurodegeneration and disease. Trends in neurosciences. 1998;21(6):249-54.
116. Fortin DL, Nemani VM, Voglmaier SM, Anthony MD, Ryan TA, Edwards RH. Neural activity controls the synaptic accumulation of alpha-synuclein. The Journal of neuroscience. 2005;25(47):10913-21.
117. McCormack AL, Mak SK, Shenasa M, Langston WJ, Forno LS, Di Monte DA. Pathologic modifications of alpha-synuclein in 1-methyl-4-phenyl-1,2,3,6-tetrahydropyridine (MPTP)-treated squirrel monkeys. Journal of neuropathology and experimental neurology. 2008;67(8):793-802.

118. Emborg ME, Ma SY, Mufson EJ, Levey AI, Taylor MD, Brown WD, et al. Age-related declines in nigral neuronal function correlate with motor impairments in rhesus monkeys. The Journal of comparative neurology. 1998;401(2):253-65.
119. McCormack AL, Di Monte DA, Delfani K, Irwin I, DeLanney LE, Langston WJ, et al. Aging of the nigrostriatal system in the squirrel monkey. The Journal of comparative neurology. 2004;471(4):387-95.
120. Collier TJ, Lipton J, Daley BF, Palfi S, Chu Y, Sortwell C, et al. Aging-related changes in the nigrostriatal dopamine system and the response to MPTP in nonhuman primates: diminished compensatory mechanisms as a prelude to parkinsonism. Neurobiology of disease. 2007;26(1):56-65.
121. Gerhardt GA, Cass WA, Yi A, Zhang Z, Gash DM. Changes in somatodendritic but not terminal dopamine regulation in aged rhesus monkeys. Journal of neurochemistry. 2002;80(1):168-77.
122. Cruz-Sanchez FF, Cardozo A, Tolosa E. Neuronal changes in the substantia nigra with aging: a Golgi study. Journal of neuropathology and experimental neurology. 1995;54(1):74-81.
123. Zecca L, Fariello R, Riederer P, Sulzer D, Gatti A, Tampellini D. The absolute concentration of nigral neuromelanin, assayed by a new sensitive method, increases throughout the life and is dramatically decreased in Parkinson's disease. FEBS letters. 2002;510(3):216-20.
124. Li W, Lesuisse C, Xu Y, Troncoso JC, Price DL, Lee MK. Stabilization of alpha-synuclein protein with aging and familial parkinson's disease-linked A53T mutation. The Journal of neuroscience. 2004;24(33):7400-9.
125. Chu Y, Kordower JH. Age-associated increases of alpha-synuclein in monkeys and humans are associated with nigrostriatal dopamine depletion: Is this the target for Parkinson's disease? Neurobiology of disease. 2007;25(1):134-49.
126. Petersen K, Olesen OF, Mikkelsen JD. Developmental expression of alpha-synuclein in rat hippocampus and cerebral cortex. Neuroscience. 1999;91(2):651-9.
127. Adamczyk A, Solecka J, Strosznajder JB. Expression of alpha-synuclein in different brain parts of adult and aged rats. Journal of physiology and pharmacology. 2005;56(1):29-37.

128. Vernace VA, Schmidt-Glenewinkel T, Figueiredo-Pereira ME. Aging and regulated protein degradation: who has the UPPer hand? Aging cell. 2007;6(5):599-606.
129. Massey A, Kiffin R, Cuervo AM. Pathophysiology of chaperone-mediated autophagy. The international journal of biochemistry & cell biology. 2004;36(12):2420-34.
130. Tabernero J, Shapiro GI, LoRusso PM, Cervantes A, Schwartz GK, Weiss GJ, et al. First-in-humans trial of an RNA interference therapeutic targeting VEGF and KSP in cancer patients with liver involvement. Cancer discovery. 2013;3(4):406-17.
131. Xu B, Wang F, Wu SW, Deng Y, Liu W, Feng S, et al. alpha-Synuclein is involved in manganese-induced ER stress via PERK signal pathway in organotypic brain slice cultures. Molecular neurobiology. 2014;49(1):399-412.
132. Zharikov AD, Cannon JR, Tapias V, Bai Q, Horowitz MP, Shah V, et al. shRNA targeting alpha-synuclein prevents neurodegeneration in a Parkinson's disease model. The Journal of clinical investigation. 2015;125(7):2721-35.
133. Takahashi M, Suzuki M, Fukuoka M, Fujikake N, Watanabe S, Murata M, et al. Normalization of Overexpressed alpha-Synuclein Causing Parkinson's Disease By a Moderate Gene Silencing With RNA Interference. Molecular therapy Nucleic acids. 2015;4:e241.
134. Cooper JM, Wiklander PB, Nordin JZ, Al-Shawi R, Wood MJ, Vithlani M, et al. Systemic exosomal siRNA delivery reduced alpha-synuclein aggregates in brains of transgenic mice. Movement disorders. 2014;29(12):1476-85.
135. Webb JL, Ravikumar B, Atkins J, Skepper JN, Rubinsztein DC. Alpha-Synuclein is degraded by both autophagy and the proteasome. The Journal of biological chemistry. 2003;278(27):25009-13.
136. Zhu M, Rajamani S, Kaylor J, Han S, Zhou F, Fink AL. The flavonoid baicalein inhibits fibrillation of alpha-synuclein and disaggregates existing fibrils. The Journal of biological chemistry. 2004;279(26):26846-57.
137. Ahsan N, Mishra S, Jain MK, Surolia A, Gupta S. Curcumin Pyrazole and its derivative (N-(3-Nitrophenylpyrazole) Curcumin inhibit aggregation, disrupt fibrils and modulate toxicity of Wild type and Mutant alpha-Synuclein. Scientific reports. 2015;5:9862.

138. Tran HT, Chung CH, Iba M, Zhang B, Trojanowski JQ, Luk KC, et al. Alpha-synuclein immunotherapy blocks uptake and templated propagation of misfolded alpha-synuclein and neurodegeneration. Cell reports. 2014;7(6):2054-65.
139. Takahashi K, Yamanaka S. Induction of pluripotent stem cells from mouse embryonic and adult fibroblast cultures by defined factors. Cell. 2006;126(4):663-76.
140. Evans MJ, Kaufman MH. Establishment in culture of pluripotential cells from mouse embryos. Nature. 1981;292(5819):154-6.
141. Martin GR. Isolation of a pluripotent cell line from early mouse embryos cultured in medium conditioned by teratocarcinoma stem cells. Proceedings of the National Academy of Sciences of the United States of America. 1981;78(12):7634-8.
142. Thomson JA, Itskovitz-Eldor J, Shapiro SS, Waknitz MA, Swiergiel JJ, Marshall VS, et al. Embryonic stem cell lines derived from human blastocysts. Science. 1998;282(5391):1145-7.
143. Thomson JA, Kalishman J, Golos TG, Durning M, Harris CP, Becker RA, et al. Isolation of a primate embryonic stem cell line. Proceedings of the National Academy of Sciences of the United States of America. 1995;92(17):7844-8.
144. Thomson JA, Kalishman J, Golos TG, Durning M, Harris CP, Hearn JP. Pluripotent cell lines derived from common marmoset (Callithrix jacchus) blastocysts. Biology of reproduction. 1996;55(2):254-9.
145. Yu J, Vodyanik MA, Smuga-Otto K, Antosiewicz-Bourget J, Frane JL, Tian S, et al. Induced pluripotent stem cell lines derived from human somatic cells. Science. 2007;318(5858):1917-20.
146. Takahashi K, Tanabe K, Ohnuki M, Narita M, Ichisaka T, Tomoda K, et al. Induction of pluripotent stem cells from adult human fibroblasts by defined factors. Cell. 2007;131(5):861-72.
147. Lee G, Papapetrou EP, Kim H, Chambers SM, Tomishima MJ, Fasano CA, et al. Modelling pathogenesis and treatment of familial dysautonomia using patient-specific iPSCs. Nature. 2009;461(7262):402-6.

148. Ebert AD, Yu J, Rose FF, Jr., Mattis VB, Lorson CL, Thomson JA, et al. Induced pluripotent stem cells from a spinal muscular atrophy patient. Nature. 2009;457(7227):277-80.
149. Robinton DA, Daley GQ. The promise of induced pluripotent stem cells in research and therapy. Nature. 2012;481(7381):295-305.
150. Chen G, Gulbranson DR, Hou Z, Bolin JM, Ruotti V, Probasco MD, et al. Chemically defined conditions for human iPSC derivation and culture. Nature methods. 2011;8(5):424-9.
151. Hu BY, Weick JP, Yu J, Ma LX, Zhang XQ, Thomson JA, et al. Neural differentiation of human induced pluripotent stem cells follows developmental principles but with variable potency. Proceedings of the National Academy of Sciences of the United States of America. 2010;107(9):4335-40.
152. Broccoli V, Giannelli SG, Mazzara PG. Modeling physiological and pathological human neurogenesis in the dish. Frontiers in neuroscience. 2014;8:183.
153. Reubinoff BE, Itsykson P, Turetsky T, Pera MF, Reinhartz E, Itzik A, et al. Neural progenitors from human embryonic stem cells. Nature biotechnology. 2001;19(12):1134-40.
154. Zhang SC, Wernig M, Duncan ID, Brustle O, Thomson JA. In vitro differentiation of transplantable neural precursors from human embryonic stem cells. Nature biotechnology. 2001;19(12):1129-33.
155. Dimos JT, Rodolfa KT, Niakan KK, Weisenthal LM, Mitsumoto H, Chung W, et al. Induced pluripotent stem cells generated from patients with ALS can be differentiated into motor neurons. Science. 2008;321(5893):1218-21.
156. Gerrard L, Rodgers L, Cui W. Differentiation of human embryonic stem cells to neural lineages in adherent culture by blocking bone morphogenetic protein signaling. Stem cells. 2005;23(9):1234-41.
157. Swistowski A, Zeng X. Scalable production of transplantable dopaminergic neurons from hESCs and iPSCs in xeno-free defined conditions. Current protocols in stem cell biology. 2012;Chapter 2:Unit2D.12.
158. Kim DS, Lee DR, Kim HS, Yoo JE, Jung SJ, Lim BY, et al. Highly pure and expandable PSA-NCAM-positive neural precursors from human ESC and iPSC-derived neural rosettes. PloS one. 2012;7(7):e39715.

159. Chambers SM, Fasano CA, Papapetrou EP, Tomishima M, Sadelain M, Studer L. Highly efficient neural conversion of human ES and iPS cells by dual inhibition of SMAD signaling. Nat Biotech. 2009;27(3):275-80.
160. Cooper O, Hargus G, Deleidi M, Blak A, Osborn T, Marlow E, et al. Differentiation of human ES and Parkinson's disease iPS cells into ventral midbrain dopaminergic neurons requires a high activity form of SHH, FGF8a and specific regionalization by retinoic acid. Molecular and cellular neurosciences. 2010;45(3):258-66.
161. Zeng X, Cai J, Chen J, Luo Y, You ZB, Fotter E, et al. Dopaminergic differentiation of human embryonic stem cells. Stem cells. 2004;22(6):925-40.
162. Shi Y, Kirwan P, Livesey FJ. Directed differentiation of human pluripotent stem cells to cerebral cortex neurons and neural networks. Nature protocols. 2012;7(10):1836-46.
163. Chung CY, Khurana V, Auluck PK, Tardiff DF, Mazzulli JR, Soldner F, et al. Identification and rescue of alpha-synuclein toxicity in Parkinson patient-derived neurons. Science. 2013;342(6161):983-7.
164. Malik N, Wang X, Shah S, Efthymiou AG, Yan B, Heman-Ackah S, et al. Comparison of the gene expression profiles of human fetal cortical astrocytes with pluripotent stem cell derived neural stem cells identifies human astrocyte markers and signaling pathways and transcription factors active in human astrocytes. PloS one. 2014;9(5):e96139.
165. Pouya A, Satarian L, Kiani S, Javan M, Baharvand H. Human induced pluripotent stem cells differentiation into oligodendrocyte progenitors and transplantation in a rat model of optic chiasm demyelination. PloS one. 2011;6(11):e27925.
166. Barker RA, Drouin-Ouellet J, Parmar M. Cell-based therapies for Parkinson disease-past insights and future potential. Nature reviews Neurology. 2015;11(9):492-503.
167. Lindvall O, Brundin P, Widner H, Rehncrona S, Gustavii B, Frackowiak R, et al. Grafts of fetal dopamine neurons survive and improve motor function in Parkinson's disease. Science. 1990;247(4942):574-7.

168. Lindvall O, Sawle G, Widner H, Rothwell JC, Bjorklund A, Brooks D, et al. Evidence for long-term survival and function of dopaminergic grafts in progressive Parkinson's disease. Annals of neurology. 1994;35(2):172-80.
169. Ben-Hur T, Idelson M, Khaner H, Pera M, Reinhartz E, Itzik A, et al. Transplantation of human embryonic stem cell-derived neural progenitors improves behavioral deficit in Parkinsonian rats. Stem cells. 2004;22(7):1246-55.
170. Kriks S, Shim JW, Piao J, Ganat YM, Wakeman DR, Xie Z, et al. Dopamine neurons derived from human ES cells efficiently engraft in animal models of Parkinson's disease. Nature. 2011;480(7378):547-51.
171. Nishino H, Hida H, Takei N, Kumazaki M, Nakajima K, Baba H. Mesencephalic neural stem (progenitor) cells develop to dopaminergic neurons more strongly in dopamine-depleted striatum than in intact striatum. Experimental neurology. 2000;164(1):209-14.
172. Kallur T, Darsalia V, Lindvall O, Kokaia Z. Human fetal cortical and striatal neural stem cells generate region-specific neurons in vitro and differentiate extensively to neurons after intrastriatal transplantation in neonatal rats. Journal of neuroscience research. 2006;84(8):1630-44.
173. Khoo ML, Tao H, Meedeniya AC, Mackay-Sim A, Ma DD. Transplantation of neuronal-primed human bone marrow mesenchymal stem cells in hemiparkinsonian rodents. PloS one. 2011;6(5):e19025.
174. Blandini F, Cova L, Armentero MT, Zennaro E, Levandis G, Bossolasco P, et al. Transplantation of undifferentiated human mesenchymal stem cells protects against 6-hydroxydopamine neurotoxicity in the rat. Cell transplantation. 2010;19(2):203-17.
175. Wernig M, Zhao J-P, Pruszak J, Hedlund E, Fu D, Soldner F, et al. Neurons derived from reprogrammed fibroblasts functionally integrate into the fetal brain and improve symptoms of rats with Parkinson's disease. Proceedings of the National Academy of Sciences. 2008;105(15):5856-61.
176. Wang S, Zou C, Fu L, Wang B, An J, Song G, et al. Autologous iPSC-derived dopamine neuron transplantation in a nonhuman primate Parkinson’s disease model. Cell Discovery. 2015;1:15012.

177. Emborg ME, Liu Y, Xi J, Zhang X, Yin Y, Lu J, et al. Induced pluripotent stem cell-derived neural cells survive and mature in the nonhuman primate brain. Cell reports. 2013;3(3):646-50.
178. Hallett PJ, Deleidi M, Astradsson A, Smith GA, Cooper O, Osborn TM, et al. Successful function of autologous iPSC-derived dopamine neurons following transplantation in a non-human primate model of Parkinson's disease. Cell stem cell. 2015;16(3):269-74.
179. Nakagawa M, Koyanagi M, Tanabe K, Takahashi K, Ichisaka T, Aoi T, et al. Generation of induced pluripotent stem cells without Myc from mouse and human fibroblasts. Nature biotechnology. 2008;26(1):101-6.
180. Soldner F, Hockemeyer D, Beard C, Gao Q, Bell GW, Cook EG, et al. Parkinson's disease patient-derived induced pluripotent stem cells free of viral reprogramming factors. Cell. 2009;136(5):964-77.
181. Caiazzo M, Dell'Anno MT, Dvoretskova E, Lazarevic D, Taverna S, Leo D, et al. Direct generation of functional dopaminergic neurons from mouse and human fibroblasts. Nature. 2011;476(7359):224-7.
182. Soldner F, Laganiere J, Cheng AW, Hockemeyer D, Gao Q, Alagappan R, et al. Generation of isogenic pluripotent stem cells differing exclusively at two early onset Parkinson point mutations. Cell. 2011;146(2):318-31.
183. Hsu PD, Lander ES, Zhang F. Development and applications of CRISPR-Cas9 for genome engineering. Cell. 2014;157(6):1262-78.
184. Capecchi MR. Altering the genome by homologous recombination. Science. 1989;244(4910):1288-92.
185. Rudin N, Sugarman E, Haber JE. Genetic and physical analysis of double-strand break repair and recombination in Saccharomyces cerevisiae. Genetics. 1989;122(3):519-34.
186. Plessis A, Perrin A, Haber JE, Dujon B. Site-specific recombination determined by I-SceI, a mitochondrial group I intron-encoded endonuclease expressed in the yeast nucleus. Genetics. 1992;130(3):451-60.
187. Rouet P, Smih F, Jasin M. Introduction of double-strand breaks into the genome of mouse cells by expression of a rare-cutting endonuclease. Molecular and cellular biology. 1994;14(12):8096-106.

188. Choulika A, Perrin A, Dujon B, Nicolas JF. Induction of homologous recombination in mammalian chromosomes by using the I-SceI system of Saccharomyces cerevisiae. Molecular and cellular biology. 1995;15(4):1968-73.
189. Bibikova M, Carroll D, Segal DJ, Trautman JK, Smith J, Kim YG, et al. Stimulation of homologous recombination through targeted cleavage by chimeric nucleases. Molecular and cellular biology. 2001;21(1):289-97.
190. Bibikova M, Beumer K, Trautman JK, Carroll D. Enhancing gene targeting with designed zinc finger nucleases. Science. 2003;300(5620):764.
191. Bibikova M, Golic M, Golic KG, Carroll D. Targeted chromosomal cleavage and mutagenesis in Drosophila using zinc-finger nucleases. Genetics. 2002;161(3):1169-75.
192. Smith J, Grizot S, Arnould S, Duclert A, Epinat JC, Chames P, et al. A combinatorial approach to create artificial homing endonucleases cleaving chosen sequences. Nucleic acids research. 2006;34(22):e149.
193. Urnov FD, Miller JC, Lee YL, Beausejour CM, Rock JM, Augustus S, et al. Highly efficient endogenous human gene correction using designed zinc-finger nucleases. Nature. 2005;435(7042):646-51.
194. Miller JC, Holmes MC, Wang J, Guschin DY, Lee YL, Rupniewski I, et al. An improved zinc-finger nuclease architecture for highly specific genome editing. Nature biotechnology. 2007;25(7):778-85.
195. Christian M, Cermak T, Doyle EL, Schmidt C, Zhang F, Hummel A, et al. Targeting DNA double-strand breaks with TAL effector nucleases. Genetics. 2010;186(2):757-61.
196. Miller JC, Tan S, Qiao G, Barlow KA, Wang J, Xia DF, et al. A TALE nuclease architecture for efficient genome editing. Nature biotechnology. 2011;29(2):143-8.
197. Boch J, Scholze H, Schornack S, Landgraf A, Hahn S, Kay S, et al. Breaking the code of DNA binding specificity of TAL-type III effectors. Science. 2009;326(5959):1509-12.
198. Moscou MJ, Bogdanove AJ. A simple cipher governs DNA recognition by TAL effectors. Science. 2009;326(5959):1501.
199. Cong L, Ran FA, Cox D, Lin S, Barretto R, Habib N, et al. Multiplex genome engineering using CRISPR/Cas systems. Science. 2013;339(6121):819-23.

200. Mali P, Yang L, Esvelt KM, Aach J, Guell M, DiCarlo JE, et al. RNA-guided human genome engineering via Cas9. Science. 2013;339(6121):823-6.
201. Maeder ML, Thibodeau-Beganny S, Osiak A, Wright DA, Anthony RM, Eichtinger M, et al. Rapid "open-source" engineering of customized zinc-finger nucleases for highly efficient gene modification. Molecular cell. 2008;31(2):294-301.
202. Brouns SJ, Jore MM, Lundgren M, Westra ER, Slijkhuis RJ, Snijders AP, et al. Small CRISPR RNAs guide antiviral defense in prokaryotes. Science. 2008;321(5891):960-4.
203. Deltcheva E, Chylinski K, Sharma CM, Gonzales K, Chao Y, Pirzada ZA, et al. CRISPR RNA maturation by trans-encoded small RNA and host factor RNase III. Nature. 2011;471(7340):602-7.
204. Jinek M, Chylinski K, Fonfara I, Hauer M, Doudna JA, Charpentier E. A programmable dual-RNA-guided DNA endonuclease in adaptive bacterial immunity. Science. 2012;337(6096):816-21.
205. Gasiunas G, Barrangou R, Horvath P, Siksnys V. Cas9-crRNA ribonucleoprotein complex mediates specific DNA cleavage for adaptive immunity in bacteria. Proceedings of the National Academy of Sciences of the United States of America. 2012;109(39):E2579-86.
206. Bolotin A, Quinquis B, Sorokin A, Ehrlich SD. Clustered regularly interspaced short palindrome repeats (CRISPRs) have spacers of extrachromosomal origin. Microbiology. 2005;151(Pt 8):2551-61.
207. Haft DH, Selengut J, Mongodin EF, Nelson KE. A guild of 45 CRISPR-associated (Cas) protein families and multiple CRISPR/Cas subtypes exist in prokaryotic genomes. PLoS computational biology. 2005;1(6):e60.
208. Makarova KS, Haft DH, Barrangou R, Brouns SJ, Charpentier E, Horvath P, et al. Evolution and classification of the CRISPR-Cas systems. Nature reviews Microbiology. 2011;9(6):467-77.
209. Makarova KS, Aravind L, Wolf YI, Koonin EV. Unification of Cas protein families and a simple scenario for the origin and evolution of CRISPR-Cas systems. Biology direct. 2011;6:38.
210. Chylinski K, Le Rhun A, Charpentier E. The tracrRNA and Cas9 families of type II CRISPR-Cas immunity systems. RNA biology. 2013;10(5):726-37.

211. Nishimasu H, Ran FA, Hsu PD, Konermann S, Shehata SI, Dohmae N, et al. Crystal structure of Cas9 in complex with guide RNA and target DNA. Cell. 2014;156(5):935-49.
212. Ran FA, Cong L, Yan WX, Scott DA, Gootenberg JS, Kriz AJ, et al. In vivo genome editing using Staphylococcus aureus Cas9. Nature. 2015;520(7546):186-91.
213. Zetsche B, Gootenberg JS, Abudayyeh OO, Slaymaker IM, Makarova KS, Essletzbichler P, et al. Cpf1 Is a Single RNA-Guided Endonuclease of a Class 2 CRISPR-Cas System. Cell. 2015;163(3):759-71.
214. Hsu PD, Scott DA, Weinstein JA, Ran FA, Konermann S, Agarwala V, et al. DNA targeting specificity of RNA-guided Cas9 nucleases. Nature biotechnology. 2013;31(9):827-32.
215. Jiang W, Bikard D, Cox D, Zhang F, Marraffini LA. RNA-guided editing of bacterial genomes using CRISPR-Cas systems. Nature biotechnology. 2013;31(3):233-9.
216. Sternberg SH, Redding S, Jinek M, Greene EC, Doudna JA. DNA interrogation by the CRISPR RNA-guided endonuclease Cas9. Nature. 2014;507(7490):62-7.
217. Kleinstiver BP, Prew MS, Tsai SQ, Topkar VV, Nguyen NT, Zheng Z, et al. Engineered CRISPR-Cas9 nucleases with altered PAM specificities. Nature. 2015;523(7561):481-5.
218. Sapranauskas R, Gasiunas G, Fremaux C, Barrangou R, Horvath P, Siksnys V. The Streptococcus thermophilus CRISPR/Cas system provides immunity in Escherichia coli. Nucleic acids research. 2011;39(21):9275-82.
219. Dianov GL, Hubscher U. Mammalian base excision repair: the forgotten archangel. Nucleic acids research. 2013;41(6):3483-90.
220. Ran FA, Hsu PD, Lin CY, Gootenberg JS, Konermann S, Trevino AE, et al. Double nicking by RNA-guided CRISPR Cas9 for enhanced genome editing specificity. Cell. 2013;154(6):1380-9.
221. Mali P, Aach J, Stranges PB, Esvelt KM, Moosburner M, Kosuri S, et al. CAS9 transcriptional activators for target specificity screening and paired nickases for cooperative genome engineering. Nature biotechnology. 2013;31(9):833-8.

222. Qi LS, Larson MH, Gilbert LA, Doudna JA, Weissman JS, Arkin AP, et al. Repurposing CRISPR as an RNA-guided platform for sequence-specific control of gene expression. Cell. 2013;152(5):1173-83.
223. Carrara M, Prischi F, Nowak PR, Kopp MC, Ali MM. Noncanonical binding of BiP ATPase domain to Ire1 and Perk is dissociated by unfolded protein CH1 to initiate ER stress signaling. eLife. 2015;4.
224. Credle JJ, Finer-Moore JS, Papa FR, Stroud RM, Walter P. On the mechanism of sensing unfolded protein in the endoplasmic reticulum. Proceedings of the National Academy of Sciences of the United States of America. 2005;102(52):18773-84.
225. Gardner BM, Walter P. Unfolded proteins are Ire1-activating ligands that directly induce the unfolded protein response. Science. 2011;333(6051):1891-4.
226. Pincus D, Chevalier MW, Aragon T, van Anken E, Vidal SE, El-Samad H, et al. BiP binding to the ER-stress sensor Ire1 tunes the homeostatic behavior of the unfolded protein response. PLoS biology. 2010;8(7):e1000415.
227. Chen Y, Brandizzi F. IRE1: ER stress sensor and cell fate executor. Trends in cell biology. 2013;23(11):547-55.
228. Tirasophon W, Welihinda AA, Kaufman RJ. A stress response pathway from the endoplasmic reticulum to the nucleus requires a novel bifunctional protein kinase/endoribonuclease (Ire1p) in mammalian cells. Genes & development. 1998;12(12):1812-24.
229. Wang XZ, Harding HP, Zhang Y, Jolicoeur EM, Kuroda M, Ron D. Cloning of mammalian Ire1 reveals diversity in the ER stress responses. The EMBO journal. 1998;17(19):5708-17.
230. Korennykh A, Walter P. Structural basis of the unfolded protein response. Annual review of cell and developmental biology. 2012;28:251-77.
231. Calfon M, Zeng H, Urano F, Till JH, Hubbard SR, Harding HP, et al. IRE1 couples endoplasmic reticulum load to secretory capacity by processing the XBP-1 mRNA. Nature. 2002;415(6867):92-6.
232. Yoshida H, Matsui T, Yamamoto A, Okada T, Mori K. XBP1 mRNA is induced by ATF6 and spliced by IRE1 in response to ER stress to produce a highly active transcription factor. Cell. 2001;107(7):881-91.

233. Yamamoto K, Sato T, Matsui T, Sato M, Okada T, Yoshida H, et al. Transcriptional induction of mammalian ER quality control proteins is mediated by single or combined action of ATF6alpha and XBP1. Developmental cell. 2007;13(3):365-76.
234. Mercado G, Valdes P, Hetz C. An ERcentric view of Parkinson's disease. Trends in molecular medicine. 2013;19(3):165-75.
235. Hetz C. The unfolded protein response: controlling cell fate decisions under ER stress and beyond. Nature reviews Molecular cell biology. 2012;13(2):89-102.
236. Liu CY, Schroder M, Kaufman RJ. Ligand-independent dimerization activates the stress response kinases IRE1 and PERK in the lumen of the endoplasmic reticulum. The Journal of biological chemistry. 2000;275(32):24881-5.
237. Bertolotti A, Zhang Y, Hendershot LM, Harding HP, Ron D. Dynamic interaction of BiP and ER stress transducers in the unfolded-protein response. Nature cell biology. 2000;2(6):326-32.
238. Harding HP, Zhang Y, Ron D. Protein translation and folding are coupled by an endoplasmic-reticulum-resident kinase. Nature. 1999;397(6716):271-4.
239. Oakes SA, Papa FR. The role of endoplasmic reticulum stress in human pathology. Annual review of pathology. 2015;10:173-94.
240. Ye J, Rawson RB, Komuro R, Chen X, Dave UP, Prywes R, et al. ER stress induces cleavage of membrane-bound ATF6 by the same proteases that process SREBPs. Molecular cell. 2000;6(6):1355-64.
241. Kim I, Xu W, Reed JC. Cell death and endoplasmic reticulum stress: disease relevance and therapeutic opportunities. Nat Rev Drug Discov. 2008;7(12):1013-30.
242. Han D, Lerner AG, Vande Walle L, Upton JP, Xu W, Hagen A, et al. IRE1alpha kinase activation modes control alternate endoribonuclease outputs to determine divergent cell fates. Cell. 2009;138(3):562-75.
243. Hollien J, Weissman JS. Decay of endoplasmic reticulum-localized mRNAs during the unfolded protein response. Science. 2006;313(5783):104-7.

244. Upton JP, Wang L, Han D, Wang ES, Huskey NE, Lim L, et al. IRE1alpha cleaves select microRNAs during ER stress to derepress translation of proapoptotic Caspase-2. Science. 2012;338(6108):818-22.
245. Lerner AG, Upton JP, Praveen PV, Ghosh R, Nakagawa Y, Igbaria A, et al. IRE1alpha induces thioredoxin-interacting protein to activate the NLRP3 inflammasome and promote programmed cell death under irremediable ER stress. Cell metabolism. 2012;16(2):250-64.
246. Upton JP, Austgen K, Nishino M, Coakley KM, Hagen A, Han D, et al. Caspase-2 cleavage of BID is a critical apoptotic signal downstream of endoplasmic reticulum stress. Molecular and cellular biology. 2008;28(12):3943-51.
247. Puthalakath H, O'Reilly LA, Gunn P, Lee L, Kelly PN, Huntington ND, et al. ER stress triggers apoptosis by activating BH3-only protein Bim. Cell. 2007;129(7):1337-49.
248. Li J, Lee B, Lee AS. Endoplasmic reticulum stress-induced apoptosis: multiple pathways and activation of p53-up-regulated modulator of apoptosis (PUMA) and NOXA by p53. The Journal of biological chemistry. 2006;281(11):7260-70.
249. Giam M, Huang DC, Bouillet P. BH3-only proteins and their roles in programmed cell death. Oncogene. 2008;27 Suppl 1:S128-36.
250. Chipuk JE, Bouchier-Hayes L, Green DR. Mitochondrial outer membrane permeabilization during apoptosis: the innocent bystander scenario. Cell Death Differ. 2006;13(8):1396-402.
251. Steiner DF. New aspects of proinsulin physiology and pathophysiology. Journal of pediatric endocrinology & metabolism. 2000;13(3):229-39.
252. Ron D. Proteotoxicity in the endoplasmic reticulum: lessons from the Akita diabetic mouse. The Journal of clinical investigation. 2002;109(4):443-5.
253. Izumi T, Yokota-Hashimoto H, Zhao S, Wang J, Halban PA, Takeuchi T. Dominant negative pathogenesis by mutant proinsulin in the Akita diabetic mouse. Diabetes. 2003;52(2):409-16.
254. Wang J, Takeuchi T, Tanaka S, Kubo SK, Kayo T, Lu D, et al. A mutation in the insulin 2 gene induces diabetes with severe pancreatic beta-cell

dysfunction in the Mody mouse. The Journal of clinical investigation. 1999;103(1):27-37.
255. Liu M, Li Y, Cavener D, Arvan P. Proinsulin disulfide maturation and misfolding in the endoplasmic reticulum. The Journal of biological chemistry. 2005;280(14):13209-12.
256. Stoy J, Edghill EL, Flanagan SE, Ye H, Paz VP, Pluzhnikov A, et al. Insulin gene mutations as a cause of permanent neonatal diabetes. Proceedings of the National Academy of Sciences of the United States of America. 2007;104(38):15040-4.
257. Delepine M, Nicolino M, Barrett T, Golamaully M, Lathrop GM, Julier C. EIF2AK3, encoding translation initiation factor 2-alpha kinase 3, is mutated in patients with Wolcott-Rallison syndrome. Nature genetics. 2000;25(4):406-9.
258. Riggs AC, Bernal-Mizrachi E, Ohsugi M, Wasson J, Fatrai S, Welling C, et al. Mice conditionally lacking the Wolfram gene in pancreatic islet beta cells exhibit diabetes as a result of enhanced endoplasmic reticulum stress and apoptosis. Diabetologia. 2005;48(11):2313-21.
259. Fonseca SG, Fukuma M, Lipson KL, Nguyen LX, Allen JR, Oka Y, et al. WFS1 is a novel component of the unfolded protein response and maintains homeostasis of the endoplasmic reticulum in pancreatic beta-cells. The Journal of biological chemistry. 2005;280(47):39609-15.
260. Fonseca SG, Ishigaki S, Oslowski CM, Lu S, Lipson KL, Ghosh R, et al. Wolfram syndrome 1 gene negatively regulates ER stress signaling in rodent and human cells. The Journal of clinical investigation. 2010;120(3):744-55.
261. Pyrko P, Schonthal AH, Hofman FM, Chen TC, Lee AS. The unfolded protein response regulator GRP78/BiP as a novel target for increasing chemosensitivity in malignant gliomas. Cancer research. 2007;67(20):9809-16.
262. Fernandez PM, Tabbara SO, Jacobs LK, Manning FC, Tsangaris TN, Schwartz AM, et al. Overexpression of the glucose-regulated stress gene GRP78 in malignant but not benign human breast lesions. Breast cancer research and treatment. 2000;59(1):15-26.
263. Song MS, Park YK, Lee JH, Park K. Induction of glucose-regulated protein 78 by chronic hypoxia in human gastric tumor cells through a protein kinase C-epsilon/ERK/AP-1 signaling cascade. Cancer research. 2001;61(22):8322-30.

264. Chen X, Ding Y, Liu CG, Mikhail S, Yang CS. Overexpression of glucose-regulated protein 94 (Grp94) in esophageal adenocarcinomas of a rat surgical model and humans. Carcinogenesis. 2002;23(1):123-30.
265. Shuda M, Kondoh N, Imazeki N, Tanaka K, Okada T, Mori K, et al. Activation of the ATF6, XBP1 and grp78 genes in human hepatocellular carcinoma: a possible involvement of the ER stress pathway in hepatocarcinogenesis. Journal of hepatology. 2003;38(5):605-14.
266. Carrasco DR, Sukhdeo K, Protopopova M, Sinha R, Enos M, Carrasco DE, et al. The differentiation and stress response factor XBP-1 drives multiple myeloma pathogenesis. Cancer cell. 2007;11(4):349-60.
267. Reimold AM, Iwakoshi NN, Manis J, Vallabhajosyula P, Szomolanyi-Tsuda E, Gravallese EM, et al. Plasma cell differentiation requires the transcription factor XBP-1. Nature. 2001;412(6844):300-7.
268. Zhang K, Wong HN, Song B, Miller CN, Scheuner D, Kaufman RJ. The unfolded protein response sensor IRE1alpha is required at 2 distinct steps in B cell lymphopoiesis. The Journal of clinical investigation. 2005;115(2):268-81.
269. Voorhees PM, Orlowski RZ. The proteasome and proteasome inhibitors in cancer therapy. Annual review of pharmacology and toxicology. 2006;46:189-213.
270. Rajkumar SV, Richardson PG, Hideshima T, Anderson KC. Proteasome inhibition as a novel therapeutic target in human cancer. Journal of clinical oncology. 2005;23(3):630-9.
271. Gu JL, Li J, Zhou ZH, Liu JR, Huang BH, Zheng D, et al. Differentiation induction enhances bortezomib efficacy and overcomes drug resistance in multiple myeloma. Biochemical and biophysical research communications. 2012;420(3):644-50.
272. Ling SC, Lau EK, Al-Shabeeb A, Nikolic A, Catalano A, Iland H, et al. Response of myeloma to the proteasome inhibitor bortezomib is correlated with the unfolded protein response regulator XBP-1. Haematologica. 2012;97(1):64-72.
273. Leung-Hagesteijn C, Erdmann N, Cheung G, Keats JJ, Stewart AK, Reece DE, et al. Xbp1s-negative tumor B cells and pre-plasmablasts mediate

therapeutic proteasome inhibitor resistance in multiple myeloma. Cancer cell. 2013;24(3):289-304.
274. Chapman MA, Lawrence MS, Keats JJ, Cibulskis K, Sougnez C, Schinzel AC, et al. Initial genome sequencing and analysis of multiple myeloma. Nature. 2011;471(7339):467-72.
275. Myoishi M, Hao H, Minamino T, Watanabe K, Nishihira K, Hatakeyama K, et al. Increased endoplasmic reticulum stress in atherosclerotic plaques associated with acute coronary syndrome. Circulation. 2007;116(11):1226-33.
276. Zhou J, Lhotak S, Hilditch BA, Austin RC. Activation of the unfolded protein response occurs at all stages of atherosclerotic lesion development in apolipoprotein E-deficient mice. Circulation. 2005;111(14):1814-21.
277. Seimon TA, Nadolski MJ, Liao X, Magallon J, Nguyen M, Feric NT, et al. Atherogenic lipids and lipoproteins trigger CD36-TLR2-dependent apoptosis in macrophages undergoing endoplasmic reticulum stress. Cell metabolism. 2010;12(5):467-82.
278. Yamaguchi O, Higuchi Y, Hirotani S, Kashiwase K, Nakayama H, Hikoso S, et al. Targeted deletion of apoptosis signal-regulating kinase 1 attenuates left ventricular remodeling. Proceedings of the National Academy of Sciences of the United States of America. 2003;100(26):15883-8.
279. Tajiri S, Oyadomari S, Yano S, Morioka M, Gotoh T, Hamada JI, et al. Ischemia-induced neuronal cell death is mediated by the endoplasmic reticulum stress pathway involving CHOP. Cell Death Differ. 2004;11(4):403-15.
280. Saxena S, Cabuy E, Caroni P. A role for motoneuron subtype-selective ER stress in disease manifestations of FALS mice. Nat Neurosci. 2009;12(5):627-36.
281. Wang L, Popko B, Roos RP. The unfolded protein response in familial amyotrophic lateral sclerosis. Human molecular genetics. 2011;20(5):1008-15.
282. Vaccaro A, Patten SA, Aggad D, Julien C, Maios C, Kabashi E, et al. Pharmacological reduction of ER stress protects against TDP-43 neuronal toxicity in vivo. Neurobiology of disease. 2013;55:64-75.
283. Matus S, Lopez E, Valenzuela V, Nassif M, Hetz C. Functional contribution of the transcription factor ATF4 to the pathogenesis of amyotrophic lateral sclerosis. PloS one. 2013;8(7):e66672.

284. Hetz C, Thielen P, Fisher J, Pasinelli P, Brown RH, Korsmeyer S, et al. The proapoptotic BCL-2 family member BIM mediates motoneuron loss in a model of amyotrophic lateral sclerosis. Cell Death Differ. 2007;14(7):1386-9.
285. Kieran D, Woods I, Villunger A, Strasser A, Prehn JH. Deletion of the BH3-only protein puma protects motoneurons from ER stress-induced apoptosis and delays motoneuron loss in ALS mice. Proceedings of the National Academy of Sciences of the United States of America. 2007;104(51):20606-11.
286. Nishitoh H, Kadowaki H, Nagai A, Maruyama T, Yokota T, Fukutomi H, et al. ALS-linked mutant SOD1 induces ER stress- and ASK1-dependent motor neuron death by targeting Derlin-1. Genes & development. 2008;22(11):1451-64.
287. Hetz C, Thielen P, Matus S, Nassif M, Court F, Kiffin R, et al. XBP-1 deficiency in the nervous system protects against amyotrophic lateral sclerosis by increasing autophagy. Genes & development. 2009;23(19):2294-306.
288. Vidal RL, Figueroa A, Court FA, Thielen P, Molina C, Wirth C, et al. Targeting the UPR transcription factor XBP1 protects against Huntington's disease through the regulation of FoxO1 and autophagy. Human molecular genetics. 2012;21(10):2245-62.
289. Casas-Tinto S, Zhang Y, Sanchez-Garcia J, Gomez-Velazquez M, Rincon-Limas DE, Fernandez-Funez P. The ER stress factor XBP1s prevents amyloid-beta neurotoxicity. Human molecular genetics. 2011;20(11):2144-60.
290. Safra M, Ben-Hamo S, Kenyon C, Henis-Korenblit S. The ire-1 ER stress-response pathway is required for normal secretory-protein metabolism in C. elegans. Journal of cell science. 2013;126(Pt 18):4136-46.
291. Yoon SO, Park DJ, Ryu JC, Ozer HG, Tep C, Shin YJ, et al. JNK3 perpetuates metabolic stress induced by Abeta peptides. Neuron. 2012;75(5):824-37.
292. Conn KJ, Gao W, McKee A, Lan MS, Ullman MD, Eisenhauer PB, et al. Identification of the protein disulfide isomerase family member PDIp in experimental Parkinson's disease and Lewy body pathology. Brain research. 2004;1022(1-2):164-72.
293. Selvaraj S, Sun Y, Watt JA, Wang S, Lei S, Birnbaumer L, et al. Neurotoxin-induced ER stress in mouse dopaminergic neurons involves

downregulation of TRPC1 and inhibition of AKT/mTOR signaling. The Journal of clinical investigation. 2012;122(4):1354-67.
294. Slodzinski H, Moran LB, Michael GJ, Wang B, Novoselov S, Cheetham ME, et al. Homocysteine-induced endoplasmic reticulum protein (herp) is up-regulated in parkinsonian substantia nigra and present in the core of Lewy bodies. Clinical neuropathology. 2009;28(5):333-43.
295. Holtz WA, O'Malley KL. Parkinsonian mimetics induce aspects of unfolded protein response in death of dopaminergic neurons. The Journal of biological chemistry. 2003;278(21):19367-77.
296. Ryu EJ, Harding HP, Angelastro JM, Vitolo OV, Ron D, Greene LA. Endoplasmic reticulum stress and the unfolded protein response in cellular models of Parkinson's disease. The Journal of neuroscience. 2002;22(24):10690-8.
297. Paisan-Ruiz C, Jain S, Evans EW, Gilks WP, Simon J, van der Brug M, et al. Cloning of the gene containing mutations that cause PARK8-linked Parkinson's disease. Neuron. 2004;44(4):595-600.
298. Zimprich A, Muller-Myhsok B, Farrer M, Leitner P, Sharma M, Hulihan M, et al. The PARK8 locus in autosomal dominant parkinsonism: confirmation of linkage and further delineation of the disease-containing interval. American journal of human genetics. 2004;74(1):11-9.
299. Greggio E, Cookson MR. Leucine-rich repeat kinase 2 mutations and Parkinson's disease: three questions. ASN neuro. 2009;1(1).
300. Steger M, Tonelli F, Ito G, Davies P, Trost M, Vetter M, et al. Phosphoproteomics reveals that Parkinson's disease kinase LRRK2 regulates a subset of Rab GTPases. eLife. 2016;5.
301. McArdle B, Hofmann A. Coronin structure and implications. Sub-cellular biochemistry. 2008;48:56-71.
302. Vitte J, Traver S, Maues De Paula A, Lesage S, Rovelli G, Corti O, et al. Leucine-rich repeat kinase 2 is associated with the endoplasmic reticulum in dopaminergic neurons and accumulates in the core of Lewy bodies in Parkinson disease. Journal of neuropathology and experimental neurology. 2010;69(9):959-72.

303. Yuan Y, Cao P, Smith MA, Kramp K, Huang Y, Hisamoto N, et al. Dysregulated LRRK2 signaling in response to endoplasmic reticulum stress leads to dopaminergic neuron degeneration in C. elegans. PloS one. 2011;6(8):e22354.
304. Samann J, Hegermann J, von Gromoff E, Eimer S, Baumeister R, Schmidt E. Caenorhabditits elegans LRK-1 and PINK-1 act antagonistically in stress response and neurite outgrowth. The Journal of biological chemistry. 2009;284(24):16482-91.
305. Kubota K, Niinuma Y, Kaneko M, Okuma Y, Sugai M, Omura T, et al. Suppressive effects of 4-phenylbutyrate on the aggregation of Pael receptors and endoplasmic reticulum stress. Journal of neurochemistry. 2006;97(5):1259-68.
306. Kitao Y, Imai Y, Ozawa K, Kataoka A, Ikeda T, Soda M, et al. Pael receptor induces death of dopaminergic neurons in the substantia nigra via endoplasmic reticulum stress and dopamine toxicity, which is enhanced under condition of parkin inactivation. Human molecular genetics. 2007;16(1):50-60.
307. Bouman L, Schlierf A, Lutz AK, Shan J, Deinlein A, Kast J, et al. Parkin is transcriptionally regulated by ATF4: evidence for an interconnection between mitochondrial stress and ER stress. Cell Death Differ. 2011;18(5):769-82.
308. Yokota T, Sugawara K, Ito K, Takahashi R, Ariga H, Mizusawa H. Down regulation of DJ-1 enhances cell death by oxidative stress, ER stress, and proteasome inhibition. Biochemical and biophysical research communications. 2003;312(4):1342-8.
309. Park JS, Mehta P, Cooper AA, Veivers D, Heimbach A, Stiller B, et al. Pathogenic effects of novel mutations in the P-type ATPase ATP13A2 (PARK9) causing Kufor-Rakeb syndrome, a form of early-onset parkinsonism. Human mutation. 2011;32(8):956-64.
310. Hoozemans JJ, van Haastert ES, Eikelenboom P, de Vos RA, Rozemuller JM, Scheper W. Activation of the unfolded protein response in Parkinson's disease. Biochemical and biophysical research communications. 2007;354(3):707-11.
311. Hirsch E, Graybiel AM, Agid YA. Melanized dopaminergic neurons are differentially susceptible to degeneration in Parkinson's disease. Nature. 1988;334(6180):345-8.

312. Baek JH, Whitfield D, Howlett D, Francis P, Bereczki E, Ballard C, et al. Unfolded protein response is activated in Lewy body dementias. Neuropathology and applied neurobiology. 2015.
313. Bellucci A, Navarria L, Zaltieri M, Falarti E, Bodei S, Sigala S, et al. Induction of the unfolded protein response by alpha-synuclein in experimental models of Parkinson's disease. Journal of neurochemistry. 2011;116(4):588-605.
314. Gorbatyuk MS, Shabashvili A, Chen W, Meyers C, Sullivan LF, Salganik M, et al. Glucose regulated protein 78 diminishes alpha-synuclein neurotoxicity in a rat model of Parkinson disease. Molecular therapy. 2012;20(7):1327-37.
315. Klein C, Westenberger A. Genetics of Parkinson’s Disease. Cold Spring Harbor Perspectives in Medicine. 2012;2(1):a008888.
316. Smith WW, Jiang H, Pei Z, Tanaka Y, Morita H, Sawa A, et al. Endoplasmic reticulum stress and mitochondrial cell death pathways mediate A53T mutant alpha-synuclein-induced toxicity. Human molecular genetics. 2005;14(24):3801-11.
317. Colla E, Coune P, Liu Y, Pletnikova O, Troncoso JC, Iwatsubo T, et al. Endoplasmic reticulum stress is important for the manifestations of alpha-synucleinopathy in vivo. The Journal of neuroscience. 2012;32(10):3306-20.
318. Jiang P, Gan M, Ebrahim AS, Lin WL, Melrose HL, Yen SH. ER stress response plays an important role in aggregation of alpha-synuclein. Molecular neurodegeneration. 2010;5:56.
319. Baumeister P, Dong D, Fu Y, Lee AS. Transcriptional induction of GRP78/BiP by histone deacetylase inhibitors and resistance to histone deacetylase inhibitor-induced apoptosis. Molecular cancer therapeutics. 2009;8(5):1086-94.
320. Suzuki M, Endo M, Shinohara F, Echigo S, Rikiishi H. Enhancement of cisplatin cytotoxicity by SAHA involves endoplasmic reticulum stress-mediated apoptosis in oral squamous cell carcinoma cells. Cancer chemotherapy and pharmacology. 2009;64(6):1115-22.
321. Rao R, Nalluri S, Kolhe R, Yang Y, Fiskus W, Chen J, et al. Treatment with panobinostat induces glucose-regulated protein 78 acetylation and endoplasmic reticulum stress in breast cancer cells. Mol Cancer Ther. 2010;9(4):942-52.

322. Castillo-Carranza DL, Zhang Y, Guerrero-Munoz MJ, Kayed R, Rincon-Limas DE, Fernandez-Funez P. Differential activation of the ER stress factor XBP1 by oligomeric assemblies. Neurochemical research. 2012;37(8):1707-17.
323. Colla E, Jensen PH, Pletnikova O, Troncoso JC, Glabe C, Lee MK. Accumulation of toxic alpha-synuclein oligomer within endoplasmic reticulum occurs in alpha-synucleinopathy in vivo. The Journal of neuroscience. 2012;32(10):3301-5.
324. Andringa G, Lam KY, Chegary M, Wang X, Chase TN, Bennett MC. Tissue transglutaminase catalyzes the formation of alpha-synuclein crosslinks in Parkinson's disease. FASEB journal. 2004;18(7):932-4.
325. Junn E, Ronchetti RD, Quezado MM, Kim SY, Mouradian MM. Tissue transglutaminase-induced aggregation of alpha-synuclein: Implications for Lewy body formation in Parkinson's disease and dementia with Lewy bodies. Proceedings of the National Academy of Sciences of the United States of America. 2003;100(4):2047-52.
326. Nemes Z, Petrovski G, Aerts M, Sergeant K, Devreese B, Fesus L. Transglutaminase-mediated intramolecular cross-linking of membrane-bound alpha-synuclein promotes amyloid formation in Lewy bodies. The Journal of biological chemistry. 2009;284(40):27252-64.
327. Schmid AW, Chiappe D, Pignat V, Grimminger V, Hang I, Moniatte M, et al. Dissecting the mechanisms of tissue transglutaminase-induced cross-linking of alpha-synuclein: implications for the pathogenesis of Parkinson disease. The Journal of biological chemistry. 2009;284(19):13128-42.
328. Segers-Nolten IM, Wilhelmus MM, Veldhuis G, van Rooijen BD, Drukarch B, Subramaniam V. Tissue transglutaminase modulates alpha-synuclein oligomerization. Protein science. 2008;17(8):1395-402.
329. Wilhelmus MM, Verhaar R, Andringa G, Bol JG, Cras P, Shan L, et al. Presence of tissue transglutaminase in granular endoplasmic reticulum is characteristic of melanized neurons in Parkinson's disease brain. Brain pathology. 2011;21(2):130-9.
330. Sugeno N, Takeda A, Hasegawa T, Kobayashi M, Kikuchi A, Mori F, et al. Serine 129 phosphorylation of alpha-synuclein induces unfolded protein

response-mediated cell death. The Journal of biological chemistry. 2008;283(34):23179-88.

331. Lin AM, Chao PL, Fang SF, Chi CW, Yang CH. Endoplasmic reticulum stress is involved in arsenite-induced oxidative injury in rat brain. Toxicology and applied pharmacology. 2007;224(2):138-46.

332. Xu B, Jin CH, Deng Y, Liu W, Yang TY, Feng S, et al. Alpha-synuclein oligomerization in manganese-induced nerve cell injury in brain slices: a role of NO-mediated S-nitrosylation of protein disulfide isomerase. Molecular neurobiology. 2014;50(3):1098-110.

333. Kabiraj P, Marin JE, Varela-Ramirez A, Zubia E, Narayan M. Ellagic acid mitigates SNO-PDI induced aggregation of Parkinsonian biomarkers. ACS chemical neuroscience. 2014;5(12):1209-20.

334. Graham DG. Catecholamine toxicity: a proposal for the molecular pathogenesis of manganese neurotoxicity and Parkinson's disease. Neurotoxicology. 1984;5(1):83-95.

335. Ben-Shachar D, Zuk R, Glinka Y. Dopamine neurotoxicity: inhibition of mitochondrial respiration. Journal of neurochemistry. 1995;64(2):718-23.

336. Gomez-Santos C, Barrachina M, Gimenez-Xavier P, Dalfo E, Ferrer I, Ambrosio S. Induction of C/EBP beta and GADD153 expression by dopamine in human neuroblastoma cells. Relationship with alpha-synuclein increase and cell damage. Brain research bulletin. 2005;65(1):87-95.

337. Ito S, Nakaso K, Imamura K, Takeshima T, Nakashima K. Endogenous catecholamine enhances the dysfunction of unfolded protein response and alpha-synuclein oligomerization in PC12 cells overexpressing human alpha-synuclein. Neuroscience research. 2010;66(1):124-30.

338. Hori O, Ichinoda F, Yamaguchi A, Tamatani T, Taniguchi M, Koyama Y, et al. Role of Herp in the endoplasmic reticulum stress response. Genes to cells. 2004;9(5):457-69.

339. Miura H, Hashida K, Sudo H, Awa Y, Takarada-Iemata M, Kokame K, et al. Deletion of Herp facilitates degradation of cytosolic proteins. Genes to cells. 2010;15(8):843-53.

340. Alberts B, Johnson, A., Lewis, J., et al. Molecular Biology of the Cell. 4th edition. 2002.

341. Chan CS, Gertler TS, Surmeier DJ. Calcium homeostasis, selective vulnerability and Parkinson's disease. Trends in neurosciences. 2009;32(5):249-56.
342. Belal C, Ameli NJ, El Kommos A, Bezalel S, Al'Khafaji AM, Mughal MR, et al. The homocysteine-inducible endoplasmic reticulum (ER) stress protein Herp counteracts mutant alpha-synuclein-induced ER stress via the homeostatic regulation of ER-resident calcium release channel proteins. Human molecular genetics. 2012;21(5):963-77.
343. Wang S, Zhang S, Liou LC, Ren Q, Zhang Z, Caldwell GA, et al. Phosphatidylethanolamine deficiency disrupts alpha-synuclein homeostasis in yeast and worm models of Parkinson disease. Proceedings of the National Academy of Sciences of the United States of America. 2014;111(38):E3976-85.
344. Munoz-Lobato F, Rodriguez-Palero MJ, Naranjo-Galindo FJ, Shephard F, Gaffney CJ, Szewczyk NJ, et al. Protective role of DNJ-27/ERdj5 in Caenorhabditis elegans models of human neurodegenerative diseases. Antioxidants & redox signaling. 2014;20(2):217-35.
345. Ray A, Zhang S, Rentas C, Caldwell KA, Caldwell GA. RTCB-1 mediates neuroprotection via XBP-1 mRNA splicing in the unfolded protein response pathway. The Journal of neuroscience. 2014;34(48):16076-85.
346. Cooper AA, Gitler AD, Cashikar A, Haynes CM, Hill KJ, Bhullar B, et al. Alpha-synuclein blocks ER-Golgi traffic and Rab1 rescues neuron loss in Parkinson's models. Science. 2006;313(5785):324-8.
347. Su LJ, Auluck PK, Outeiro TF, Yeger-Lotem E, Kritzer JA, Tardiff DF, et al. Compounds from an unbiased chemical screen reverse both ER-to-Golgi trafficking defects and mitochondrial dysfunction in Parkinson's disease models. Disease models & mechanisms. 2010;3(3-4):194-208.
348. Thayanidhi N, Helm JR, Nycz DC, Bentley M, Liang Y, Hay JC. Alpha-synuclein delays endoplasmic reticulum (ER)-to-Golgi transport in mammalian cells by antagonizing ER/Golgi SNAREs. Molecular biology of the cell. 2010;21(11):1850-63.
349. Credle JJ, Forcelli PA, Delannoy M, Oaks AW, Permaul E, Berry DL, et al. alpha-Synuclein-mediated inhibition of ATF6 processing into COPII vesicles

disrupts UPR signaling in Parkinson's disease. Neurobiology of disease. 2015;76:112-25.
350. Devine MJ, Ryten M, Vodicka P, Thomson AJ, Burdon T, Houlden H, et al. Parkinson's disease induced pluripotent stem cells with triplication of the alpha-synuclein locus. Nature communications. 2011;2:440.
351. Flierl A, Oliveira LM, Falomir-Lockhart LJ, Mak SK, Hesley J, Soldner F, et al. Higher vulnerability and stress sensitivity of neuronal precursor cells carrying an alpha-synuclein gene triplication. PloS one. 2014;9(11):e112413.
352. Reyes JF, Olsson TT, Lamberts JT, Devine MJ, Kunath T, Brundin P. A cell culture model for monitoring alpha-synuclein cell-to-cell transfer. Neurobiology of disease. 2015;77:266-75.
353. Byers B, Cord B, Nguyen HN, Schule B, Fenno L, Lee PC, et al. SNCA triplication Parkinson's patient's iPSC-derived DA neurons accumulate alpha-synuclein and are susceptible to oxidative stress. PloS one. 2011;6(11):e26159.
354. Chambers SM, Fasano CA, Papapetrou EP, Tomishima M, Sadelain M, Studer L. Highly efficient neural conversion of human ES and iPS cells by dual inhibition of SMAD signaling. Nature biotechnology. 2009;27(3):275-80.
355. Ran FA, Hsu PD, Wright J, Agarwala V, Scott DA, Zhang F. Genome engineering using the CRISPR-Cas9 system. Nat Protocols. 2013;8(11):2281-308.
356. Chen B, Gilbert LA, Cimini BA, Schnitzbauer J, Zhang W, Li G-W, et al. Dynamic Imaging of Genomic Loci in Living Human Cells by an Optimized CRISPR/Cas System. Cell. 2013;155(7):1479-91.
357. Untergasser A, Cutcutache I, Koressaar T, Ye J, Faircloth BC, Remm M, et al. Primer3—new capabilities and interfaces. Nucleic Acids Research. 2012;40(15):e115.
358. Koressaar T, Remm M. Enhancements and modifications of primer design program Primer3. Bioinformatics. 2007;23(10):1289-91.
359. Stock JK, Giadrossi S, Casanova M, Brookes E, Vidal M, Koseki H, et al. Ring1-mediated ubiquitination of H2A restrains poised RNA polymerase II at bivalent genes in mouse ES cells. Nature cell biology. 2007;9(12):1428-35.

360. Ibanez P, Bonnet AM, Debarges B, Lohmann E, Tison F, Pollak P, et al. Causal relation between alpha-synuclein gene duplication and familial Parkinson's disease. Lancet. 2004;364(9440):1169-71.
361. Pchelina SN, Nuzhnyi EP, Emelyanov AK, Boukina TM, Usenko TS, Nikolaev MA, et al. Increased plasma oligomeric alpha-synuclein in patients with lysosomal storage diseases. Neuroscience letters. 2014;583c:188-93.
362. Schondorf DC, Aureli M, McAllister FE, Hindley CJ, Mayer F, Schmid B, et al. iPSC-derived neurons from GBA1-associated Parkinson's disease patients show autophagic defects and impaired calcium homeostasis. Nature communications. 2014;5:4028.
363. Barlow BK, Cory-Slechta DA, Richfield EK, Thiruchelvam M. The gestational environment and Parkinson's disease: evidence for neurodevelopmental origins of a neurodegenerative disorder. Reproductive toxicology. 2007;23(3):457-70.
364. Gorba T, Conti L. Neural stem cells as tools for drug discovery: novel platforms and approaches. Expert opinion on drug discovery. 2013;8(9):1083-94.
365. Gore A, Li Z, Fung HL, Young JE, Agarwal S, Antosiewicz-Bourget J, et al. Somatic coding mutations in human induced pluripotent stem cells. Nature. 2011;471(7336):63-7.
366. Hussein SM, Batada NN, Vuoristo S, Ching RW, Autio R, Narva E, et al. Copy number variation and selection during reprogramming to pluripotency. Nature. 2011;471(7336):58-62.
367. Lengner CJ, Gimelbrant AA, Erwin JA, Cheng AW, Guenther MG, Welstead GG, et al. Derivation of pre-X inactivation human embryonic stem cells under physiological oxygen concentrations. Cell. 2010;141(5):872-83.
368. Ran FA, Hsu PD, Wright J, Agarwala V, Scott DA, Zhang F. Genome engineering using the CRISPR-Cas9 system. Nature protocols. 2013;8(11):2281-308.
369. Gonzalez-Horta A, Hernandez BG, Chavez-Montes A. Fluorescence as a Tool to Study Lipid-Protein Interactions: The Case of ¦Á-Synuclein. Open Journal of Biophysics. 2013;Vol.03No.01:8.

370. Waxman EA, Mazzulli JR, Giasson BI. Characterization of hydrophobic residue requirements for alpha-synuclein fibrillization. Biochemistry. 2009;48(40):9427-36.
371. Bertoncini CW, Jung YS, Fernandez CO, Hoyer W, Griesinger C, Jovin TM, et al. Release of long-range tertiary interactions potentiates aggregation of natively unstructured alpha-synuclein. Proceedings of the National Academy of Sciences of the United States of America. 2005;102(5):1430-5.
372. Atarashi R, Sano K, Satoh K, Nishida N. Real-time quaking-induced conversion: A highly sensitive assay for prion detection. Prion. 2011;5(3):150-3.
373. Alvarez-Erviti L, Seow Y, Schapira AH, Gardiner C, Sargent IL, Wood MJ, et al. Lysosomal dysfunction increases exosome-mediated alpha-synuclein release and transmission. Neurobiology of disease. 2011;42(3):360-7.
374. Luk KC, Kehm VM, Zhang B, O'Brien P, Trojanowski JQ, Lee VM. Intracerebral inoculation of pathological alpha-synuclein initiates a rapidly progressive neurodegenerative alpha-synucleinopathy in mice. The Journal of experimental medicine. 2012;209(5):975-86.
375. Fasano A, Visanji NP, Liu LW, Lang AE, Pfeiffer RF. Gastrointestinal dysfunction in Parkinson's disease. The Lancet Neurology. 2015;14(6):625-39.
376. Dreos R, Ambrosini G, Cavin Perier R, Bucher P. EPD and EPDnew, high-quality promoter resources in the next-generation sequencing era. Nucleic acids research. 2013;41:D157-64.
377. Gilbert LA, Larson MH, Morsut L, Liu Z, Brar GA, Torres SE, et al. CRISPR-mediated modular RNA-guided regulation of transcription in eukaryotes. Cell. 2013;154(2):442-51.
378. Chen B, Gilbert LA, Cimini BA, Schnitzbauer J, Zhang W, Li GW, et al. Dynamic imaging of genomic loci in living human cells by an optimized CRISPR/Cas system. Cell. 2013;155(7):1479-91.
379. Irizarry MC, Growdon W, Gomez-Isla T, Newell K, George JM, Clayton DF, et al. Nigral and cortical Lewy bodies and dystrophic nigral neurites in Parkinson's disease and cortical Lewy body disease contain alpha-synuclein immunoreactivity. Journal of neuropathology and experimental neurology. 1998;57(4):334-7.

380. Spillantini MG, Crowther RA, Jakes R, Cairns NJ, Lantos PL, Goedert M. Filamentous alpha-synuclein inclusions link multiple system atrophy with Parkinson's disease and dementia with Lewy bodies. Neuroscience letters. 1998;251(3):205-8.
381. Irwin DJ, Lee VM, Trojanowski JQ. Parkinson's disease dementia: convergence of alpha-synuclein, tau and amyloid-beta pathologies. Nature reviews Neuroscience. 2013;14(9):626-36.
382. McLean CA, Cherny RA, Fraser FW, Fuller SJ, Smith MJ, Beyreuther K, et al. Soluble pool of Abeta amyloid as a determinant of severity of neurodegeneration in Alzheimer's disease. Annals of neurology. 1999;46(6):860-6.
383. Selkoe DJ. The molecular pathology of Alzheimer's disease. Neuron. 1991;6(4):487-98.
384. Ballatore C, Lee VM, Trojanowski JQ. Tau-mediated neurodegeneration in Alzheimer's disease and related disorders. Nature reviews Neuroscience. 2007;8(9):663-72.
385. Wszolek ZK, Tsuboi Y, Ghetti B, Pickering-Brown S, Baba Y, Cheshire WP. Frontotemporal dementia and parkinsonism linked to chromosome 17 (FTDP-17). Orphanet journal of rare diseases. 2006;1:30.
386. Moussaud S, Jones DR, Moussaud-Lamodiere EL, Delenclos M, Ross OA, McLean PJ. Alpha-synuclein and tau: teammates in neurodegeneration? Molecular neurodegeneration. 2014;9:43.
387. Larson MH, Gilbert LA, Wang X, Lim WA, Weissman JS, Qi LS. CRISPR interference (CRISPRi) for sequence-specific control of gene expression. Nature protocols. 2013;8(11):2180-96.
388. Gilbert LA, Horlbeck MA, Adamson B, Villalta JE, Chen Y, Whitehead EH, et al. Genome-Scale CRISPR-Mediated Control of Gene Repression and Activation. Cell. 2014;159(3):647-61.
389. Lawhorn IE, Ferreira JP, Wang CL. Evaluation of sgRNA target sites for CRISPR-mediated repression of TP53. PloS one. 2014;9(11):e113232.
390. Rach EA, Winter DR, Benjamin AM, Corcoran DL, Ni T, Zhu J, et al. Transcription initiation patterns indicate divergent strategies for gene regulation at the chromatin level. PLoS genetics. 2011;7(1):e1001274.

391. Wasserman WW, Sandelin A. Applied bioinformatics for the identification of regulatory elements. Nature reviews Genetics. 2004;5(4):276-87.
392. Gilbert LA, Horlbeck MA, Adamson B, Villalta JE, Chen Y, Whitehead EH, et al. Genome-Scale CRISPR-Mediated Control of Gene Repression and Activation. Cell. 2014.
393. Du Y, Meng Q, Zhang J, Sun M, Shen B, Jiang H, et al. Functional annotation of cis-regulatory elements in human cells by dCas9/sgRNA. Cell research. 2015;25(7):877-80.
394. Gao X, Tsang JC, Gaba F, Wu D, Lu L, Liu P. Comparison of TALE designer transcription factors and the CRISPR/dCas9 in regulation of gene expression by targeting enhancers. Nucleic acids research. 2014;42(20):e155.
395. Kearns NA, Pham H, Tabak B, Genga RM, Silverstein NJ. Functional annotation of native enhancers with a Cas9-histone demethylase fusion. Nature methods. 2015;12(5):401-3.
396. Maeder ML, Linder SJ, Cascio VM, Fu Y, Ho QH, Joung JK. CRISPR RNA-guided activation of endogenous human genes. Nature methods. 2013;10(10):977-9.
397. Cheng AW, Wang H, Yang H, Shi L, Katz Y, Theunissen TW, et al. Multiplexed activation of endogenous genes by CRISPR-on, an RNA-guided transcriptional activator system. Cell research. 2013;23(10):1163-71.
398. Kearns NA, Genga RM, Enuameh MS, Garber M, Wolfe SA, Maehr R. Cas9 effector-mediated regulation of transcription and differentiation in human pluripotent stem cells. Development. 2014;141(1):219-23.
399. Hu J, Lei Y, Wong WK, Liu S, Lee KC, He X, et al. Direct activation of human and mouse Oct4 genes using engineered TALE and Cas9 transcription factors. Nucleic acids research. 2014;42(7):4375-90.
400. Hilton IB, D'Ippolito AM, Vockley CM, Thakore PI, Crawford GE, Reddy TE. Epigenome editing by a CRISPR-Cas9-based acetyltransferase activates genes from promoters and enhancers. Nature Biotechnology. 2015;33(5):510-7.
401. Tanenbaum ME, Gilbert LA, Qi LS, Weissman JS, Vale RD. A protein-tagging system for signal amplification in gene expression and fluorescence imaging. Cell. 2014;159(3):635-46.

402. Zalatan JG, Lee ME, Almeida R, Gilbert LA, Whitehead EH, La Russa M, et al. Engineering complex synthetic transcriptional programs with CRISPR RNA scaffolds. Cell. 2015;160(1-2):339-50.
403. Konermann S, Brigham MD, Trevino AE, Joung J, Abudayyeh OO, Barcena C, et al. Genome-scale transcriptional activation by an engineered CRISPR-Cas9 complex. Nature. 2015;517(7536):583-8.
404. Chavez A, Scheiman J, Vora S, Pruitt BW, Tuttle M, P R Iyer E, et al. Highly efficient Cas9-mediated transcriptional programming. Nat Meth. 2015;12(4):326-8.
405. Fujita T, Fujii H. Efficient isolation of specific genomic regions and identification of associated proteins by engineered DNA-binding molecule-mediated chromatin immunoprecipitation (enChIP) using CRISPR. Biochemical and biophysical research communications. 2013;439(1):132-6.
406. Fujita T, Fujii H. Isolation of specific genomic regions and identification of associated molecules by engineered DNA-binding molecule-mediated chromatin immunoprecipitation (enChIP) using CRISPR. Methods in molecular biology. 2015;1288:43-52.
407. Wu X, Scott DA, Kriz AJ, Chiu AC, Hsu PD, Dadon DB, et al. Genome-wide binding of the CRISPR endonuclease Cas9 in mammalian cells. Nature biotechnology. 2014;32(7):670-6.
408. Kuscu C, Arslan S, Singh R, Thorpe J, Adli M. Genome-wide analysis reveals characteristics of off-target sites bound by the Cas9 endonuclease. Nature biotechnology. 2014;32(7):677-83.
409. Oakes BL, Nadler DC, Savage DF. Protein engineering of Cas9 for enhanced function. Methods in enzymology. 2014;546:491-511.
410. Josephs EA, Kocak DD, Fitzgibbon CJ, McMenemy J, Gersbach CA, Marszalek PE. Structure and specificity of the RNA-guided endonuclease Cas9 during DNA interrogation, target binding and cleavage. Nucleic acids research. 2015.
411. Xu H, Xiao T, Chen CH, Li W, Meyer CA, Wu Q, et al. Sequence determinants of improved CRISPR sgRNA design. Genome research. 2015;25(8):1147-57.

412. Kuscu C, Arslan S, Singh R, Thorpe J, Adli M. Genome-wide analysis reveals characteristics of off-target sites bound by the Cas9 endonuclease. Nat Biotech. 2014;32(7):677-83.
413. Kim YK, Bourgeois CF, Isel C, Churcher MJ, Karn J. Phosphorylation of the RNA Polymerase II Carboxyl-Terminal Domain by CDK9 Is Directly Responsible for Human Immunodeficiency Virus Type 1 Tat-Activated Transcriptional Elongation. Molecular and cellular biology. 2002;22(13):4622-37.
414. Wu H, Wang Y, Wang Y, Cao X, Wu Y, Meng Z, et al. Quantitatively relating gene expression to light intensity via the serial connection of blue light sensor and CRISPRi. ACS synthetic biology. 2014;3(12):979-82.
415. Polstein LR, Gersbach CA. A light-inducible CRISPR-Cas9 system for control of endogenous gene activation. Nature chemical biology. 2015;11(3):198-200.
416. Balboa D, Weltner J, Eurola S, Trokovic R, Wartiovaara K, Otonkoski T. Conditionally Stabilized dCas9 Activator for Controlling Gene Expression in Human Cell Reprogramming and Differentiation. Stem cell reports. 2015;5(3):448-59.
417. Tsai SQ, Wyvekens N, Khayter C, Foden JA, Thapar V, Reyon D, et al. Dimeric CRISPR RNA-guided FokI nucleases for highly specific genome editing. Nat Biotech. 2014;32(6):569-76.
418. Hara S, Tamano M, Yamashita S, Kato T, Saito T, Sakuma T, et al. Generation of mutant mice via the CRISPR/Cas9 system using FokI-dCas9. Scientific reports. 2015;5:11221.
419. Nakagawa Y, Sakuma T, Sakamoto T, Ohmuraya M, Nakagata N, Yamamoto T. Production of knockout mice by DNA microinjection of various CRISPR/Cas9 vectors into freeze-thawed fertilized oocytes. BMC biotechnology. 2015;15:33.
420. Wyvekens N, Topkar VV, Khayter C, Joung JK, Tsai SQ. Dimeric CRISPR RNA-Guided FokI-dCas9 Nucleases Directed by Truncated gRNAs for Highly Specific Genome Editing. Human gene therapy. 2015;26(7):425-31.
421. Wyvekens N, Tsai SQ, Joung JK. Genome Editing in Human Cells Using CRISPR/Cas Nucleases. Current protocols in molecular biology. 2015;112:31.3.1-.3.18.

422. Piatek A, Ali Z, Baazim H, Li L, Abulfaraj A, Al-Shareef S, et al. RNA-guided transcriptional regulation in planta via synthetic dCas9-based transcription factors. Plant biotechnology journal. 2015;13(4):578-89.
423. Lin S, Ewen-Campen B, Ni X, Housden BE, Perrimon N. In Vivo Transcriptional Activation Using CRISPR-Cas9 in Drosophila. Genetics. 2015.
424. Choudhary E, Thakur P, Pareek M, Agarwal N. Gene silencing by CRISPR interference in mycobacteria. Nature communications. 2015;6:6267.
425. Tong Y, Charusanti P, Zhang L, Weber T, Lee SY. CRISPR-Cas9 Based Engineering of Actinomycetal Genomes. ACS synthetic biology. 2015;4(9):1020-9.
426. Zhao Y, Dai Z, Liang Y, Yin M, Ma K, He M, et al. Sequence-specific inhibition of microRNA via CRISPR/CRISPRi system. Scientific reports. 2014;4:3943.
427. Zhang WW, Tong HL, Sun XF, Hu Q, Yang Y, Li SF, et al. Identification of miR-2400 gene as a novel regulator in skeletal muscle satellite cells proliferation by targeting MYOG gene. Biochemical and biophysical research communications. 2015;463(4):624-31.
428. Hawkins JS, Wong S, Peters JM, Almeida R, Qi LS. Targeted Transcriptional Repression in Bacteria Using CRISPR Interference (CRISPRi). Methods in molecular biology. 2015;1311:349-62.
429. Ji W, Lee D, Wong E, Dadlani P, Dinh D, Huang V, et al. Specific gene repression by CRISPRi system transferred through bacterial conjugation. ACS synthetic biology. 2014;3(12):929-31.
430. Lv L, Ren YL, Chen JC, Wu Q, Chen GQ. Application of CRISPRi for prokaryotic metabolic engineering involving multiple genes, a case study: Controllable P(3HB-co-4HB) biosynthesis. Metabolic engineering. 2015;29:160-8.
431. Nielsen AA, Voigt CA. Multi-input CRISPR/Cas genetic circuits that interface host regulatory networks. Molecular systems biology. 2014;10:763.
432. Pan A, Weintraub NL, Tang Y. Enhancing stem cell survival in an ischemic heart by CRISPR-dCas9-based gene regulation. Medical hypotheses. 2014;83(6):702-5.

433. Falahi F, Sgro A, Blancafort P. Epigenome engineering in cancer: fairytale or a realistic path to the clinic? Frontiers in oncology. 2015;5:22.
434. Sun Y, Oravecz-Wilson K, Mathewson N, Wang Y, McEachin R, Liu C, et al. Mature T cell responses are controlled by microRNA-142. The Journal of clinical investigation. 2015;125(7):2825-40.
435. Citorik RJ, Mimee M, Lu TK. Sequence-specific antimicrobials using efficiently delivered RNA-guided nucleases. Nature biotechnology. 2014;32(11):1141-5.
436. Bikard D, Euler CW, Jiang W, Nussenzweig PM, Goldberg GW, Duportet X, et al. Exploiting CRISPR-Cas nucleases to produce sequence-specific antimicrobials. Nature biotechnology. 2014;32(11):1146-50.
437. Ebina H, Misawa N, Kanemura Y, Koyanagi Y. Harnessing the CRISPR/Cas9 system to disrupt latent HIV-1 provirus. Scientific reports. 2013;3:2510.
438. Hu W, Kaminski R, Yang F, Zhang Y, Cosentino L, Li F, et al. RNA-directed gene editing specifically eradicates latent and prevents new HIV-1 infection. Proceedings of the National Academy of Sciences of the United States of America. 2014;111(31):11461-6.
439. Liao HK, Gu Y, Diaz A, Marlett J, Takahashi Y, Li M, et al. Use of the CRISPR/Cas9 system as an intracellular defense against HIV-1 infection in human cells. Nature communications. 2015;6:6413.
440. Kampmann M, Horlbeck MA, Chen Y, Tsai JC, Bassik MC, Gilbert LA, et al. Next-generation libraries for robust RNA interference-based genome-wide screens. Proceedings of the National Academy of Sciences of the United States of America. 2015;112(26):E3384-91.
441. Anton T, Bultmann S, Leonhardt H, Markaki Y. Visualization of specific DNA sequences in living mouse embryonic stem cells with a programmable fluorescent CRISPR/Cas system. Nucleus. 2014;5(2):163-72.
442. Chen B, Huang B. Imaging genomic elements in living cells using CRISPR/Cas9. Methods in enzymology. 2014;546:337-54.
443. Ma H, Naseri A, Reyes-Gutierrez P, Wolfe SA, Zhang S, Pederson T. Multicolor CRISPR labeling of chromosomal loci in human cells. Proceedings of

the National Academy of Sciences of the United States of America. 2015;112(10):3002-7.
444. Deng W, Shi X, Tjian R, Lionnet T, Singer RH. CASFISH: CRISPR/Cas9-mediated in situ labeling of genomic loci in fixed cells. Proceedings of the National Academy of Sciences of the United States of America. 2015;112(38):11870-5.
445. Agne M, Blank I, Emhardt AJ, Gabelein CG, Gawlas F, Gillich N, et al. Modularized CRISPR/dCas9 effector toolkit for target-specific gene regulation. ACS synthetic biology. 2014;3(12):986-9.
446. Cress BF, Toparlak OD, Guleria S, Lebovich M, Stieglitz JT, Englaender JA, et al. CRISPathBrick: Modular Combinatorial Assembly of Type II-A CRISPR Arrays for dCas9-Mediated Multiplex Transcriptional Repression in E. coli. ACS synthetic biology. 2015;4(9):987-1000.
447. Pardridge WM, Boado RJ. Reengineering biopharmaceuticals for targeted delivery across the blood-brain barrier. Methods in enzymology. 2012;503:269-92.
448. Pardridge WM. Targeted delivery of protein and gene medicines through the blood-brain barrier. Clinical pharmacology and therapeutics. 2015;97(4):347-61.
449. Alvarez-Erviti L, Seow Y, Yin H, Betts C, Lakhal S, Wood MJA. Delivery of siRNA to the mouse brain by systemic injection of targeted exosomes. Nat Biotech. 2011;29(4):341-5.
450. Misra S, Chopra K, Sinha VR, Medhi B. Galantamine-loaded solid-lipid nanoparticles for enhanced brain delivery: preparation, characterization, in vitro and in vivo evaluations. Drug delivery. 2015:1-10.
451. Pardridge WM. Drug Delivery to the Brain. J Cereb Blood Flow Metab. 1997;17(7):713-31.
452. Schmidt F, Grimm D. CRISPR genome engineering and viral gene delivery: a case of mutual attraction. Biotechnology journal. 2015;10(2):258-72.
453. Shalem O, Sanjana NE, Hartenian E, Shi X, Scott DA, Mikkelsen TS, et al. Genome-scale CRISPR-Cas9 knockout screening in human cells. Science. 2014;343(6166):84-7.

454. Cheng R, Peng J, Yan Y, Cao P, Wang J, Qiu C, et al. Efficient gene editing in adult mouse livers via adenoviral delivery of CRISPR/Cas9. FEBS letters. 2014;588(21):3954-8.
455. Malina A, Mills JR, Cencic R, Yan Y, Fraser J, Schippers LM, et al. Repurposing CRISPR/Cas9 for in situ functional assays. Genes & development. 2013;27(23):2602-14.
456. Senis E, Fatouros C, Grosse S, Wiedtke E, Niopek D, Mueller AK, et al. CRISPR/Cas9-mediated genome engineering: an adeno-associated viral (AAV) vector toolbox. Biotechnology journal. 2014;9(11):1402-12.
457. Swiech L, Heidenreich M, Banerjee A, Habib N, Li Y, Trombetta J, et al. In vivo interrogation of gene function in the mammalian brain using CRISPR-Cas9. Nature biotechnology. 2015;33(1):102-6.
458. Barrangou R, Birmingham A, Wiemann S, Beijersbergen RL, Hornung V, Smith A. Advances in CRISPR-Cas9 genome engineering: lessons learned from RNA interference. Nucleic acids research. 2015;43(7):3407-19.
459. Heintze J, Luft C, Ketteler R. A CRISPR CASe for high-throughput silencing. Frontiers in Genetics. 2013;4:193.
460. Fu Y, Foden JA, Khayter C, Maeder ML, Reyon D, Joung JK, et al. High-frequency off-target mutagenesis induced by CRISPR-Cas nucleases in human cells. Nature biotechnology. 2013;31(9):822-6.
461. Jackson AL, Bartz SR, Schelter J, Kobayashi SV, Burchard J, Mao M, et al. Expression profiling reveals off-target gene regulation by RNAi. Nature biotechnology. 2003;21(6):635-7.
462. Pattanayak V, Lin S, Guilinger JP, Ma E, Doudna JA, Liu DR. High-throughput profiling of off-target DNA cleavage reveals RNA-programmed Cas9 nuclease specificity. Nature biotechnology. 2013;31(9):839-43.
463. Haeusler AR, Donnelly CJ, Periz G, Simko EA, Shaw PG, Kim MS, et al. C9orf72 nucleotide repeat structures initiate molecular cascades of disease. Nature. 2014;507(7491):195-200.
464. Bonifati V. Parkinson's disease: the LRRK2-G2019S mutation: opening a novel era in Parkinson's disease genetics. European journal of human genetics. 2006;14(10):1061-2.

465. A novel gene containing a trinucleotide repeat that is expanded and unstable on Huntington's disease chromosomes. The Huntington's Disease Collaborative Research Group. Cell. 1993;72(6):971-83.
466. Ueda M, Ando Y. Recent advances in transthyretin amyloidosis therapy. Translational neurodegeneration. 2014;3:19.
467. Farooqi AA, Rehman ZU, Muntane J. Antisense therapeutics in oncology: current status. OncoTargets and therapy. 2014;7:2035-42.
468. Kim JE, O'Sullivan ML, Sanchez CA, Hwang M, Israel MA, Brennand K, et al. Investigating synapse formation and function using human pluripotent stem cell-derived neurons. Proceedings of the National Academy of Sciences of the United States of America. 2011;108(7):3005-10.
469. Zhao A, Tsechansky M, Ellington AD, Marcotte EM. Revisiting and revising the purinosome. Molecular bioSystems. 2014;10(3):369-74.
470. Ltic S, Perovic M, Mladenovic A, Raicevic N, Ruzdijic S, Rakic L, et al. Alpha-synuclein is expressed in different tissues during human fetal development. Journal of molecular neuroscience. 2004;22(3):199-204.
471. Bialecka M, Robowski P, Honczarenko K, Roszmann A, Slawek J. Genetic and environmental factors for hyperhomocysteinaemia and its clinical implications in Parkinson's disease. Neurologia i neurochirurgia polska. 2009;43(3):272-85.
472. Hosoi T, Ogawa K, Ozawa K. Homocysteine induces X-box-binding protein 1 splicing in the mice brain. Neurochemistry international. 2010;56(2):216-20.
473. Yang W, Tiffany-Castiglioni E, Koh HC, Son IH. Paraquat activates the IRE1/ASK1/JNK cascade associated with apoptosis in human neuroblastoma SH-SY5Y cells. Toxicology letters. 2009;191(2-3):203-10.
474. Niso-Santano M, Bravo-San Pedro JM, Gomez-Sanchez R, Climent V, Soler G, Fuentes JM, et al. ASK1 overexpression accelerates paraquat-induced autophagy via endoplasmic reticulum stress. Toxicological sciences. 2011;119(1):156-68.
475. Sado M, Yamasaki Y, Iwanaga T, Onaka Y, Ibuki T, Nishihara S, et al. Protective effect against Parkinson's disease-related insults through the activation of XBP1. Brain research. 2009;1257:16-24.

476. Valdes P, Mercado G, Vidal RL, Molina C, Parsons G, Court FA, et al. Control of dopaminergic neuron survival by the unfolded protein response transcription factor XBP1. Proceedings of the National Academy of Sciences of the United States of America. 2014;111(18):6804-9.
477. Janyou A, Changtam C, Suksamrarn A, Tocharus C, Tocharus J. Suppression effects of O-demethyldemethoxycurcumin on thapsigargin triggered on endoplasmic reticulum stress in SK-N-SH cells. Neurotoxicology. 2015;50:92-100.
478. Duplan E, Giaime E, Viotti J, Sevalle J, Corti O, Brice A, et al. ER-stress-associated functional link between Parkin and DJ-1 via a transcriptional cascade involving the tumor suppressor p53 and the spliced X-box binding protein XBP-1. Journal of cell science. 2013;126(Pt 9):2124-33.
479. Hely MA, Reid WG, Adena MA, Halliday GM, Morris JG. The Sydney multicenter study of Parkinson's disease: the inevitability of dementia at 20 years. Movement disorders. 2008;23(6):837-44.
480. Hoozemans JJ, van Haastert ES, Nijholt DA, Rozemuller AJ, Scheper W. Activation of the unfolded protein response is an early event in Alzheimer's and Parkinson's disease. Neuro-degenerative diseases. 2012;10(1-4):212-5.
481. Rujano MA, Bosveld F, Salomons FA, Dijk F, van Waarde MA, van der Want JJ, et al. Polarised asymmetric inheritance of accumulated protein damage in higher eukaryotes. PLoS biology. 2006;4(12):e417.
482. Liu B, Larsson L, Caballero A, Hao X, Oling D, Grantham J, et al. The polarisome is required for segregation and retrograde transport of protein aggregates. Cell. 2010;140(2):257-67.

Appendix

A.1 Publications

1. **Heman-Ackah, S.M.**, Bassett, A.R., Wood, M.J.A. 2016. “Precision Modulation of Neurodegenerative Disease-Related Gene Expression in Human iPSC-Derived Neurons.” Accepted for Publication in *Scientific Reports*.

2. Thompson, A.G., Gray, E., **Heman-Ackah, S.M.**, Mäger, I., Talbot, K., Andaloussi, S.E., Wood, M.J., Turner, M.R. 2016. “Extracellular vesicles in neurodegenerative disease: pathogenesis to biomarkers.” *Nat Rev Neurol* no.12 (6):346-57. doi: 10.1038/nrneurol.2016.68.

3. Hasson, S. A., A. I. Fogel, C. Wang, R. MacArthur, R. Guha, **S. M. Heman-Ackah**, S. Martin, R. J. Youle, and J. Inglese. 2015. "Chemogenomic profiling of endogenous PARK2 expression using a genome-edited coincidence reporter." *ACS Chem Biol* no. 10 (5):1188-97. doi: 10.1021/cb5010417.

4. Malik, N., X. Wang, S. Shah, A. G. Efthymiou, B. Yan, **S. M. Heman-Ackah**, M. Zhan, and M. Rao. 2014. "Comparison of the gene expression profiles of human fetal cortical astrocytes with pluripotent stem cell derived neural stem cells identifies human astrocyte markers and signaling pathways and transcription factors active in human

astrocytes." *PLoS One* no. 9 (5):e96139. doi: 10.1371/journal.pone.0096139.

5. Efthymiou, A., A. Shaltouki, J. P. Steiner, B. Jha, **S. M. Heman-Ackah**, A. Swistowski, X. Zeng, M. S. Rao, and N. Malik. 2014. "Functional screening assays with neurons generated from pluripotent stem cell-derived neural stem cells." *J Biomol Screen* no. 19 (1):32-43. doi: 10.1177/1087057113501869.

6. Hasson, S. A., L. A. Kane, K. Yamano, C. H. Huang, D. A. Sliter, E. Buehler, C. Wang, **S. M. Heman-Ackah**, T. Hessa, R. Guha, S. E. Martin, and R. J. Youle. 2013. "High-content genome-wide RNAi screens identify regulators of parkin upstream of mitophagy." *Nature* no. 504 (7479):291-5. doi: 10.1038/nature12748.

7. **Heman-Ackah, S. M.**, M. Hallegger, M. S. Rao, and M. J. Wood. 2013. "RISC in PD: the impact of microRNAs in Parkinson's disease cellular and molecular pathogenesis." *Front Mol Neurosci* no. 6:40. doi: 10.3389/fnmol.2013.00040.

8. Erskine, C.L., Krco, C.C., Hedin, K.E., Borson, N.D., Kalli, K.R., Behrens, M.D., **Heman-Ackah, S.M.**, von Hofe, E., Wettstein, P.J., Mohamadzadeh, M., and Knutson, K.L. 2011. MHC Class II Epitope Nesting Modulates Dendritic Cell Function and Improves Generation of Antigen-Specific CD4 Helper T Cells. *J Immunol.* 2011 Jul 1. 187(1): 316-24.

A.2 Book Chapters

1. Heman-Ackah S.E., **Heman-Ackah S.M.**, Lalwani A.K. Chapter: Genetics in Otolaryngology. Encyclopedia of Otolaryngology. Ed. S Kountakis New York: Springer Berlin Heidelberg, 2013, p 1001-1011.

A.3 Published Medical Illustrations

1. Heman-Ackah Y.D., Goding G.S. Jr., Rao V. Laryngotracheal trauma. In: Diagnosis and Treatment of Voice Disorders, 3rd edition. Rubin J.S., Sataloff R.T., Korovin G.S., eds. San Diego, CA: Singular Publishing Group, Inc. 2006.

2. Heman-Ackah Y.D., Goding G.S. Jr., Rao V. Laryngotracheal trauma. In: Diagnosis and Treatment of Voice Disorders, 2nd edition. Rubin J.S., Sataloff R.T., Korovin G.S., eds. San Diego, CA: Singular Publishing Group, Inc. 2002.

A.4 Conference Presentations

1. **Heman-Ackah, S.M.**, Flynn, R., Cowley, S.A., Fulga, T.A., Bassett, A.R., Wood, M.J.A. Correction of Alpha-Synuclein Gene Triplication by Double-Nicking CRISPR/Cas9 in Parkinson's Disease Patient-Derived iPSCs. Poster Presentation. Oxford Parkinson's Disease Research Day. April 20, 2015.

2. **Heman-Ackah, S.M.**, Flynn, R., Cowley, S.A., Fulga, T.A., Bassett, A.R., Wood, M.J.A. Correction of Alpha-Synuclein Gene Triplication by Double-Nicking CRISPR/Cas9 in Parkinson's Disease Patient-Derived iPSCs. Poster Presentation. Keystone Symposium on Precision Genome Engineering and Synthetic Biology. January 13, 2015.

3. **Heman-Ackah, S.M.**, Wood, M.J.A., Rao, M.S. Establishing SH-SY5Y and iPSC-Derived Neuron Models for Studying Molecular Mechanisms of Neurodegeneration in Parkinson's Disease. Poster Presentation. NIAMS Intramural Research Program Retreat. June 5, 2013.

4. **Heman-Ackah, S.M.**, Wood, M.J.A., Rao, M.S. Establishing SH-SY5Y and iPSC-Derived Neuron Models for Studying Molecular Mechanisms of Neurodegeneration in Parkinson's Disease. Poster Presentation. NIH Center for Regenerative Medicine Symposium. May 31, 2013.

A.5 Awards

1. John Fell Fund, "Developing a Reporter to Purify Dopamine Neurons from iPS Cells", £7,500

2. Cure Parkinson's Trust, "Mitochondrial piRNAs: Role in PD Pathogenesis and Novel Targets for Therapeutic Intervention", £45,000

A.6 Leadership

1. Student Representative for the Department of Physiology, Anatomy and Genetics (2013 – 2014)
    a. Departmental Management Committee (Michalemas, Hilary and Trinity Terms 2013 – 2014)
    b. Departmental Safety Advisory Committee (Michalemas, Hilary and Trinity Terms 2013 – 2014)
    c. Student Organizer of Brain Awareness Week at the Museum of the History of Science (10 – 17 March 2014)